Characterisation of Implant Supported Soft Tissue Prostheses Produced with 3D Colour Printing Technology

School of Clinical Dentistry
The University of Sheffield

A PhD thesis submitted by
Faraedon M. M. Zardawi
November 2012

Dedication

I lovingly dedicate this thesis to my wife Wasnaa, who has supported me each step of the way.

To my parents, who always stood by me, gone now, but never forgotten. I will miss them always and love them forever.

To my lovely daughter Farah, my sons Ahmed and Ali, their wives Marwa and Israa and my sweet grand kids Lavin, Lana and Meran; that is my lovely family.

Acknowledgments

I would like to convey my gratitude to my supervisors, Professor Julian Yates and Professor Richard van Noort for providing me with the inspiration and support during my PhD work. Their kind but rigorous oversight of this project constantly gave me the motivation to perform to my maximum ability. I was very fortunate to have been able to work with them; their detailed and constructive comments were vital to the development of this thesis.

I would also like to extend my gratitude to Mr. David Wildgoose for his advice and support

I am most grateful to the other members of the project team at Sheffield based Industrial Design Company, Fripp Design and Research: Mrs Sue Roberts, Tom Fripp, Neil Frewer and Steve Roberts for their time and expertise throughout this project.

Very special thanks to Neil Frewer for his great help in designing the alignment process and producing the magnet boss designs for the prostheses.

Without Dr. Nishant Yadev the biocompatibility tests would not have taken place; he promised to help till the end and he did. So thank you so much Nish.

I am grateful to my friend and colleague Dr. Kaida Xiao; we worked side by side on this project for 3 years, it was more than nice to work with him and I really appreciate his support and the great work we have done in colour reproduction and colour measurements.

My thanks must go also to Mrs L. Gill, a senior lecturer in maxillofacial technology at Manchester University for being very kind and helpful to me in designating the skin colour shade guide used for colour reproduction.

Many thanks to Mr. Frank Johnson, a maxillofacial technician at the Northern General Hospital in Sheffield for his kind help and being generous in answering all my questions about handmade facial prostheses.

I must say thank you to Dr. Duncan Wood for his help with the spectrophotometer.

My special thanks to Dr. Rob Moorehead for being always nearby to help.

I must acknowledge as well the many friends and colleagues who have supported me in one way or another during my studies, Haitham Almansour, Salam Al Zahawi, Raad Al Marza, Ahmed Abusarwel, Omar Alsadon, Shreen shahrabaf, Neda akaisy, Hawa Fathi. and Dalal Alotaibi.

I would like to thank the staff in the Academic Unit of Restorative Dentistry for being so friendly and helpful.

Finally I wish to express my most sincere gratitude and appreciation to the Iraqi Ministry of Higher Education and Scientific Researches for their sponsorship of this Doctoral Scholarship with a very special thanks to the staff of the Iraqi Cultural Attaché in London for their kind help and support during the period of my PhD study.

Summary

The numbers of patients needing facial prostheses has increased in the last few decades due to improving cancer survival rates. The many limitations of the handmade prostheses together with rapid expansion of prototyping in all directions, particularly in producing human anatomically accurate parts, have raised the question of how to employ this technology for rapid manufacturing of facial soft tissue prostheses.

The idea started to grow and the project was implemented based on CAD/CAM principles – additive manufacturing technology, by employing layered fabrication of facial prostheses from starch powder and a water based binder and infiltrated with a silicone polymer (SPIS).

The project aimed to produce a facial prosthesis by using 3D colour printing, which would match the patient's skin shade and have the desirable mechanical properties, through a relatively low cost process that would be accessible to the global patient community. This was achieved by providing a simple system for data capture, design and reproducible method of manufacture with a clinically acceptable material. The prosthesis produced has several advantages and few limitations when compared to existing products/prostheses made from silicone polymer (SP).

The mechanical properties and durability were not as good as those of the SP made prosthesis but they were acceptable, although the ideal properties have yet to be identified. Colour reproduction and colour matching were more than acceptable, although the colour of the SPIS parts was less stable than the SP colour under natural and accelerated weathering conditions. However, it is acknowledged that neither of the two methods used represent the natural life use on patients and the deficiencies demonstrated in terms of mechanical properties and colour instability were partially inherent in the methodology used, as the project was still at the developmental stage and it was not possible to apply real

life tests on patients. Moreover, deficiencies in mechanical and optical properties were probably caused by the starch present, which was used as a scaffold for the SP.

Furthermore, a suitable retention system utilising existing components was designed and added to the prosthesis. This enabled the prosthesis to be retained by implants with no need for the addition of adhesive. This would also help to prolong the durability and life span of the prosthesis.

The capability of the printer to produce skin shades was determined and it was found that all the skin colours measured fall within the range of the 3D colour printer and thereby the printer was able to produce all the colours required. Biocompatibility was also acceptable, with a very low rate of toxicity. However, no material is 100% safe and each material has a certain range of toxicity at certain concentrations.

At this stage of the project, it can be confirmed that facial prostheses were successfully manufactured by using 3D colour printing to match the patient's skin shade, using biocompatible materials and having the desirable mechanical properties. Furthermore, the technology used enabled prostheses to be produced in a shorter time frame and at a lower cost than conventional SP prostheses. They are also very lightweight, easier to use and possibly more comfortable for the patients. Moreover, this technology has the capability of producing multiple prostheses at the time of manufacture at reduced extra cost, whilst the data can be saved and can be utilised/modified for producing further copies in the future without having to going through all the steps involved with handmade prostheses.

Based on the mechanical properties and colour measurements the prostheses will have a finite service life and the recommendation is that these prostheses will need replacing every 6 to 12 months, depending on how the patient handles and maintains the prostheses and whether the prosthesis is being used as an interim or definitive prosthesis. This was largely comparable to existing prostheses but without the time and cost implications for replacement.

However, it is acknowledged that further investigations and clinical case studies are required to investigate the “real life” effect on the prostheses and to get feedback from the patients in order to make appropriate improvements to the mechanical properties and the durability of the prosthesis.

Table of Contents

DEDICATION ..... **II**
ACKNOWLEDGMENTS ..... **III**
LIST OF ABBREVIATIONS ..... **XII**
LIST OF FIGURES ..... **XIV**
LIST OF TABLES ..... **XIX**
1 INTRODUCTION **1**
2 LITERATURE REVIEW **5**
2.1 Maxillofacial Prostheses – Past and Present Trends **6**
2.2 Current Facial Prostheses **13**
2.2.1 Materials Available 13
2.2.2 Fabrication 19
2.2.3 Requirements: 21
2.2.4 Limitations of Current Prostheses 25
2.3 Material Properties **25**
2.3.1 The Mechanical Properties 26
2.3.2 Optical Properties 28
2.4 Durability **28**
2.4.1 Changes in the Mechanical Properties 29
2.4.2 Changes in the Optical Properties: 30
2.4.3 Aging Mechanism and Effect of Accelerated Weathering Conditions on Maxillofacial Silicone Polymers 31
2.4.4 Evaluation of Material Degradation: 33
2.5 Additive Manufacturing **35**
2.5.1 Evolution of CAD/CAM Technology 36
2.5.2 Medical Rapid Prototyping 37
2.5.3 Data Capturing, Data Processing 38
2.5.4 Utilization of Captured Data: 42
2.5.5 The Manufacturing Processes 43
2.5.6 Dental Application of Additive Manufacturing 44
2.5.7 Soft Tissue Facial Prostheses and Additive Manufacturing Technology 47
2.6 Challenges and Summary: **49**
3 AIMS & OBJECTIVES **52**
3.1 Introduction **53**
3.2 The Aim **54**
3.3 The Objectives **54**

4 INVESTIGATION INTO ELASTOMER INFILTRATION DEPTH AND METHODS OF ENHANCING THEIR CHARACTERISTICS . 56

4.1 Introduction 57
4.2 Aim.....58
4.3 Materials.....58
4.4 Methods.....59
4.4.1 Group 1 - Starch Cubes.....59
4.4.2 Group 2 - Plaster Cubes.....64
4.4.3 Group 3 - Starch Cubes and Two Other SPs.....64
4.4.4 Statistical Analysis.....65
4.4.5 Silicone/Starch Ratio by Weight 65
4.4.6 SEM Analysis 65
4.5 Results 65
4.5.1 Infiltration Depth of Sil-25 Inside Starch and Plaster Cubes: 65
4.5.2 Silicone/Starch Ratio by Weight 73
4.5.3 Scanning Electron Microscopy 74
4.6 Discussion 77
4.7 Conclusions.....80

5 THE MECHANICAL PROPERTIES OF THE 3D PRINTED SILICONE POLYMER INFILTRATED STARCH MODELS..... 81

5.1 Introduction 82
5.2 Aim.....83
5.3 Materials and Methods.....83
5.3.1 Silicone Infiltrated Starch Specimens 83
5.3.2 Silicone/Control Specimens:.....87
5.3.3 Statistical Analysis.....89
5.4 Results 89
5.4.1 Tensile Strength and Tear Strength:.....89
5.4.2 Percentage Elongation: 90
5.4.3 Hardness Test: 91
5.5 Discussion 92
5.6 Conclusion:.....95

6 EFFECT OF WEATHERING CONDITIONS ON THE MECHANICAL PROPERTIES OF SILICONE POLYMER INFILTRATED STARCH SAMPLE 96

6.1 Introduction 97
6.2 Aim.....98
6.3 Materials and Methods.....98
6.3.1 Part 1: Exposure to Natural Weathering Conditions 98
6.3.2 Statistical Analysis.....99
6.3.3 Part 2: Exposure to Artificial Weathering Conditions 100
6.4 Results 102
6.4.1 Part 1 - Exposure to Natural Weathering Conditions: 102
6.4.2 Part 2- Exposure to Artificial Weathering Conditions: 106
6.5 Discussion 110
6.6 Conclusion:.....114

7 RETENTION OF SOFT TISSUE PROSTHESES USING MAGNETS 115

7.1 Introduction 116
7.2 Materials and Methods 120
7.2.1 Boss Designs 120
7.2.2 Preparation of the Specimens 122
7.2.3 Data Analysis 125
7.3 Results 125
7.4 Discussion 127
7.5 Conclusion 129

8 SKIN COLOUR MEASUREMENT' 130

8.1 Introduction 131
8.2 Aim 133
8.3 Materials and Methods 133
8.4 Results 134
8.5 Discussion 143
8.6 Conclusion 145

9 SKIN COLOUR REPRODUCTION USING 3D COLOUR PRINTING 146

9.1 Introduction 147
9.2 Aims 148
9.3 Materials and Methods 149
9.3.1 Part One - Testing the Performance of Z-Printer for Colour Reproduction 149
9.3.2 Part two - Colour Correction 152
9.4 Results 155
9.4.1 Part One - Testing the Performance of the Printer for Colour Reproduction 155
9.4.2 Part Two – Colour Correction 165
9.4.3 Performance with Time Spent 168
9.5 Discussion 169
9.6 Conclusion 172

10 EFFECT OF WEATHERING AND EXPOSURE TO UV LIGHT ON THE COLOUR STABILITY OF SILICONE POLYMER INFILTRATED STARCH MODELS 173

10.1 Introduction 174
10.2 Aim 174
10.3 Materials and Methods 174
10.3.1 Part one – Exposure to Accelerated Weathering Conditions 174
10.3.2 Part two – Exposure to Natural "Outdoor" Weathering Conditions 176
10.3.3 Part Three - Exposure to Ambient Room Environments 177
10.4 Results 177
10.4.1 Part one - Exposure to Accelerated Weathering Conditions 177
10.4.2 Part two - Exposure to Natural Weathering Conditions 183

10.4.3 Part three – Exposure to Ambient Room Environments 185
10.5 Discussion 186
10.6 Conclusion 188

11 BIOCOMPATIBILITY OF THE MATERIALS USED FOR PRINTING SOFT TISSUE PROSTHESES' 189

11.1 Introduction 190
11.2 Aim 191
11.3 Materials and Methods 191
11.3.1 Part one - Biocompatibility of the Binders 191
11.3.2 Part two - Biocompatibility of the Starch Powder 193
11.3.3 Part three - Biocompatibility of Manufactured Prosthesis 194
11.4 Results 195
11.4.1 Part one - Biocompatibility of the Binders 195
11.4.2 Part Two – The Starch 203
11.4.3 Part three – Manufactured Prosthesis 207
11.5 Discussion: 211
11.6 Conclusion 214

12 GENERAL DISCUSSION, GENERAL CONCLUSIONS AND RECOMMENDATIONS FOR FUTURE WORK 215

12.1 General Discussion 216
12.2 General conclusions 220
12.3 Recommendations for Future Work 221
12.4 Novelty 223

13 REFERENCES 225

14 APPENDICES 241

14.1 Appendix A 242
14.2 Appendix B 244
14.3 Appendix C 245
14.4 Appendix D 246
14.5 Appendix E 248
14.6 Appendix F 251
14.7 Appendix G 254

LIST OF ABBREVIATIONS

%	percentage
°C	centigrade
CO_2	Carbon dioxide
O_2	Oxygen
µm	micrometer
ΔE	Delta E
L929	Mouse fibroblast cells
p/s	Penicillin and Streptomycin
2D	Two Dimensional
3D	Three Dimensional
3DP	Three Dimensional Printing
AM	Additive Manufacturing
AF	Additive Fabrication
ANOVA	Analysis of Variance
ARP	Additive Rapid Prototyping
ASTM	American Society for Testing Materials
AV	Average
BCS	Bovine Calf Serum
BPS	Buffered Phosphate Saline
CAD	Computer Aided Design
CAM	Computer Aided Manufacture
CIE	International Commission on Illumination
CIELAB	CIE L*a*b* (CIE colour model)
cm	centimetre
CMM	Coordinate Measuring Machine
CT	Computerised Tomography
DICOM	Digital Imaging and Communications in Medicine
DMEM	Dulbecco's Modified Eagle's Medium
EBM	Electron Beam Melting
FDM	Fused Deposition Modelling
EDTA	Ethylene diamine tetra acetic acid
FFF	Fused Filament Fabrication
HSD	honestly significant difference
HTV	High Temperature Vulcanized
i3DP	inkjet 3D printing
LDH	Lactate Dehydrogenase
LM	layered Manufacturing

LOM	Lamination Object Manufacturing
mm	millimetre
mg	milligram
ml	millilitre
MTT	Methylthiazol Tetrazolium
MPa	Mega Pascal
MRI	Magnetic Resonance Imaging
MSP	Maxillofacial Silicone Polymer
N	Newton
NAD	Nicotinamide adenine dinucleotide
PASW	Predictive analytics software
PDMS	Poly-dimethylsiloxane
RGB	Read, Green, Blue
REDOX	Reduction Oxidation
PHMS	Poly-hydromethylsiloxane
ROS	Rat Osteosarcoma
RPM	Revolutions Per Minute
RP	Rapid Prototyping
RTV	Room Temp. Vulcanization
SD	Standard Deviation
SE	Silicone Elastomer
SEM	Scanning Electron Microscopy
SLS	Selective Laser Sintering
SLM	Selective Laser Melting
SP	Silicone Polymer
SPIS	Silicone Polymer Infiltrated Starch
SR	Silicone Rubber
STL	Stereolithography
TCT	Time Compressing Technology
UV	Ultra Violate
VCM	Vinyl chloride monomer
W	Watt
Z-Corp	Z Corporation
Z-Printer	Z Corporation printer

List of Figures

Figure 2-1: Mummy (a) and (b) of an elderly male with artificial eyes inserted in the orbits (dynasty 21-22), (c) artificial eyes used in mummification, (Roberts, 1971a). 6
Figure 2-2: Tycho Brahe (1564-1901), (Roberts, 1971a). 8
Figure 2-3: Ambroise Pare (1510-1590), (Roberts, 1971a). 8
Figure 2-4: Prosthetic reconstruction by Pare (Roberts, 1971a). 9
Figure 2-5: Spectacles used to achieve retention (a) nose prosthesis (b) eye prosthesis, (Roberts, 1971a). 11
Figure 2-6: Clip type design. 12
Figure 2-7: Magnet design. 12
Figure 2-8: Professor Per-Ingvar Brånemark, the inventor of osseointegration. 13
Figure 2-9: Condensation curing system for silicone rubber. 14
Figure 2-10: Addition curing system of silicone rubber. 15
Figure 2-11: Peroxide curing system for poly (dimethylsiloxane). 15
Figure 2-12: Chemical structure of polyurethane. 18
Figure 2-13: Poly vinyl chloride. 18
Figure 2-14: Auricular prosthesis made from a maxillofacial silicone elastomer. 22
Figure 2-15: Eye Prosthesis and the skin around it. 22
Figure 2-16: Nose prosthesis made from a maxillofacial silicone elastomer. 23
Figure 2-17: Q-Sun Xenon test chamber (ASTM G155). 34
Figure 2-18: QUV accelerated test chamber (ASTM G 154). 34
Figure 2-19: CT Image. 39
Figure 2-20: MRI the craniofacial region. 39
Figure 2-21: 3D image for a face scanned by laser scanning. 41
Figure 2-22: Images captured by 3dMD camera. 41
Figure 2-23: An overview of rapid manufacturing technology applied to fabricate soft tissue facial prostheses. 51
Figure 4-1: Z-Corp (Z510) 3D Printer. 60
Figure 4-2: Sensitive digital balance (Navigator). 60
Figure 4-3: Sectional blocks showing the staining due to the dye and identifying the extent of silicone polymer infiltration. 61
Figure 4-4: Travelling Microscope (Mitutoyo TM). 62
Figure 4-5: Measurement field as viewed under the travelling microscope. 62
Figure 4-6: Measurement's lines on a half cube. 62
Figure 4-7: Dental pressure bath. 63
Figure 4-8: Infiltration depth of Sil-25 in mm into starch cubes in air. 66
Figure 4-9: Infiltration depth of Sil-25 in mm into plaster cubes in air. 67
Figure 4-10: Infiltration depth of Sil-25 in mm into starch cubes at 2 bar pressure. 67
Figure 4-11: Infiltration depth of Sil-25 in mm into starch cubes at 3 bar pressure. 68

Figure 4-12: Effect of time and pressure on the infiltration of Sil-25 into starch. 69
Figure 4-13: Infiltration depth of Sil-25 into plaster cubes under 3 bar pressure. 70
Figure 4-14: Comparison of infiltration of Sli-25 into plaster cubes under air and 3 bar pressure. 70
Figure 4-15: Comparison of infiltration depth for starch and plaster for Sil-25 at 3 bar pressure. 71
Figure 4-16: Infiltration of Promax-10 under 3 bar. 72
Figure 4-17: Infiltration of M-3428 under 3 bar. 72
Figure 4-18: Comparison of infiltration depth between Sil-25, M-3428 and Promax-10 at 3 bar. 73
Figure 4-19: Percentages of starch and SP in fully infiltrated blocks. 74
Figure 4-20: SEM starch particles x50. 74
Figure 4-21: SEM starch particles x341. 75
Figure 4-22: SEM for starch infiltrated Sil-25 (x180). 75
Figure 4-23: SEM for starch infiltrated Promax10 (x189). 76
Figure 4-24: SEM for Sil-25 hand mixed with 40% starch by weight (x178). 76
Figure 4-25: SEM for Sil-25 hand mixed samples showing spaces around the starch particles (x707). 77
Figure 5-1: Dumbbell-shaped specimens ASTM-D412/ISO34. 84
Figure 5-2: Tensil tester used for testing tensile strength. 84
Figure 5-3: Trouser-shaped specimens ASTM-D624-07/ISO34. 85
Figure 5-4: Tensile tester used for testing tear strength. 86
Figure 5-5: Hardness Test Specimens ASTM-D1415-06/ISO48. 87
Figure 5-6: Shore Scale Durometer Hardness Tester (England). 87
Figure 5-7: Stainless steel moulds designed according to ASTM specification for production of tensile, tear, hardness and percentage elengation test. 88
Figure 5-8: SP – Sil-25 specimens for tensile, tear, hardness and elongation testing. 88
Figure 5-9: Tensile strength for SP& SPIS specimens. 90
Figure 5-10: Tear strength for SP& SPIS specimens. 90
Figure 5-11: Percentage elongation for SP& SPIS specimens. 91
Figure 5-12: Hardness test Shore A for SP& SPIS specimens. 91
Figure 6-1: Q-Sun Xe-1 Xenon test chamber. 100
Figure 6-2: Tensile strength for SP & SPIS specimens before & after natural weathering. 104
Figure 6-3: Tear strength for SP & SPIS specimens before & after natural weathering. 104
Figure 6-4: Elongation for SP & SPIS specimens before & after natural weathering. 105
Figure 6-5: Hardness for SP & SPIS specimens before & after natural weathering. 106
Figure 6-6: Tensile strength for SP & SPIS specimens before and after 2 & 6 weeks weathering. 108
Figure 6-7: Tear strength for SP & SPIS samples before and after 2 &6 weeks weathering. 109
Figure 6-8: Percentage elongation for SP and SPIS samples before and after 2&6 weeks weathering. 109

Figure 6-9: Hardness test for SP & SPIS specimens before and after 2 & 6 weeks weathering. 110
Figure 7-1: The magnet and the plastic Pole. 117
Figure 7-2: 3D image with the magnet poles in place. 117
Figure 7-3: The stock library nose with the magnet pole in place. 118
Figure 7-4: Blending the library part into the patient's face. 118
Figure 7-5: Fitting the final position of the library part. 119
Figure 7-6: The inner surface of the prostheses with the magnet bosses. 119
Figure 7-7: Boss design 1. 120
Figure 7-8: Boss design 2 121
Figure 7-9: Boss design 3. 121
Figure 7-10: Boss design 4. 121
Figure 7-11: The magnet fixed by pink acrylic into the magnet boss. 122
Figure 7-12: cross sectional illustration of the magnet boss and the magnet retained by self cured acrylic. 123
Figure 7-13: Grips added to the stock implant and the magnet. 123
Figure 7-14: Grip added to the magnet boss. 124
Figure 7-15: Four test designs with grips attached from both sides. 124
Figure 7-16: A steel pin with grips inserted inside the acrylic resin when fill the boss. 125
Figure 7-17: Load at failure for the 4 magnet boss model. 126
Figure 7-18: Comparison of load at failure between the 4 magnet boss models and the stock implants. 127
7-19: Different shapes and sizes of magnet (Technovent, 2012). 128
Figure 8-1: L*a*b* colour model. 131
Figure 8-2: A suntanned arm showing colour differences between the exposed parts, which are browner than the covered parts. 132
Figure 8-3: Body position for skin measurements. 134
Figure 8-4: Average and SD of L*a*b* colour Value for the ethnic groups. 136
Figure 8-5: Comparison for L*a*b* values according to gender between the groups. 136
Figure 8-6: Higher and lower range of L*a*b* values recorded within each ethnic group compared to mean value of each group. 140
Figure 8-7: Vertical (a) and horizontal (b) appearance of the skin colour gamut for Caucasian shade. 140
Figure 8-8: Vertical (a) and horizontal (b) appearance of the skin colour gamut for 141
Figure 8-9: Vertical (a) and horizontal (b) appearance of the skin colour gamut for Middle East shade. 141
Figure 8-10: Vertical cluster distribution for all colour gamuts (a), overlapped with the printer's colour gamut (b). 142
Figure 8-11: Horizontal cluster distribution for all colour gamuts (a), overlapped with the printer's colour gamut (b). 142
Figure 9-1: Minolta spectrophotometer (Model: CM-2600d). 150
Figure 9-2: PerkinElmer "Lambda 25" spectrophotometer. 150
Figure 9-3: Diagram illustrating the position of the sample and the reflectance light. 151
Figure 9-4: The sample compartment and the sample. 151
Figure 9-5: GretagMacbeth colour checker DC chart. 153

Figure 9-6: Skin colour chart. 153
Figure 9-7: Coloured discs for the Asian and Pakistan ethnic group (original rubber and printed starch). 157
Figure 9-8: Coloured discs for the Caribbean and African ethnic group (original rubber and printed starch). 157
Figure 9-9: Coloured discs for the Caucasian ethnic group (original rubber and printed starch). 157
Figure 9-10: Spectral reflectance curve Pakistan 2. 158
Figure 9-11: Spectral reflectance curve African 4. 158
Figure 9-12: Spectral reflectance curve Asian 1. 158
Figure 9-13: Spectral reflectance curve Caribbean 2. 159
Figure 9-14: Spectral curve Caucasian 1. 159
Figure 9-15: Spectral reflectance curve Caucasian 3. 159
Figure 9-16: Coloured discs for the Asian and Pakistan ethnic group (original rubber and printed plaster). 162
Figure 9-17: Coloured discs for Caucasian ethnic group (original rubber and printed plaster). 162
Figure 9-18: Coloured discs for the Caribbean and African ethnic group (original rubber and printed plaster). 162
Figure 9-19: Spectral reflectance curve Caucasian 2. 163
Figure 9-20: Spectral reflectance curve Caucasian 3. 163
Figure 9-21: Spectral reflectance curve Asian 1. 164
Figure 9-22: Spectral reflectance curve Caribbean 1. 164
Figure 9-23: Spectral reflectance curve African 1. 164
Figure 9-24: Spectral reflectance curve African 3. 165
Figure 9-25: Performance of colour reproduction for Printed starch+Z510 profile, printed starch+standard printer profile and cyanoacrylate infiltrated plaster+ standard printer profile. 167
Figure 9-26: Colour reproduction using direct RGB transforms – (a) the original input – (b) the printed output. 167
Figure 9-27: Colour reproduction using Z-Corp printer profile – (a) the original input – (b) the printed output. 167
Figure 9-28: Colour correction by multiple reproduction of the skin colour chart. 168
Figure 9-29: Performance of the colour reproduction system within 20 days. 169
Figure 10-1: SP discs and the printed discs exposed to outdoor weathering. 177
Figure 10-2: L*a*b* values for SR (control) discs before (B) and after (A) 6 weeks weathering time. 179
Figure 10-3: L*a*b* values for SPIS (test) samples before (B) and after (A) 6 weeks weathering time. 179
Figure 10-4: L*a*b* values for SP (control) discs before (B) and after (A) 2 weeks weathering time. 180
Figure 10-5: L*a*b* values for clear SP infiltrated coloured starch (test) samples before (B) and after (A) 2 weeks weathering time. 182
Figure 10-6: L*a*b* colour values for coloured SP infiltrated plain starch (test) 182
Figure 10-7: L*a*b* colour values for SP (control) discs before and after 4 months natural weathering time. 184

Figure 10-8: L*a*b* colour values for SPIS (test) discs before and after 4 months natural weathering time. 184
Figure 10-9: The noses at fabrication (A) and after 18 months (B). 185
Figure 11-1: Alamar Blue assay of ROS cells for the four binders at day 3. 197
Figure 11-2: The Alamar Blue assay of L929 for the four inks at day 3. 198
Figure 11-3: Light microscopy of L929 cell line for control well. 198
Figure 11-4: Light microscopy of L929 cell line at 1.0% cyan binder. 198
Figure 11-5: Light microscopy of L929 cell line at 0.5% magenta binder 199
Figure 11-6: Light microscopy of ROS cell line for the control group. 199
Figure 11-7: Light microscopy of ROS cell lines at 0.1% clear binder. 199
Figure 11-8: Light microscopy of ROS cell lines at 0.1% magenta binder. 200
Figure 11-9: Alamar Blue assay of ROS cells for the four binders at day 5. 200
Figure 11-10: Alamar Blue assay of L929 cells for the four binders at day 5. 201
Figure 11-11: Alamar Blue assay of ROS cells for the four binders at day 7. 201
Figure 11-12: Alamar Blue assay of L929 cells for the four binders at day 7. 202
Figure 11-13: Clear binder 1.0% at day 7. 202
Figure 11-14: Cyan binder 0.5 % few cells were detected at day 7. 203
Figure 11-15: Alamar Blue assay for 3 starch concentrations on ROS at day 3. 204
Figure 11-16: Alamar Blue assay for 3 starch concentrations on L929 at day 3. 204
Figure 11-17: Alamar Blue assay for 3 starch concentrations on ROS at day 5. 205
Figure 11-18: Alamar Blue assay for 3 starch concentrations on L929 at day 5. 205
Figure 11-19: Alamar Blue assay for 3 starch concentrations on ROS at day 7. 206
Figure 11-20: Alamar Blue assay for 3 starch concentrations on L929 at day 7. 206
Figure 11-21: Histological section for the control EpiDerm showing normal tissue architecture. 207
Figure 11-22: Histological section for sample A showing significant disruption of the cellular architecture. 208
Figure 11-23: Histological section for sample B showing no evidence of tissue disruption. 208
Figure 11-24: Optical density obtained from the MTT assay for the test and control samples. 209
Figure 11-25: histogram demonstrating the optical density obtained from the LDH assay for the test and control samples. 210

List of Tables

Table 4-1: Materials used and their manufacture specifications. 59
Table 4-2: Infiltration depth of Sil-25 in mm under different pressures into 20 mm starch and plaster cubes for different times.....66
Table 4-3: Infiltration depth of Promax-10, Sil-25 and M-3428 in mm under 3 bar pressure into 2 cm starch cubes for different time schedule. 72
Table 4-4: Percentage of the starch powder and the silicone polymer in fully infiltrated blocks. 73
Table 5-1: Average and standard deviation values of the printed and control samples. 89
Table 6-1: Types and number of samples (SP & SPIS) used for each test group. 99
Table 6-2: The 24 hour cyclic exposure in Q-Sun test chamber. 101
Table 6-3: Mechanical behaviour of SP and SPIS specimens under natural weathering conditions. 103
Table 7-1: Load (N) at failure for the 2 stock implants. 126
Table 7-2: Load (N) at failure for the 4 magnet boss models. 126
Table 8-1: Numbers of volunteers and their ethnic groups. 135
Table 8-2: Average and SD of L*a*b* colour Value for the ethnic groups. 135
Table 8-3: Average L*a*b* Values for different body parts according to gender for Caucasian skin shade. 137
Table 8-4: Average L*a*b* Values for different body parts according to gender for Middle East skin shade. 138
Table 8-5: Average L*a*b* Values for different body parts according to gender for Chinese skin shade. 139
Table 8-6: Higher and lower range of L*a*b* values recorded within each ethnic group. 139
Table 9-1: L*a*b* values for the original rubber and the printed starch shade guides and there colour difference using directly converted RGB values. 156
Table 9-2: L*a*b* values for the original rubber and the plaster printed and cyanoacrylate infiltrated shade guides and their colour difference using directly converted RGB values. 161
Table 9-3: Effect of infiltration with coloured silicone polymers. 165
Table 9-4: Average ΔE Values for printed starch+Z510 profile, printed starch+ standard printer profile and cyanoacrylate infiltrated plaster+standard printer profile. 166
Table 9-5: Performance of the colour reproduction system within 20 days. 168
Table 10-1: L*a*b* colour values for SP (control) discs before and after 6 weeks weathering time. 178
Table 10-2: L*a*b* colour values for coloured SPIS discs before and after 6 weeks weathering time. 178

Table 10-3: L*a*b* colour values for SP (control) discs before and after 2 weeks weathering time. 180
Table 10-4: L*a*b* colour values for the clear SP infiltrated coloured starch and. coloured SP infiltrated white starch following 2 weeks weathering time. . 181
Table 10-5: L*a*b* colour values for SP (control) discs before and after 4 months natural weathering time. 183
Table 10-6: L*a*b* colour values for SPIS (test) discs before and after 4 months natural weathering time. 183
Table 10-7: L*a*b* values and ΔE value for nose sample at fabrication and after 18 months lifetime. 185
Table 11-1: Alamar Blue assay for the binders on ROS cell lines. 196
Table 11-2: Alamar Blue assay for the binders on L929 cell lines. 197
Table 11-3: Alamar Blue assay for 3 concentrations of starch on ROS & L929 cell lines at days 3, 5, & 7. 203
Table 11-4: MTT assay for test samples SP and the whole compound SP+Starch powder after 12 and 25 hours contact. 209
Table 11-5: LDH assay for test samples SP and the whole compound SP+Starch powder after 12 and 25 hours contact. 210

1 Introduction

Maxillofacial prosthodontics or anaplastology refers to the specialty that designs and manufactures prostheses used to replace part or all of any stomatognathic and/or craniofacial structure. The prostheses provide descriptive evidence of the prosthesis, including location, retention, support, time, materials, and form (glossary, 2005). It is both an art and a science of cosmetics, anatomical and functional reconstruction that is achieved by means of artificial substitutes of head and neck structures that are missing or defective. It is the branch of dentistry that rehabilitates intra and extra-oral deformities (Worthington and Branemark, 1992.). Maxillofacial prostheses are often constructed to correct facial disfiguration or deficiencies. These can be due to surgical ablation of cancer, severe facial trauma or congenital craniofacial anomalies (Khan et al., 1992).

Extensive tissue loss of facial (or body) structures often cannot be corrected surgically because of lack of sufficient donor tissue required for surgical repair and reconstruction. Furthermore, the patient's age and general condition may not permit extensive surgical procedures or allow for the often protracted course of reconstructive surgery, recovery and associated morbidity. Additionally, the final outcome can often be aesthetically and functionally compromised. In such cases, defects may be replaced artificially by the provision of facial prostheses to provide functional rehabilitation and aesthetic repair. Often there is an associated improvement in social, emotional status and overall quality of life (Leonardi et al., 2008). Conventional/traditional methods of prosthesis production are well established and are used even today. These include taking an impression, manufacturing a cast and ultimately, hand crafting a polymeric prosthesis. The provision of prostheses in this manner has provided considerable comfort and support to many patients, and allowed them to continue with normal activities and social life (Markt and Lemon, 2001). Despite the great advantages that this method has achieved, its application has shown some limitations and shortcomings. These are primarily related to the processing strategy, technical expertise required, time, effort, cost and retention problems. Furthermore, there are durability problems due to the material's degradation and colour fade after a relatively short period of servicing and exposure to ultraviolet radiation from sunlight. For these reasons, facial prostheses require renewing and replacement periodically, which is a costly and time-intensive - both burdening patients and prosthodontists alike (Valauri, 1982).

Time compression technologies (TCT) are beginning to be more widely explored to provide customised prostheses. The use of TCT has the potential to offer significant advantages over traditional processing techniques with enormous potential for improving savings in time and cost of production, and consistency in quality. Although the importance of medical rapid prototyping, and three-dimensional (3D) computer aided design and computer aided manufacturing (CAD/CAM) in designing and manufacturing maxillofacial prostheses is acknowledged, its potential is far from being fully explored. These technologies have added considerably to the field of maxillofacial prosthetics. In terms of data capture, more recently the development of non-contact scanning methods including, computed tomography (CT) and magnetic resonance imaging (MRI) – for surface and deep tissue scanning, and laser surface scanning and structured light scanning for data acquisition when information about deep tissues is not required, have revolutionised the way we can assess and plan how prostheses can be designed and manufactured. Non-contact scanning has minimized time and cost, and provided an alternative to capturing accurate surface details for designing maxillofacial prostheses (Kai et al., 2000, Jin Sun et al., 2011, Sun et al., 2011).

However, to date these technologies contributed to the pathway of rapid manufacturing – the use of CT/MRI or surface scanning to produce moulds to manufacture prostheses, or RP manufacturing techniques to make non-colour matched prostheses out of inflexible and unsuitable materials e.g. plastic. A manufacturing method, using rapid prototyping techniques to produce bespoke, lightweight, biocompatible prostheses in a suitable material is now required to complete the process - 3D data acquisition, analyzing data and structure 3D models for maxillofacial prostheses. The 3D rapid manufacturing of models in a more accurate way both in shape and colour would be a significant advance in medical technology (Vannier et al., 1993, Chen et al., 1997a). Time compression technology or medical rapid prototyping is an advanced and new technology used in different high-tech industries, with potential for use in a wide range of applications in the fields of medicine and surgery. However, not all aspects of this technology have been fully explored or applied to the field of maxillofacial reconstruction (Cheah et al., 2003a, Cheah et al., 2003b). Therefore, the challenge will be to determine what technologies can be used to address the problems of data capture, design and manufacture.

The scope of this study was to utilize and evaluate an additive method of manufacturing namely 3D printing, to fabricate soft tissue facial prostheses following the capture of 3D geometric and colour data. More importantly the project will hope to identify:

1) What kind of difficulties could be encountered during the 3D printing process?
2) The capability of the 3D printing to print colour that could match the original skin shade and the degree of colour shift that could occur during the printing process.
3) How to control printing errors and colour deviations.
4) What kind of materials are needed to perform the printing processes to produce a facial prosthesis with the quality required to fulfil the "ideal" properties.
5) Finally, can 3D printing technology replace the traditional methods of manufacture in the area of craniofacial or maxillofacial prostheses in producing more realistic facial structures regarding surface anatomy details, colour matching and durability?

Furthermore, it is hoped this technology could identify additional advantages over traditional methods and could overcome the many shortcomings associated with this method of manufacture. Also, it is hoped that this application could render facial models with higher accuracy, lower cost, shorter manufacturing time, and easier storage, which would be more convenient for the patient and the prosthodontist.

2 Literature Review

2.1 Maxillofacial Prostheses – Past and Present Trends

Although official documentation is scant, it is believed that maxillofacial prostheses in one form and another are as old as modern "mankind". Excavations of tombs within the Egyptian dynasty (1613-2494 BC) have provided evidence of some facial prostheses: artificial eyes, ears and noses have been found in Egyptian mummies. Eyes made from precious stones, earthenware, enamelled bronze, copper, and gold within eye sockets (Roberts, 1971b). However, it is thought that these may have been inserted after death to fulfil the religious demands and beliefs of that era (Moore, 1994, McKinstry, 1983), (Figure 2-1). Additionally there is no formal documentation to indicate the presence of facial rehabilitation.

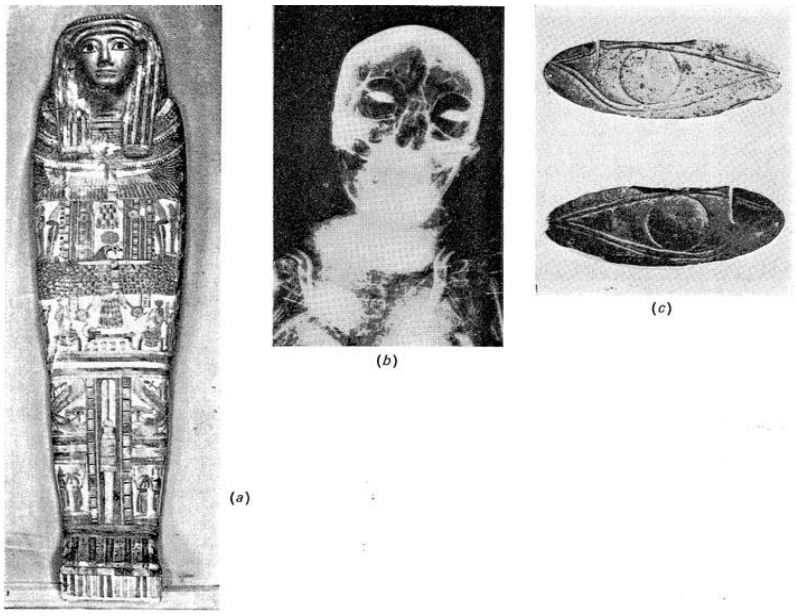

Figure 2-1: Mummy (a) and (b) of an elderly male with artificial eyes inserted in the orbits (dynasty 21-22), (c) artificial eyes used in mummification, (Roberts, 1971a).

The only materials that could have been used would have been limited to animal skin, clay and wood. This would have severely limited what could have been provided as these materials are degradable. As a result any prostheses made from such materials would undoubtedly have degraded throughout time in their final resting place. Indeed the only early evidence to suggest these methods were explored is found in a scripture from the Egyptian era (Edwin Smith, Papyrus). A summarising copy of the ancient Egyptian scripture from 16th century BC has been translated and published in a modern medical test (Wilkins 1964). This document details the medical and surgical cases of battlefield injuries, including the head, and face, and their management.

Early prosthetic replacements of acquired maxillofacial defects date back to the sixteen century and used different materials and methods (Chalian and Barnett, 1972). Some of the first reports were by Tycho Brahe (1546-1601) (Fig. 2-2) and Ambroise Pare (1510-1590) (Fig 2-3). There are many documented incidents incorporating the use of prostheses – one such report from the life history of the Danish astronomer Tycho Brahe (1546-1601) highlights a reconstructed nose (Bulbulian, 1954b). Tycho and his enemy arranged to meet for a duel in the dead of night. It was entirely dark and they found each other only by ear. After a fierce fight, Tycho lost his nose after it came in the way of his opponent's sword. It was difficult for Tycho to go through life without his nose so he decided to make one for himself out of gold and silver and using a paste to keep it attached. Interestingly, after his enemies had seen his nose cemented in place, they said it looked better than the old one (Roberts, 1971a). Despite this interesting account of an artificial nose from the life of Tycho Brahe, Ambroise Pare (1510-1590) can well be considered the father of facial prostheses. His work and fabrication of these appliances is considered the foundation stone of modern anaplastology. He established the first base line principles for prosthetic reconstruction of facial prostheses by describing the indications and appliances used (Gibson, 1955), (Figure 2-3, Figure 2-4).

As time has progressed, ever more adventurous cases have been undertaken. Pierre Facular (1678-1761) replaced part of the lower jaw of a soldier with a cast silver mask painted with oil paint in order to achieve the same skin colour (Beumer et al., 1996).

Figure 2-2: Tycho Brahe (1564-1901), (Roberts, 1971a).

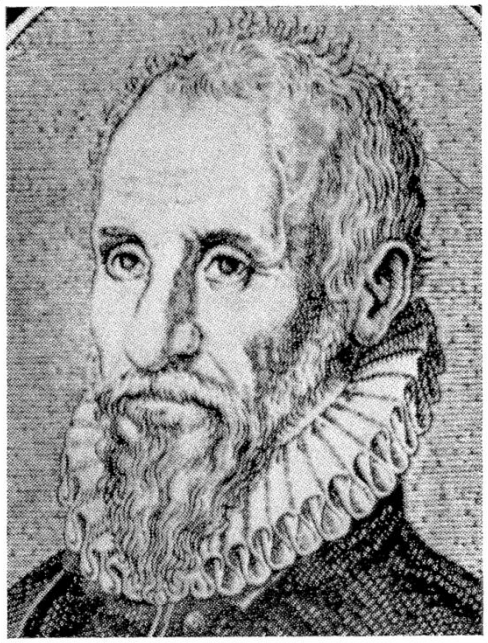

Figure 2-3: Ambroise Pare (1510-1590), (Roberts, 1971a).

Between 1800 and 1900, William Morton (1819), Kingsley (1880) and Claude Martin (1889) all attempted to replace nasal defects by using ceramic material (Beder, 1974). In 1913, attempts were made to produce nasal and ocular prostheses from vulcanite rubber.

Other materials including gelatin glycerin have also been used to produce facial prostheses, but practically, they showed high levels of degradation and short service life.

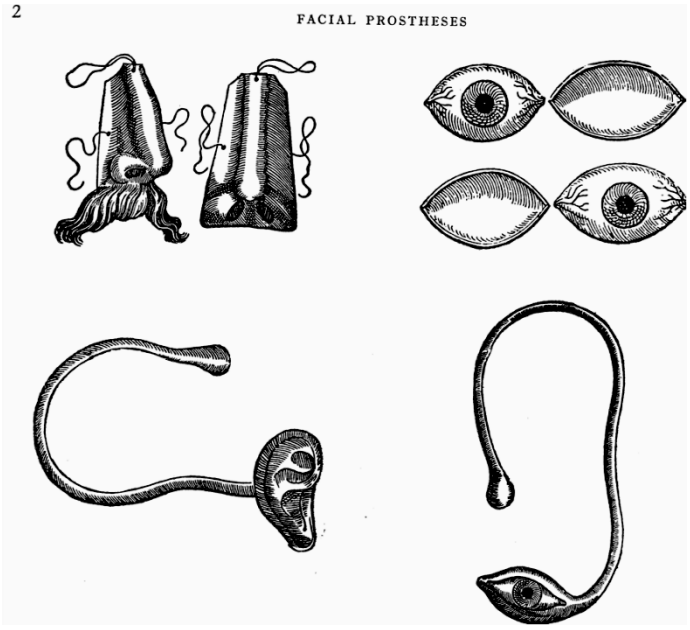

Figure 2-4: Prosthetic reconstruction by Pare (Roberts, 1971a).

However, this transition from hard metallic materials, to softer and more rubber like materials was a huge step and enabled the production of more "life like" prostheses (Beumer et al., 1996). In the 1930's vulcanite rubber was replaced by acrylic resin in fabricating maxillofacial prostheses - Tylman used soft vinyl copolymer for the replacement of soft facial parts. In the mean time Brasier used acrylic stain as an intrinsic colorant and oil colour mixed with acrylic resin monomer as extrinsic colorant (Beumer et al., 1996). In 1945 soft and flexible maxillofacial prostheses were described by Bulbulian (Bulbulian, 1954a). Later, between 1960 and 1970, various kinds of elastomers were introduced. Barnhart, in 1960, introduced a special silicone rubber for construction of facial prostheses; this was the major revolution in the history of maxillofacial prostheses (Barnhart, 1960, Udagama and Drane, 1982). From 1970 to 1990, different authors described many types of maxillofacial elastomers. Gonzalez described polyurethane for maxillofacial prostheses (Gonzalez, 1978). Lontz described the use of modified polysiloxane elastomers (Lontz, 1990). Lewis and Castleberry used

phenylene compound to fabricate facial prostheses (Lewis and Castleberry, 1980). By the 1990s polyphosphazenes, a class of metallo-organic polymers, has also been investigated for their suitability for facial prostheses by Lawrence Gettleman (Khan et al., 1992, Beumer et al., 1996).

Recently however, prosthetic rehabilitation has been considered as an alternative to surgery in cases of severe functional and aesthetic defects for extensive maxillofacial tissue lost as a result of cancer and its surgical resection, trauma and congenital abnormalities (Leonardi et al., 2008). Facial reconstruction is not only beneficial for re-establishing patient's aesthetics or their functional rehabilitation or speech correction. It is also notable for supporting the patient's mental health and helping them to re-engage the society again, the outcome of which is directly dependent on the level of satisfaction with the prosthetic rehabilitation (Goiato et al., 2009). Maxillofacial prostheses are considered by many the primary choice of treatment for functional rehabilitation, aesthetic reconstruction and rebuilding the patient's confidence. It provides comfort and support to the patient on many levels including socially and psychologically. Maxillofacial prosthetic patients usually encounter social, psychological and economic challenges, which vary from fear of not being accepted in society, and being stigmatized as an outcast. This can often lead to long-term problem and is a source of severe depression and rejection of life (Sykes et al., 1972).

Studies have shown overall improvements in the psychological condition of the patients after the provision of maxillofacial prostheses (Lowental and Sela, 1982). Rehabilitation provides patient satisfaction and well-being in the family and society (Goiato et al., 2009). Maxillofacial prostheses can be a permanent or temporary substitute, depending on the size of the facial defect, the patient's age and general health, and the progression/stasis of the condition (Valauri, 1982). Furthermore, facial prostheses retained by implants have demonstrated significantly higher levels of contentment and acceptance than adhesive retained prostheses in terms of ease of use, and retention with different daytime activities (Chang et al., 2005).

However, maxillofacial prosthetic aids and devices produced for these patients are considered less than optimal, with a basic problem of insufficient retention and stability of the prosthesis. Several methods of retention of soft facial prostheses can be applied according to the size and morphology of the defect, presence or absence of mechanical retention means and undercuts used to engage the prosthesis. The later

method of retention may traumatise the soft tissue at the contact areas within the undercuts. The prostheses can also be retained mechanically in rare cases by extending the components of the prostheses to attach to the patient's eyeglasses or denture as seen in Figure 2-5.

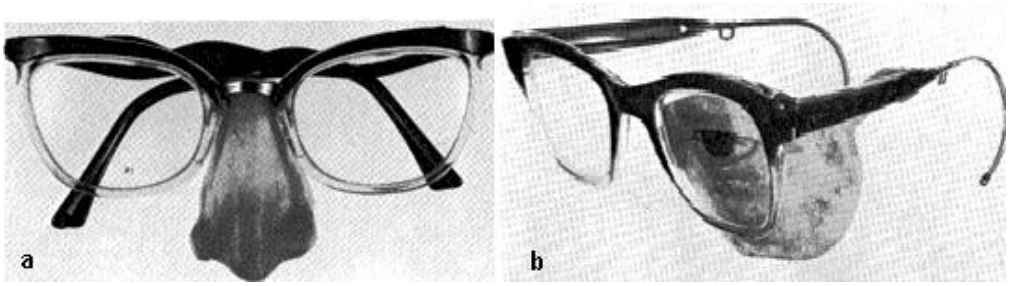

Figure 2-5: Spectacles used to achieve retention (a) nose prosthesis (b) eye prosthesis, (Roberts, 1971a).

Another method of holding the prosthesis is by using medical grade adhesives added to the margins of the prosthesis. It could be either in the form of a liquid, spray emulsion, or double-sided tape, which is the most commonly used adhesive. It has the advantages of easy application and removal from the prostheses (Chen et al., 1981). Each method has advantages and limitations; bio-adhesives has been widely used for retention of extraoral prostheses (Ismail and Zaki, 1990). However, a major limitation is achieving optimal adhesion of the prostheses for long periods of time. Another disadvantage of this method of retention is the interaction of the adhesive material with the patient's skin – perspiration, movement, sensitivity/allergy to the adhesive material. Furthermore, there is the issue of cleaning and removal of the adhesive material from the prostheses and the skin on a daily bases, which increases the possibility of tearing the prosthetic margin during maintenance (Kiat-amnuay et al., 2000). Another critical problem relating to adhesive retained prostheses, and in fact prostheses in general, is colour fade. In addition to these problems, there are also concerns with alteration to the material consistency and properties with an increase in potential damage to the prosthesis (Chen et al., 1981).

The second major evolution came in 1979 – this was the use of osseointegrated implants with bar/clips and magnets to retain soft tissue facial prostheses, as shown in

Figures 2-6 and 2-7 respectively. The technique was based on the initial concept by Branemark (Figure 2-8) and involves inserting the implant into the facial bones to act as anchors in order to hold different types of prostheses. Parel et al (1986), considered the use of implants for retention of facial prostheses as the most important event in the last 25 years in field of maxillofacial prosthetic (Parel et al., 1986). This was primarily because implant retained prostheses could overcome a lot of retention problems with the limitations and disadvantages of medical-grade skin adhesives.

Figure 2-6: Clip type design.
http://www.anaplastology-clinic.com/home/implant-retention

`

Figure 2-7: Magnet design.

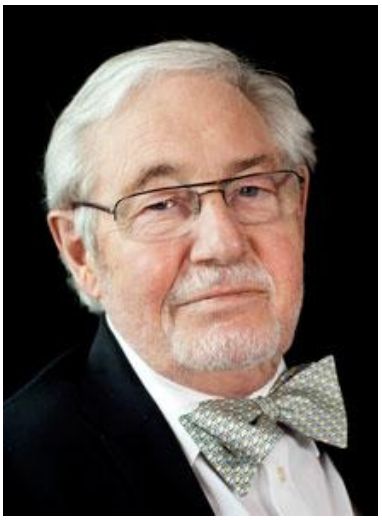

Figure 2-8: Professor Per-Ingvar Brånemark, the inventor of osseointegration.
http://www.informatik.gu.se/digitalAssets/1314/1314015_branemark.jpg

2.2 Current Facial Prostheses

2.2.1 Materials Available

There is no single material to date that fulfils all the ideal properties or requirements of maxillofacial prostheses. A wide variety of materials, with a range of characteristics and properties have been used in maxillofacial prosthetic reconstruction. They have different physical properties, ranging from hard and inflexible but durable, to soft and flexible but fragile. These include alloys, ceramics, hard and soft polymers and elastomers. The most widely used materials for fabrication of maxillofacial prostheses are:

2.2.1.1 Silicone Polymers

Poly-dimethylsiloxane (PDMS), often referred to simply as silicone, is an important class of organo-silicon synthetic material based on molecular chains of alternate silicon and oxygen atoms. It is a combination of organic and inorganic components (Rahimi, 2004). It was first applied to maxillofacial prosthetics by Barnhart in the 1960's (Barnhart, 1960, Beumer et al., 1996). To date, it is the most widely used maxillofacial material for extra oral prosthetic devices. This is because its physical properties make it suitable for use when adaptability and accommodation of soft tissue movement is

required during contact between the device and the patient's soft tissues. The material can also be manufactured so that it has translucent properties and enhances the aesthetic outcomes of the prosthesis.

There are several types of PDMS curing reactions. The condensation type of reaction PDMS polymer is terminated with hydroxyl groups and it is of adequate molar mass to achieve sufficient degree of viscosity, whilst the crosslinking agent is an oligomeric poly (hydromethylsiloxane) (PHMS). The process of crosslinking takes place by the reaction of the Si-H and Si-OH groups. The reaction is accompanied by hydrogen release and is accelerated either by an amine or tin octate (Saunders, 1985, Taylor et al., 2003). The process occurs at room temperature, and is called room temperature vulcanized (RTV). With this silicone rubber there are two systems for this type of curing reaction occur; one-compound and two-compound systems. In the first, the catalyst and the cross-linking agents are incorporated within the base material during manufacturing , whereas with the two-compound system both the catalyst and the base are added from separate components and mixed together just before use, as demonstrated in Figure 2-9. This reaction leaves a fraction of the unbounded portion of PHMS to PDMS which can contribute to an increased free volume. This excess of PHMS together with the low molecular mass PDMS plasticiser can leach from the bound compound and subsequently lead to an increased free volume and microscopic permeability at the surface. This may lead to problems clinically including the potential for microbial/bacterial or fungal ingrowths within the silicone elastomer (Verran and Maryan, 1997b). It may also contribute to colour fade and deterioration of the prosthesis soon after being in service. However, these compounds are considered very biocompatible (Verran and Maryan, 1997a).

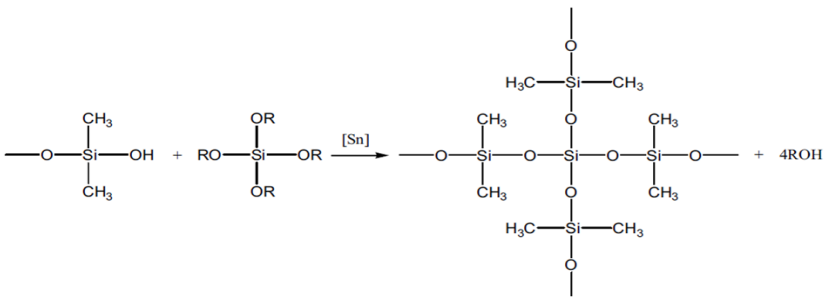

Figure 2-9: Condensation curing system for silicone rubber.

Another type of PDMS curing reaction is the additive reaction. This type of reaction also takes place at room temperature. Cross linking takes place by attachment of Si-H group to double bonds. Platinum or palladium could be used as the catalyst (Figure 2-10).

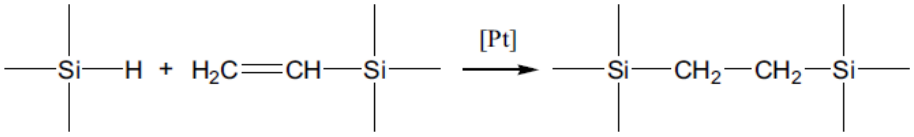

Figure 2-10: Addition curing system of silicone rubber.

A further method of curing is the peroxide curing method, used with high temperature vulcanized (HTV) silicone polymers. This follows a free radical curing mechanism and requires a certain amount of heat for initiation. The curing reaction by organic peroxides free radicals is shown in Figure 2-11.

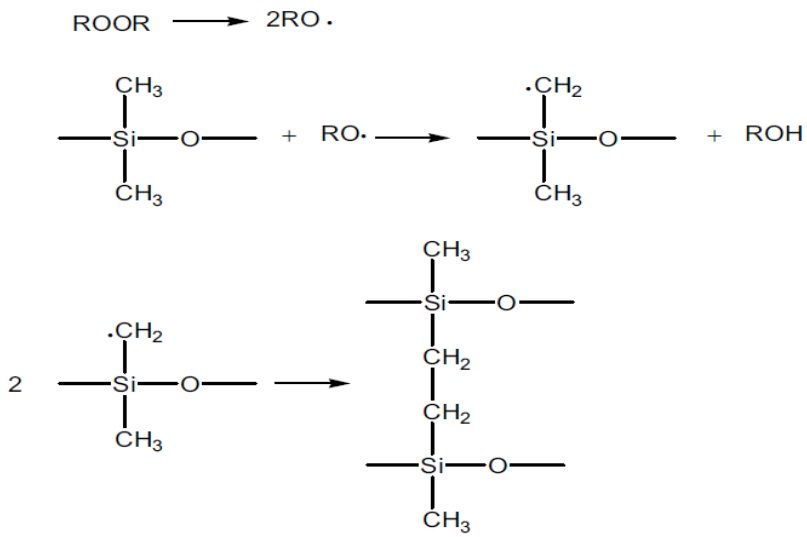

Figure 2-11: Peroxide curing system for poly (dimethylsiloxane).

Finally there is the irradiation curing system, where cross-linking is induced by radiation including gamma ray or high energy electron beam (Morton M, 1987). The length of the polymer chain within the silicone determines the viscosity of the material, as does the addition of fillers or other compounds. Other additives can

incorporated into the compound such as colorants, antioxidants and crosslinking agents, in order to transfer the material from a liquid to a rubber during processing.

The cross links between the long polymer chains create a strong inter-linking between the components, that can't be separated easily and provide the silicone with resistance to heat and degradation during exposure to ultraviolet light (Beder, 1974).

The mechanical behaviour of silicone polymers are strongly correlated to three main factors:

1) The molecular weight distribution - blending both long and short chains of the same polymer creates a broader bimodal network which combines mechanical properties of high tensile strength, tear resistance and elasticity (Shah and Winter, 1996).
2) Incorporation of a hydrophilic surface treated silica fillers (with dimethyl silyl or trimethyl silyl groups) into the base polymer allows the polymer chains to uncoil and slide past neighbouring filler particles. This increases the crosslinking between neighbouring PDMS chains, and thus provides the elastomer with a higher strength under deformation (Raymond, 1977).
3) Degree of crosslinking - elastomeric chains are essential in order to optimise tensile and tear strength. The higher the crosslinking, the harder, more brittle elastomeric material is produced, whereas low cross-link density provides lower tensile and tear strength (Raymond, 1977).

The two major groups of poly-dimethylsiloxane silicone elastomers used for fabrication of maxillofacial prostheses are:

1) Room-temperature vulcanizing (RTV) silicones – these include a filler of diatomaceous earth particles and are composed of two main parts; a catalyst (stannous octate) and a cross linking agent, ortho-alkyl silicate. This group includes a variety of materials namely Silastic 382 and 399. They are inert, colour stable viscous polymers. MDX4-4210 is also widely used in the manufacture of maxillofacial prostheses (Beumer et al., 1996). These materials are translucent so they can be blended with suitable earth pigments to replicate the patient's basic skin colour, with higher colour stability. The material is biologically inert and processed easily. Furthermore, it can retain physical and mechanical properties at a wide range of temperatures. The main disadvantage of these materials is poor edge strength (Maller et al., 2010).

2) Heat-temperature vulcanizing (HTV) is used when higher tear strength is required. Tear strength is determined by the type and nature of the cross linking in the catalyst. Different heat vulcanized silicone elastomers exist and include: Silastic 370, 372, 373, 4-4514, and 4-4515. They are highly viscous white/opaque materials with a Dichlorobenzyl peroxide/platinum salt catalyst. Different amounts of silica fillers are added according to the degree of hardness, tensile and tear strength that is required. The material has thermal and colour stability but it lacks flexibility and restricts movement. It has poor aesthetic output because the material is opaque and many consider it to have an artificial or lifeless appearance. A new generation of (HTV) are Q7-4635, Q7-4650, Q7-4735, SE-4534U and these have shown improved mechanical properties compared to MDX4-4210 and MDX4-4514 RTV Silicone (Beumer et al., 1996, Lontz, 1990).

2.2.1.2 Polyurethane:

Polyurethane polymers are formed by combining two functional groups. One of these groups contains two or more isocyanate functional groups and the other contains two or more hydroxyl groups (Figure 2-12). It is a soft polymer and has elastic properties with sufficient strength to allow the production of thin and soft margins, therefore increasing its potential to "blend" in with surrounding tissue and avoiding irritation to the movable soft tissues around the margin. However polyurethane has several disadvantages. Isocyanate is hydrophilic and absorbs moisture, which could lead to the formation of gas bubbles, which affects the characteristics of the material. This property makes it difficult to work with in a humid environment. Another disadvantage of these compounds is the relatively quick loss of the plasticiser, which leads to rapid discolouration and loss of strength of the prostheses. The material is not colour stable under ultraviolet light and with a relatively rapid surface degradation after cleaning and removal of the adhesive from the prostheses, means that it is not ideal for this purpose (Beumer et al., 1996, Gonzalez, 1978).

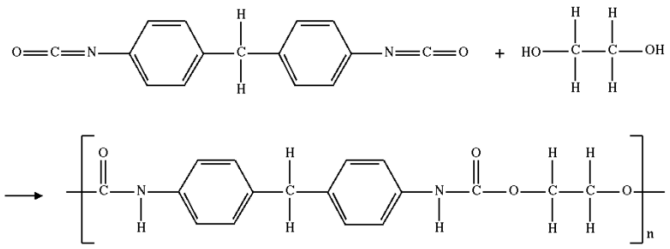

Figure 2-12: Chemical structure of polyurethane.

2.2.1.3 Polyvinylchloride and co-polymers:

Polyvinyl chloride is produced by polymerization of the monomer vinyl chloride (VCM), as shown in Figure 2-13. They have some desirable properties, especially when used in combination with 5-20% vinylacetate, which acts as a plasticiser. The reactant in these elastomer is a hydroxyl terminated polymer and isocyanate terminating catalyst. Again, a wide variation in properties can be obtained by altering the proportion of the reactant and catalyst. These properties include increased flexibility and adaptability to both intrinsic and extrinsic colouration. However, the disadvantages of this material is the early loss of plasticisers, resulting in colour loss, increased permeability, easy tearing of the prosthetic edges and absorption of body secretion. These factors can result in rapid degradation of the physical properties of the material (Maller et al., 2010).

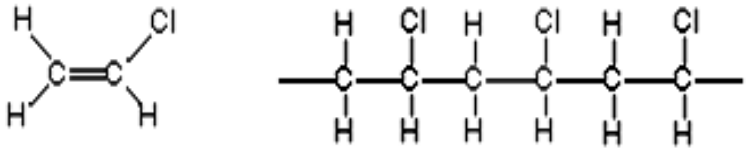

Figure 2-13: Poly vinyl chloride.

2.2.1.4 Acrylic resin and acrylic co-polymer:

The use of acrylic is limited to those defects where limited movement occurs in the area of the defect. This is because it is a hard material and can cause physical irritation to the tissue bed if there is excessive movement around the prosthesis. These include intra-oral obturators and ophthalmic prostheses. However it has the advantage of being easy to

process, produce very thin margins, and can be coloured to achieve skin colour easily. It also has a good strength and a long "shelf life". Different monomer viscosities and infiltrate powder granulate sizes can be used to alter the characteristics of the finished prosthesis, however the ingredients are usually standardised for this process in order to achieve predictable results.

Although acrylic co-polymer has some acceptable properties i.e. soft and flexible, it has a major disadvantage of poor marginal adaptation and poor durability on exposure to outdoors weathering. It also has a poor surface texture, which can facilitate stain collection (Khindria et al., 2009).

2.2.2 Fabrication

With the development of soft and flexible materials and their application by maxillofacial prosthodontists/anaplastologists, the basic technique of fabrication has been modified in the past to follow the processing demands of these materials. Different methods of fabrication of facial prostheses have been described by different authors based on type of the facial prostheses and thus, the particular demand for each specific prosthesis (Wang, 1999, Marion et al., 1997, Craig et al., 1978, Coward et al., 1999, Al Mardini et al., 2005). The steps of making a prosthesis can be summarised as follows:

1) Taking an accurate impression for the area requiring a prosthesis and obtaining fine detail of the affected area. This is performed by selecting the suitable impression material according to site and size of the defect, and presence or absence of any undercuts in the area of the defect. Many impression materials are available, ranging between soft/flexible to hard/rigid. Among these materials are hydrocolloid alginates, elastic silicone polymer impression materials, and rigid materials like plaster of Paris. Although plaster of Paris can achieve excellent details of the defect it has disadvantages and limitations in the presence of undercuts. Plaster of Paris can't be used in the presence of severe undercuts as fracture of the impression material will occur on removal and/or damage to the soft tissue might occur. Therefore, it is preferable to use flexible or elastic material in cases of moderate to severe undercuts. Sometimes a combination of both soft and rigid impression materials gives an optimal result. The area of the undercut can be recorded first with a soft elastic/hydrocolloid material, whilst any area of defect or impression that required re-

enforcement could be reinforced by a rigid jacket of plaster of Paris. Furthermore, the impression can be removed from the undercut without fracture of the material or causing injury to the soft tissues.

Pre-surgical impressions are also an important step in saving the details of the diseased area that is going to be replaced following resection, and again, a combination of impression techniques may be used.

2) An accurate master cast is obtained from the impression. It should be remembered that the impression is the negative "picture" of the defect; this is then converted to an accurate "positive" cast for the defect by pouring up the impression with stone.
3) With this cast the maxillofacial technician builds up the lost structure from wax or clay. The wax model is carved until the natural morphological details of the defect are obtained. The technician bases this design on information obtained from the patient. This can be detail from the pre-operative condition i.e. mould or photos, or from characteristics obtained from contralateral structure, if available i.e. ear or eye. Furthermore, information can be obtained from one of the patient's relatives that have some similarity in their facial features. This relative may have features that could be used as a reference (Beumer et al., 1996). More modern techniques include computer software packages including image-editing software such as Adobe Photoshop or CAD software such as Mimics or Freeform to help in building and carving the prostheses. For fabrication of complex prosthesis, several methods could be applied when a pre-surgical cast is not available.
4) Checking the wax or clay model of the missing part on the patient to check the details and inspect the margin of the model for any gaps or space between the model and the surrounding tissue. Special attention must be paid to the marginal adaptation and fit for better aesthetic results.
5) Transferring the model into the final material - The wax pattern is returned to the master cast and conventional flasking methods are undertaken using dental stone. The wax is then removed and the cast is lubricated with a suitable lubricant/separator.
6) A suitable maxillofacial silicone rubber is then selected and mixed according to the manufacturer's directions. Colouring agents are then added to the mixture and checked against the patient's skin colour until the appropriate colour will be achieved

– this will produce the base colour of the patient's skin. The silicone rubber is then applied to the mould and the flasking process completed.

7) After setting of the silicone rubber within the cast the facial prosthesis is recovered from the mould, trimmed and extrinsic colorant added if necessary. The prosthesis can then be delivered to the patient after giving carful instruction about using adhesives and/or other retentive features to position the prostheses, and instruction for cleaning and maintenance.

2.2.3 Requirements:

A meeting of the American Academy of Maxillofacial Prosthetics, held in Washington in 1966, stated that the materials used in maxillofacial reconstruction should be biocompatible and safe so they can be used in contact with human skin without causing any irritation (Report, 1966). This meeting also confirmed that it should resemble human skin in texture and colour and be flexible enough to show similar properties and mimic the natural feeling of skin and human tissues, as shown in Figures 2-14, 2-15 and 2-16. The material should also be translucent enough so it can show the vitality of natural tissues around the prosthesis. Durability and environmental resistance (including sunlight, hot and cold temperatures), plus resistance to body secretion and wettability were also considered to be principal characteristics of these materials. Additionally, easy processing, weight and thermal conductivity and finally the hygienic properties, such as ease of cleaning without damage or changes to the basic properties of the materials, were also discussed by the authors at the workshop and focused on in this meeting.

Figure 2-14: Auricular prosthesis made from a maxillofacial silicone elastomer.
http://www.colombiasaludybelleza.com/images/articulos/012a.jpg

Figure 2-15: Eye Prosthesis and the skin around it.
http://farm7.static.flickr.com/6232/6252788772_fb77d318f5.jpg

Figure 2-16: Nose prosthesis made from a maxillofacial silicone elastomer.
http://a.abcnews.com/images/GMA/ht_glasses_051129_ssh.jpg

There appears to be some consensus about the properties of the materials used, and Andres et al (1992) characterized the properties of the ideal maxillofacial materials as follow;

1) Materials used for maxillofacial prostheses must match the human tissue in colour and anatomical and morphological details. In other words it must be able to provide human skin colour and morphological details of the maxillofacial soft and hard tissues and match these tissues in terms of consistency of detail. For the maxillofacial region, different consistencies of these materials are required according to the type of tissue that are being replaced, and whether it is a soft tissue replacement or a hard tissue replacement or combination of both tissues. Furthermore it must be highly elastic with high edge strength so it can resist tearing at the periphery, and it must be soft and comfortable to the surrounding tissues in order to permit tissue movement without irritation to the areas of contact with the surrounding tissues. It should also be lightweight.
2) The material must be highly compatible with human tissue; it must not be toxic, cause allergic reaction or sensitivity/irritation. It should be hygienic and easily cleaned and maintained. It should also be permeable so that moisture levels are kept

to a minimum and have no odour (or at least no bad odours) released from it. It must resist bacterial growth and not elicit microbial infections.

3) The material must not show adhesion problems with human tissue when aided by adhesive materials, or any other means of adhesion or mechanical methods of attachment. The adhesive used must be removed from the material and from the skin easily without irritating the skin or causing damage to the prosthesis.
4) The material must be durable and strong so it can hold mechanical attachment aids without displacement.
5) The material must be able to accept both extrinsic and intrinsic colouring agents without releasing them during service and it must show the same characteristics such as vitality and translucency as human tissue without an outer surface glaze.
6) The material should demonstrate easy processing regarding its polymerization and other moulding processes, and it must be repairable, relinable, and able to maintain or modify the marginal integrity of the model.
7) The material should be able to produce durable models with high resistance to outdoor and other deteriorating factors during service in order to last for at least one year with the above-mentioned properties and characteristics (Andres et al., 1992).

Of course, it should be remembered that these are ideal properties and that not all of these are achieved on every occasion.

Others have also described "ideal" properties. Lewis and Castleberry (1980) characterized the "ideal" properties of maxillofacial materials into three groups. The material should possess the following properties:

1) Low viscosity, long working time, able to accept colorations, low processing temperature and it should be moulded easily.
2) Show optimal mechanical properties including tensile strength, tear strength and percentage of elongation. It must also show enough hardness to resist environmental factors, outdoor weathering and chemicals, stains, and body secretions.
3) The material must be inert, non-toxic, not cause any kind of sensitivity or allergy to the patient, and must be hygienic, not heavy in weight and not expensive (Lewis and Castleberry, 1980).

Although considerable advances have been made in both treatment modalities for patients suffering from facial disfiguration and materials used in maxillofacial reconstruction, there is still no "ideal" material for facial prostheses. Despite the

improvements that have been made in recent years, significant work in this aspect is still required in order to achieve the ideal material (Moore, 1994).

2.2.4 Limitations of Current Prostheses

Conventional methods for producing facial prostheses have several limitations. Firstly, they are manually grafted prosthesis and require a high degree of technical skill. Secondly, they are relatively expensive and time consuming to produce. A facial prosthesis takes many complex steps to complete - as described previously. These are time consuming and expensive in both time and materials (Bulbulian, 1973). Furthermore, these prostheses do not last indefinitely, and once delivered to the patient undergo deterioration. These changes occur with the colour and consistency of the prostheses. This can in turn create problems in terms of colour matching the patient's skin to the prostheses, and for this reason the prosthetic must be changed regularly. Once fitted the facial prostheses will be in contact with human skin/mucosa for a long period of time and my absorb skin/oral secretion including sweat, sebaceous secretions and saliva which may lead to degradation of the material (Lewis and Castleberry, 1980). Indeed it can be argued that the characteristics of the prosthesis – colour, consistency, mechanical properties, are only optimal at the time of delivery and only ever decrease from that point onwards.

The limited service of maxillofacial prostheses is usually a consequence of deterioration of the elastomer and colour change under environmental exposure to sunlight and change in temperature, humidity and hand contact during cleaning and adhesive use on a daily basis (Chen et al., 1981, Hanson et al., 1983).

2.3 Material Properties

Maxillofacial silicone elastomers are used to achieve functional and aesthetic characteristics while in service. The durability of facial prostheses is dependent on the mechanical and physical properties of the materials used in the fabrication of these prostheses.

2.3.1 The Mechanical Properties

Silicone rubber is the most widely used material in maxillofacial prostheses because of its mechanical properties including ease of processing, biocompatibility and chemical inertness (Lai et al., 2002). However its mechanical properties do not fulfill the ideal requirements (Hatamleh and Watts, 2010c). Variations in mechanical properties for different maxillofacial elastomers are attributed to different manufacturing formulations; including chain length of the polymers, types, amount and size of fillers, degree of crosslinking and molecular weight (Aziz et al., 2003, Lai et al., 2002).

Variation in crosslinker/elastomer ratio can significantly affect the mechanical properties of these materials and in turn can have a great impact on their "shelf life" after being delivered to the patient. Clinically, this can have consequences including colonization with micro-organisms - including Candida albicans (Taylor et al., 2003).

Maxillofacial material must be tested for different mechanical properties in order to fulfil the criteria of "ideal material" and the requirement of the most suitable and durable material. These tests include:

1) Hardness test: Hardness is defined as the resistance to indentation under specific conditions. The hardness of an elastomer is the result of two related properties; the inherent, and the processed hardness. This is based on the chemical structure of the material. Each elastomer has its own inherent hardness, which can be modified by vulcanisation - the hardness of the processed moulded elastomer is determined by the degree of adjusted inherent cross-linking within the material. Hardness test is related to the material softness and flexibility and shows how soft and pliable the material is. It can also be used to see how close to the consistency/properties of human's soft tissues they are. The ideal hardness is that which mimics the properties of the lost tissue (Lewis and Castleberry, 1980).
2) Ultimate elongation determines the maximum flexibility of the material – elongation values are essential to assess the material's ability to accommodate the movement of the adjacent soft tissue during function. It also determines material's resistance to rupture during service and maintenance (Waters et al., 1997).
3) Tensile strength is an indication of the material's overall strength in general and its resistance to "pulling" forces. Consequently this characteristic will contribute to the

ability of the maxillofacial prostheses to overcome general wear and tear and weathering over time (Waters et al., 1997).

4) Tear strength is a material's ability to resist transverse forces and relates to the marginal strength and resistance to shearing forces during service. For an optimal and successful aesthetic outcome marginal integrity and accurate marginal adaptation is necessary in order to blend the facial prosthesis to the patient's own tissue. Very thin edges can appear merged with the patient's own tissues if they are thin enough. However, it results in a very fragile margin that may rupture/tear easily during service. Therefore high tear strength is required for better marginal integrity (Aziz et al., 2003). Although softness and flexibility of soft tissue prostheses are required, high strength is also an essential property for life extension and durability of these models (Dootz et al., 1994). Tear strength is an important characteristic of prostheses durability, especially when the method of retention involves the use of adhesives. Low tear strength would increase the possibility of tearing during removal of the prosthesis for maintenance and/or removal of adhesive from the margin for the purpose of cleaning. However, if the prostheses are retained by implants, tear strength is not as essential as the mechanism of retention would not involve excessive pressure being exerted on the margins of the prostheses during insertion and removal.

In 1971, Roberts evaluated the physical properties of different maxillofacial elastomers and he reported the following range of measurements:

1) Hardness of maxillofacial silicone ranged between 45 and 55 indentation hardness (Shore-A Durometer) test.
2) Tensile strength varied between 2.1- 6.9 MPa
3) Percentage of elongation ranged between 100% and 350%.
4) Tear energy was around 17.51 N/mm, (Roberts, 1971b).

Furthermore a table presenting the mechanical data for a range of maxillofacial elastomers is attached to this thesis[1].

[1] Table for the mechanical properties for a range of maxillofacial silicone polymers is attached to appendix G.

2.3.2 Optical Properties

The ideal maxillofacial materials must accept and retain both intrinsic and extrinsic coloration without changes in the general appearance of the prostheses and preserving the initial mechanical properties (Lewis and Castleberry, 1980). Several methods of colouring and tinting have been developed for these materials. These include intrinsic and extrinsic methods of colouration or a combination of these methods have been widely practiced during fabrication of maxillofacial prostheses. According to the condition and requirements of each individual case, a combination of these methods is used to obtain the optimal colour match, and therefore achieve the best aesthetic outcome. When colouring prostheses, an accurate base colour is used to colour the prostheses intrinsically i.e. within the silicone. After its production further colour can be added extrinsically to obtain the most accurate colour match at the time of delivery of the prosthesis. To colour the prosthesis various pigments are used. Colouration of soft tissue facial prostheses is achieved by adding oil based or dry-earth pigments (intrinsic colouration) to the silicone polymer at an early stage of processing, before adding the accelerator and final polymerization. The second step is adding the individual/patient specific colours (extrinsic colouration) which is added as a thin layer to the outer surface of the prosthesis in order to optimize colour matching with the patient's own skin colour (Beatty et al., 1999).

Pigments can be classified in three main ways - their colour, their origin and according to their major constituents. The first organic pigments are those that are formed from carbon-hydrogen compounds, and are generally derived from animal, plant or synthetic origin. The second group are inorganic pigments, and these are of mineral origin. It is thought that organic pigments are subjected to more deterioration and have a shorter life span when exposed to environmental factors when compared to inorganic ones.

2.4 Durability

The patient's major complain about his or her prosthesis is colour instability and alteration in the properties of the materials used in the production of facial prostheses (Cantor et al., 1969). Success of treatment depends on the mechanical and physical

properties of the material used and their ability to resist alterations in these properties under different weathering conditions (Craig et al., 1978). Deterioration of the delivered prosthesis starts immediately after it has been made and fitted – the resultant material degradation will affect both the colour and overall integrity of the prosthesis and will eventually lead to a prosthesis that neither looks acceptable or fits appropriately (Goldberg et al., 1978, Beumer, 1996).

2.4.1 Changes in the Mechanical Properties

Another concern when providing soft tissue facial prostheses is the service – there is inherent deterioration of the silicones mechanical properties over time (Chen et al., 1981, Lemon et al., 1995). The prostheses lose elasticity and become increasingly rigid. The areas that are most susceptible are the peripheries of the prosthesis – early rigidity is then followed by marginal tear due to daily application and removal of medical adhesive and exposure to the patient's skin secretions. Contact between the skin and the rigid border of the prosthesis can also lead to abrasion and ulceration of the underlying skin at the boundaries of the prosthesis and at portions where the prosthesis moves against a fixed tissue bed or when the tissue moves against a fixed portion of the prosthesis. This movement usually creates an area of conflict at the elastomer-tissue interface, which then leads to irritation of the skin and oral mucosa, and is uncomfortable for the patient (Waters et al., 1999). When assessing the effects of environmental factors many articles have discussed the use of artificial weathering and weathering chambers to simulate normal life weathering conditions to assess the overall deterioration of the materials used in this process (Sweeney et al., 1972, Gary et al., 2001, Kiat-Amnuay et al., 2002). Fading of pigments and/or dye and changes in mechanical properties during exposure to sunlight is the result of a chemical reaction that occur when UV radiation, in the presence of oxygen and moisture breaks down the silicone and pigment within the prosthesis and therefore alters the reflective properties of the material and changes its colour (Patton, 1973). This is problematic and is a key point in the overall deterioration of any prosthesis. Yu et al (1981) evaluated 4 types of silicone, polyvinyl chloride and polyurethane polymers for their physical properties after exposure to artificial weathering conditions. They concluded that the 4 types of silicone polymers reported no changes in physical properties on accelerated aging and

they attributed this important characteristic to the inert inorganic backbone of the molecular chain (Yu et al., 1980).

Articles show that the mean lifetime of elastomeric prostheses is between 6 months to 3 years and the limited service of facial prostheses results from material degradation and colour change (Haug et al., 1999b, Hulterstrom and Ruyter, 1999, Polyzois, 1999). Therefore, patients must be made aware of deteriorating factors and must be instructed on how to avoid prolonged exposure to sunlight. They must also be advised to wear sun protecting hats and sunglasses if they work or spend extended periods of time outside. They must also be familiar with appropriate cleaning of the prostheses to prolong the life span. The use of cosmetics on the facial prostheses (Yu et al., 1981, Yu et al., 1982) and/or repeated washing/cleaning, including the use of solvents like isopropyl alcohol, which dissolves the pigments, should be avoided. Smoking may also cause discoloration of nasal prostheses and therefore must be avoided. Finally, the patients must be instructed on how to apply and remove the prosthesis and how to clean and store the prosthesis (Yu et al., 1983).

2.4.2 Changes in the Optical Properties

The ability of the soft and flexible maxillofacial materials to lose their colour is considered one of the greatest shortcomings of these types of treatment. Therefore prostheses require regular replacement, which could be considered a burden to the patient in terms of time, effort and cost (Valauri, 1982). Environmental factors including exposure to ultra violet light, air pollution and humidity are considered the most common factors when deterioration of the prosthesis is observed. Other factors including cosmetics and strong solvents for cleaning and removal of the adhesive from the prostheses (such as benzene and xylene) also have negative effects on the longevity of prostheses. Testing the colour stability of maxillofacial prostheses, usually involves exposing the prostheses to environmental factors over extended periods in a controlled manner. Samples of pigmented facial elastomers were tested by Lemon et al (1995) under artificial weathering and outdoor weathering conditions. The samples did show slight colour changes but in a perceptible manner. Bigger changes were observed and caused by artificial weathering than outdoors. Addition of a UV absorber to the elastomer did not protect the samples from colour change (Lemon et al., 1995).

Sweeney et al (1972) used an accelerated aging chamber to simulate the effect of outdoor weathering on colour stability of maxillofacial silicone materials. They recommended two thousand hours of exposure for evaluation of maxillofacial materials (Sweeney et al., 1972).

In 1978 Craig et al used a similar method to test colour stability of polyvinylchloride, polyurethane and 4 other silicones (Silastic 382, Silastic 399 and Silastic 44210, Dow corning, Midland, Mich.). The materials were evaluated by Spectrophotometer before and after exposure to weathering condition with a 2500W xenon light source. The results demonstrated that all silicone elastomers showed good colour stability, although Silastic 44210 elastomers were demonstrably better. The study also suggested that decreased stain resistance and increased permeability of the elastomers were partly responsible for the colour degradation that occurs during service (Craig et al., 1978). Colour fade can be preserved by adding colour/pigment stabilizers. Addition of intrinsic UV light absorber such as benzotriazole compounds in a concentration between 0.5% and 1.0% by weight can improve the longevity of the colour.

A literature review by Gary and Smith (1998) stated that colour change is expected after exposing silicone elastomers to aging factors. Furthermore, intrinsic pigments may resist fade/change following exposure to UV light or solvents more effectively than extrinsic pigments, and the use of UV absorbers reduces the effect of extrinsic weathering factors (Gary and Smith, 1998).

2.4.3 Aging Mechanism and Effect of Accelerated Weathering Conditions on Maxillofacial Silicone Polymers

Aging mechanism refers to material degradation of the polymers and changes to their properties under the environmental factors. Several factors are responsible for the chemical and physical deterioration of the polymers either individually, or combined - light, temperature and humidity are considered a triple threat for polymers. Alone any of these factors can cause damage, however, combined they act synergistically and cause further damage to the polymer. These factors cause damage to the polymer coating and inks/pigments and this phenomenon leads to gloss loss, colour fade, surface cracks and

crazing. Materials under these conditions lose their tensile and tear strength. An increase in the stiffness and hardness of the material also takes place. Material degradation, loss of dyes and pigments, also occur under sunlight through windows (QUV&Q-Sun, 2012).

2.4.3.1 Ultraviolet (UV) radiation from sunlight:

The primary cause of material degradation is exposure to UV radiation from sunlight, also referred to as photo-oxidation. Photo-oxidation of the polymers occur due to absorption of radiation which results in physical and chemical changes (Brown et al., 1995). Energy from sunlight activates free radical formation by dissociation of hydrogen-carbon bonds within the polymer chain (White and Turnbull, 1994). The effect of UV light is usually primarily affects the surface layer, however this effect shows fewer reactions in the deeper layers. The free radicals utilize surface oxygen at the surface where there is the exchange between UV light and oxygen diffusion promotes the reaction. The presence of heat is a key determinant of the kinetics of this reaction. Other weathering factors such as heat, humidity and air pollution can facilitate the effect of UV radiation from sunlight on the mechanical breakdown, thus enhance the ageing process of the polymers.

2.4.3.2 Thermal factor:

Elevated temperatures influence chemical and physical reactions within the material and promote changes in the mechanical and optical properties of the polymer (Wright, 2001). Degradation processes such as oxidation, chemical attack and mechanical creep take place and their effect increase under increased temperature. Oxidation is one of the key determinants that cause material degradation by potentiating the thermo-oxidation process. The process starts by oxygen response from peroxide with free radicals P*

$P^* + O_2 \rightarrow POO^*$

The formation of free radicals at the point of polymerization for HTV silicone polymers is increased when combined with light and/or ionizing radiation. After free radical formation, low rate propagation of the peroxide radicals takes place under the effects of light and increased temperature. This propagation reaction breaks down the polymer chains and leads to material degradation although this can take a long time.

However, the rate can be increased when under the influence of higher temperatures (Wright, 2001), Additionally thermal induced expansion, albeit a reversible reaction in elastic polymers, can effect material integrity (especially in composite types of polymers with fibrous matrices), which may also lead to thermo-mechanical failure during thermal processing (Brown et al., 1995).

2.4.3.3 Chemical degradation:

Chemical damage involves the positive reaction of polymers to fluid. Hydrolysis takes place in the presence of different types of liquids including acid and alkaline. These fluids include amides, esters and carbon groups located within the back bone chains of the polymer. This leads to chain scission and a reduction in the polymer's inherent stability thus, producing a reduction in the toughness, fracture strain, and failure of the polymer (Brown et al., 1995).

2.4.4 Evaluation of Material Degradation

In Recent years several devices have been developed for testing the influence of environmental conditions on colour stability and mechanical properties of polymers. These devices include the Q-sun Xenon test chamber (ASTM G155) and QUV accelerated weathering tester (ASTM G 154)**,** as shown in Figures 2-17 and 2-18 respectively.

Both devices perform the same testing function using different test methods. These differences are in the way in which they apply the humidity and light spectrum emission. The QUV emits the violet wavelength of sunlight between 300 nm to 400 nm, while Xenon lamp emits the entire spectrum of the sunlight. This spectrum ranges between 295 nm to 800 nm. Short wave ultra-violet wavelengths from outdoor sunlight cause the greatest degree of damage to these polymers.

Figure 2-17: Q-Sun Xenon test chamber (ASTM G155).
http://2.imimg.com/data2/PC/SX/IMFCP-659792/qsun-250x250.jpg

Figure 2-18: QUV accelerated test chamber (ASTM G 154).
http://www.nhplcolour.com/Stability/IMAGES/quv1.png

These devices simulate the natural detrimental effects of long-term exposure to outdoor weathering conditions and UV radiation from sunlight, moisture and heat. Although it is a matter of debate, if there is a direct correlation between the accelerated weathering simulations and natural weathering conditions, they could be the only time compression method available for testing the effects of different weathering conditions on materials within a shorter timeframe. These devices expose the test materials to extreme and highly aggressive weathering conditions, and have the advantage of saving extended testing time, which is considered crucial for many manufacturers (QUV&Q-Sun, 2012).

The effect of accelerated weathering on mixed polyethylene and polypropylene products has been evaluated and it was found that 1000 hours exposure to UV light and moisture, corresponds to 1 year of exposure to out-door, natural weathering conditions.

However, several factors must be taken in to consideration when making such comparisons. These include the thermal background of the polymer, test conditions and the nature of the polymer in use. Accurate relationships between the natural and accelerated weathering of a material in this context must be considered with these difficulties in mind (Philip et al., 2004).

2.5 Additive Manufacturing

Additive manufacturing (AM) or additive fabrication (AF) refers to the process of automated production of 3D models in layers by applying solid freeform technology based on computer aided design and computer aided manufacture CAD/CAM. The process is also described as Rapid Prototyping (RP), Additive Rapid Prototyping (ARP) or Layered Manufacturing (LM) (Honiball, 2010).

CAD/CAM technology first emerged in the late 1980's as rapid prototyping technology. However the history relating to the development of rapid prototyping can be traced back to the late sixties, when Herbert Voelker, an engineering professor, started to investigate the possibility of computer controlled machines which were involved in manufacturing machine made components that otherwise would have been handmade by machine workers (Hogan, 2009).

In the 1970's, Voelker transferred his ideas from theory into practice by designing basic algorithms and mathematical formulae for building solid structures on computers.

In 1987, Voelker's idea was strongly supported by Carl Deckard (from Texas University) and together the process of RP with layer-based manufacturing came into being and implemented on a practical level. This became the first application of selective laser sintering technology, then Stereolithography, became the first commercially available Rapid Prototyping (RP) technique (Williams et al., 1996, Levy et al., 2003).

Additive manufacturing is a revolutionary technology which was originally based on rapid fabrication of a working model for testing, examination and study purposes (Wohlers, 2009). It has a wide range of application with the benefit of time and cost reduction. AM also enables the user to give immediate feedback to the designing system. The technology has now been developed such that it is not only used

for the rapid manufacturing of models but also to produce definitive functional parts/components.

2.5.1 Evolution of CAD/CAM Technology

Computer-assisted design and computer-assisted manufacturing (CAD/CAM) were first developed in the 1970s. However, they became available for dental practice only in the late 1980s (Duret and Preston, 1991). Today CAD/CAM has many applications; however, the technology can be divided into two broad forms of automated manufacturing techniques: additive or subtractive.

Initially CAD/CAM technology started with subtractive techniques as a numerically controlled process – generally machine milling (Petzold et al., 1999). The basic principle of subtractive rapid prototyping technology is cutting though solid blocks, i.e. metal or ceramic, to produce 3D solid models. Fine steel or diamond burs (with or without lubrication) rotate in harmony with the material to cut through blocks according to selected data sorted as STL files/data in a CAD pack in order to produce a 3D model. The main application of subtractive CAD/CAM technology, more specifically computer controlled milling or machining, is the use of the CEREC® system in most modern dental laboratories for crown and bridge construction (Miyazaki et al., 2009). However, this method has some limitations as the construction process is performed by a milling machine with restricted motion capability; it can be difficult to program complex geometry with several undercuts and geometric details (Potamianos et al., 1998). The other limitation is that only hard materials with a certain degree of toughness can be employed in this technique (Klein et al., 1992). Another limitation of subtractive machining is the material waste; by its very nature the process removes material from a pre-determined volume and discards what is not needed – this can be quite wasteful if the design process is not planned efficiently. This is not only a matter of material waste, it is also a matter of time consumed to produce a single piece since the machine may only accept one part at any one time (van Noort, 2011) .

Therefore, although the subtractive method of fabrication has its place in manufacturing, it does have its drawbacks and limitations. Today, additive manufacturing techniques have the geometric flexibility to produce more complex internal geometries. Therefore they are more attractive for dental applications and more

suited to producing arbitrary complex physical models with undercuts, cavities within and deep internal complex geometries such as those of canals and sinuses. This kind of manufacturing flexibility can overcome many problems associated with the milling process and it is the outcome of the additive nature via discretization "slicing" and sequential stacking of "2D" layers which can overcome design and manufacturing complexities (Liu et al., 2006).

In recent years rapid prototyping (RP) evolved to rapid manufacturing (RM) as a result of technical improvements in layer manufacturing methods, and the capability of these technologies to employ a wide range of materials, including various types of metals (Kruth et al., 2004, Kruth et al., 2005).

Today, CAD/CAM describes methods of additive fabrication, which are based on data acquisition, data processing and manufacturing.

2.5.2 Medical Rapid Prototyping

Although AM is a relatively new technology, it has expanded quickly within the last few years and has been adapted to a wide range of applications within industry, including healthcare.

Medical Rapid Prototyping was first described by Mankovich et al. in 1990 as the production of 3D dimensionally accurate anatomical models of the human body using a range of rapid prototyping technologies - SLA, SLS, FDM and 3DP (Mankovich et al., 1990). Following their inception these technologies started to play a more and more essential role in medicine due to their advantages of reducing time and cost in developing and manufacturing models/implants/prostheses. With the limitations of more conventional methods of manufacture they also improved the quality, accuracy of fit and performance (Liu et al., 2006). The most common application of medical rapid prototyping can be described as biomodelling, which includes the production of physical and biological models illustrating human anatomy for diagnostic purposes and surgical planning. Bio-Models can also be utilised to conduct the operation as intra-operation guides, assuring the accuracy and the quality of outcomes (D'Urso et al., 1999). These models were produced using SLA; the source of image data for 3D modelling is primarily the patient's CT images. MRI has also been used to produce soft tissues models of such body parts as arteries and nasal passages. These anatomical

models have been successfully applied as customised implants for surgical reconstruction of the orbital floor and for cranioplasties. MRP has also been used widely in maxillofacial surgery and orthopaedics for production of customised implants and in neurosurgery and dental implantology (Anderl et al., 1994, Arvier et al., 1994, Heckmann et al., 2001, Winder, 1999, Minns et al., 2003). Other medical applications of AM are the design and construction of customised implants for individual demands and production of scaffolds for tissue engineering as well as drug delivery systems and fabrication of specific surgical tools (Giannatsis and Dedoussis, 2009).

2.5.3 Data Capturing, Data Processing

The development of different types of digital scanners with a wide range of scanning capacity has made it possible to create 3D models of the oral cavity directly with no need for time consuming impressions or model pouring. In recent years, intraoral scanners have had a significant impact on the expansion of dental applications using CAD/CAM technology. Today a wide range of tasks, including planning, design and manufacture of restorations/orthodontic appliances, can be performed with the help of intra oral scanners. The development of these types of digital scanners has been accompanied by the advancement of several software packages that facilitate the design and manufacture of any dental restorations within a short period of time (van Noort, 2011).

2.5.3.1 Deep structures - CT/MRI:

For deeper structures with a bigger volume or obscured by surface details – bones under skin, data acquisition has to be achieved by other means. These can include computerised tomography (CT) or magnetic resonance imaging (MRI). Both can be used to produce dimensionally accurate virtual and physical models of human anatomy derived from medical imaging data (DICOM data) using different methods of additive manufacturing methods. CT is a medical imaging scanning device using x-ray. This method of imaging combines x-rays with computer technology to produce and then combine cross sectional images of the object/body and display them on a screen. CT scans can outline tissues of different densities – bone inside the body, very accurately (Figure 2-19). Magnetic resonance imaging (MRI) is another medical diagnostic

imaging technique and is primarily used to display soft tissue images (Gianluca et al., 2010) (Figure 2-20).

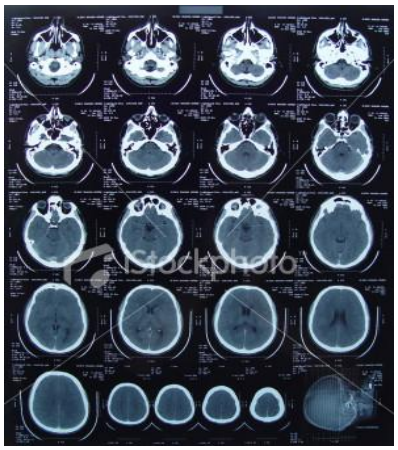

Figure 2-19: CT Image.
http://two-views.com/images/istockphoto_1026283-ct-scan-skull-slices.jpg

Figure 2-20: MRI the craniofacial region.
http://emedtravel.files.wordpress.com/2010/03/brainmri.jpg

2.5.3.2 Surface details - contact and non-contact systems

At its simplest, surface digital data capture can be performed by using a coordinate measuring machine (CMM) in two different ways – contact or non-contact digitalizing systems (Chang et al., 2006). These two systems can create digitized surface data automatically and the contact methods can generate the surface data from a physical

model by a touch probe; however, this is a slow method of data capturing and time consuming. Furthermore, the contact method has a limited capability for measuring complex physical models.

The process of non-contact digitalization is achieved by an optical method using a laser beam in order to capture the surface data; this method is more efficient and less time consuming because a mass of data can be acquired in a shorter time.

The data can then be transferred to a 3D CAD package for visualisation and manipulation of a virtual 3D computer model. This kind of data capturing can only be used with digitally controlled machining to create small models for crown or bridge construction (Kelly, 2007).

Digitalized surface data capturing is becoming a well-acknowledged system that is used where precise, non-contact measurements of a 3D surface are required (Leifer, 2003). Non-contact 3D surface imaging systems have started to replace traditional methods of detail capture. This method captures quantitative information about the facial soft tissues by using non-contact optical scanning techniques. This system of data capture developed rapidly as a result of the introduction of different types of devices that can scan the facial soft tissue faster by using non-invasive methods (Kau et al., 2007).

For maxillofacial soft tissue prostheses data can be captured by laser surface digitalizing technique (Figure 2-21) or Stereophotogrammetry system (Figure 2-22); these are considered the two most acknowledged methods of surface imaging, because they are non-invasive, non-ionizing and non-contact methods of data capturing. Both are highly sensitive methods of surface imaging which optimize the image capturing system (Ireland et al., 2008, Heike et al., 2010)

Figure 2-21: 3D image for a face scanned by laser scanning.

Figure 2-22: Images captured by 3dMD camera.

On the other hand, only the external data is captured by a laser scan or 3dMD camera, whereas CT and MRI collect both external and internal data; this reduces the size of the image file and the processing time while converting the scanned data to CAD data.

Laser scanning is a non-invasive method of soft tissue imaging with successful clinical output. However, this method of scanning has several disadvantages, including, firstly, the scanning process takes from eight to nineteen seconds, and therefore the patient must stay fixed during the time of scanning in order to avoid technical image distortion in the captured image being caused by any movement. Furthermore, the laser scanning system is not able to provide surface details and tissue texture precisely. Another limitation of laser scanning in the field of maxillofacial reconstruction is that the process of laser scanning of the human face may endanger the eyes, therefore, in order to protect eyes, the patients must keep their eyes closed during scanning, and this

may capture an inaccurate facial expression, especially for the landmarks around the eyes (Hajeer et al., 2002).

Photogrammetry is the process of producing quantitative 3D information about the external geometry of an object via the use of photographs. Photogrammetry deals with measurements of photographs and reconstructs the measurements of 3D objects from photographic reproductions. This can be achieved by using two or more cameras arranged as stereo-pairs to obtain 3D coordinates of facial geometry. Stereophotogrammetry can simply be defined as creation of a 3D image from multiple views of photos (Leifer, 2003, Kau et al., 2007). The photogrammetric system is based on high-resolution digital cameras, set up as three pods, positioned at three locations, to the right, front and left of the object. The combination of the three cameras allows for greater accuracy of facial anatomy within 360 degrees. Two lenses are used to capture separate images of the same object but from different angles. This technique is a novel technique called natural features technique. The acquired data is transferred to a 3D CAD package for processing and designing a 3D image (Majid et al., 2008).

This method of 3D imaging has some advantages over the other methods. It is a rapid image system, capturing the anatomical facial details achieved within 0.5 min with rapid generation of the 3D display. Thus young children's and babies' imaging can be performed with minimum risk of data distortion. Furthermore, this method of imaging is a non-contact and non-invasive method of 3D surface data capturing (Majid et al., 2008).

2.5.4 Utilization of Captured Data

The data obtained is then transferred in a format that can be used for CAD/CAM purposes. Data is converted to an STL type file, and then manipulated within a suitable CAD. The completed 3D design can then be transferred to a suitable RM system to perform layered fabrication of the requested design (Kai et al., 2000). The stored data is analysed by a slicing algorithm which breaks the 3D parts into 2D layers, this data is then used to guide the additive prototyping machine to fabricate 3D models from the bottom up, one layer at a time (Carrion, 1997). Several rapid prototyping software packages are available and are widely used for designing medical models for additive

fabrication. These include Mimics, 3-Matic, SolidWorks, Magics and FreeForms and each can perform general and specific tasks.

2.5.5 The Manufacturing Processes

The manufacturing process of CAD/CAM now involves numerous additive processes; the main difference between various types of additive technologies is the method in which the material is built up to produce a 3D models. In general, this technology employs layered manufacturing techniques. Some of these processes melt or soften materials to produce the layers i.e. Selective Laser Sintering (SLS) and Fused Deposition Modelling (FDM). Other technologies lay down liquid material called thermodynamic sets, and these are then cured by using different methods i.e. stereolithography (SLA), light/temperature. In the case of lamination systems, thin layers are cut to shape and joined together.

Advances in rapid prototyping have been significant – from subtractive techniques to the former additive manufacturing technologies including stereolithography, laser sintering, and fused deposition modelling, to the newer "3D printing" technologies with bigger reductions in cost and time (Sherman, 2004, Sherman, 2009). To summarise additive manufacturing techniques applied to layered fabrication using different material include (Giannatsis and Dedoussis, 2009).

1) Stereolithography (SLA) used with photopolymers.
2) Fused Deposition Modelling (FDM) used with thermoplastics.
3) Three Dimensional Printing (3DP) used with different materials i.e. cornstarch and plaster of Paris etc.
4) Selective laser sintering (SLS) used with thermoplastics, metals and sand.
5) Electron Beam Melting (EBM) used with titanium alloys.
6) Lamination Object Manufacturing (LOM) used with paper and plastic.

The additive manufacturing techniques have shown many advantages over its short period of development. This relatively new technology can be used to produce complex, three-dimensional solid structures in extremely fine detail to a high degree of accuracy. Furthermore, this can be done on a large scale. Therefore the following advantages are accounted for this recent technology.

1) Applicable to many industries.

2) Rapid construction - saving time.
3) Testing products for effectiveness of function and performance in an efficient manor and prior to definitive manufacture.
4) Reducing cost of the end product.
5) Easy adaptation of existing designs or, creating new designs from scratch.
6) Detection of design flaws at an early stage, before manufacturing.
7) The potential for early feedback by the user often in the design stage.
8) Better product quality, highly detailed and accurate objects are possible with rapid prototyping technology (eBook-1).

2.5.6 Dental Application of Additive Manufacturing

Since their development, many AM technologies have been employed for the fabrication of those items listed in the previous paragraphs. A list of technologies such as stereolithography (SLA), selective laser sintering (SLS), ink-jet 3D printing (i3DP) and fused deposition modelling (FDM) with a variety of materials such as wax, resin, metal and ceramics have been practiced in the field of medicine and dentistry, with numerous articles published under the topic of additive manufacturing or CAD/CAM technology.

2.5.6.1 Stereolithography (SLA):

SLA was developed by Hull in 1984. The system builds acrylic/plastic parts or objects by curing consecutive layers of a photosensitive liquid resin by tracing UV laser beam on the surface of the liquid resin to form a sold model (Hull, 1986). This allows the construction of anatomically accurate 3D models that can be utilized for surgical planning and rehearsing, especially with the current facilities of performing some simple colour-changing for biomedical applications providing greater inventiveness by highlighting meticulous/fine features in a different colour (Liu et al., 2006). RP biomodels have facilitated the diagnosis and treatment planning significantly in the past, and this has enabled the surgeon to understand the anatomy of each particular area (even on an individual level). In complex parts of the body, including the facial region, this has enhanced the level of knowledge and allowed the surgeon to understand the difficulties that may arise. Furthermore, with presurgical interpretation and planning, a

biomodel allows the clinician to predict possible difficulties or complications and, thus decrease surgical errors or misinterpretation and the operation time may be reduced too. These anatomical models can also be used for teaching, educational and motivation purposes (Winder and Bibb, 2005).

SLA has also been used to fabricate customized implants for cranial and orbital floor reconstruction. Another application of SLA modelling is construction of surgical drilling templates/"drill guides" for dental implant insertion, and recently the development of translucent coloured resins allow appropriate visualization and distinction of anatomical landmarks (Azari and Nikzad, 2009). Additionally, and very recently, SLA has also been used for fabrication of customised orthodontic aligners (Invisalign, Clearstep) from a thin transparent resin produced by CAD/CAM methods with considerable accuracy of fit and aesthetic outcome - each aligner designed to establish about 0.2 mm of sequential predicted CAD/CAM tooth movement, each one to be used approximately 14 days apart to produce the desired amount of tooth movement (Phan and Ling, 2007). It is also possible to design and fabricate customised study models for lingual orthodontic devices by scanning the patient's dental arches with an intraoral scanner. This allows the technician/clinician to build up a picture of the patients precise tooth position, and thus produce models to which more comfortable and well fitting appliances can be fabricated (Liu et al., 2006). In 2003 a study by Wiechmann et al, investigated the effectiveness of producing custom made models and guides to align brackets in patients undergoing lingual orthodontics. The study, based on 600 bonded arches over a 20 month clinical testing period, concluded that this kind of guide provided new opportunities for problem solving in relation to the bonding and frequent de-bonding of brackets, patient discomfort and problematic finishing process (Wiechmann et al., 2003).

SLA has also been used in dental laboratories to fabricate both temporary or definitive crowns and bridges following the preparation of teeth and geometric data captured by any array of digital laser scanners.

2.5.6.2 Selective laser sintering (SLS):

SLS or selective laser melting (SLM) technology enables the construction of solid 3D objects by fusing consecutive layers of a powder melt utilising high power 'co_2' laser. The laser used hits and melts the powder and then fuses them together. SLS can utilize a

wide range of powder materials – including ceramics and metals. It also has the added advantage of manufacturing objects to a very high degrees of precision and this can be utilised for different types of customized implants in maxillofacial region and/or other parts of the body (Giannatsis and Dedoussis, 2009). Another application for this type of additive manufacturing is the fabrication of bespoke dental implants and implant abutments for patient specific cases. Owing to the anatomical variations between different individuals, there are always cases that are outside the "standard" or "off the shelf" range as these may sometimes not fitful every case - in some cases the implant must be tailored according to the individual anatomical requirements (Liu et al., 2006).

2.5.6.3 Fused deposition modeling (FDM):

FDM or fused filament fabrication (FFF) was first developed by S. Scott Crump in the late 1980s. This method of additive manufacturing is based on laying down plastic materials (or metals) in layers through a pre heated nozzle moving in different directions under the control of a software package to produce 3D models. In dental practice it is used as an aid for the production of wax patterns for subsequent casting. Bioplotter is a commercially available FDM machine and is able to print in multiple materials. It can also be used in tissue engineering for the constructing of biocompatible tissue/organ scaffolds.

2.5.6.4 3D printing:

3D printing is a type of additive manufacturing technique that involves similar technology to that used in ink-jet printing systems, for manufacturing 3D models in full colour. Instead of ink the printing heads releases a binder onto a powder foundation according to CAD information provided to the printer, and this allows printing in a cross sectional 2D layer. The process is then repeated to produce a new 2D layer on the top of the previous layer. The process of printing continues until a full 3D model is built. The unbounded powder acts as support for the object during the printing process. Thus, the subject does not require supporting piles during at the time of printing – as with other techniques involving wax or acrylic (Cheung et al., 2001). It is this technology that has been adapted and developed to print 3D soft tissue prostheses for the facial region.

2.5.7 Soft Tissue Facial Prostheses and Additive Manufacturing Technology

The current method of constructing maxillofacial prostheses is considered less than ideal because of the limitations and drawbacks related to impression taking and impression materials used, time required producing the prostheses, convenience, cost and high technical skill needed to fabricate these prostheses. Furthermore, there are the problems of colour matching and manufacturing accuracy, which requires special laboratory techniques and expertise (Beumer et al 1995). The disadvantages of conventional method can however, potentially be overcome by applying a digital techniques based on facial defect measurements in three dimensions for data capturing and also applying digital technologies for the manufacturing process (Chen et al., 1997b).

An additional and relatively new strategy to overcome these disadvantages is the use of cameras or optical data acquisition. Some of the first optical data acquisition systems for reconstruction of facial deformity were introduced in 2000 (Runte et al., 2002). Cheah et al presented an application of CAD/CAM as an intermediary manufacturing method for automatic fabrication of anatomically accurate extra-oral structures. The fabrication protocol includes a laser scan of the face and rapid prototyping of the model without taking an impression. This was one of the first indications that human anatomical data could be acquired, and an accurate model produced without the need for an impression (Cheah et al., 2003a, Cheah et al., 2003b). Numerous studies have detailed the application of CAD/CAM for the indirect fabrication of facial prostheses. Several procedures have also been published detailing the fabrication of mirror-image casts and wax copies for maxillofacial prostheses (Nusinov and Gay, 1980, Coward et al., 1999). However, these techniques require more time and are much more costly than the traditional manual procedures.

Attempts have also been made to produce parts or anatomical models that could be used as an aid for the manufacture of other parts (with suitable materials) and used for secondary processing i.e. moulds. Recently, Eggbeer et al (2012) evaluated a direct and an in-direct additive manufacture of maxillofacial prostheses AM method of production for a nasal prosthesis. The direct AM prosthesis production included production of the body of the prosthesis from a digital design and manufactured from a

soft transparent acrylic based material – polyjet modeling 3D printing process. The body then wrapped with a layer of 0.4 mm thick HC20 silicone after it has been mixed with base shade and flocking using a strong adhesive - G604. The indirect technique employed using two mould sections fabricated using 3D printing (ProJet HD 3000 Plus, 3D-Systems, Rock Hill, USA). The 3D printed mould was used to complete the prosthesis body by moulding silicone in a manner similar to conventional methods using a base shade colour-matched silicone. Both approaches relied on 3D photogrammetry to capture patient anatomy data and FreeForm CAD for the initial design of the prosthesis form. Critical evaluation has shown that utilising a computer-aided workflow can produce a prosthesis body that is comparable to that produced using existing best practice. However to date there has been no reports of studies being able to integrate this technology to directly fabricate facial prostheses (Eggbeer et al., 2012).

In addition to laser scanning, rapid prototyping technology has most commonly been used for the production of moulds to fabricate customised prostheses using highly detailed CT data. However, this method is far from ideal as CT data is costly to obtain in terms of time and money (Cheah et al., 2003a, Cheah et al., 2003b). Furthermore, these investigations were not able to integrate this technology into prosthetic practice, and lacked proper evaluation of required physical and mechanical properties of the prostheses. It also lacked the effectiveness to develop an integrated and efficient manufacturing process – it was not automated and utilised many steps.

Therefore, the project within this thesis attempts to fabricate soft tissue facial prostheses by using full colour printing technology, utilising 3D data capture, data processing and designing 3D models, and manufacturing coloured prostheses using 3D colour printing. A reduction in the final product's cost and manufacturing time is expected with this project (Dimitrov et al., 2006a, Carrion, 1997). We also expect that the outcome of this automated technology could be available for the majority of patients who require soft tissue facial prostheses worldwide rather than to be confined to only a small group of patients that can afford the high cost of the handmade prostheses - the current technique requires highly skilled manpower, technical and artistic expertise, which is not always available around the world.

Fabrication of soft tissue facial prostheses starts with data acquisition by using 3D surface imaging methods, such as laser scan or 3D photogrammetry system - both are methods of capturing quantitative information about the facial soft tissues using

non-contact techniques in order to create virtual images. It is acknowledged that highly sensitive methods of data capture are required to optimize the image capturing process (Ireland et al., 2008, Heike et al., 2010).

Stereophotogrammetry is a method of achieving a three dimensional image by using one or more pairs of photographs taken simultaneously. This system obtains quantitative 3D information of the surface geometry of an object (Leifer, 2003). It has several advantages over other methods including rapid image capture - hence making it possible for patients who could not tolerate laser scanning (need to be still), CT or MRI (often need to lie down for extended periods of time). Using 3D photogrammetry accurate capture of anatomical facial details can be achieved - within 0.5 mm depending on the resolution of the system, as well as rapid generation of 3D display.

Within these investigations we have managed to develop a unique and innovative manufacturing process using a Z-Corp 3D colour printer - based on the data received from the software package. The printer then starts layered printing using starch powder bound together by a water soluble binder. These layers are then produced in a continuous sequence, one on top of the other and are essentially stacked into a 3D form - it essentially adds 2D layer to construct 3D objects (Sachs et al., 1993).

3D Printing has several advantages over other types of rapid prototyping processes. It is considered one of the fastest additive fabrication processes available. Production time has been reduced up to ten times when compared to other additive processes (Wohlers, 2009). Furthermore, 3D printers are easy to use and the printed parts are cheaper than other additive processes by up to 50% (Sherman, 2004). However, the disadvantages are that the 3D printed subject possesses limited mechanical properties, because only few materials are used suitable for this process and potentially renders the 3D printed parts very fragile after printing. Subsequently may require post-manufacturing infiltration to achieve additional strength (Dimitrov et al., 2006b, Dimitrov et al., 2008).

2.6 Challenges and Summary

Over the decades, maxillofacial prosthetics has been used to rehabilitate patients with facial deformities by reconstructing these deformities using artificial material – primarily silicone polymer based. Over the last 40 years cancer survival rates have

increased as a result of early diagnosis, improvements in surgical techniques and post treatment adjunct therapies. However, this has also been complemented by an increase in life span. Subsequently, this has led to an increase in the number of patients that require treatment and from a maxillofacial perspective has also resulted in increased patient numbers demanding facial prostheses. The demand for increasing numbers of highly skilled maxillofacial technicians and the cost of customised prosthesis has increased too – but is often not attained (Wolfaardt et al., 2003). This problem has led the researchers to investigate the role of new and innovative technologies to produce facial prostheses, and thus, utilise 21st century techniques to address an increasing modern day problem. The general disadvantages of the conventional methods of fabrication include high cost, shortage of technical staff with increasing demand for this kind of prosthetics. It is hoped our work will deliver a relatively low cost process that will be accessible to the global patient community.

The challenge then is to provide a simple system for data capture, design, accurate and consistent manufacture method with a clinically acceptable material.

This project focuses on the manufacturing aspect of the digital processing of soft tissue facial prostheses by a layered fabrication method. As demonstrated in Figure 2-23, the project could be summarised as - 3D data capturing and manipulation of data in a 3D CAD package for designing the prostheses and layered printing using Z510-3D colour printer. Data can be saved and additional copies could be printed on demand in the future.

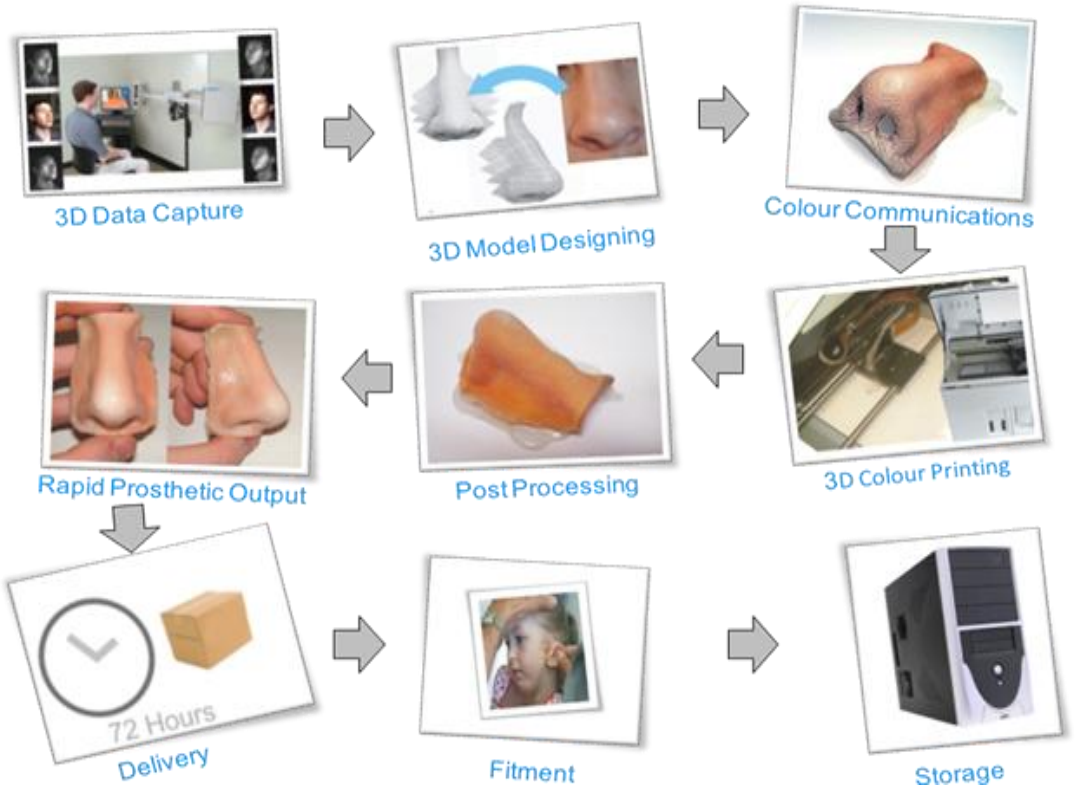

Figure 2-23: An overview of rapid manufacturing technology applied to fabricate soft tissue facial prostheses.

3 Aims & objectives

3.1 Introduction

Additive manufacturing technology is based on computer aided design and manufacturing (CAD/CAM). The project is concerned with the possible application of the technologies in the fabrication of maxillofacial prostheses in order to improve accuracy (Sun et al., 2011), reduce manufacture time (Azari and Nikzad, 2009), effort and the final cost of the prostheses (Davis and Emert, 2010). The patient's own data is captured and stored in an appropriate manner so that it could be utilized to provide or replace a prosthesis.

As the project is a novel project, the baseline data published about the fundamental components were scant. Therefore, it was necessary to investigate different aspects of the project and collect the required mechanical, physical and biological data.
The majority of 3D objects printed using the Z-Corp 3D colour printer are satisfactory with a sufficient degree of infiltration of the surface layer to produce a reasonably robust item that can be handled. In the case of flexible facial prostheses to be constructed in this project it is important that the printed item is fully infiltrated with the flexible silicone elastomer as this will ensure optimum performance of the prosthesis. The printed parts can perform better after infiltration with a suitable infiltrant in order to hold all the components together and provide the printed parts with the strength to enable them to function appropriately (Gatto et al., 2011). Thus, determination of the depth of penetration of the infiltrant inside the printed structures is an essential task. Increasing the depth of penetration and improving the quality of infiltration should improve the service life of the final product – indeed to reduce the ratio of filler/silicone polymer would enable optimisation of many of its qualities.

The mechanical properties of the materials used for the fabrication of facial prostheses would determine the durability and service life of the prostheses (Beumer et al., 1996), and thus the patient's satisfaction with the prostheses (Chang et al., 2005). Therefore, it is necessary to determine the mechanical properties and the optical properties of the material used and understand the effect of natural weathering conditions on the prostheses in order to utilise the appropriate materials for fabrication

of the facial soft tissue prostheses and to motivate and help the patients to maintain their own prosthesis (Yu et al., 1981).

As endosseous implants provide the prostheses with better retention and longer service life, it was necessary to add a suitable attachment to the prosthesis provided with different mechanical means in order to hold the magnet in the exact position and orientation to that of the implant.

Human skin shade varies considerable - from very light as in Caucasians to dark in Africans. For the Z-Printer to be able to print the whole spectrum of skin colour required, the skin colour gamut should be compatible with the printer's colour gamut as this will determine the capability of the printer to produce the whole range of human skin colour.

Reproducing the exact human skin colour by 3D colour printing is a function of several factors: the RGB colour profile of the 3D printer and the colour capture device (Coward et al., 2008), also the type and nature of the colorant added to the binder and the nature of the materials used in 3D printing. Finally the infiltrate used in post manufacture processing has a great influence on the produced colour (Walters et al., 2009). It was also necessary to investigate the novel prostheses for their ability to retain colour and their ability to resist colour changes under different weathering conditions.

The materials utilised by the Z-Printer are designed for industrial purposes and not for medical purposes (Lam et al., 2002), and therefore the biocompatibility of the materials used is an important considerations.

3.2 The Aim

The aim of this project was to produce soft tissue facial prostheses by using 3D colour printing, which has a patient matched skin shade and the desirable mechanical properties for service.

3.3 The Objectives

1- To investigate the elastomer infiltration depth and methods to enhance the infiltration depths of the silicone polymer infiltrates and thereby achieve the optimal infiltration depth of the silicone polymers inside the printed parts.

2- To assess the mechanical properties of the final material used.

3- To evaluate the effect of natural and artificial weathering conditions on the product.

4- To assess the colour reproduction capability of the Z-Printer and colour stability of the prostheses under natural and artificial weathering conditions.

5- To determine the capability of the colour printer to print the human skin colour via an investigation into human skin shade of a wide range of ethnicity.

6- To provide a suitable attachment when an endosseous implant is the means of retention.

7- To formulate a combination of materials that yields a biocompatible composite with properties similar to that of traditional prostheses.

4 Investigation into Elastomer Infiltration Depth and Methods of Enhancing Their Characteristics

4.1 Introduction

3D printing is a branch of rapid prototyping and a method of additive manufacturing. The use of 3D printing has added some additional advantages to the process of prototyping by producing more accurate virtual 3D models, improving product quality, reducing production time and reducing final product cost (Carrion, 1997, Dimitrov et al., 2006a). 3D printing allows printing of consecutive layers of various materials, one after the other until a 3D structure is completely built. The 3D printer prints by using "inkjet-printing" systems and acts to bind fine powder together according to information or data derived from the 3D design/CAD software (Sherman, 2004, Chiu and Yu, 2008).

The chemical binder is acts as an "ink" to hold the powder together in cross sections as each set of data is sent to the printer. The printer can also use coloured "ink" for printing the 3D model, and then for the first time there is a technology that prints full colour prototypes (Ming and Gibson, 2009). The powder that is used by the Z-Printer can be cornstarch/cellulose, plaster with a water based binder, and is dependent on what is trying to be achieved and according to the requirement and quality of the printed structures (Steinhilp and Kias, 2009). In this study cornstarch powder is used for construction of facial soft tissues prostheses. This makes it possible for the printed structure to be infiltrated with a maxillofacial elastomer in order to achieve skin texture and softness (Gatto et al., 2011). Commonly plaster powder, infiltrated with cyanoacrylate, is used for printing hard models. The highest concentration of the binder is located at the outermost layers, to form an external shell in order to provide the printed model with certain degree of strength and hardness, whereas the amount of the binder inside is very little leaving the starch powder almost unbound. Consequently, the final product consists of areas/surfaces that are solid and composed of powder and binder and the remaining areas within the internal volume of the solid model remain as unbound powder. This renders very fragile models that may crush easily under a slight pressure at the time of their extraction from the printer. Therefore, these models must be infiltrated with a suitable polymer to achieve structural integrity and provide either strength/or flexibility (Gatto et al., 2011).

In the majority of cases 3D objects printed using the Z-Corp colour printer are satisfactory with a sufficient degree of infiltration of the surface layer to produce a

reasonably robust item that can be handled (Upcraft and Fletcher, 2003, McMains, 2005). However, in the case of flexible facial prostheses it is important that the printed item is fully infiltrated with the flexible silicone elastomer (SE), as this will ensure optimum performance of the prosthesis (Dimitrov et al., 2006a). The elastomer acts as the main binder for the printed powders and areas that are not infiltrated will be exceedingly fragile, as the powder will readily disintegrate.

4.2 Aim

The aim of this part of the project was to establish the optimum conditions for infiltration with a silicone polymer (SP) into starch and plaster produced objects.

4.3 Materials

Table 4-1 illustrates the manufacturing specifications of the materials used in the study, which include the two powders utilised by the Z-Corp (Z510) 3D colour printer and the different binders used in the printing process. The table also presents the maxillofacial silicone polymers (MSP) that were used as infiltrant.

Table 4-1: Materials used and their manufacture specifications.

Material	Name	Type	Components				
Powder Z-Corp	zp™15e	Starch/cellulose Powder	Starch Gum 0-100%	Confectioners Sugar 5-30%	Cellulose Fiber 5-30%	Sorbitan Fatty Acids 0-1%	
	zp®131	Plaster Powder	50-95% Plaster	Vinyl Polymer 2-20%	Sulphate Salt 0-5%		
Binder Z-Corp	zb™58	Liquid	Glycerol 1-10%	Preservative 0-2%	Surfactant < 1%	Pigment < 20%	Water 85-95%
	zb@60	Clear Binder	Humectant 1 < 10%	Humectant 2 < 8%	Polymer < 4%	Non	Water 85-95%
	zb@60	Yellow Binder	Humectant 1 < 10%	Humectant 2 < 8%	Polymer < 4%	Yellow Dye < 10%	Water 85-95%
	zb@60	Cyan Binder	Humectant 1 < 10%	Humectant 2 < 5%	Polymer < 4%	Dye 5- 40%	Water 65-95%
	zb@60	Magenta Binder	Humectant 1 < 10%	Humectant 2 < 8%	Polymer < 4%	Dye < 20%	Water 65-95%
Maxillofacial Silicone Polymer	Sil-25 Silicone polymer Abacus	Component A- Base – 10	Polydimethyl Siloxane	Functional group Cross-Linking	Additives	Addition cross-linking	RTV
		Component B- Catalyst - 1	Polydimethyl Siloxane	Functional group Cross-Linking	Additives	Addition cross-linking	RTV
	PROMA X-10-SLOW Abacus	Component A- Base-1	Polydimethyl Siloxane	Platinum – Cure	Additives	Addition cross-linking	RTV
		Component B- Catalyst-1	Polydimethyl Siloxane	Platinum – Cure	Additives	Addition cross-linking	RTV
	Platinum MATRIX M-3428 Abacus	Component A- Base – 10	Polydimethyl Siloxane	Platinum – Cure	Additives	Addition cross-linking	RTV&HTV
		Component A- Catalyst – 1	Polydimethyl Siloxane	Platinum –Cure	Additives	Addition cross-linking	RTV&HTV

4.4 Methods

The experiment to investigate the infiltration depth was divided in to three groups:

4.4.1 Group 1 - Starch Cubes

Three sets of 20 x 20 x 20 mm, starch cubes were infiltrated with Sil-25 maxillofacial silicone polymer MSP under different conditions.

4.4.1.1 Group 1 – Series 1: Infiltrations of starch cubes with Sil-25 under normal air pressure:

The cubes were infiltrated with Sil-25 under standard air pressure and at room temperature.

1) A set of 30 cubes measuring 20x20x20 mm were printed in starch, using the Z-Corp (Z510) 3D printer (Figure 4-1).

Figure 4-1: Z-Corp (Z510) 3D Printer.

2) Two part addition curing silicone (Sil-25) maxillofacial translucent SP, ratio (1-10) was used as an infiltrate for the starch cubes.
3) Two-silicone parts were proportioned by weight to an accuracy of 0.1 gm by using a digital balance - Navigator (Figure 4-2). One part weight of the accelerator was mixed with 10 parts of the silicone base for one minute in order to achieve a uniform consistency within the mix.

Figure 4-2: Sensitive digital balance (Navigator).

4) To prevent the most inferior aspects of the cubes touching the bottom of the container they were suspended on a wire platform constructed out of 0.7 mm stainless steel wire. This allowed a few millimetres of separation in order for silicone to be evenly distributed under the cubes. Another wire frame was placed on the top of the cubes to avoid them floating out of the SP.
5) The plastic container was then left at room temperature. After 5 minutes one cube was removed from the container and left on a glass slab to allow complete drainage of the residual SP. After a further 5 minutes another cube was removed from the container and left on the glass slab for full drainage. This continued until the last cube was removed. This meant the cubes had been submerged in SP for the following times: 5 minutes, 10 minutes, 15 minutes, 20 minutes and 25 minutes. The cubes were then left for 24 hours before the infiltration depths measurements.
6) After 24 hours the cubes were bisected into equal halves using No. 11 scalpel blade. Any residual non-infiltrated starch powder was removed by using a lacron carver. The internal aspect of the cube was then stained by using Cochineal dye to highlight the silicone infiltration boundary and facilitated measurement taking, as seen in Figure 4-3.
7) The bisected cubes were then orientated under a travelling microscope (Mitutoyo TM) with X-Y coordinates as shown in Figure 4-4 and Figure 4-5 and measurements taken at three points on each face. This enabled 12 measurement points on any of the two halves of the cube as shown in Figure 4-6.
8) This experiment was repeated on six sets of cubes, for each time period. A total of 30 cubes were used for each series.

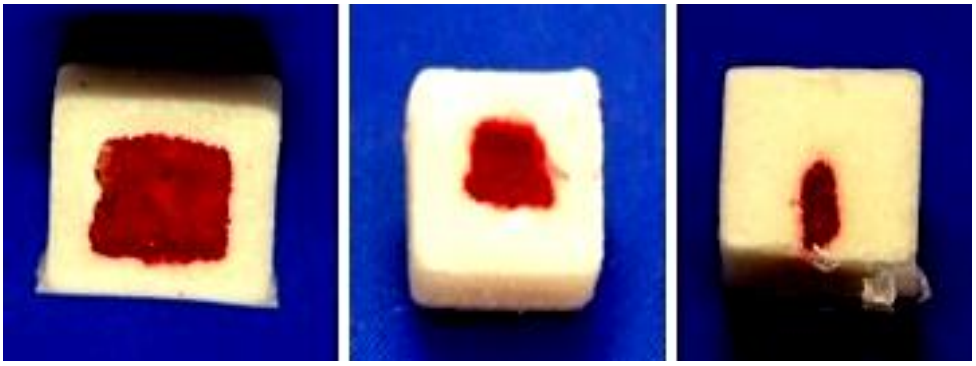

Figure 4-3: Sectional blocks showing the staining due to the dye and identifying the extent of silicone polymer infiltration.

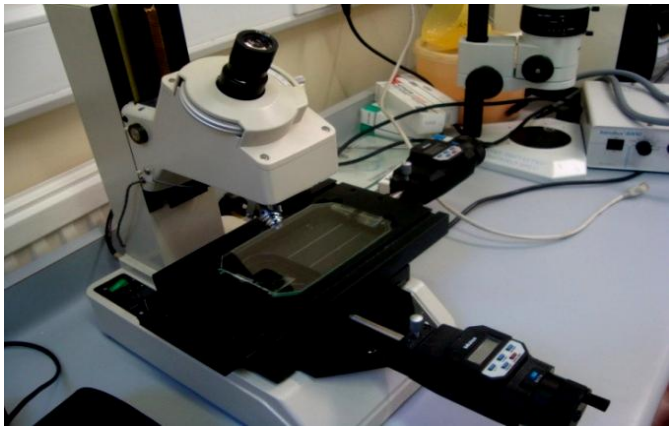

Figure 4-4: Travelling Microscope (Mitutoyo TM).

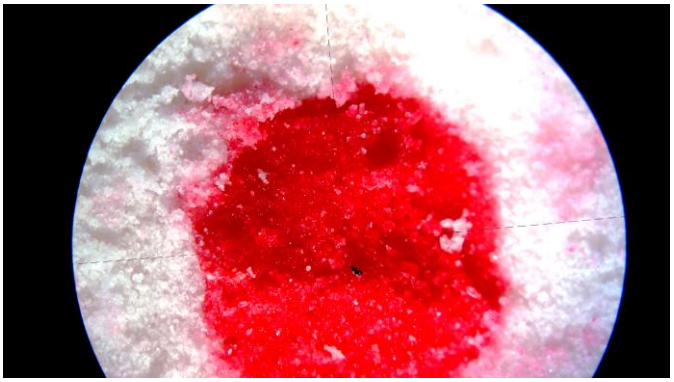

Figure 4-5: Measurement field as viewed under the travelling microscope.

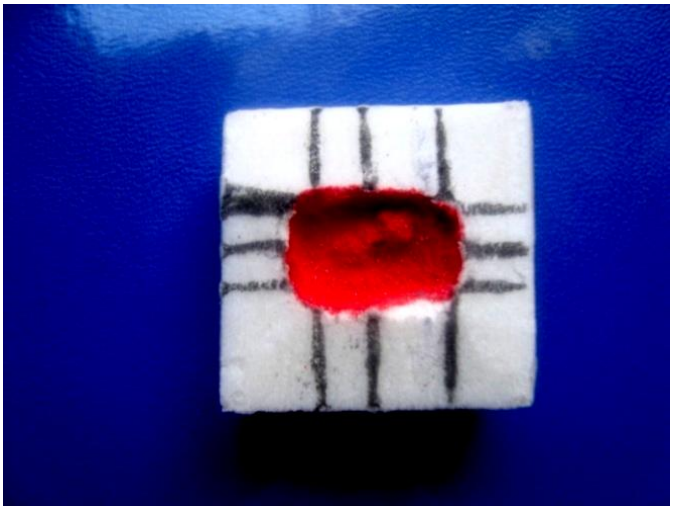

Figure 4-6: Measurement's lines on a half cube.

4.4.1.2 Group 1 - Series 2: Infiltrations of starch cubes with Sil-25 under 2 bar pressure:

20x20x20 mm starch cubes were infiltrated with Sil-25 MSP under 2 bars pressure and room temperature. Similarly another set of 30 starch cubes measuring 20x20x20 mm in dimensions were printed and used in this series of experiments – see section 4.4.1.1. However in this series the experiments infiltration was carried out under 2 bar pressure, by placing the cubes into a dental pressure bath in order to undertake the infiltration process under pressure at identical times (5 min, 10 min, 15 min, 20 min and 25 min) (Fig. 4-7). The cubes were again removed and left on a glass slab for drainage of the residual SP. Measurements of penetration depth were also carried out under the travelling microscope after 24 hours.

Figure 4-7: Dental pressure bath.

4.4.1.3 Group 1 - Series 3: Infiltrations of starch cubes with Sil-25 under 3 bar pressure:

20x20x20 mm starch cubes infiltrated with Sil-25 MSP under 3 bars pressure and room temperature. The previous experiment was repeated at similar times (5 min, 10 min, 15 min, 20 min and 25 min) but the infiltration process was performed under 3 bar pressure instead of 2 bar.

4.4.2 Group 2 - Plaster Cubes

Identical experiments were repeated on another 2 sets of 30 cubes measuring 20x20x20 mm in dimensions. However these were printed in plaster by the same printer. The same translucent SP - Sil-25 was used for infiltration.

4.4.2.1 Group 2 - Series 1: Infiltrations of plaster cubes with Sil-25 under normal air:

A set of 30 plaster cubes measuring 20x20x20 mm were infiltrated with Sil-25 MSP, under normal air pressure for (5 min,10 min, 15 min, 20 min and 25 min).

4.4.2.2 Group 2 - Series 2: Infiltrations of plaster cubes with Sil-25 under 3 bar:

20x20x20 mm plaster cubes were infiltrated with Sil-25 MSP, under 3 bar pressure and identical times.

4.4.3 Group 3 - Starch Cubes and Two Other SPs

In this group of experiments, two other MSP were used as infiltrant instead of Sil-25 MSP, the Promax-10-Slow and Platinum Matrix M-3428.

4.4.3.1 Group 3 - Series 1: Infiltrations with Promax-10-Slow at 3 bar pressure:

A set of 30 starch cubes, measuring 20x20x20 mm in dimensions were infiltrated with a two part addition curing maxillofacial translucent SP (Promax-10), ratio (1-1). The infiltration process was performed under 3 bar pressure for the same duration (5 min. 10 min. 15 min. 20 min and 25 min).

4.4.3.2 Group 3 - Series 2: Infiltrations with Platinum-Matrix M-3428 at 3 bar:

Infiltration of 30 starch cubes measuring 2x2x2 mm was performed under 3 bar pressure by using two part additive curing (Matrix M-3428) MSP, ratio (1-10) at identical times.

4.4.4 Statistical Analysis

The collected data were subjected to PASW statistics 18, employing one-way ANOVA on each group of data collected from each experiment in order to make the comparison between the subgroups – time intervals. Furthermore, two-way ANOVA – Tukey's HSD was performed between groups.

4.4.5 Silicone/Starch Ratio by Weight

The percentage of each component (the starch powder and the SP) was determined by weight in the final models. 8 starch blocks (45mmx45mmx4mm) were printed by the Z-Printer (Z510) and weighed by using sensitive digital balance (Mettler AJ100). Then, the blocks were infiltrated with Sil-25 under 3 bars for 25 minutes and left for 24 hours. Weight measurements were performed again for the infiltrated blocks to estimate the percentage of each component (the starch powder and the SP) within fully infiltrated blocks.

4.4.6 SEM Analysis

SEM (Scanning Electron Microscopy) was undertaken. Slides were prepared for 12 different samples of silicone polymer infiltrated starch (SPIS) - printed blocks of starch infiltrated with Sil-25 and Promax10 in order to examine the quality of the infiltration of the silicone inside the printed structures. In addition SEM analysis was performed for a hand mixed composite of 40% starch powder incorporated into 60% Sil-25 SP by weight. The two components were mixed until a homogenous mixture was achieved. The mixture then poured into a 75x75x4 mm stainless steel mould, pressed and left at room temperature for 24 hours. After complete set, the block was cut in thin slices with a surgical blade and examined under the SEM.

4.5 Results

4.5.1 Infiltration Depth of Sil-25 Inside Starch and Plaster Cubes:

The dye coloration in the non-infiltrated areas of the blocks clearly defined the areas that were and were not infiltrated with the SP (Figure 4-3). Figure 4-8 illustrates the

depth of infiltration of Sil-25 into the starch cubes under normal air pressure. It can be seen that under normal air pressure the SP was unable to infiltrate deep inside the starch cubes. Time alone didn't show any obvious effect on SP penetration. Penetration depths for starch cubes under air pressure varied between 0.9±0.1 mm at 5 minutes to 1.4±0.1 mm at 25 minutes and for the plaster cubes under air pressure varied between 0.7±0.1 mm, at 5 minutes to 0.9±0.1 mm at 25 minutes (Figure 4-9).

Table 4-2, shows the penetration depth and standard deviation of Sil-25 into 20 mm starch cubes under air, 2 bar pressure and 3 bar pressure, it also shows the data for 20 mm plaster cubes under air and 3 bar pressure for different time period.

Table 4-2: Infiltration depth of Sil-25 in mm under different pressures into 20 mm starch and plaster cubes for different times.

Infiltration depth in mm					
Starch	5 min	10 min	15 min	20 min	25 min
Air	0.9±0.1	1.2±0.1	1.2±0.1	1.3±0.1	1.4±0.1
2 Bar	2±0.1	2.8±0.2	3.3±0.2	3.8±0.2	3.9±0.2
3 Bar	3.9±0.2	5.4±0.2	6.4±0.5	7.7±0.3	8.7±0.5
Plaster	5 min	10 min	15 min	20 min	25 min
Air	0.7±0.1	0.9±0.1	0.9±0.2	0.9±0.1	0.9±0.1
3 Bar	3.2±0.4	4.7±0.3	6.3±0.4	7.6±0.4	8.2±0.3

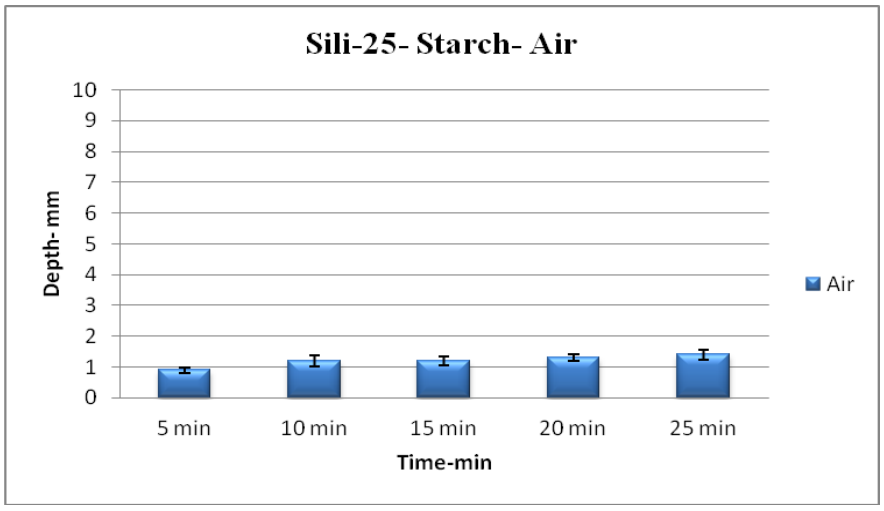

Figure 4-8: Infiltration depth of Sil-25 in mm into starch cubes in air.

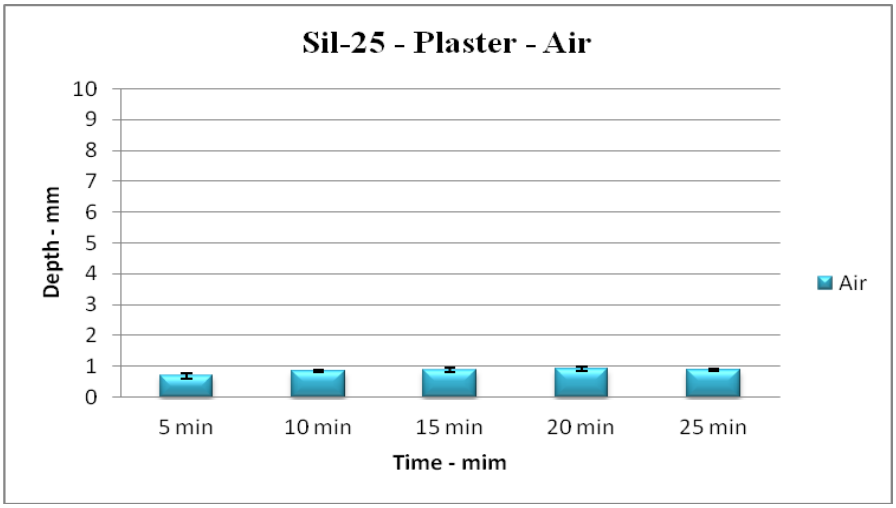

Figure 4-9: Infiltration depth of Sil-25 in mm into plaster cubes in air.

In contrast, applying 2 and 3 bar pressure had greater influence on the infiltration of SP inside the starch and plaster cubes as shown in Table 4-2. There was a significant differences *($p<0.05$)* between the subgroups – time intervals, and no significant difference *($p=0.26$)* was noticed for the infiltration depths between 20 minute and 25 minute. Two bar pressure showed less influence on the infiltration depth of Sil-25 inside the starch cubes than 3 bar pressure.

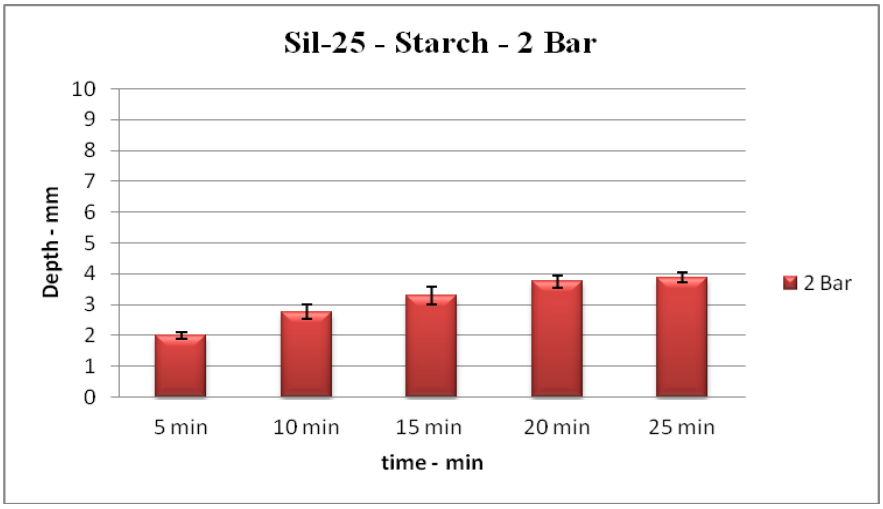

Figure 4-10: Infiltration depth of Sil-25 in mm into starch cubes at 2 bar pressure.

The infiltration depth of Sil-25 inside the starch cubes under 2 bar pressure varied between 2±0.1 mm at 5 minutes to 3.9±0.2 mm at 25 minutes (Figure 4-10). Under 3 bar pressure, the infiltration depth of Sil-25 varied between 3.9±0.2 mm at 5 minutes to 8.7±0.5 mm at 25 minutes (Figure 4-11). Statistically there was a significant difference *($p<0.05$)* between all subgroups - time intervals. Figure 4-12, illustrates the effect of time and pressure on the infiltration depth of Sil-25 into the starch cubes. Applying pressure had a significant effect on the degree of infiltration of the starch blocks. 2-way ANOVA revealed a significant difference *($p<0.05$)* in the infiltration depths between the 3 groups – under air pressure, 2 bar and 3 bar.

Figure 4-11: Infiltration depth of Sil-25 in mm into starch cubes at 3 bar pressure.

Under air pressure the depth of infiltration remained around 1mm and was not affected by the length of time of the infiltration process. The infiltration of Sil-25 under 2 bar pressure was higher than at normal air. However, application of 3 bars pressure increased the depth of penetration significantly and after 20-25 minutes the depth of penetration was of the order of 8 mm.

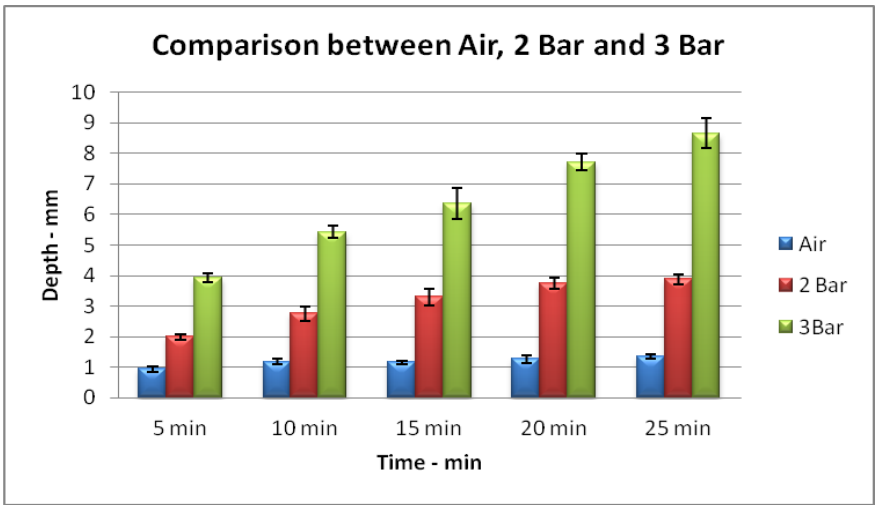

Figure 4-12: Effect of time and pressure on the infiltration of Sil-25 into starch.

Figure 4-13 reveals the infiltration rate of Sil-25 into plaster cubes under 3 bar pressure for identical time schedules. Again this chart illustrates the effect of pressure on the infiltration depth of Sil-25 into the plaster cubes. Under normal air pressure, the maximum penetration depth was less than 1 mm, while the penetration depth at 3 bar pressure at 25 minutes was more than 8 mm. One-way ANOVA showed a significant difference *($p<0.05$)* between all subgroups.

As with the starch cubes, Figure 4-14 shows a chart comparing the infiltration rate of Sil-25 into plaster under normal air pressure and 3 bar pressure. 2-way analysis of variance demonstrates that pressure significantly *($p<0.05$)* improves infiltration rates of Sil-25 into these cubes.

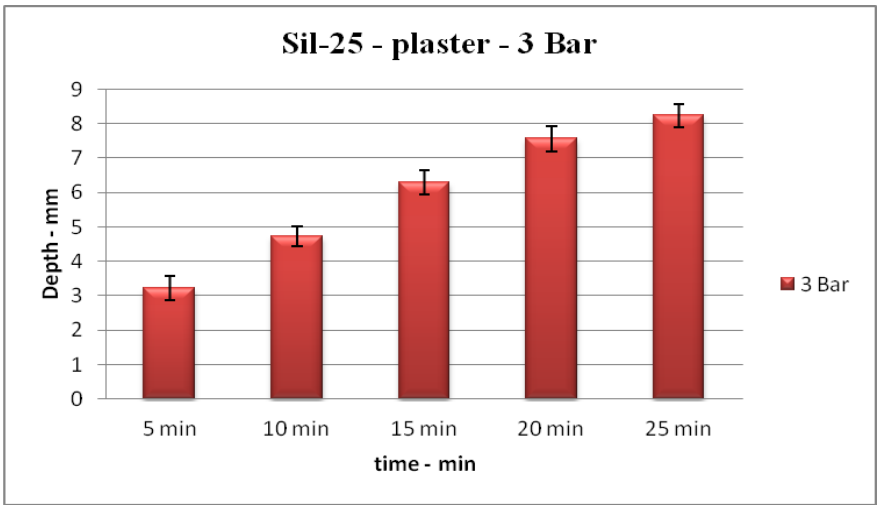

Figure 4-13: Infiltration depth of Sil-25 into plaster cubes under 3 bar pressure.

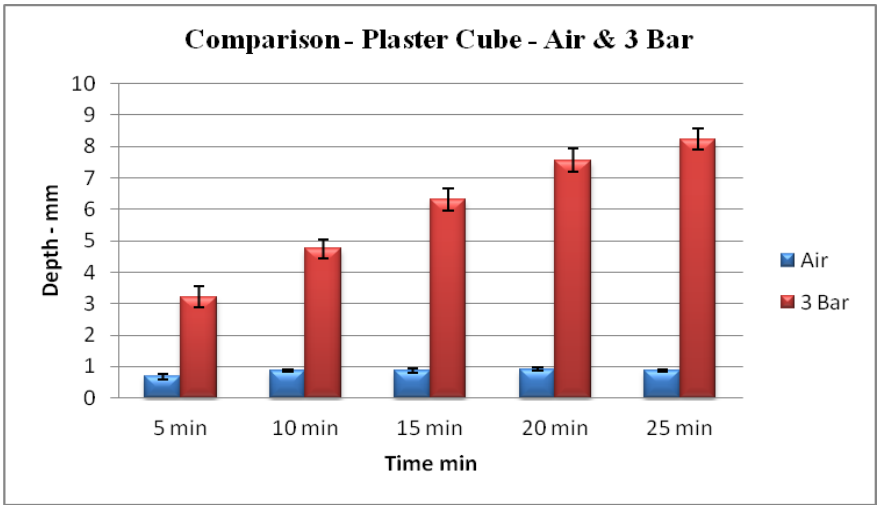

Figure 4-14: Comparison of infiltration of Sli-25 into plaster cubes under air and 3 bar pressure.

In Figure 4-15, the infiltration depths of Sil-25 into starch and plaster cubes at 3 bar pressure are compared. From these data it is clear that the infiltration into the starch and plaster cubes is similar (7-8 mm) for 20-25 minutes. 2-way analysis of variance showed no significant difference ($p>0.05$) in penetration depth of the SP between the starch cubes and plaster cubes.

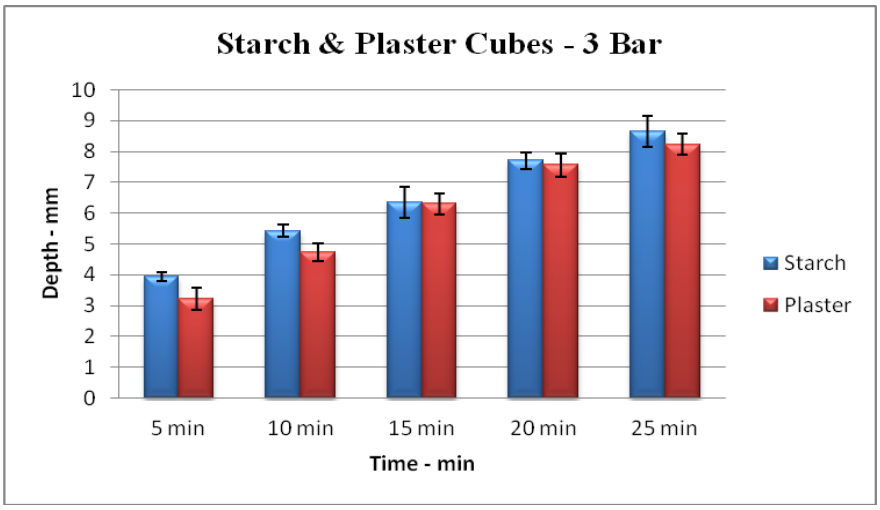

Figure 4-15: Comparison of infiltration depth for starch and plaster for Sil-25 at 3 bar pressure.

4.5.1.1 Infiltration of Promax-10 and M-3428 into starch cubes under 3 bar:

Table 4-3 shows the results for group 3 for Infiltration depth of Promax-10 and M-3428 compared to Sil-25 into 20x20x20 mm starch cubes under 3 bar pressure. Results demonstrate a minimum infiltration of 1.9±0.2 mm at 5 minutes and a maximum of 2.4±0.3 mm at 25 minutes for Promax-10 (Figure 4-16). Statistically, the only significant difference *($p<0.05$)* was between 5 minutes and 25 minutes, whereas no significant differences was recorded between the other subgroups *($p>0.05$)*. While M-3428 shows a minimum infiltration of 1.4±0.1 mm at 5 minutes and a maximum of 7.5±0.3 mm at 25 minutes (Figure 4-17). One-way ANOVA – Post Hoc tests showed a significant infiltration depth differences between all subgroups *($p<0.05$)*. This illustrates that there was no denotable increase in the penetration depths with Promax-10 under the same conditions as M-3428 and Sil-25.

When the infiltration depths of Promax-10 and M-3428 into the starch cubes at 3 bar pressure are compared to Sil-25 (Figure 4-18) it can be seen that Sil-25 has penetrated deeper than Promax10 and M-3428. A maximum of 8.7 mm is registered for Sil-25 at 3 bar pressure after 25 minutes against 2.4 mm and 7.5 mm for Promax-10 and M-3428 respectively under similar conditions. The Tukey's test revealed a significant difference *($p<0.05$)* in the infiltration depth between the 3 Silicone polymers for the scheduled times.

Table 4-3: Infiltration depth of Promax-10, Sil-25 and M-3428 in mm under 3 bar pressure into 2 cm starch cubes for different time schedule.

Infiltration depth in mm					
SP	**5 min**	**10 min**	**15 min**	**20 min**	**25 min**
Promax-10	1.9±0.2	2.1±0.3	2.1±0.1	2.2±0.2	2.4±0.3
M-3428	1.4±0.1	2.8±0.2	3.2±0.3	6.6±0.2	7.5±0.3
Sil-25	3.9±0.2	5.5±0.2	6.5±0.5	7.7±0.3	8.7±0.5

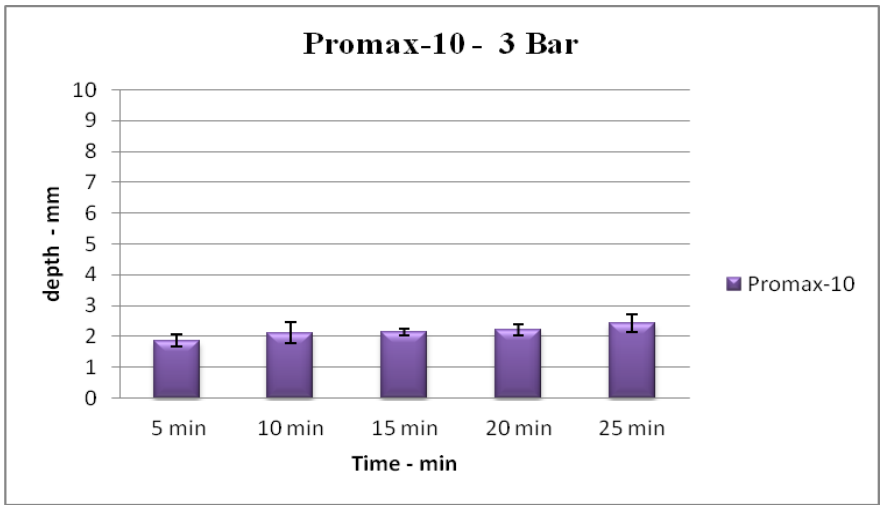

Figure 4-16: Infiltration of Promax-10 under 3 bar.

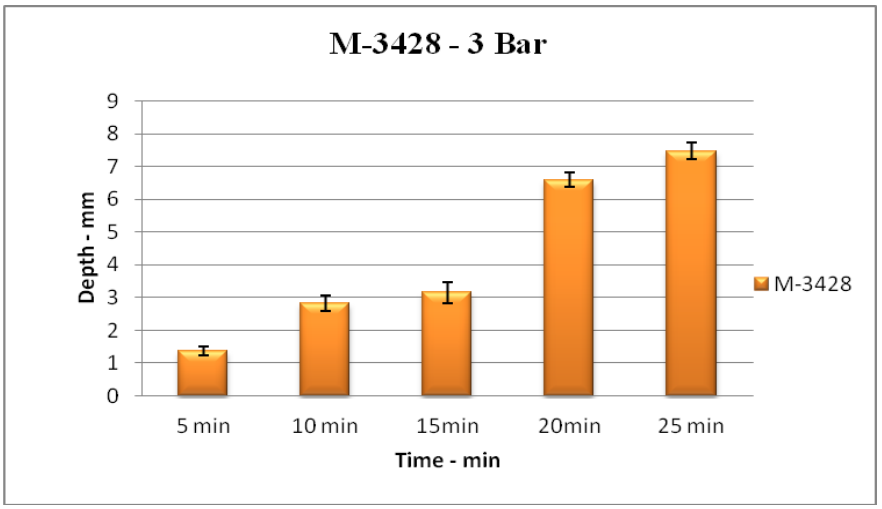

Figure 4-17: Infiltration of M-3428 under 3 bar.

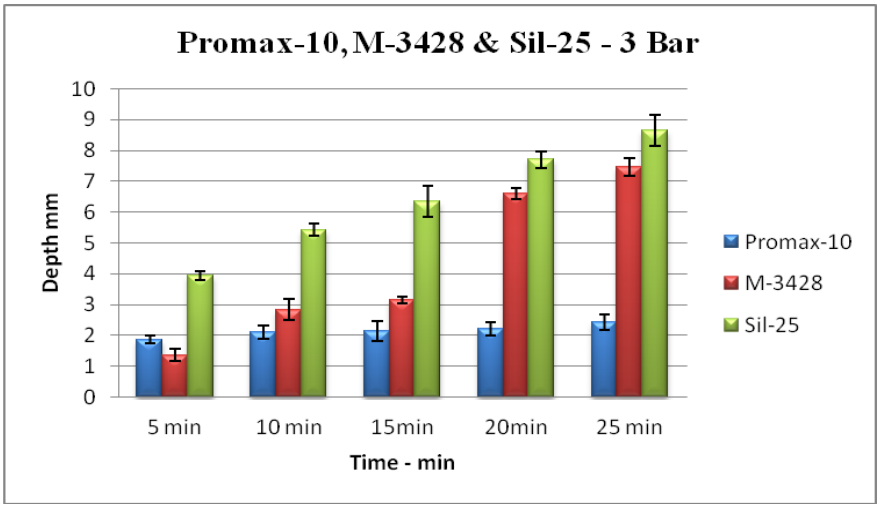

Figure 4-18: Comparison of infiltration depth between Sil-25, M-3428 and Promax-10 at 3 bar.

4.5.2 Silicone/Starch Ratio by Weight

Average weight and standard deviation of the starch blocks and the SPIS blocks, and percentage of each component within the fully infiltrated models are shown in Table 4-4 and Figure 4-19. Starch powder comprises about 40% of the total weight, whereas the SP adds up to 60% of the fully infiltrated blocks.

Table 4-4: Percentage of the starch powder and the silicone polymer in fully infiltrated blocks.

Weight in gm & SD		% by weight	
Starch	**Starch + Silicone P.**	**Starch**	**Silicone P.**
3.5±0.04	8.50±0.07	41.5%	58.5%

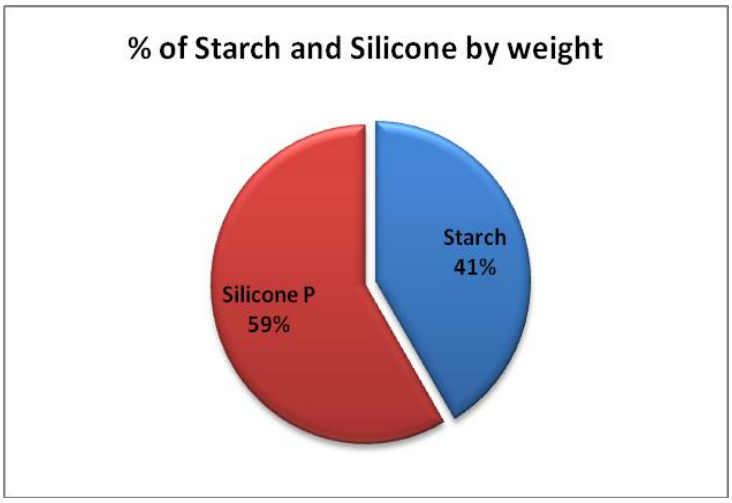

Figure 4-19: Percentages of starch and SP in fully infiltrated blocks.

4.5.3 Scanning Electron Microscopy

The SEM results for the silicone infiltrated samples showed amorphous, non-crystalline shaped particles with an associated variation in particle sizes. These particles appeared to be randomly orientated and showed a loosely packed arrangement with a small amount of spacing in between. Figures 4-20 and 4-21 demonstrate the shape and arrangement of starch powder under SEM at x50 and x340 magnification.

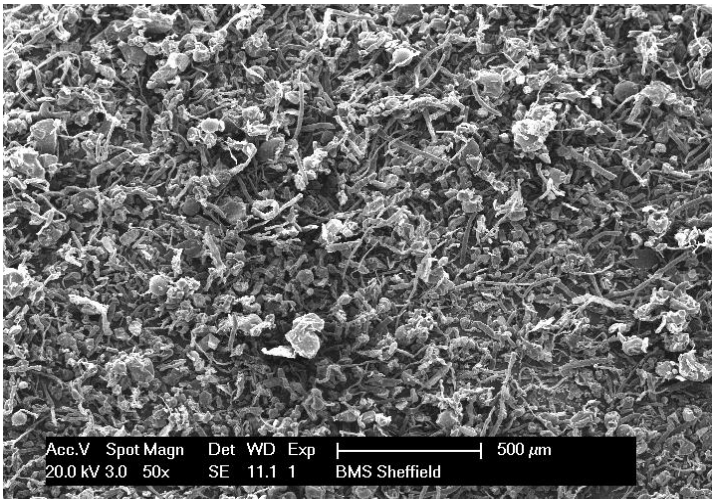

Figure 4-20: SEM starch particles x50.

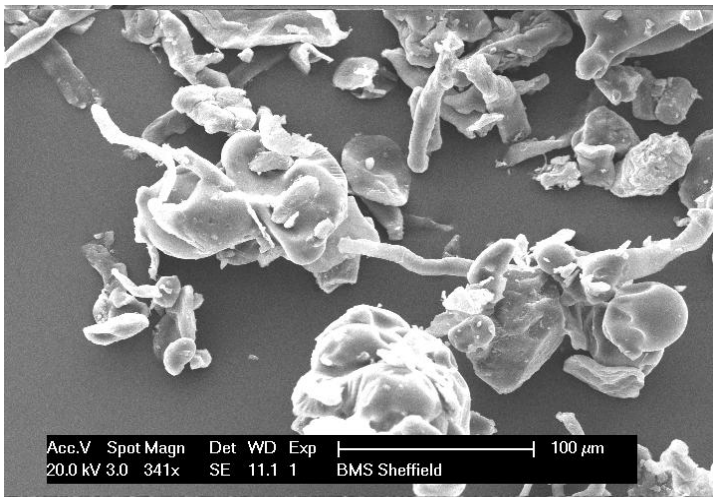

Figure 4-21: SEM starch particles x341.

SEM further indicates that there is a relatively disorganised distribution of starch particles within the silicone infiltrate for two of the MSPs used in this study, as SEM (x180) for Sil-25 and Promax-10 infiltrated inside starch blocks under 3 bar showing in Figure 4-22 and Figure 4-23.

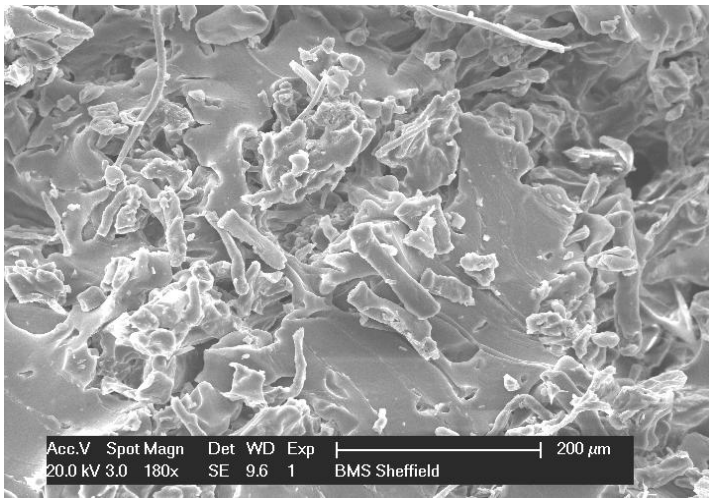

Figure 4-22: SEM for starch infiltrated Sil-25 (x180).

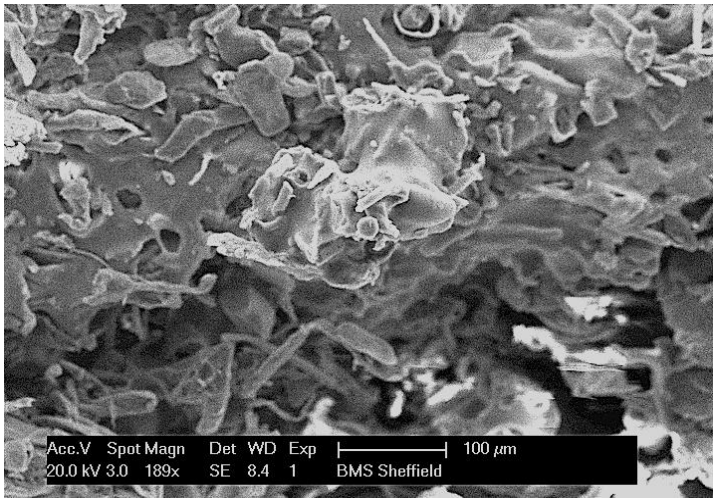

Figure 4-23: SEM for starch infiltrated Promax10 (x189).

However, SEM for 40 wt% starch powder incorporated into 60 wt% Sil-25 SP by hand mixing is shown in Figure 4-24 and Figure 4-25. This revealed a more homogeneous and coherent distribution of the starch powder and the SP with fewer gaps and spaces in between, higher magnification revealed narrow gaps or spaces around the starch particles as an indication for lack of integration between the starch particles and the SP (Figure 4-25).

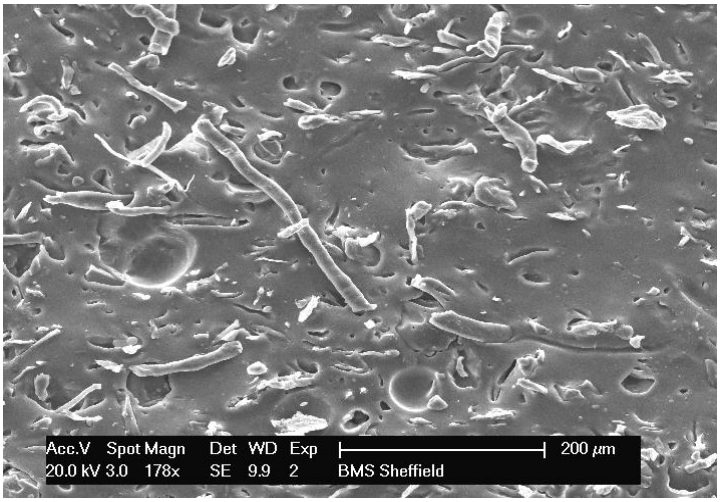

Figure 4-24: SEM for Sil-25 hand mixed with 40% starch by weight (x178).

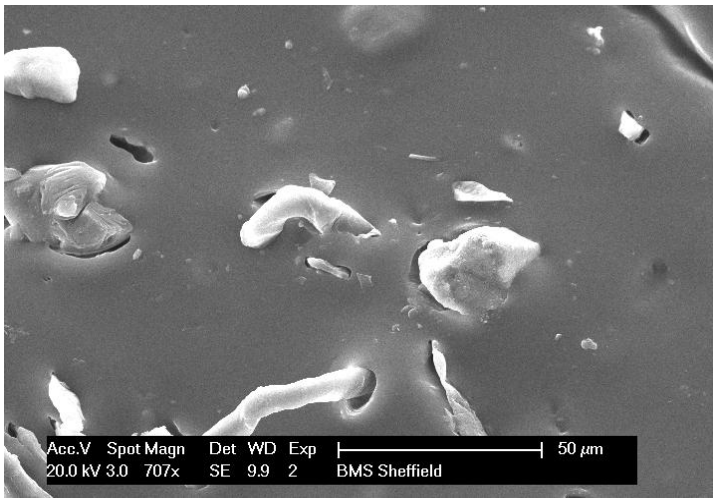

Figure 4-25: SEM for Sil-25 hand mixed samples showing spaces around the starch particles (x707).

4.6 Discussion

The penetration of the infiltrant inside the printed models is determined by the time and pressure that the samples were subjected to and these were influenced by the degree of viscosity of the polymers used as infiltrants and their curing rates. This view has been supported previously - (Gatto et al., 2011). Therefore, a higher penetration rate could be achieved with a low viscosity SP.

The infiltration depth of Sil-25 SP inside the two different cubes; the starch cubes and the plaster cubes were evaluated in order to explore if the type of the powder used for printing could have had any influence on the penetration depth. Moreover, the infiltration depth of 3 different SPs; Sil-25, Promax-10 and M-3428 inside the starch cubes were evaluated to explore if different infiltrants possessing different physical properties have a different effect on the penetration depth. Furthermore, different pressures and different time frames were applied to assess the penetration depth of Sil-25 SP inside the starch cubes. The objective was to explore if the infiltration depth can be influenced by different conditions including type of the powder and infiltrant used and time and pressure.

The data obtained clearly show that the use of ambient air pressure has no real influence on the penetration of SPs into starch or plaster printed cubes. That is probably due to the relatively high viscosity of the SPs used and the higher concentration of the

likely hood that the binder at the external surfaces of the printed blocks acted as a barrier to the flow of the SP inside the blocks. It was therefore concluded that an increase in pressure was required to try and improve the rate of infiltration. The data obtained clearly show that the use of pressure has a very positive influence on the depth of penetration of the SPs. again this is supported by previous reports (Quail et al., 2009). It can also be seen that time alone was unable to help the SP infiltrate deep inside the starch and plaster cubes. Furthermore, the results showed that the infiltration depth was not affected by type of the powder used for printing the cubes, since no significant differences in the infiltration parameters were shown between the starch cubes and the plaster cubes. It was also been observed that printing with starch produces softer and more flexible parts after their infiltration with SP and thus appear to be more suitable for producing soft tissue prostheses. Therefore, group 3 experiments; promax-10 and M-3428 were evaluated for their infiltration depths on starch cubes only.

Data showed that pressure has a significant impact on the penetration depth. When the infiltration process was performed at 2 and 3 bar pressure, the penetration of the SP increased considerably. However, the penetration depth of the SP under 2 bar pressure was less than at 3 bar pressure. This indicates that higher infiltration depth can be achieved by increasing the pressure applied. Since the items printed can be infiltrated from all sides this would suggest that the maximum depth of infiltration for a prosthesis will be 16 mm. Therefore as long as the prosthesis is not more than 16 mm thick full penetration with Sil-25 and Matrix M-3428 SPs can be achieved. It can also be reasonably argued that a depth of penetration of 15 mm will be adequate for most applications for this project.

When comparing the penetration depth under pressure between Sil-25, Matrix M-3428 and Promax-10 into the starch cubes, the data showed significantly higher effectiveness of Sil-25 and M-3428 in penetrating the cubes when compared to Promax-10. These differences can be attributed to the setting time and viscosity of the different maxillofacial SPs. Promax-10 has a quicker setting time and therefore gets more viscous after a shorter period of time after mixing both silicone components. In other words, Promax-10 has a shorter working time than Sil-25 and M-3428 to permit penetration of the SP inside the printed structures. The infiltration process slows down when the viscosity starts to increase as part of the normal setting reaction.

Although we determined in group 2 of these experiments that we could achieve a maximum infiltration depth of 8 mm, we did not understand how consistent/homogeneous this infiltration was. The SEM analysis was undertaken to answer this specific question. Macroscopically the samples look fully infiltrated and smooth. However, under SEM the infiltrated blocks show evidence of porosity that look like patches or small spaces within a confluent albeit textured base (Figures 4-22 and 4-23). This may be related to the viscosity of the silicone polymer used and/or wettability factors of the individual constituents. Silicone polymers generally have a low surface-free energy and are very hydrophobic (Waters et al., 1999), whilst starch is hydrophilic. The presence of unfilled patches potentially occurs when air is trapped at the central part of the cubes after the SP starts to penetrate inside from all aspects under the effect of pressure. These factors may explain the reduced homogeneity and coherence between the SP and the starch particles as shown in Figure 4-25. This magnified (707x) image for mixed starch particles and SP shows gaps around each particle, which indicates a lack of interaction and coherence between the starch particles and the SP even when the two components were mixed adequately for one minute. This phenomenon is attributed to the hydrophobic nature of the SP (Jayasekara et al., 2004), and this will influence the general properties of the final product. Figure 4-24 shows a more homogeneous distribution of the starch powder inside the SP with fewer voids shown after hand mixing of both components compared to starch infiltrated silicone samples (Figure 4-22 and Figure 4-23). This is probably caused because the printed samples are sealed from outside by the binder, which acts as barrier for infiltration of the SP inside the printed blocks.

An additional point to consider in our experience is that the infiltration depth appears to be relatively dependent on the setting time of the SP. Therefore, although the preferred SP - Sil-25, may allow for maximum infiltration (increased setting time) it may compromise the homogeneity of the test sample/prosthesis and thus the mechanical properties. In contrast, reducing the setting time will reduce infiltration depth and compromise the test samples/prosthesis as a whole. We feel the former is preferable especially when investigations assessing the two SPs under SEM revealed very little difference in terms of homogeneity. This is demonstrated in Figure 4-22 and Figure 4-23. Therefore, Sil-25 was selected rather than Promax-10 and Matrix M-3428 as an

infiltrant for the mechanical properties samples and colour samples. In the next sections when we refer to silicone polymer (SP) that means Sil-25.

4.7 Conclusions

1- Pressure has a significant impact on infiltration depth of the silicone polymers. The depth of penetration of Sil-25 and Matrix M-3428 into starch under 3 bar pressure is sufficient for prostheses that are upto15 mm thick.
2- Two bar pressure is less effective than 3 bar for infiltration of the starch models.
3- Promax-10 is considered a poor infiltrate, because it has a quick setting time and poor penetration rate.
4- SEM revealed the presence of porosity and lack of integration between the starch particles and the silicone polymers within the infiltrated areas of the printed blocks, whereas samples prepared by hand mixing of starch particle into the SP revealed fewer voids.

5 The Mechanical Properties of the 3D Printed Silicone Polymer Infiltrated Starch Models

5.1 Introduction

Any facial prosthesis is an artificial appliance used to correct a facial deformity; it is used as a temporary or a permanent substitute. However, it supports the patient's psychological wellbeing and social life and improves his or her self-esteem by restoring aesthetical and functional demands (Haug et al., 1999b).

Reproducing the patients' morphology and colour details appropriately is a challenge; it requires highly skilled maxillofacial technicians in order to achieve patient satisfaction with the prosthesis. Although optimal aesthetics are the patients' main concern when using facial soft tissue prostheses, the short service life is also considered one of the patient's main complaints following deliver (Chang et al., 2005). Periodic replacement of these prostheses requires an intensive fabrication schedule, which burdens both the patient and technician in term of time and convenience. In order to achieve optimal aesthetics the prostheses must be fabricated from highly characterised materials that possess suitable mechanical properties to resist chemical and physical deterioration (Mancuso et al., 2009c, Mancuso et al., 2009b).

After delivery, the prostheses lose elasticity and become rigid especially at the peripheries. This usually manifests itself as early marginal tearing following daily removal of the prosthesis and application and removal of a medical adhesive. Therefore improved mechanical properties are required to achieve a more comfortable and more durable prostheses that can resist degradation in mechanical and optical properties of the prostheses (Farah et al., 1987).

Although most of the maxillofacial SPs used now do not fulfill the ideal properties, they have shown mechanical properties and material biocompatibility that keep them in service for sufficient time.

High tear strength and low hardness are essential factors for functional maxillofacial SP (Chalian and Phillips, 1974). Tensile strength indicates overall strength characteristic of the prosthesis (Waters et al., 1997), while high tear strength secures the marginal integrity and durability of the prosthesis in practical service, especially for adhesive retained prostheses (Aziz et al., 2003). Hardness contributes to the flexibility and softness of the final prostheses (Lewis and Castleberry, 1980), whereas percentage

elongation is a feature of the overall flexibility of the prostheses and defines their resistance to tear during maintenance.

The printed starch models produced by the Z-Corp printer are solid but fragile; they are robust enough to be manipulated but must be handled carefully prior to infiltration. The infiltrated silicone rubber provides them with strength and elasticity.

The mechanical properties and the final product are influenced by three factors;

1) Type, amount, size and configuration of the filler particles within printed models; starch powder is used by Z-Printer (Z510) to act as a structural framework for the prostheses.
2) Type of the binders and the colorants used to hold the starch particles together and adding colour to the printed models. The binder not only provides the printed models with colour, it also acts as the glue for holding the starch particles together during the printing process. The printer is supplied with four different water based binders, the clear, yellow, cyan and the magenta, which feed the inkjet with different coloured binders according to colour information received by the printer at the time of printing.
3) Type and the characteristics of the infiltrant used to infiltrate the printed models. In this instance maxillofacial SPs are used for infiltration of the printed facial prostheses.

5.2 Aim

The aim of this part of the project was to evaluate the mechanical properties of the starch printed models infiltrated with maxillofacial silicone polymer, and compare them to the existing maxillofacial materials used.

5.3 Materials and Methods

5.3.1 Silicone Infiltrated Starch Specimens

Test specimens were designed using SolidWorks 2008 software and then printed by the Z-Corp printer. The test specimens were printed in starch and allowed a 24 hours post printing “dry” and then infiltrated with Sil-25 maxillofacial SP under 3 bar pressure for 25 min in order to achieve total infiltration. The specimens were left for 24 hours in

order to achieve complete set before performing the mechanical tests. The test specimens were designed according to industry standards and set out to evaluate key mechanical properties.

5.3.1.1 Test designs and measurements:

1- Tensile strength:

Ten dumbbell shaped specimens were produced for testing tensile strength and percentage of elongation in accordance with ASTM-D412/ISO (ASTM-D412, 1981), (Figure 5-1).

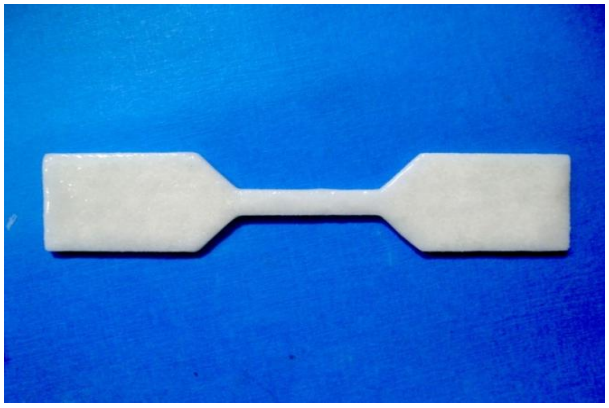

Figure 5-1: Dumbbell-shaped specimens ASTM-D412/ISO34.

Figure 5-2: Tensil tester used for testing tensile strength.

Tensile strength testing was conducted using a Lloyd LRX tensile instrument; load rating 100 N at a constant crosshead speed of 25 mm/min (Figure 5-2). The tensile strength was calculated using the following equation:

$\sigma_f = F/A$

Where: σ_f = tensile strength (MPa), F = force at failure (N),
A = original cross-sectional area (mm^2).

2- Tear strength:

Ten test specimens, in accordance with ASTM D624-07/ISO34 (trouser leg) (ASTM-D624, 1981) for testing tear strength, were fabricated for this test (Figure 5-3). Tear strength was conducted using a Lloyd tensile tester (Figure 5-4) and calculated by the following equation:

T=F/D

Where: T is tear strength (N/mm), F is the force required to break the specimen (N), D is thickness of the specimen (mm).

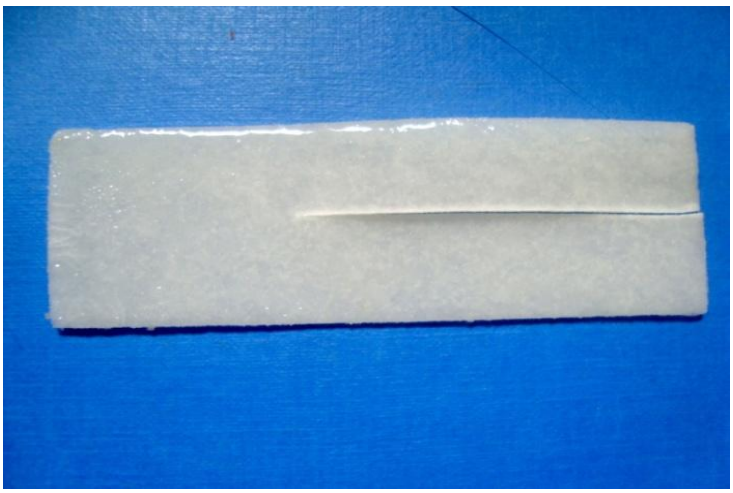

Figure 5-3: Trouser-shaped specimens ASTM-D624-07/ISO34.

Figure 5-4: Tensile tester used for testing tear strength.

3- Percentage elongation:

Elongation prior to failure was performed at the time of measuring tensile strength. Ultimate elongation was calculated using the equations below:

% Elongation = $100\times(L-L_0)/L_0$.
Where: L represents extension at break, L_0 represents the original length.

4- Hardness:

Test specimens, in accordance with ASTM D1415-06 ISO48 (solid blocks) for testing Shore A Durometer hardness, were produced. Four specimens were fabricated for this purpose (Figure 5-5) and the hardness test carried out using a Shore Scale Durometer, Hardness Tester (England) (Figure 5-6), with 6 mm measurement course, 6 mm distance between the measurements and keeping 6 mm away from the border.

Figure 5-5: Hardness Test Specimens ASTM-D1415-06/ISO48.

Figure 5-6: Shore Scale Durometer Hardness Tester (England).

5.3.2 Silicone/Control Specimens

In order to provide a comparison, control specimens were made from pure SP. The samples used as controls were manufactured to the exact dimensions as the test samples. They were prepared from pure SP (Sil-25) using custom made stainless steel moulds (Figure 5-7). These were designed and manufactured according to ASTM specifications and were made specifically for this project. Specimens for tensile strength, elongation, tear strength and hardness were fabricated by mixing the two 2 components of the SP, Sil-25 (10:1) for one minute – as per the manufacturer's instructions. The mix was then

poured into the stainless steel mould, pressed and left under pressure at room tempreture for 24 hours (Figure 5-8).

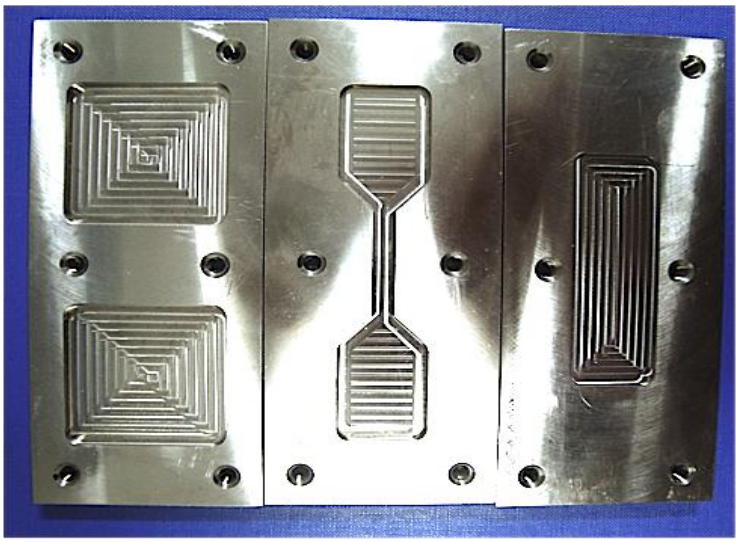

Figure 5-7: Stainless steel moulds designed according to ASTM specification for production of tensile, tear, hardness and percentage elengation test.

Figure 5-8: SP – Sil-25 specimens for tensile, tear, hardness and elongation testing.

5.3.3 Statistical Analysis

The entire resultant data was collected and subjected to PASW statistics 18 in order to make the comparison between the test group (SPIS) and the control group pure (SP). Independent sample T test was employed for the analysis.

5.4 Results

5.4.1 Tensile Strength and Tear Strength

Following testing the SPIS specimens demonstrated a lower tensile strength and tear strength than the pure SP test samples. The average tensile strength for SP specimens was 3.5±0.3 MPa, while the average value of tensile strength for the SPIS samples was 1.2±0.2 MPa. Similarly tear strength was decreased from 12.2±1.5 N/mm for the SP specimens to 8.5±1.1 N/mm for the SPIS printed samples (Table 5-1). However, it could be seen that the percentage reduction in tear strength was demonstrably less when compared to the reduction in tensile strength, 64 % and 30 % respectively. The data described in Figures 5-9 and 5-10 for tensile strength and tear strength respectively and according to the statistical analysis the differences were significant *($p<0.05$)*.

Table 5-1: Average and standard deviation values of the printed and control samples.

Sample	Tensile Strength MPa	Tear Strength N/mm	Hardness Shore A	Elongation %
Control	3.5 ± 0.3	12.2 ± 1.5	30.9 ± 0.7	511 ± 57.5
Printed	1.2 ± 0.2	8.5 ± 1.1	62.8 ± 2.8	244 ± 36.1

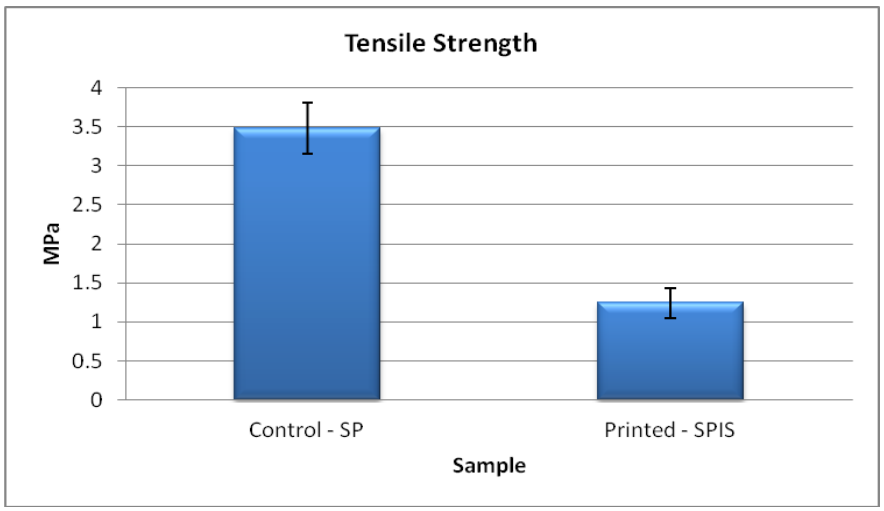

Figure 5-9: Tensile strength for SP& SPIS specimens.

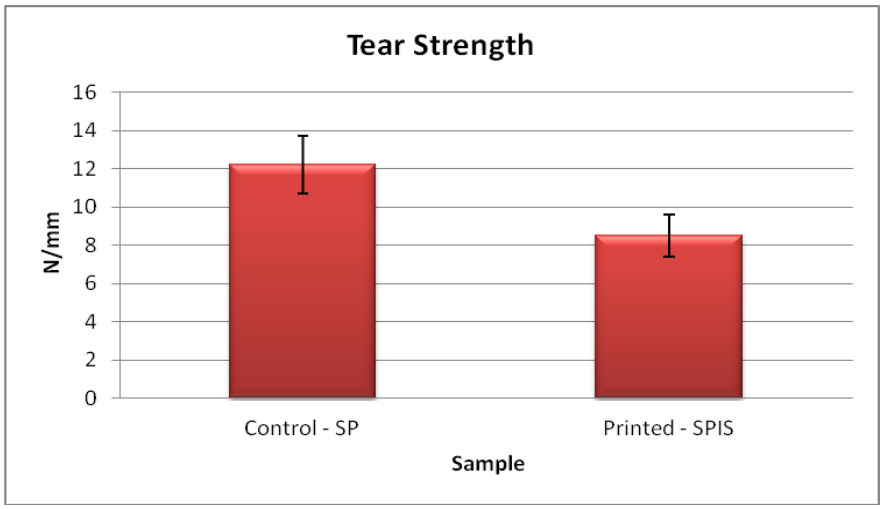

Figure 5-10: Tear strength for SP& SPIS specimens.

5.4.2 Percentage Elongation:

The SP control specimens demonstrated a 511% elongation prior to fracture, while the SPIS printed specimens demonstrated a lower percentage elongation of 244% (Table 5-1 and Figure 5-11). There was a significant difference *($p<0.05$)* in the data for Pure SP and SPIS samples.

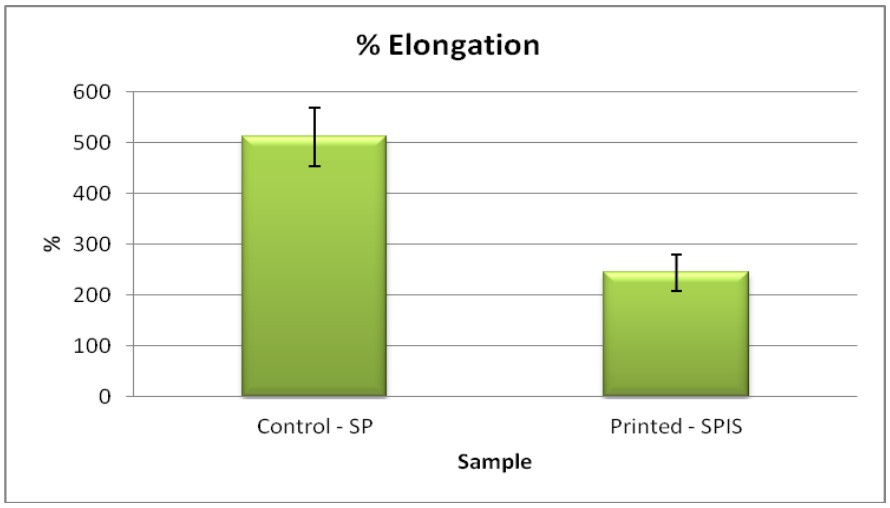

Figure 5-11: Percentage elongation for SP& SPIS specimens.

5.4.3 Hardness Test:

Shore (Durometer) hardness A for Sil-25 was 30.9±0.7 and this is shown in Table 5-1. However, the hardness of the Silicone polymer infiltrated starch (SPIS) test specimens was more than double that demonstrated by the pure SP test specimens - 62.8±2.8. The data is illustrated in Figure 5-12, and according to the statistical analysis, the difference was significant *($p<0.05$)*.

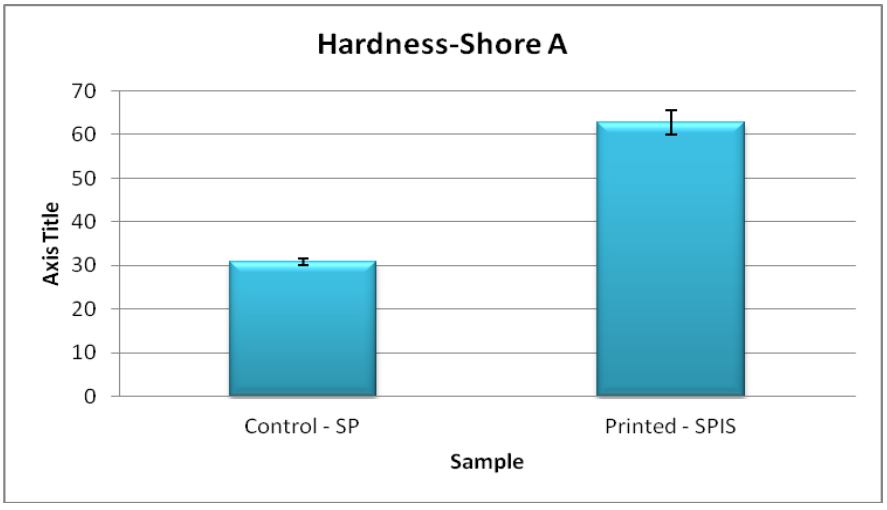

Figure 5-12: Hardness test Shore A for SP& SPIS specimens.

5.5 Discussion

The method of assessment that has been adopted was to assess a range of properties according to ASTM standards. These properties are: tensile, strength, tear strength, hardness and percentage of elongation. In terms of measurement of these properties, there were no technical problems relating to the methodology applied since ASTM standards were followed. However it could be argued that there was some reservation about the elongation percentage evaluation as this was measured from the extension of the tensile machine at the time of measuring tensile strength rather than an extensometer, which may not present a fully accurate measurement of extension. During the measurement some of the materials may pull out of the grips and this may lead to disproportion degree of extension and not the true extension.

In terms of selection of the properties measured, this study aimed to follow previous researchers and reports that have been performed and seemed to be the properties that have been measured: these would provide good characterisation of the materials evaluated and how these properties would be compared with the measurements undertaken by other researches (Polyzois et al., 2000, Li et al., 2007, Eleni et al., 2009a, Hatamleh and Watts, 2010c).

Variation in the mechanical data between the samples can be attributed to the weight or volume ratio of silicone (infiltrate) to starch (filler). In this project the starch provides a scaffold for the SP that is used when making prostheses. Inevitably the presence of a filler material is going to affect the properties of the samples produced. However, these changes may be irrelevant – or may even be an advantage. As detailed, the presence of a filler tended to increase the hardness of the samples whilst reduce the tensile and tear strength.

As shown in a previous chapter - section 4.5.2., the percentage of starch powder by weight in a fully infiltrated block is about 40% of the total weight, and the infiltrant constituted 60% of the total weight. In this series of experiments it is acknowledged that the amount of starch added is significant – approximately 40 %. This is the proportion used by Z-Corp printer to produce the printed 3D models. Although the density can be adjusted this amount of starch is the minimum that can be produced – any less and the model becomes too fragile. However, this does allow for the maximum proportion of silicone to be added.

SEM also showed lack of coherence between the starch particles and the silicone polymer, the two components have different behaviour toward each other. The SP is extremely hydrophobic with very low surface energy, while starch is extremely hydrophilic. The SEM pictures demonstrated textures filled with gaps and spaces around the starch particles which indicates lack of integration between the starch particles and the SP, in other word the starch within the samples can be consider as a potential space inside the silicone rubber. Thus, it was expected that this would lower the values of the mechanical data especially tear strength, tensile strength and elongation of the test printed (SPIS) samples compared to control (SP) samples. It was also expected that there would be an increase in the Shore A hardness as 40% of the total weight replaced by starch.

These characteristics may, in part, be dictated by the material used. We know the SPs are not "ideal", but are the best available at present. In this study we used SP as an infiltrant because it is the material always used for producing soft tissue facial prostheses, moreover we considered it a control group for comparison purposes despite not being the ideal material, and thereby the material we used could have characteristics are potentially more favourable - the mechanical properties of the printed samples could be perfectly adequate or in some respects better when compared to traditional SP.

Furthermore, the differences in the mechanical properties could be explained by starch powder comprising approximately half of volume within the sample with the quantity of silicone infiltrate reduced when compared to the control samples. In order to explain these results the SEM experiments have provided some answers – although not all – see section 4.5.3.

In these investigations hardness test values increased and the samples had lost some flexibility in the SPIS (printed) when compared to pure SP (control group). However, hardness itself is not the only determination criteria for the "overall" toughness of the printed parts; the design can also influence the flexibility of the prostheses. In this project we utilised CAD/CAM principles to design and manufacture soft tissue facial prostheses. Unlike the handmade prostheses, CAD allows the production of shell prostheses which are lighter and more flexible than those produced by hand (Ciocca et al., 2010). Due to technical limitations, the maxillofacial technicians are not always able to produce shell prostheses. Therefore, despite the higher values of Shore A hardness for the SPIS samples compared to the pure SP samples, the prostheses

produced by applying CAD/CAM technology can be more flexible than the handmade SP prostheses.

Tear strength values for the printed samples reduced after infiltration with SP about 30%. However, this is not a critical problem since the 3D printed prostheses in this project were designed to be infiltrated with silicone rubber which would extend to the peripheries to achieve a feathered edged prosthesis in order to blend the margin of the prosthesis with the patient's natural skin tissues. Tears usually start at the flange which is finished with pure silicone rubber and the prosthesis is going to tear there during cleaning and removal of the adhesive from the margin. Therefore, as with a traditional prosthesis a tear will start in the silicone rubber at the periphery and not in the starch itself. It may well become an issue when the feathered edge has torn through the silicone into the starch, but it could be argued that by that stage the prosthesis should be replaced anyway. Hence, the reduction in tear strength is not a critical point especially with implant retained prostheses when no adhesive is required for retention. The drawback in tensile strength and percentage of elongation values will not be a critical problem if the patient looked after his/her prosthesis properly. It would be dependent on how the patient follows the instructions of maintenance and how to take care of the prosthesis in order to optimise service life. Indeed the patient may not have to stretch the prosthesis for maintenance purposes and during placement and removal. As a matter of fact very high tear strength is not required for facial soft tissue prostheses unless the patient manipulates the prosthesis harshly.

In this study the results of the mechanical tests performed on tensile strength, tear strength, the percentage of elongation and hardness for the printed samples were found to be significantly different from the control samples. This does not necessarily means that the new material would be worse or better. Indeed we really don't know because it is yet not clear what the optimal properties are for making facial prostheses. The ideal properties have not been standardised yet in terms of the mechanical properties.

On the basis of the information obtained from the mechanical data, there is nothing to suggest that these prostheses shouldn't last as long as the existing handmade silicone prostheses. Furthermore, the feel and handing characteristics of the new material appear as good as if not better as the existing silicone rubber prostheses. Although it is acknowledged that this is a subjective evaluation.

5.6 Conclusion:

1- The mechanical properties of the SPIS specimens are different to those made of pure SP.
2- There is an increase in Shore A hardness, but a decrease in tensile strength, tear strength and percentage of elongation.

6 Effect of Weathering Conditions on the Mechanical Properties of Silicone Polymer Infiltrated Starch Sample[2]

[2] Part of this work on mechanical durability of SP prostheses has been presented as a poster at the BDOSR 2011, Sheffield 12th – 15th September – Appendix A - The Abstract.

6.1 Introduction

Facial prostheses need to be replaced on a regular base as a result of degradation of the physical properties of the SPs, (Haug et al., 1999b, Takamata et al., 1989), mainly resulting in tearing of the feathered edges and colour fade of the prostheses (Jani and Schaaf, 1978, Hooper et al., 2005). In general it can be expected that the prosthesis needs to be replaced every 6-12 months (Jebreil, 1980, Chen et al., 1981, Haug et al., 1999b), although a range from 3 to 14 months service life has been suggested by (Polyzois et al., 2011, Hooper et al., 2005, Lemon et al., 1995). Ultimately the life span of the facial prostheses is dependent on the inherent properties of the material used and behavioural factors of the patients using the prostheses (Stathi et al., 2010).

Deterioration of the delivered prosthesis starts immediately after it has been made and fitted, and will affect both the colour and overall integrity of the prosthesis (Goldberg et al., 1978, Beumer, 1996). The degree of success or failure of this type of treatment is dependent on the ability of the prostheses to resist alteration in the mechanical and optical properties under natural weathering conditions (Craig et al., 1978). Factors affecting the prosthesis are UV radiation from sunlight and other weathering conditions including temperature, moisture and hand contact during removal and cleaning (Chen et al., 1981, Hanson et al., 1983). Furthermore, the use of adhesives for retention can also lead to changes in colour and stiffness of the prosthesis. With time the prosthesis loses its elastic properties and becomes rigid. This can become a significant problem at the margin of the prosthesis as it can lead to lack of adaptation to the surrounding tissues and tearing.

Many articles have discussed the use of accelerated weathering and weathering chambers to simulate normal life weathering conditions and to assess the overall deterioration of materials (Sweeney et al., 1972, Gary et al., 2001, Kiat-Amnuay et al., 2002). Accelerated weathering is used to simulate the long term effect of outdoor natural weathering conditions by utilizing the most aggressive components of weathering - ultraviolet radiation, moisture and heat. The two widely used accelerated weathering testers are the Q-Sun and QUV. Each produce light, temperature, and moisture in different ways. The major difference is the type of light used by both machines, Q-Sun utilizes xenon light, which is similar to sunlight (295nm - 800nm),

while QUV uses the most harmful part of sunlight which is UV light with a spectrum of electromagnetic wavelength from 300 nm- 400 nm (QUV&Q-Sun, 2012).

6.2 Aim

The aim of this part of the project was to test the effect of natural and accelerated weathering conditions on the mechanical properties of 3D printed starch samples infiltrated with a maxillofacial silicone polymer.

6.3 Materials and Methods

6.3.1 Part 1: Exposure to Natural Weathering Conditions

6.3.1.1 Test design and measurements:

The test specimens were designed according to industry standards as detailed before (Chapter 5), and set out to evaluate key mechanical properties of the SPIS (Sil-25) under different natural weathering conditions. These conditions included day light room ambiance and a dark room ambiance and the outdoor weather conditions to expose the samples to natural weathering. Test groups included pure SP and SPIS specimens. Types and the total number of samples used in this study are demonstrated in Table 6-1 A total of 72 samples were used in this study[3], one set produced from printed starch and infiltrated SP, and the second set were produced from pure SP 'Sil-25'.

Two sets of 15 dumbbell-shaped and 15 trouser-legs samples – 5 for each subgroup for testing tensile strength, tear strength and another 2 sets of 6 for hardness SP and SPIS samples, 2 samples were allocated for testing Shore A durometer for each group.

6.3.1.2 Group 1 - Outdoors weathering group:

Specimens were exposed to natural weathering and UV light from sunlight; these specimens were placed in a plastic container in the garden for 4 months during July, August, September and October 2011.

[3] Power analysis test was performed to define the sample size by using "nQuery" software and test results are attached to Appendix F.

Table 6-1: Types and number of samples (SP & SPIS) used for each test group.

Samples	Dark Group	Indoor Group	Outdoor Group	No. of Samples
	Number of samples - (SP)			
Dumbbell-shaped	5	5	5	15
Trouser-legs	5	5	5	15
Hardness	2	2	2	6
	Number of samples - (SPIS)			
Dumbbell-shaped	5	5	5	15
Trouser	5	5	5	15
Hardness	2	2	2	6
Total	24	24	24	72

6.3.1.3 Group 2 - Indoors 'window' weathering group:

Specimens were left on a window ledge in order to be exposed the samples to sun light at daytime and ambient room temperature and humidity for 4 months.

6.3.1.4 Group 3 - Time passing 'dark' group:

Samples were stored in a sealed glass container in complete darkness at room temperature and humidity for 4 months (Polyzois et al., 2011).

Results were compared to a previously tested control group at 'zero' time, 24 - 48 hours after complete setting was achieved.

6.3.2 Statistical Analysis

Statistical analysis was performed for the resultant data by using PSAW statistics 18, one way analysis of variance ANOVA was employed in order to make comparisons between the control groups and each test group for the SP and the SPIS specimens to determine the effect of different natural weathering conditions on the mechanical properties of the SP and SPIS specimens used in this study.

6.3.3 Part 2: Exposure to Artificial Weathering Conditions

6.3.3.1 Test design and measurements:

The method used for testing the effect of UV light and weathering on the mechanical properties of the printed specimens (SPIS) and pure SP specimens was to expose them to accelerated weathering conditions for 2 and 6 weeks. A Q-Sun Xenon test chamber (Xe-1-BC1/SC) was used and a window glass filter was added in order to produce a spectrum in the critical short wave UV region (295 nm - 400 nm), (Figure 6-1). Test samples were exposed to cycles of UV light and moisture at 50-70° C, as shown in Table 6-2.

At the end of the experiment tensile strength, tear strength, Shore A durometer hardness test and percentage elongation were measured and the results were compared to that of the control group. The experiment was divided into 2 main groups.

Figure 6-1: Q-Sun Xe-1 Xenon test chamber.
http://www.q-lab.com/en-us/products/q-sun-xenon-arc-test-chambers/q-sun-xe-1

Table 6-2: The 24 hour cyclic exposure in Q-Sun test chamber.

N.	Accelerated Weathering	hrs per day
1	UV	6
2	UV + Water	2
3	UV	2
4	UV + Water	2
5	Dark	8
6	UV	2
7	UV + Water	2

6.3.3.2 Group 1 - Silicone polymer specimens:

Group 1 - Series 1: Samples exposed to artificial weathering for 2 weeks:

Ten dumb-belled shaped and 10 trouser-shaped samples were produced according ASTM-D412/ISO 037 (ASTM-D412, 1981) and ASTM D624-07/ISO34 (trouser leg) (ASTM-D624, 1981) respectively from pure SP (Sil-25) for testing tensile strength, tear strength and percentage of elongation. Furthermore, 4 hardness test specimens ASTM D1415-06 ISO48 (solid blocks) for testing Shore A Durometer hardness were produced. Specimens were inserted into the Q-Sun weathering chamber and at the end of 2 weeks the specimens were removed from the simulators and their mechanical properties tested.

Group 1 - Series 2: Samples exposed to artificial weathering for 6 weeks:

Ten dumb-belled shaped, 10 trouser-shaped and 4 hardness Sil-25 pure SP specimens exposed to UV Light and weathering conditions for 6 weeks. Test specimens were inserted into the Q-Sun weathering machine, and at the end of the 6 weeks specimens were removed and the mechanical properties were tested.

6.3.3.3 Group 2 - Silicone polymer infiltrated starch (SPIS) specimens:

Group 2 - Series 1: Samples exposed to artificial weathering for 2 weeks:

Dumbbell-shaped, trouser-shaped and hardness test specimens were printed as documented before and infiltrated with Sil-25 maxillofacial SP to investigate the effect of UV light and weathering conditions on the mechanical properties of the printed test samples 'SPIS'. 24 specimens were produced and inserted into the Q-Sun for two weeks then, the mechanical tests were measured.

Group 2 - Series 2: Samples exposed to artificial weathering for 6 weeks:

The starch printed dumbbell-shaped, trouser-shaped and hardness specimens and infiltrated maxillofacial 'Sil-25' SP were used to test the effect of 6 weeks accelerated weathering conditions inside the Q-Sun weathering chamber. After 6 weeks time the samples were removed and their mechanical properties were measured.
Data was analysed by one way analysis of variance (ANOVA), post hoc tests *($p<0.05$).*

6.4 Results

6.4.1 Part 1 - Exposure to Natural Weathering Conditions

Table 6-3 presents the data (average and standard deviation) for the mechanical properties obtained from specimens tested under different natural weathering conditions: samples left in complete dark ambient conditions, samples left on the window ledge and samples exposed to outdoor natural weathering conditions for 4 months. The table also shows a comparison with the control data that has been obtained 24 to 48 hours after complete setting of the specimens.

6.4.1.1 Tensile strength:

There was a slight but demonstrable reduction in tensile strength for the pure SP samples under natural weathering conditions compared to the control "SP" results. Average tensile strength for the dark group, the indoor group and the outdoor group was 3.1 MPa, 3.0 MPa and 2.9 MPa respectively against 3.5 MPa for the control group. In

contrast the average values of the printed samples "SPIS" showed a minimal increase in tensile strength for the dark and the outdoor samples, whilst the indoor samples were not affected when compared to the control results. Tensile strength values of the printed samples left in dark, indoors and outdoors were 1.3 MPa, 1.2 MPa and 1.4 MPa respectively against 1.2 MPa for the control group (Figure 6-2).

Following statistical analysis there was a significant difference between the control group and the three test groups for SP samples *($p<0.05$)* but no significant differences between the three test groups *($p>0.05$).* Furthermore, on significant differences for SPIS samples were detected between the control group and samples *($p>0.05$)* or the 3 test groups *($p>0.05$).* The only significant difference in this group was between the indoor samples and the outdoor samples for SPIS test groups *($p=0.029$).*

Table 6-3: Mechanical behaviour of SP and SPIS specimens under natural weathering conditions.

Test	Sample	Control	Natural Weathering conditions		
			Dark	Indoor	Outdoor
Tensile-MPA	Silicone	3.5±0.3	3.1±0.2	3.0±0.1	2.9±0.1
	Printed	1.2±0.2	1.3±0.2	1.2±0.2	1.4±0.1
Tear-N/mm	Silicone	12.2±1.5	6.9±1.2	7.4±1.5	8±0.8
	Printed	8.5±1.1	8.6±1	10.5±2.2	8.3±0.9
Hardness- Shore A	Silicone	30.9±0.7	31.9±1.5	31.7±0,5	30,8±0.7
	Printed	62.8±2.8	45.3±5.2	55.1±2.7	37.7±3.8
Elongation-%	Silicone	511±57.5	474±37.9	487±59.6	437±22.6
	Printed	244±36.1	309±60.0	179.4±14.9	281±53.5

6.4.1.2 Tear strength:

There was a considerable reduction in the tear strength values of the pure SP samples for the dark group, the indoor and the outdoor specimens 6.9 N/mm, 7.4 N/mm and 8.0 N/mm respectively against 12.2 N/mm control group. The values of tear strength for the printed samples for the dark group, the indoor and the outdoor groups were 8.6 N/mm, 10.5 N/mm and 8.3 N/mm respectively against 8.5 N/mm for the control group. Interestingly there appear to be a slight increase in tear strength of the dark samples and

the window samples (Figure 6-3). Statistical analysis showed a significant differences between the control group for the SP samples and the other three test samples *(p<0.05)*. Statistically, SPIS samples demonstrated a significant increase in tear strength of the indoor samples compared to the control samples and the outdoor samples *(p<0.05)*, but no significant difference *(p>0.05)* was observed between the control values and the two other test groups.

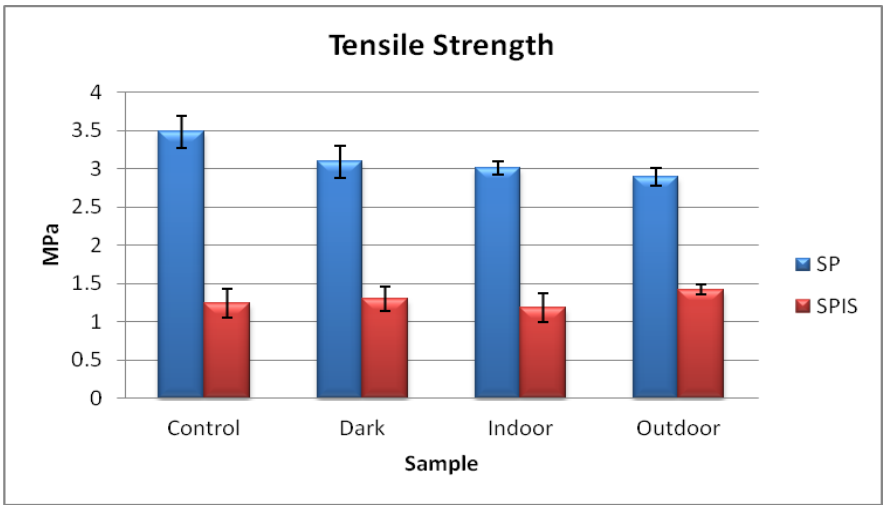

Figure 6-2: Tensile strength for SP & SPIS specimens before & after natural weathering.

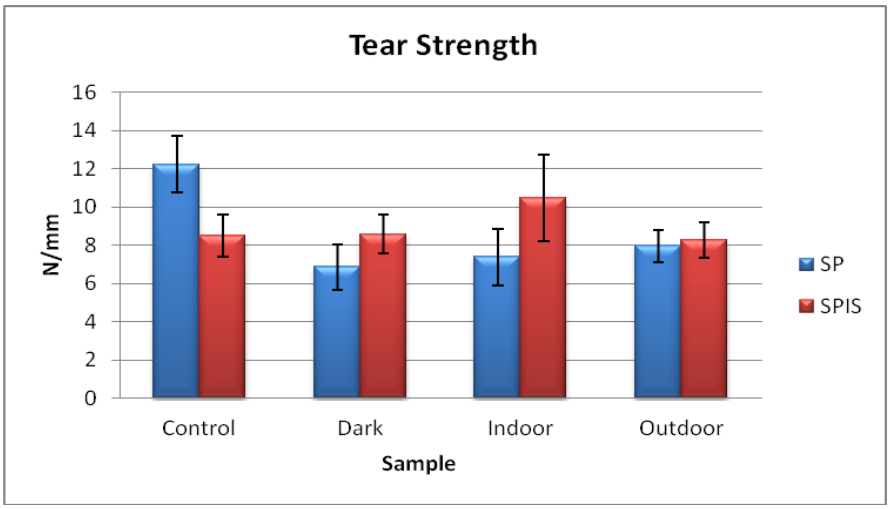

Figure 6-3: Tear strength for SP & SPIS specimens before & after natural weathering.

6.4.1.3 Percentage elongation:

The percentage elongation was slightly reduced for all groups of the pure SP specimens, the dark, the indoor and the outdoor, 474%, 487% and 437% respectively against 511% for the control group. In contrast there was an increased percentage elongation in the printed dark and outdoor samples. The percentage of elongation for the dark, the window and the outdoor samples were 309%, 179% and 281% respectively against 244% for the control group (Figure 6-4).

Statistically there was no significant differences between the control group and the test groups for SP samples, or between the test samples in the same group *($p>0.05$)*. Percentage elongation for SPIS recorded non-significant differences *($p>0.05$)* between the control values and the dark samples. However, when compared to the outdoor samples there was a significant difference *($p<0.05$)* between the control and the indoor samples. Results also showed a significant difference between the indoor samples and the dark samples *($p<0.05$)* and between the indoor and outdoor samples *($p<0.05$)*.

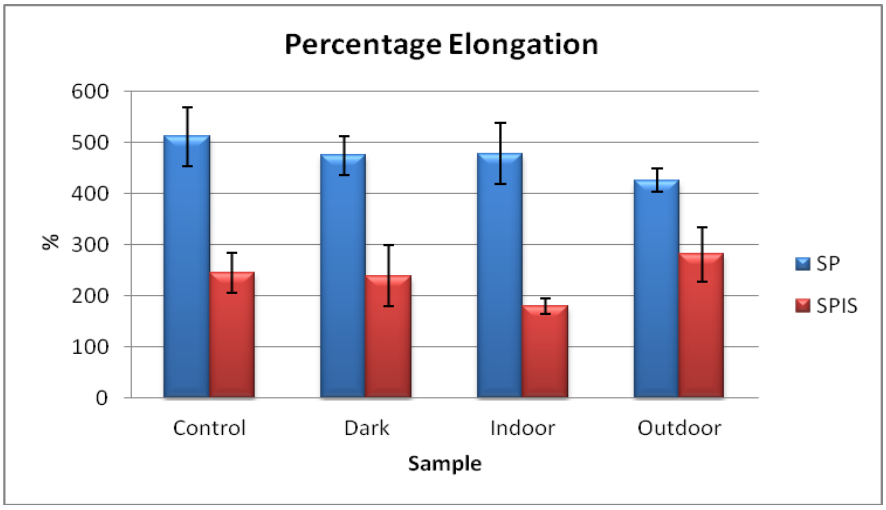

Figure 6-4: Elongation for SP & SPIS specimens before & after natural weathering.

6.4.1.4 Hardness:

Data showed a change in Shore A hardness values for all SP groups exposed to natural weathering, the average shore A for the dark, indoor, and outdoor specimens were 31.9, 31.7. 30.8 respectively against 30.9 for the control group. A considerable reduction in

Shore A values was recorded for the printed specimens - dark, indoor and outdoor 45.3, 55.1, and 37.7 respectively against 62.8 Shore A value for the control group (Figure 6-5). Significant differences *($p<0.05$)* were observed statistically between the control data and the test data for both SP and SPIS samples, the only non-significant differences were observed between the control group of SPIS sample and indoor samples *($p=0.17$)* and in the hardness between the dark and the window samples for SP group *($p=0.96$)*.

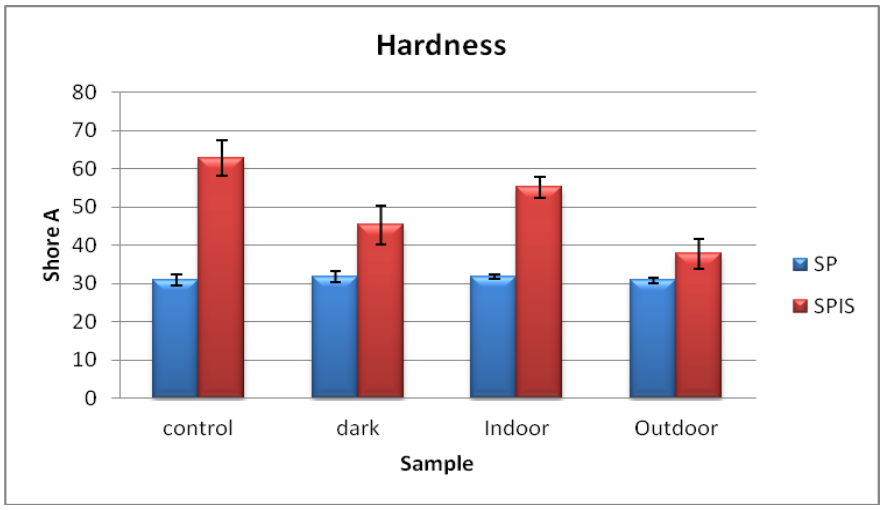

Figure 6-5: Hardness for SP & SPIS specimens before & after natural weathering.

6.4.2 Part 2- Exposure to Artificial Weathering Conditions

Table 6-4, illustrates the tensile strength, the tear strength, the hardness and the percentage elongation values for each test group, the pure SP and the SPIS samples for 2 weeks and 6 weeks exposure to accelerated weathering conditions. Results are compared to the control data of the un-weathered samples.

Table 6-4: Mechanical behaviour of SP & SPIS specimens before & after 2 &6 weeks exposure to artificial weathering.

Test	Sample	Before weathering (control)	2 Weeks Weathering	6 Weeks weathering
Tensile Strength MPa	Silicone	3.5±0.3	2.9±0.4	2.9±0.2
	Printed	1.2±0.2	1.1±0.2	0.9±0.1
Tear Strength N/mm	Silicone	12.2±1.5	10.7±1.6	6.4±1.5
	Printed	8.5±1.1	8.1±0.8	7.5±1.6
Hardness Shore A	Silicone	30.9±0.7	32.3±0.8	34.4±1.9
	Printed	62.8±2.7	58.1±2.2	29.1±4.7
Elongation %	Silicone	511±57.5	479±32.7	468±52.2
	Printed	244±36.1	204±55.6	158±30.6

6.4.2.1 Tensile strength, tear strength and percentage elongation:

Average values of tensile strength, tear strength and percentage elongation for the pure SP specimens before and after weathering are shown in Table 6-4. Before weathering they were 3.5 MPa, 12.2 N/mm and 511% respectively as against 2.9 MPa, 10.7 N/mm and 479% respectively after 2 weeks weathering and 2.9 MPa, 6.4 N/mm and 468% respectively after 6 weeks exposure to UV Light and weathering conditions. The average values of tensile, tear strength and percentage elongation for SPIS samples before exposure were 1.2 MPa, 8.5 N/mm and 244% respectively as against 1.1, 8.1 N/mm and 204% respectively after two weeks weathering, and 0.9 MPa, 7.5 N/mm and 158% respectively after 6 weeks weathering, (Figures 6-6, 6-7 and 6-8).

A significant overall difference *($p<0.05$)* was detected by ANOVA for tensile strength for both the SP and the SPIS test data after weathering when compared to the control data. No significant differences *($p>0.05$)* in tensile strength were recorded between 2 weeks and 6 weeks exposure for both SP and SPIS samples. Also the tear strength for SP groups showed significant differences *($p<0.05$)* between the groups, whereas SPIS showed no significant differences *($p>0.05$)* between the test groups and the control group. Statistically SP percentage elongation results showed no significant differences *($p>0.05$)* between the test samples and the control samples, but SPIS data

showed a significant difference *(p<0.05)* between the control data and the test data (2 weeks and 6 weeks).

6.4.2.2 Hardness test:

The test results for SPIS samples showed a slight reduction in hardness from an average of 62.8 indentation shore A hardness for the SPIS test samples before weathering to 58.1 Shore A after 2 weeks, and a significant reduction to 29.1 after 6 weeks exposure to UV light and weathering conditions. In contrast the SP samples demonstrated a slight increase in the indentation Shore A value after weathering and exposure to UV light. Their Shore A values were 30.9 before weathering, this increased to 32.3 after 2 weeks and 34.4 after 6 weeks exposure to weathering (Figure 6-9). A significant overall difference *(p<0.05)* was detected by ANOVA between the samples for both SP and SPSI samples for 2 and 6 weeks exposure to accelerated weathering compared to the control groups.

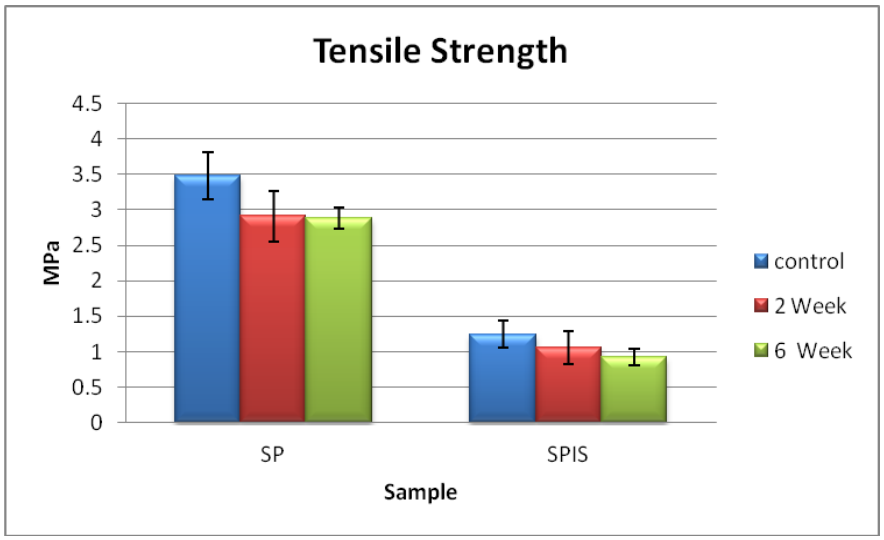

Figure 6-6: Tensile strength for SP & SPIS specimens before and after 2 & 6 weeks weathering.

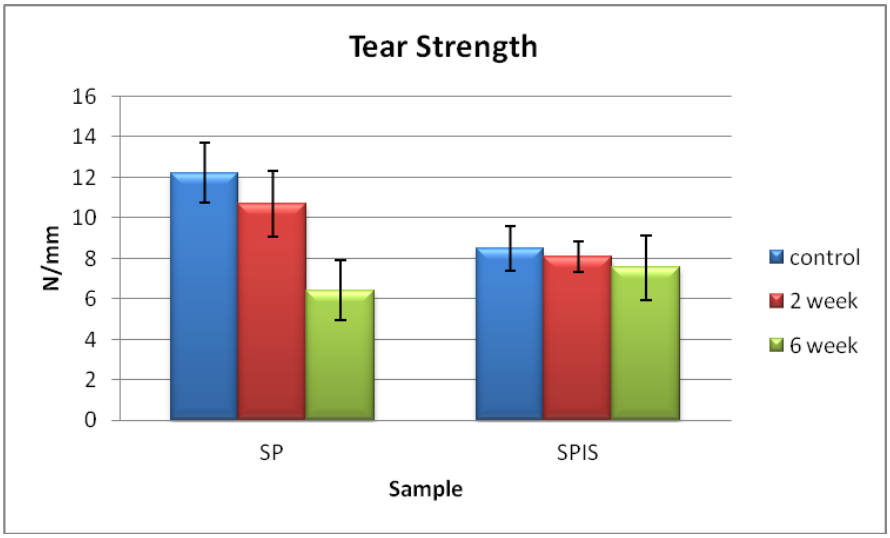

Figure 6-7: Tear strength for SP & SPIS samples before and after 2 &6 weeks weathering.

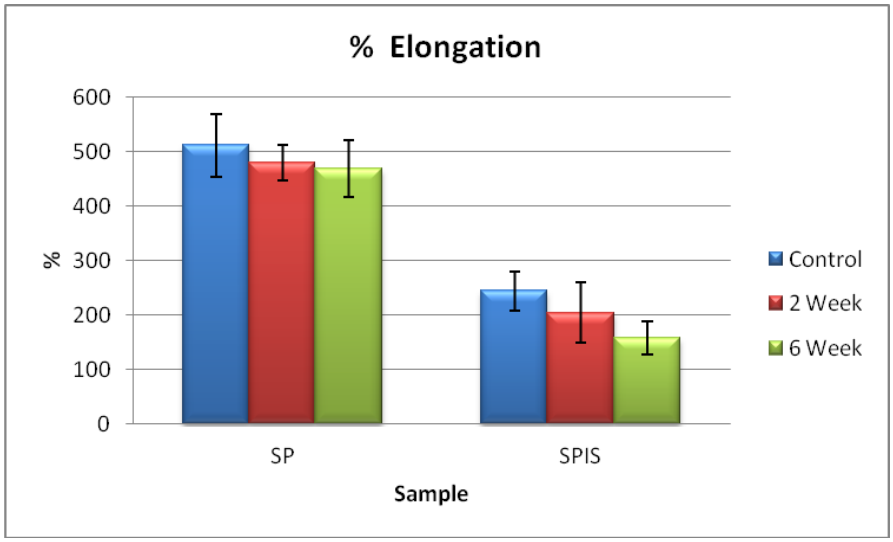

Figure 6-8: Percentage elongation for SP and SPIS samples before and after 2&6 weeks weathering.

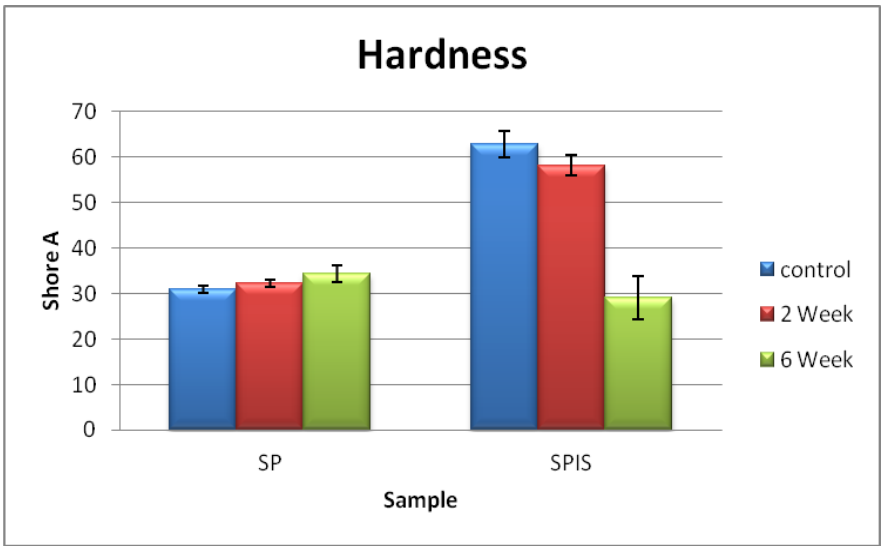

Figure 6-9: Hardness test for SP & SPIS specimens before and after 2 & 6 weeks weathering.

6.5 Discussion

Natural outdoor weathering and artificial accelerated weathering tests are usually undertaken to assess the durability of maxillofacial facial materials. These methods involve exposing the samples to different factors that induce chemical, physical and mechanical degradation such as UV light, humidity and temperature.

The outdoor weathering exposes the samples to natural weathering conditions but it is an un-controlled subjective method of testing. There is no control over the amount of each factor causing the deterioration which include, geographic location, season, weathering condition, time of day and length of exposure (Eleni et al., 2009a).

The accelerated weathering condition is a controlled method of testing the effect of the most deteriorating factors on the SP and they do condense the process in a shorter time frame. However, it does expose the samples to extreme and aggressive weathering condition. It is still not clear how effectively the artificial weathering process simulates the natural process and it may well present an incorrect estimation about service life of the materials used for fabrication of these prostheses (Maxwell et al., 2003). The use of accelerated weathering to replicate outdoor weathering was brought into question by different results presented by two different studies. In 1994 Dootz et al reported no

difference in the hardness and percentage elongation of Silastic 4-4210 before and after exposure to accelerated weathering (Dootz et al., 1994), while Haug et al (1999) showed a significant differences in the percentage elongation and hardness of the same maxillofacial silicone before and after exposure to accelerated weathering (Haug et al., 1999a).

It has been suggested that 1000 hours of exposure to UV light and other weathering conditions by using accelerated weathering chambers is equivalent to one year of natural outdoors exposure (Wolf et al., 1999, Philip et al., 2004). Thus one hour exposure to artificial weathering corresponds to 8.76 hours of natural weathering conditions. Therefore, the 2 weeks time frame exposure to accelerated weathering that has been applied in this study should be equivalent to 4 months of natural weathering conditions. Furthermore, 6 weeks exposure to artificial weathering would represent longer time period correspondent to one year natural weathering; hence it was expected to find much bigger changes in the mechanical properties of the specimens.

In this project both methods of weathering have been applied, but it should be noted that neither of them represent true clinical use and the way that prostheses are being used by the patients in “real life”. It can only be seen as an indication of the kind of problems that may arise. In real life there are issues of hand contact, applying and removing the prostheses, bodily secretions and of course the use of make up or adhesive to help disguise and retain the prosthesis. Furthermore, the patient does not spend all the time outdoors to be exposed to the full period of natural weathering used in this study. Polyzois (1999) suggested 4 months exposure to natural outdoors weathering is probably equivalent to 8-12 months actual clinical service time; yet a patient with facial prosthesis is unlikely to stay outdoors for 24 hours a day. A maximum of 8-12 hours daily outdoor time by the patient might expected, thus the time frame in this study could be equivalent to 8 -12 months clinical service life of the prosthesis (Polyzois, 1999). Nevertheless, it is not possible to apply the real life experiments at an early stage of the project as the clinical component of the project is still developing.

The specimens were exposed to three different methods of natural weathering conditions, the dark, the indoor and the outdoor, which showed different effects on the mechanical properties of the SPIS used for producing soft tissue facial prostheses. Exposure of the SPIS to different natural weathering conditions for 4 months showed no significant effect on tensile strength and tear strength of the test specimens compared

with the control specimens, whereas there was a significant increase in the tear strength of the indoor specimens. In contrast, statistically the pure SP control samples showed a significant difference in tensile strength and tear strength with the 3 test methods, the dark, the indoor and the outdoor group. Furthermore, statistical analysis of percentage elongation didn't show any significant changes when the control data are compared to the test data of the outdoor and the dark samples. Data showed a slight reduction in percentage elongation for the indoor samples. On the other hand, statistical analysis showed a significant reduction in Shore A hardness values for all test groups.

In this study the effect of accelerated weathering was also tested on SP and SPIS specimens for 2 weeks and 6 weeks. The device used 'Q-Sun' for testing the effect of accelerated weathering exposes the samples to extreme and aggressive weathering conditions. The results demonstrated a considerable reduction in the mechanical properties of the pure SP and the SPIS specimens.

Following exposure to accelerated weathering for 2 weeks, statistical analysis of the results showed a significant reduction in tensile strength of the printed samples, consequently the percentage of elongation was also reduced, and this is shown in Table 6-4. The 2 weeks exposure induced a significant effect on the tear strength of the pure SP but no significant effect on the tear strength for the SPIS samples.

Six weeks exposure induced more reduction in the mechanical properties of the SPIS values compared to SP group. The effect of weathering on SP samples was non-significant on tensile strength and the percentage elongation specimens when compared to the tear strength and hardness values which demonstrated significant changes statistically. Additionally there was a significant reduction in tensile strength, percentage of elongation and hardness values for SPIS samples after 6 weeks exposure to UV light and weathering conditions and this is shown in Table 6-4. One notable feature was the significant reduction of the Shore durometer A values for the printed samples after 6 weeks exposure to accelerated weathering, which was also accompanied by a considerable reduction in their percentage elongation. This shows the consequence of harsh and extreme nature of artificial weathering conditions and the length of time used for testing. Furthermore, the SPIS is a composite and starch constitutes 40% of the whole component by weight as detailed in section 4.5.2. Inevitably starch is a soft hydrophilic material and the accelerated weathering condition is beyond the starch's ability to resist deterioration under these extreme artificial weathering conditions.

The results indicate that exposure to 2 weeks and 6 weeks accelerated weathering had a more severe effect on both SP and SPIS. In theory the 2 weeks weathering should be equivalent to four month natural weathering but when the results were compared with each other, the two weeks weathering were found to show a much more severe effect than the 4 months natural weathering conditions. Thus 2 weeks of accelerated weathering may be more representative to a year of natural weathering conditions. The 6 weeks exposure to accelerated weathering was found not to be comparable to the results of natural weathering in this study and may well be representative of many years of clinical use.

The mechanical data obtained from the SP samples under artificial weathering condition are comparable with other reports that evaluated clear and coloured maxillofacial silicone polymers under accelerated ageing mechanisms (Andres et al., 1992, Dootz et al., 1994, Eleni et al., 2009a, Eleni et al., 2009b). However, it contradicts the results achieved by Yu et al (1981), who evaluated 4 types of silicone, polyvinyl chloride and polyurethane polymers for their physical properties. They tested hardness, percentage of elongation and tear strength, before and after exposure to 600-900 hours weathering. They concluded that the 4 types of silicone polymers reported no changes in physical properties on accelerated ageing and they attributed this important characteristic to the inert inorganic backbone of the molecular chain. The high percentage of silicone elongation was attributed to the nature of fillers and configurations of crosslinkages. In contrast the polyurethane showed complete deterioration and failed entirely after 600 hours of testing (Yu et al., 1980). Moreover the results of natural weathering conditions of the SP samples is also found to be consistent with the results of Eleni et al, 2009, (Eleni et al., 2009a).

Although there are inherent differences in these values for each group before weathering the SPIS appear to be able to resist extreme weathering conditions well and as a result of this, the SPIS could potentially be used to replace facial defects without going through significant deterioration during the service life of the prostheses.

Therefore, it would appear that this method of producing the prostheses has no demonstrable detrimental effect on the mechanical properties when compared to the material already used today ‘SP’. However, it is acknowledged that the mechanical properties are different when compared to pure silicone and extended period of

exposure to extreme weathering conditions does adversely affect the samples tested ‘SPIS’.

According to the mechanical data obtained from these studies, there is some loss in properties but it is hard to judge how that will be reflected in the day to day clinical use of these prostheses. The results obtained suggest that the SPIS formulation is adequate for the purpose when compared to SP alone and the prostheses will last between 6 – 12 months, thereby one can overcome the degradation process by making multiple prostheses and when the prostheses are used as interim replacements for patients with defects during any post operative healing period, it is only required to last for a shorter time and it would be perfectly adequate.

6.6 Conclusion:

1- The silicone polymer prostheses showed very little degradation in both the natural and the accelerated weathering conditions.
2- For the printed prostheses there was no significant effect for the natural weathering conditions, while accelerated weathering conditions showed a significant effect on some mechanical properties of the printed samples.

7 Retention of Soft Tissue Prostheses Using Magnets[4]

[4] Acknowledgment - This work was performed in collaboration with Neil Frewer AB (HONS), MA at Fripp Design and Research Ltd.

7.1 Introduction

Surgical treatment of maxillofacial cancer can result in extensive loss of soft and hard tissues and frequently leaves the patients with facial disfiguration, living in isolation and despair. When surgical correction of the resultant defects cannot be performed surgically due to technical/patient limitations, the alternative treatment involves making a prosthesis with a secure means of retention. One of the common problems with soft tissue facial prostheses relates to the retention and the stability of the prosthesis during service (Goiato et al., 2007, Goiato et al., 2009). Prostheses are provided with suitable means of retention according to type, size and site of the replacement part and it is important that the retention method is strong, easy to use and simple enough to be built into the prosthesis.

Today maxillofacial prostheses are retained either by using medical adhesives or endosseous implants, or a combination of both. Despite the limitations associated with the application of medical adhesive it is often used as an alternative method of retention to endosseous implants when there are technical/surgical problems with using implants or because of economic considerations.

The new 3D designed and printed prostheses can be retained by both endosseous implants and adhesives. The adhesive can be applied to the margins of the prosthesis since the starch shell is encapsulated in the maxillofacial elastomer; in other words, the adhesive is applied to the silicone elastomer rather than the starch as is the case with conventional soft tissue prostheses.

Endosseous implants are small metal screws retained inside the patient's bone around the defective area in order to hold the prosthesis in place. They can be used with two different retention systems: the magnet type and the bar-clip type. Each is incorporated into the prosthesis through a different attachment design (Hatamleh and Watts, 2010a). A bar-clip allows retention at the bar site but therefore does not provide maximum integrity of the margins with the surrounding skin (Wazen et al., 1999), whereas magnets can achieve better marginal adaptation with the patient's tissues, especially with large facial prostheses (Parel et al., 1986).

Since the 3D soft tissue facial prosthesis is designed by CAD, a suitable retention design for the prosthesis can be provided according to the requirements of the individual patient. This includes adding a number of sockets to the inner aspect of the prosthesis to hold magnets in the exact position of the corresponding implant studs on the patient's face.

The creation of the magnet fixture has to start at the stage of 3D imaging of the patient. A magnet fixture boss, in the form of a tube, is attachment to either the implant head or magnet (if already in-situ) – this is required as image captured of the implant head is not accurate enough to translate its position on fitting surface of the prosthesis in the design process. This is due to size and reflection constraints associated with the implant, the production of the boss requires perfect alignment with the implant of the patient. The procedure can be summarised as follows:

1) A plastic cylinder designed for use with a stock magnet insert is clicked onto the implant during the 3D photogrammetry process (Figure 7-1). The magnet pole is utilised at this stage in order to locate the exact position and orientation of each implant stud (Figure 7-2).

Figure 7-1: The magnet and the plastic Pole.

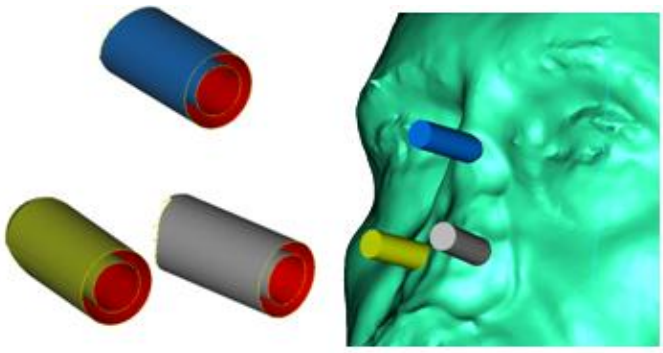

Figure 7-2: 3D image with the magnet poles in place.

2) The 3D image is then imported to the 3Matic software for processing. In the case of a missing nose, this includes importing the scan data from the 3D camera and matching the missing part with a stock library part, which is suitable for the patient (Figure 7-3). In the case of a missing ear or other parts of the face it is possible to capture a mirror image of the contralateral part of the patient that has not suffered any deformity/intervention.

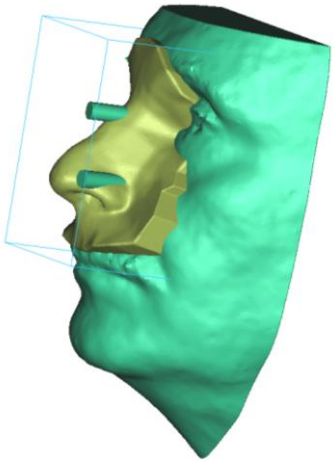

Figure 7-3: The stock library nose with the magnet pole in place.

3) The next phase is to blend the library part into the patient's face in order to ensure that the prosthetic looks realistic. It is important that the stock library part is blended into the patient's face in order to produce a good peripheral fit at the margins of the prosthesis (Figure 7-4).

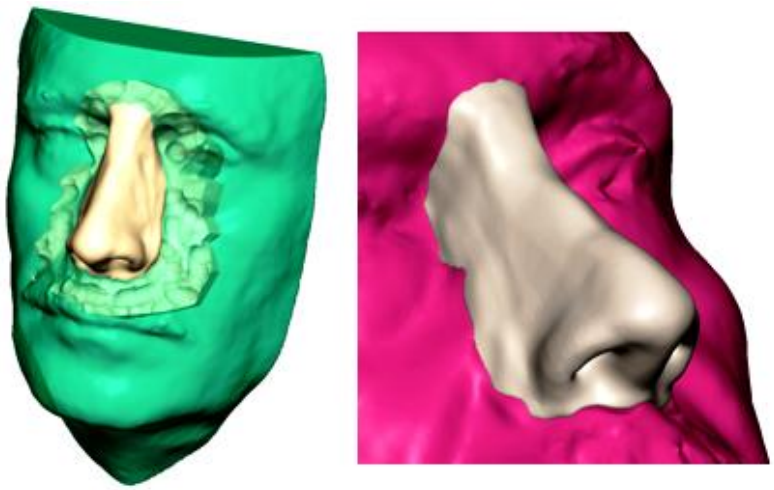

Figure 7-4: Blending the library part into the patient's face.

4) The library part is adapted to the model and manipulated until a good fit is achieved. This may involve moving the part in all three planes to allow the “best fit” along with manipulation of the margins to blend into the patients existing skin. Then several detailed processes are applied using 3Matic to achieve the final positioning of the magnet’s sockets on the inner aspects/fitting surface of the prosthesis (Figure 7-5).

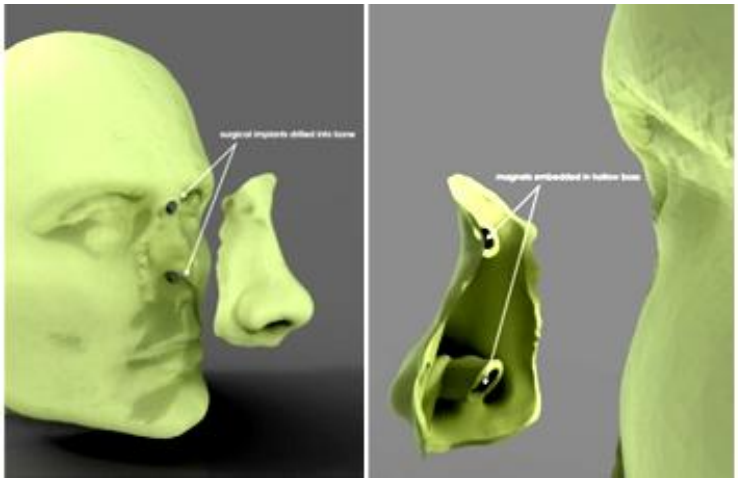

Figure 7-5: Fitting the final position of the library part.

5) A suitable mechanical retention for the magnet is incorporated into the final design during the generation of the magnet boss (Figure 7-6).

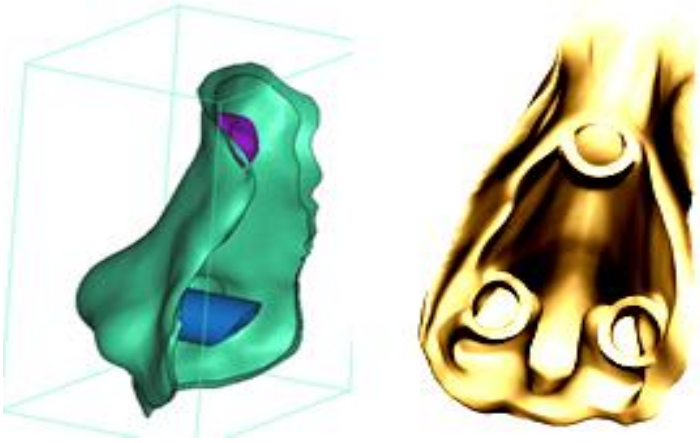

Figure 7-6: The inner surface of the prostheses with the magnet bosses.

Therefore, the aim of this part of the project was to present suitable retention designs for the implant retained prosthesis and test the potential retention methods in order to assess the feasibility of securing the prosthesis to the underlying skin.

7.2 Materials and Methods

7.2.1 Boss Designs

Four boss designs provided with different mechanical means of retention were applied in this test in order to adopt the most appropriate retention boss design for the prosthesis.

Boss design 1:

Boss design 1 is a simple tapered design provided with an internal shelf in order to secure the resin and the magnet (Figure 7-7).

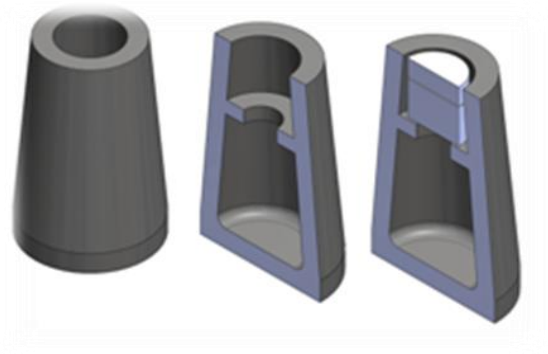

Figure 7-7: Boss design 1.

Boss design 2:

Boss design 2 is also a tapered cylinder but provided with an additional groove around the magnet in order to allow the resin to anchor itself to the boss (Figure 7-8).

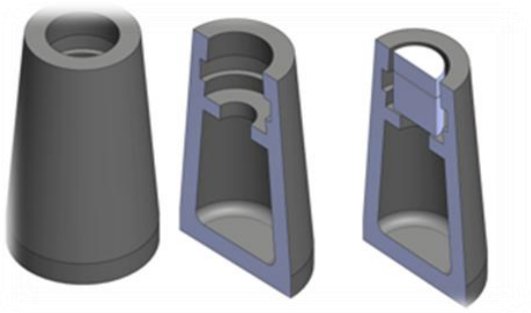

Figure 7-8: Boss design 2.

Boss design 3:

Boss design 3 is a straight sided cylinder with a similar internal feature to the boss design 2 (Figure 7-9).

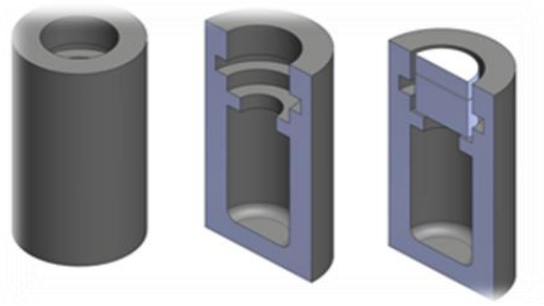

Figure 7-9: Boss design 3.

Boss design 4:

As with designs 1 and 2, the boss design 4 is also tapered; however, it has a greater number of indented grooves in order to provide additional retention (Figure 7-10).

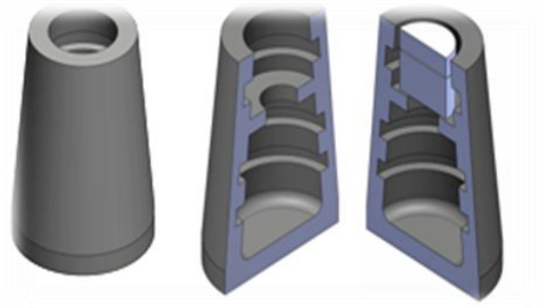

Figure 7-10: Boss design 4.

7.2.2 Preparation of the Specimens

7.2.2.1 Preparation of stock magnet samples:

Self/cold cure acrylic resin was used to bond the magnet to the boss as this is a standard and commonly used approach**.** The magnet was attached to the acrylic mechanically via a retentive groove around the magnet, and the acrylic part including the magnet was retained inside the magnet boss by mechanical methods of retention as shown in Figure 7-11. However, as there is no chemical adhesion between the acrylic resin and the silicone elastomer; retention was principally mechanical in the form of undercuts added to the internal part of the magnet boss in order to provide secure retention of the prosthesis by the magnet. Figure 7-12 illustrates a cross section of the design of the magnet boss filled with acrylic resin. It also shows the position of the magnet and the implant stud centred on the upper part of the magnet boss.

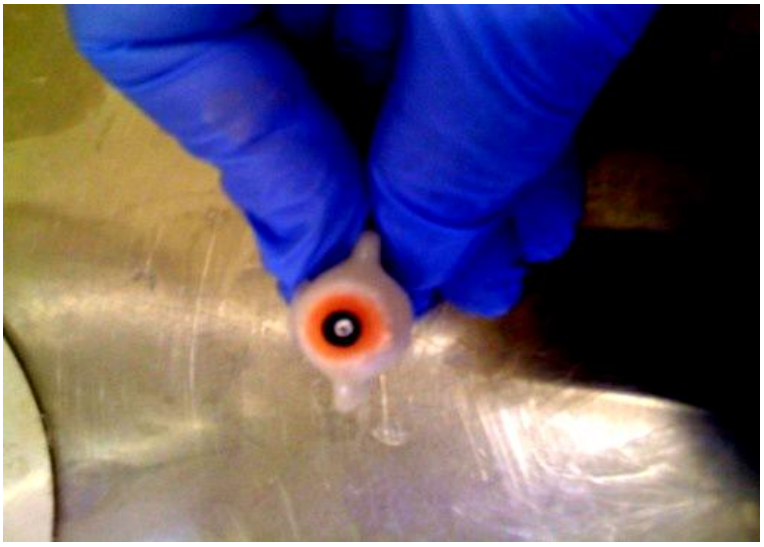

Figure 7-11: The magnet fixed by pink acrylic into the magnet boss.

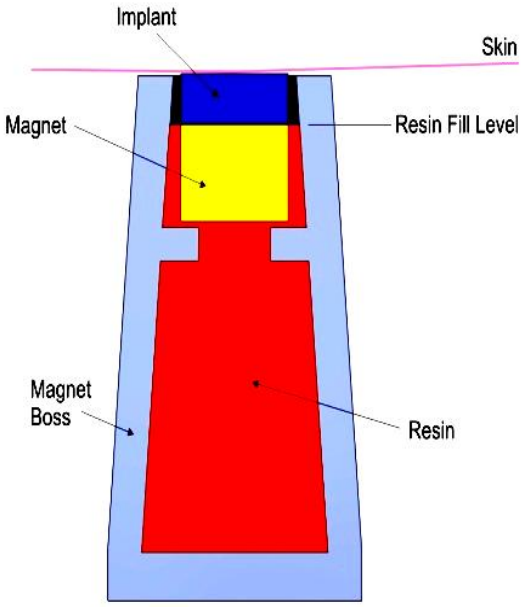

Figure 7-12: cross sectional illustration of the magnet boss and the magnet retained by self cured acrylic.

Two stock implants from Technovent – Maxi Magnabutment, 5.1 mm diameter and 2.1 mm height were used and provided with acrylic grips for positioning on the Lloyd instrument. Retention force was measured and repeated 5 times for each stock magnet; then the average force value was calculated and used as a control force at break (Figure 7-13).

Figure 7-13: Grips added to the stock implant and the magnet.

7.2.2.2 Preparation of the magnet boss specimens:

Four designs with different undercut details were created (Section 7.2.1.) to provide anchor points when the resin was set, and a suitable grip was added to each design (Figures 7-14 and 7-15). Three test specimens for the 4 different magnet boss models were printed by the Z-Printer from starch and infiltrated with SP according to the standard infiltration protocol. Each boss was printed and assessed for its strength. The magnet was represented as a static steel pin which was bonded to each boss design using the self/cold cure acrylic resin (figure 7-16). Retention force was measured using a Lloyd LRX tensile instrument; with a 100 N load cell at a constant speed of 5mm/min. Then retention force for implant-magnet was compared to that of magnet-boss.

Figure 7-14: Grip added to the magnet boss.

Figure 7-15: Four test designs with grips attached from both sides.

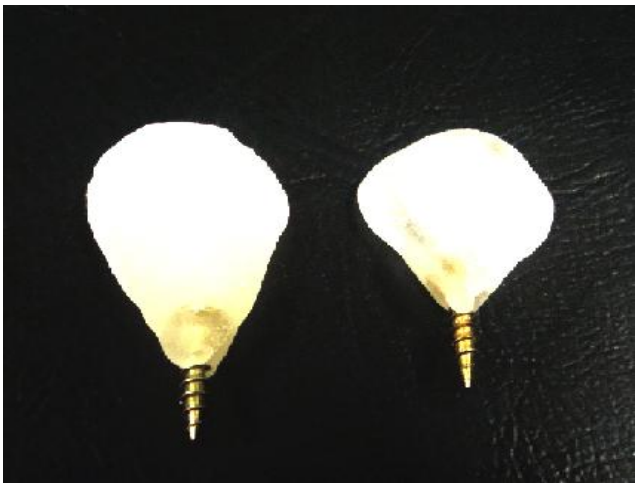

Figure 7-16: A steel pin with grips inserted inside the acrylic resin when fill the boss.

7.2.3 Data Analysis

Statistical analysis was performed for the resultant data using PSAW statistics 18, whilst one way variance statistical analysis (ANOVA) was employed in order to compare the amount of force at break between the four boss designs. An independent samples test t-test was employed to determine the level of significance between the forces required to separate the magnet from the boss and the magnet from the implant.

7.3 Results

The average separating forces of the stock implants were 7.9±0.4 N and 7.8±0.1 N (Table 7-1), whereas the average forces for the four boss designs at failure were 22.7±4.9 N, 27.6±5.4 N, 22.1±1.4 N and 21.3±6.7 N for boss models 1, 2, 3 and 4 respectively (Table 7-2**).** The data in Figure 7-17, showed no significant differences *($p>0.05$)* between the four test models. The force required to dislodge the 4 magnet bosses was significantly higher *($p<0.05$)* in fact some 3 times higher than the force required for separating the magnets from the implants (Figure 7-18).

Table 7-1: Load (N) at failure for the 2 stock implants.

Test No.	Implant 1 Failure load (N)	Implant 2 Failure load (N)
Test 1	7.4	7.7
Test 2	8.2	7.7
Test 3	8.2	7.8
Test 4	7.7	7.9
Test 5	7.8	8.0
Average & SD	7.9±0.4	7.8±0.1

Table 7-2: Load (N) at failure for the 4 magnet boss models.

Test No.	Failure Load (N)			
	Model 1	**Model 2**	**Model 3**	**Model**
Test 1	25.1	23.4	21.1	20.7
Test 2	26.0	33.7	21.6	15.0
Test 3	17.1	25.8	23.7	28.3
Average & SD	22.7±4.9	27.6±5.4	22.1±1.4	21.3±6.7

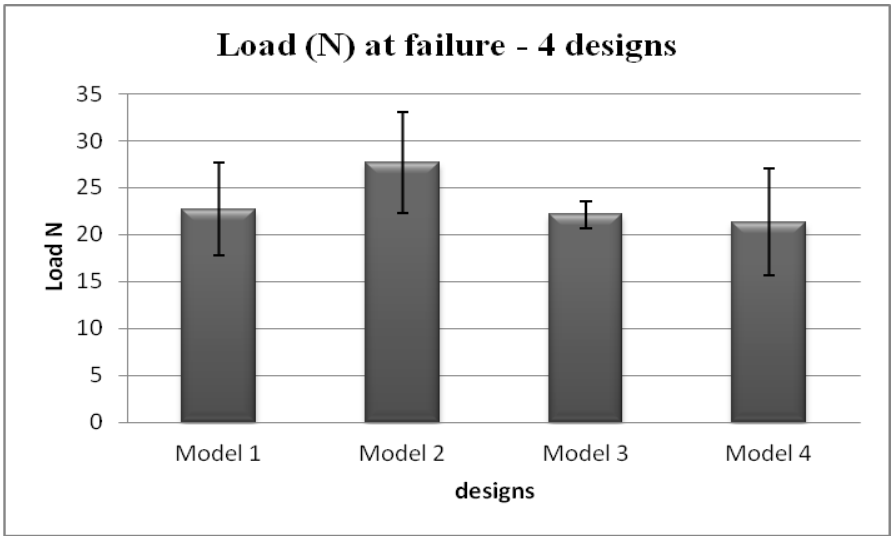

Figure 7-17: Load at failure for the 4 magnet boss model.

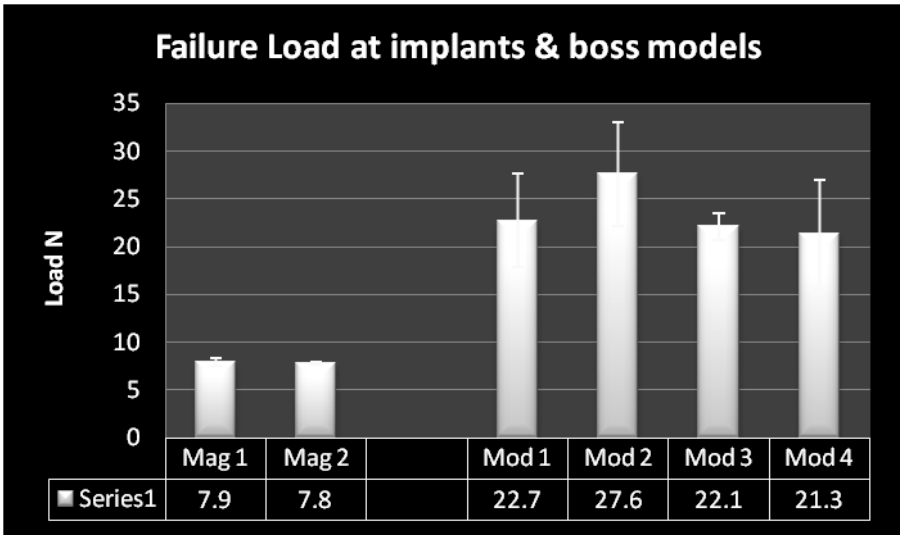

Figure 7-18: Comparison of load at failure between the 4 magnet boss models and the stock implants.

7.4 Discussion

To date, magnets are considered the most efficient means of retention for facial prostheses and avoid some of the limitation associated with adhesives (Parel et al., 2001). Implant retained facial prostheses have better durability with an increased service life, since no adhesive needs to be added to the prosthesis, no solvents are required for adhesive removal and no excessive pressure is exerted on the thin margins of the prosthesis. Furthermore, retention provided by magnets is considered more secure than that provided by adhesives, and thus prostheses retained with magnets achieve greater patient acceptance and satisfaction (Chang et al., 2005).

In order to ensure magnets are retained in the prosthesis when it is removed, the magnet must fit into a suitable retentive component part made from acrylic resin; this can be achieved by processing the silicone polymer onto the acrylic part during the production process. Retention between the acrylic and the maxillofacial silicone polymer is achieved mechanically by creating a number of small holes with a 1.5 – 2.0 mm round bur in the acrylic or by using a medical adhesive or combination of both (McKinstry, 1995, Brånemark and de Oliveira, 1997, Chang et al., 2006, Chung et al., 2003).

In this project, development of an appropriate retention system for the magnetic prosthesis design is a key to meeting the general requirements of a functional prosthesis and providing an accurate method of attachment between the magnet and the prosthesis. Therefore, a number of magnet bosses were added to the design in order to hold the magnet in exactly the same position and orientation as that of the implant stud, and self cure acrylic was used to retain the magnet inside the magnet boss.

Magnet designs can vary in shape, length, diameter and retention force. The diameters of the magnets used to retain facial prostheses vary from 4.4 mm to 5.5 mm, with retention force ranging between 3.8 N and 11.5 N (Figure 7-19). However, magnets of larger diameter (9.4 mm), with a much higher attraction force, are also available and used occasionally according to the technical requirements of the individual patient (Technovent, 2012). The stock magnet used in this study was 5.1 mm in diameter and had a separating force of 7.5 N as it is the commonly used endosseous implant in the maxillofacial region to provide retention to the nasal, auricular and eye prostheses.

The four designs were evaluated and all showed retention of the magnet boss at approximately 3 times the force required to separate the magnets. Thus the magnets should separate before the magnet boss is dislodged from the prosthesis. Among the four designs used there was no significant difference in the quality of retention. The retention force was in the region of 22 N; the force required to dislodge the magnet was 7.5 N. Therefore, the logical solution was to use the simplest of the four designs.

7-19: Different shapes and sizes of magnet (Technovent, 2012).

Results demonstrated a safety margin of x3; however, although a satisfactory margin in these cases the larger magnets could still incur problems as any further increase in the size of the magnet produces a proportional increase in separating load. Hence, the greater diameter of the larger magnets will cause the force to increase. Therefore, the recommendation is that magnets larger than those used in this project should not be used due to the potential problem of the magnet boss being pulled out of the prosthesis prior to separation of the magnets.

Retention could be improved further by using an appropriate adhesive between the acrylic and the silicone polymer. For example, silicone adhesives are used to prevent silicone impression materials from separating from the tray and indeed this maybe a solution. However, this requires further investigation.

7.5 Conclusion

1- All the test designs are capable of retaining a magnet of up to 5.1 mm within the magnet boss without risk of displacement during placement and removal of the prosthesis.
2- It is recommended that the simplest magnet boss designs – 1 or 2 is used as a standard retention pattern.

8 Skin colour measurement[5,6]

[5] Acknowledgment - This work was performed in collaboration with Dr. Kaida Xiao – PhD in colour imaging – Research Fellow- University of Sheffield.
[6] Part of this work on skin colour measurement has been published in Chinese Optics Letters – August 10, 2012, Appendix B – The Abstract.

8.1 Introduction

Colour is the visual perceptual property to the reflected light from an object within the range of the visible light spectrum (400 -700 nm) that can be detected by a human eye and it is directly related to the reflective property of a material. Recently the optical properties of the skin have been attracting much attention; today a number of scientific, medical and industrial disciplines such as medical imaging (DICOM), computer graphics, cosmetics, and display industries are showing great interest in skin colour. In the field of medicine, skin colour has attracted particular interest in relation to diagnosis of skin lesions, micro-vascular surgery or plastic surgery and soft tissue prostheses that restore the function and appearance of missing biologic structures of maxillofacial, craniofacial and head and neck regions as a result of cancer, birth deformities and trauma (Paravina et al., 2009).

In order to measure objectively the skin colour appearance and evaluate skin colour differences, CIE Colorimetry has been widely used for specifying skin colours into CIELAB uniform colour space. The L*a*b* is described as the vertical (L*) axis which represent lightness, ranging from 0-100 and two other horizontal axis values (a*) and (b*). Each has an "axis" that can range from (–a) to (+a) and (–b) to (+b). More specifically, (–a) represents green and (+a) represents red, whilst (b+) is represented by yellow and (b-) is represented by blue, as is shown in Figure 8-1 (Hunter, 1948, Honiball, 2010).

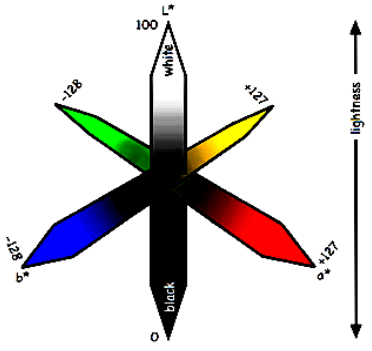

Figure 8-1: L*a*b* colour model.
http://www.termseekinc.com/raw-conversion/lab-color-model.html

Several factors affect human skin colour; these include thickness of the keratin layer, amount of blood supply perfusing the skin and degree of melanin pigmentation. Moreover, genetic and geographic factors can also play an important role in skin colour variations among various ethnic groups (Thong et al., 2003, Ito and Wakamatsu, 2003, Walters and Roberts, 2008). Skin shades also vary according to the part of the body, these variations may lead to colour mismatching after surgery including micro-vascular reconstruction (Feldman, 1990, Shaw and Ahn, 1992). In many cases although a defect may be surgically reconstructed a desirable (aesthetic – shape and colour) result may not be achieved due to site differences of the transplanted tissue. To complicate matters further skin colour is not statics – it can also be affected by exposure to temperature, exercise and sunlight. The later causes tanning of the exposed skin, leading it to exhibit a darker colour than non-exposed parts (Jablonski and Chaplin, 2010) (Figure 8-2).

Figure 8-2: A suntanned arm showing colour differences between the exposed parts, which are browner than the covered parts.
http://en.wikipedia.org/wiki/File:Skin_tanning.JPG

Skin colour measurements have seldom been conducted among individual ethnic groups (Over et al., 1998, Han et al., 2006, Coward et al., 2008, Xiao et al., 2012) and some of these were performed only for limited purposes. To date, no comprehensive global database for skin colour among the main ethnic groups is available. Generation of a global skin shade guide requires comprehensive measurement of skin colour to be conducted among groups of people from different ethnic back grounds and different geographic locations around the world.

The complete colour range that can be achieved under a specific viewing condition is referred to as the colour gamut. The skin colour gamut represents the complete range of colour appearance for a defined group of people, which provides

clear information about the range and distribution of skin colour values across the entire colour space (Stone et al., 1988).

8.2 Aim

The aim of this part of the project was to collect skin colour data from a wide range of people from different ethnic backgrounds by using a spectrophotometer in order to generate a comprehensive skin colour database, to identify their colour gamut and to analyse factors that might affect the skin colour's appearance. These would then be used to determine if there were limitations within the data capture or manufacturing process when producing prostheses within the "whole" colour gamut of skin shades.

8.3 Materials and Methods

1) Ethical approval was obtained from the Research Ethics Committee - School of Clinical Dentistry - University of Sheffield[7] for measuring skin colours among a group of volunteers. An information sheet that included all information and details about the colour measurement procedure and a consent form to be signed by the volunteer were produced.
2) A Minolta CM-2600d spectrophotometer using SpectraMagic NX Colour Data Software was employed to measure the skin colour in CIELAB tristimulus values with a 2 degree standard observer. The illuminate was set to the CIE standard D65 to simulate skin colour in daylight conditions. During the measurement, a viewing geometry of d/8 (diffuse illumination, 8-degree viewing), was used with the specular component included and the aperture size was set to 3mm.
3) Skin colour measurement was conducted for each subject in a total of nine body areas – forehead, tip of nose, cheek, earlobe, chin, back of hand, palm, outer forearm and inner forearm (Figure 8-3). L*a*b* colour values were recorded for each measurement. Each subject also provided further information relating to age, gender and ethnicity.

[7] A Copy of ethical approval is attached to appendix C

4) A Skin Colour Database was established and based upon 3933 (437 subjects x 9 body areas) items of skin colour data in terms of CIELAB tristimulus values. Based on these data, skin colour appearance was analysed using Caucasian, Chinese and Middle Eastern skin colour data and the skin colour gamut for each ethnic group and the entire sample was determined.
5) One way analysis of variance ANOVA was conducted that examined the statistical differences of each colour attribute of the L*a*b* value between the three ethnic groups. While independent-samples T-Test was conducted to analyze the differences of the three colour attributes (L*, a* and b*) between male and female for each ethnic group separately.

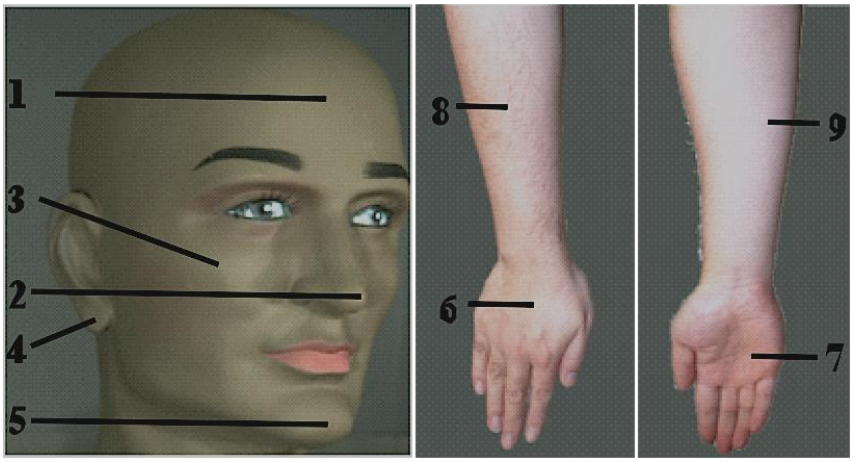

Figure 8-3: Body position for skin measurements.

8.4 Results

Information on the volunteers is detailed in Table 8-1. To date 437 volunteers – 275 male and 162 female, covering five different ethnic groups, participated in this study. The colour measurements were conducted in the UK, China and Iraq. The volunteers included university staff and students, but the majority of the participants were students aged from 20-40 years.

Table 8-2 presents the average and standard deviation for L*, a* and b* values for Caucasians, Chinese and Middle Eastern skin tones. In general, the results demonstrate a clear trend that Chinese and Middle Eastern skins are significantly

(p<0.05) darker than Caucasian shade, while there was no significant differences *(p>0.05)* in the L* values between Middle Eastern and Chinese shade.

Table 8-1: Numbers of volunteers and their ethnic groups.

Gender	Caucasian	Chinese	M. East	Asian	African
Male	43	137	72	4	1
Female	33	65	74	2	1
Total	73	202	146	6	2

Chinese and Middle Eastern Skins were also found to be significantly *(p<0.05)* more yellow when compared with Caucasian skin (Figure 8-4). Caucasian shades demonstrated a higher L* value and lower b* value than Chinese and Iraqi shades (Table 8-2). However, in the case of individuals, the skin colours of these three ethnic groups might not be easily distinguishable. Furthermore, skin colour variations were predicted for each ethnic group and compared to other ethnic groups. It was found that Caucasians have the largest variation in skin tones, whereas the Chinese have the least skin colour variation.

From Table 8-2, it can be seen that, in general, Caucasians have the lightest skin - highest L* values, whereas Iraqis have the darkest skin - Lowest L* values. Furthermore, Caucasian skin appears to be more reddish and this is presented in Table 8-2 as the highest a* value, whilst the lowest b* value was recorded for Caucasians when compared to Chinese and Iraqi shades.

Table 8-2: Average and SD of L*a*b* colour Value for the ethnic groups.

Ethnic Group	Total L*a*b* Value		
	L*	a*	b*
Caucasian	60.3±2.1	11.8±3.9	13.9±1.2
Chinese	58.6±2	10.1±2	15.3±1.3
Middle East	56.4±2.8	10.2±2.3	15.8±0.9

Figure 8-5 presents the average L*a*b* values and standard deviation for males and females and Tables 8-3, 8-4 and 8-5 detail the L*a*b* colour distribution according to

gender and body part. It can be seen that females have significantly *(p<0.05)* lighter skin shades in all groups as 2 tailed independent samples t-test showed; however, the greatest variation in L* values (lightness) is between males and females of Iraqi skin shade, statistically a significant difference *(p<0.05)* of L* Value was recorded between Iraqi males and females. Whereas, no significant differences *(p>0.05)* in a* and b* values between male and female was reported in the 3 ethnic groups. However, males have slightly more colourful skin than females in all groups and this is represented by higher a* values for males against females.

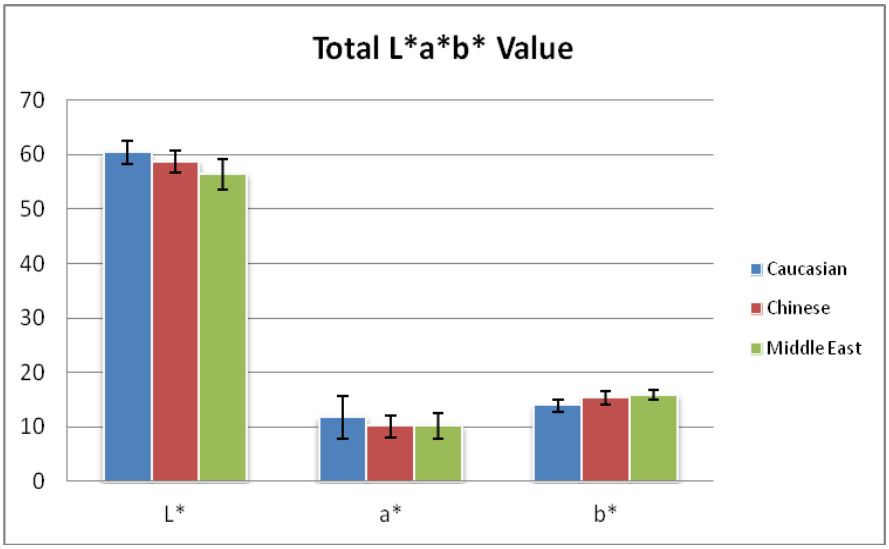

Figure 8-4: Average and SD of L*a*b* colour Value for the ethnic groups.

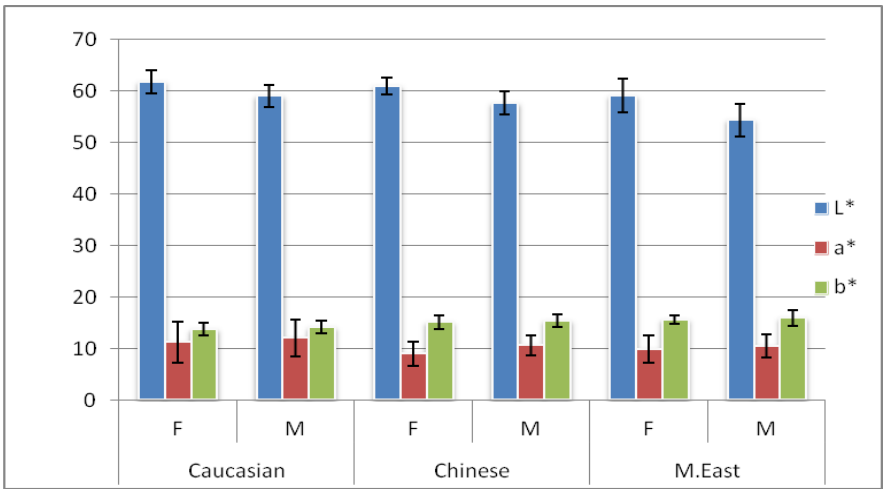

Figure 8-5: Comparison for L*a*b* values according to gender between the groups.

Table 8-3: Average L*a*b* Values for different body parts according to gender Caucasian skin shade.

Position	L*a*b* - Caucasian					
	L*a*b* - Female			L*a*b* - Male		
	L*	a*	b*	L*	a*	b*
	FACE					
Forehead	60.6	12.8	14.2	59	15.8	14.9
Nose	59.3	15.3	14.5	58.3	15.8	15
Cheek	61	13.7	13.6	58.4	14.6	14.9
Ear	60.4	13.9	13	58.5	14.6	12.9
Chin	59.6	16.5	13.6	55.9	14.1	13.6
AV&SD	60.2±0.7	14.4±1.4	13.8±0.6	58±1.2	15±0.8	14.3±1
	ARM					
Back hand	63.3	7.2	14.3	59.1	9	14.2
Palm	61.6	8.6	11.7	59.3	10.1	12.2
Outer arm	63	7.3	16	58.6	8.3	16.1
Inner arm	66.3	5.6	12.5	64.3	6.3	13.1
AV&SD	63.6±2	7.2±1.2	13.6±1.9	60.3±2.7	8.4±1.6	13.9±1.7
Total AV+SD	61.7±2.2	11.2±4.0	13.7±1.2	59.0±2.2	12.1 ±3.6	14.1±1.2

Variations of L*a*b* colour attributes in the ‘colour gamut’ among the three groups are presented in Table 8-6 and Figure 8-6. The average value for each attribute L*, a*, b* and the highest and lowest values for these components were marked in order to determine the range of colour distribution for each group compared to the other groups. The greatest variation of a* and b* values was for Caucasian skin shades, ranging from 4 to 24.8 with a mean value of 11.8 and 6.3 to 24.2 with a mean value of 13.9 respectively. This indicates that Caucasian skin has a more colourful spectrum than Chinese and Middle Eastern skin. The greatest variation for L* value was for Middle Eastern shades, which ranged from 32 to 70.7 with a mean value of 56.4. This indicates

that the skin of Middle Eastern people, in comparison to that of Caucasians and the Chinese, is a combination of light and dark skin tones.

Table 8-4: Average L*a*b* Values for different body parts according to gender for Middle East skin shade.

Position	L*a*b* - Middle East					
	L*a*b* - Female			L*a*b* - Male		
	L*	a*	b*	L*	a*	b*
	FACE					
Forehead	57.2	10.4	15.7	54.8	12.2	17.1
Nose	57.9	13.2	15.9	54.5	14	16.1
Cheek	60.4	11.7	15.6	55.6	11.7	16.1
Ear	51.8	10.4	15.2	51.6	12.3	15.7
Chin	59	13.5	15.9	49.2	9	13.1
AD&SD	57.3±3.2	11.8±1.5	15.7±0.3	53.1±2.7	11.8±1.8	15.6±1.5
	ARM					
Back hand	60	7.9	16.6	55	9.2	16.3
Palm	61.4	9.1	14	59	10.7	14.1
Outer arm	59.9	6.8	16.5	50.9	7.8	17.6
Inner arm	63.4	5.7	15.4	57.9	7.4	17.3
AV&SD	61.2±1.6	7.4±1.5	15.6±1.2	55.7±3.6	8.8±1.5	16.3±1.6
Total AV&SD	59±3.3	9.9±2.7	15.6±0.8	54.3±3.2	10.5±2.3	15.9±1.5

Table 8-5: Average L*a*b* Values for different body parts according to gender for Chinese skin shade.

Position	L*a*b* - Chinese					
	L*a*b* - Female			L*a*b* - Male		
	L*	a*	b*	L*	a*	b*
	FACE					
Forehead	58.6	10.6	16.1	55.3	12.2	16.4
Nose	60.1	9.9	17.1	57.3	12	16.6
Cheek	61.7	10.2	13.3	57.5	11.9	14.6
Ear	61.3	10.8	14.1	59.1	12.7	14.2
Chin	59.5	12.5	15.8	54.4	11.9	15.1
AV&SD	60.2±1.3	10.8±1	15.3±1.5	56.7±1.9	12.1±0.3	15.4±1.1
	ARM					
Back hand	59.8	7.9	16.3	57	9.9	16.1
Palm	63.6	7.2	13.1	61.4	8.2	13.3
Outer arm	60.3	6.5	15.7	56.5	9	17.1
Inner arm	63.3	5.5	14.1	59.7	7.7	15.5
AV&SD	61.8±2	6.8±1	14.8±1.5	58.7±2.3	8.7±1	15.5±1.6
Total AV&SD	60.9±1.7	9.0±2.3	15.1±1.4	57.6±2.2	10.6±1.9	15.4±1.2

Table 8-6: Higher and lower range of L*a*b* values recorded within each ethnic group.

Ethnic Group	Total L*a*b* Value		
	L*	a*	b*
Caucasian- Mean	60.3	11.8	13.9
Min – Max	49.5 – 70.7	4 – 24.8	6.3 – 24.2
Chinese – Mean	58.6	10.1	15.3
Min – Max	47.1 – 69.7	3.8 – 16.8	3.8 – 17.7
Middle East – Mean	56.4	10.2	15.8
Min – Max	32 – 70.7	3.8 – 19.1	7.5 – 22

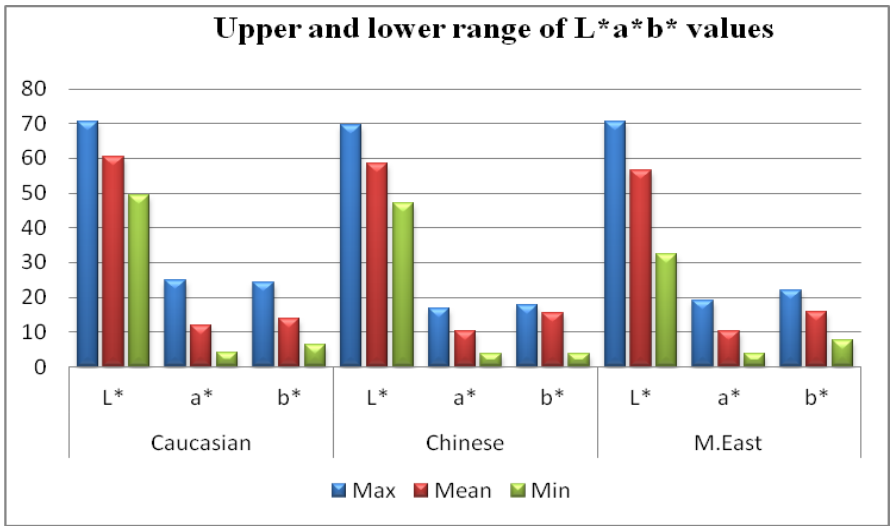

Figure 8-6: Higher and lower range of L*a*b* values recorded within each ethnic group compared to mean value of each group.

In order to further demonstrate skin colour variations between different ethnic groups, the skin colour gamut for each group is plotted in Figures 8-7, 8-8 and 8-9. The Caucasian skin colour gamut appears to be slightly different when compared to either the Chinese or the Iraqi colour gamut; Caucasians have a wider range of colour and more limited range of lightness whereas the Chinese have a limited range of colour, and the Middle Eastern colour gamut presents a wider lightness range compared to that of the Caucasians and the Chinese.

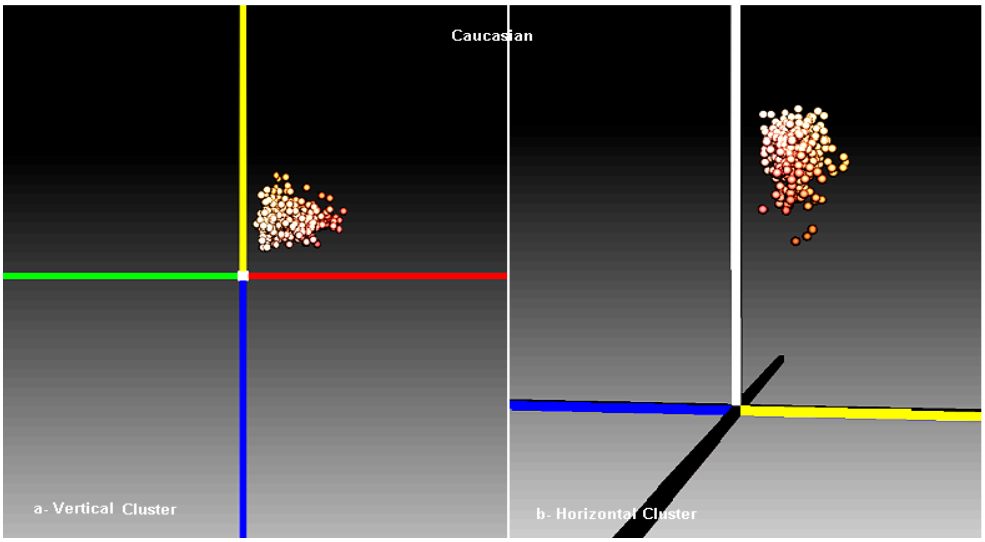

Figure 8-7: Vertical (a) and horizontal (b) appearance of the skin colour gamut for Caucasian shade.

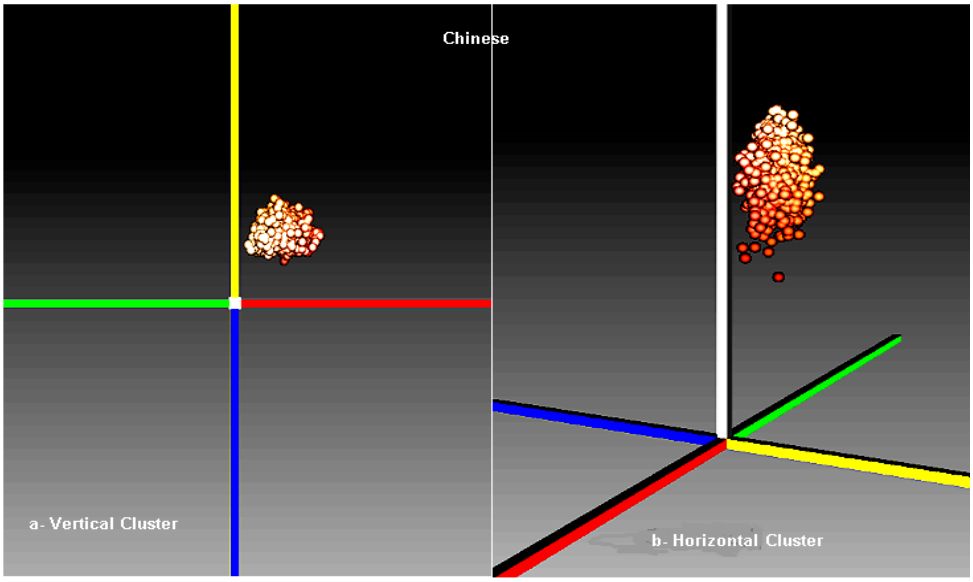

Figure 8-8: Vertical (a) and horizontal (b) appearance of the skin colour gamut for Chinese shade.

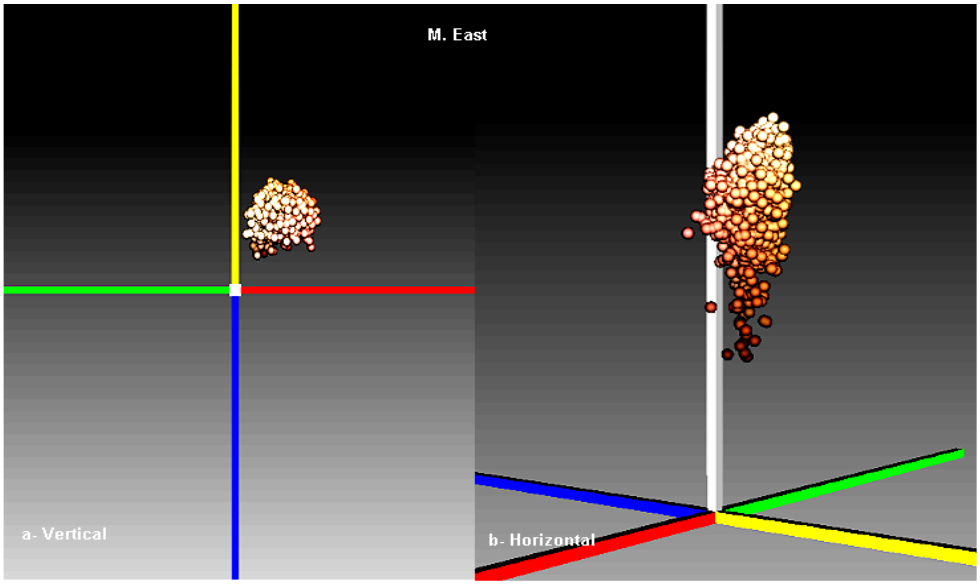

Figure 8-9: Vertical (a) and horizontal (b) appearance of the skin colour gamut for Middle East shade.

The skin colour gamuts for the three ethnic groups overlapped with each other as presented in Figures 8-10 - a and 8-11- a, which show that the Chinese colour range is almost entirely enveloped by the Caucasians' wide range of colour and the Iraqis' wide range of lightness. The resulting colour gamut also overlapped with the printer's colour gamut (Figures 8-10 - b and 8-11- b) and the outcome showed that the skin colour

gamuts for the 3 ethnic groups measured in this study are compatible with the colour range of the printer and this makes it possible for the printer to print the full extent of these colours accurately.

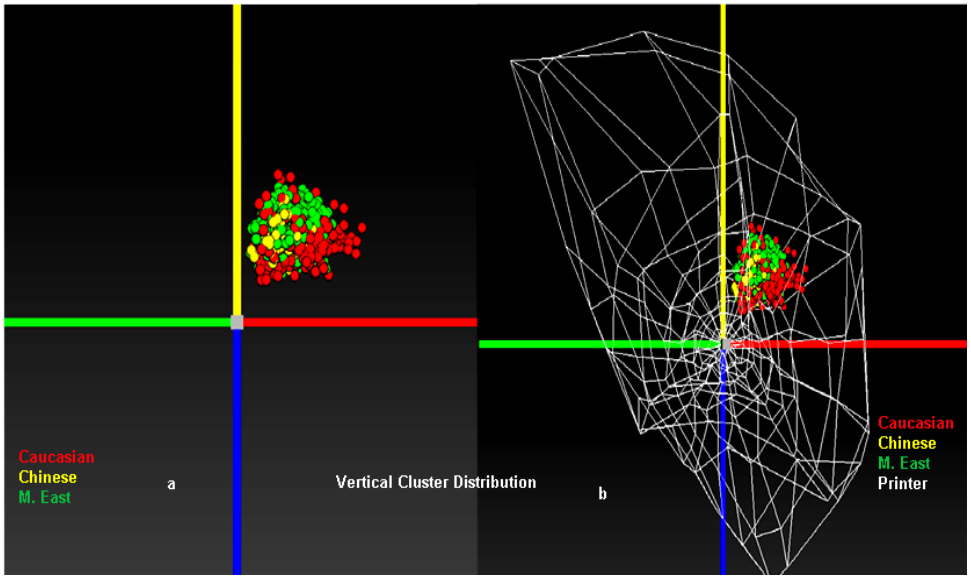

Figure 8-10: Vertical cluster distribution for all colour gamuts (a), overlapped with the printer's colour gamut (b).

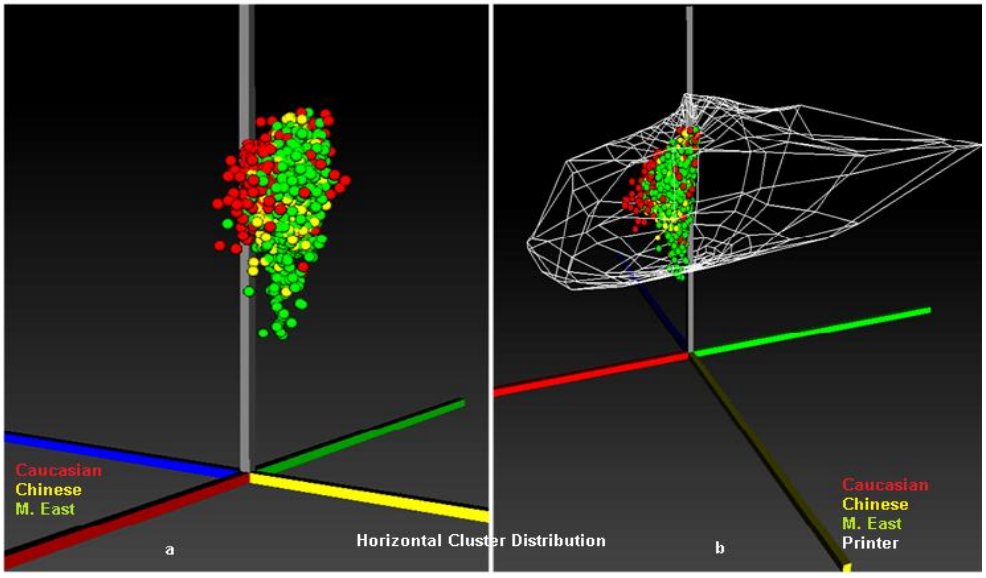

Figure 8-11: Horizontal cluster distribution for all colour gamuts (a), overlapped with the printer's colour gamut (b).

8.5 Discussion

In this study, colour measurements were conducted in three countries for over 400 subjects in 9 body areas using a spectrophotometer. The current study aimed to generate a comprehensive skin colour database and skin colour information based on CIELAB tristimulus values for volunteers representing Caucasians, Chinese and Middle Eastern people. A small number of people of Asian and African origin also participated in this study. Human skin colour shows variations throughout life, and human skin undergoes several structural and functional alterations caused by intrinsic aging and independent environmental insults (Roh et al., 2001). This often results in hyper pigmentation spots by erratic melanocyte activity as a result of cumulative UV exposure. Also white spots or hypopigmantation can be detected in aged skin. Structurally the aged epidermis likely becomes thinner and less coloured than the young epidermis, with age human skin loses colour and presents a significant reduced in (a*) and (b*) values (Fullerton and Serup, 1997). Therefore, and in order to collect more valid and representative skin colour data, the majority of data were collected from younger age group – mainly students aged from 20 to 40 years.

Skin colour appearance differences between ethnic groups were investigated. Then, the skin colour gamut for each ethnic group and colour variations according to gender and body part were also determined. The amount of data obtained from Asian and African participants was too small to be included in the data analysis processes of this study. Further data collection is required in order to establish the skin colour and appearance for other ethnic groups and thereby represent a wider range of skin colours worldwide.

The results provided some important evidence about the skin colour of the three ethnic groups investigated in this study. This evidence indicates that Caucasian shade is more reddish and lighter than Chinese and Iraqi shades, whereas Iraqi shades are darker than Caucasian and Chinese; this could be due to geographic and/or genetic factors. Also, the skin of the Chinese and people of Middle Eastern decent is more yellow than that of Caucasians. Furthermore, Caucasian, Chinese and Middle Eastern females exhibited lighter skin shade than males, while males exhibited redder skin colour than females: the redness is because of the greater blood volume in the male's body (Fortney et al., 1981), while the lightness is probably due to genetic factors, such as the male

having more melanin in his skin or the fact that most outdoor labour is undertaken by males. Also, females are more likely to use makeup, which provides some protection from sunlight (Brown et al., 1962, Frost, 2006). The data also revealed that faces are of darker and more colourful shades than the arms for all three ethnic backgrounds. This is probably due to the fact that the face is an uncovered part of the body and exposed to more sunlight than the covered parts. The natural skin colour can darken as a result of tanning due to exposure to sunlight. Either the UV-radiation creates oxidative stress, which in turn oxidizes existing melanin and leads to rapid darkening of the melanin or there is an increase in production of melanin to provide protection to the skin (Agar and Young, 2005). It is very important to consider these facts when applying data acquisition or manufacturing processes to skin colour reproduction. Human skin shades can be digitally represented using cameras (2D or 3D) and then physically reproduced using additive manufacturing techniques, including layered fabrication techniques such as 3D colour printing. For this process to be successful, the appropriate skin colour gamut has to be used as a true reference in order to achieve an accurate skin colour reproduction and/or translation between different media.

Another important advantage of skin colour measurement is that it can provide each population group/ethnic group with a dedicated skin colour shade guide instead of one shade guide representing the entire skin colour range. If, for example, one wants to produce a prosthesis for a patient in China, all that is needed is to refer to the Chinese skin shade guide. This will allow much more focused and more accurate colour matching. One skin shade guide for the whole population of the world cannot be as accurate as a range of dedicated skin shade guides. If we look at the Chinese skin shade guide or any other ethnic shade, for example, it is possible to produce a skin shade guide for an ethnic group, perhaps comprising no more than eight or nine skin shades. This kind of very simple shade guide can be created for the purpose of producing prosthetic devices.

This provides the option of producing a clear prosthesis and then infiltrating it with an appropriately shaded silicone polymer selected from a dedicated skin shade guide. The use of such a shade guide may offer a simple and effective solution when dealing with large numbers of people, when the primary consideration is not aesthetics but to produce a prosthesis that is

reasonably well matched anatomically. It might not be perfect but it can help people worldwide who need prostheses and do not have access to maxillofacial technicians.

The anaplastologist can select the appropriate skin colour from a dedicated skin shade guide and pass the colour code to a maxillofacial technician anywhere in the world who can then perform the infiltration process for a colourless prosthesis using a coloured silicone polymer based on the colour information that has already been collected visually from the patient. This can overcome the problems of digital colour reproduction that can arise due to limitations related to the colour capture devices/ printer colour profiling. In this case the entire digital colour reproduction process is bypassed and replaced by a visual colour matching process.

8.6 Conclusion

Analysis of a skin colour database for Caucasian, Chinese and Iraqis was performed and this revealed that, in general, Caucasian skin appears to be more reddish and lighter in colour than either Chinese skin or Iraqi skin. However, individuals across the three ethnic groups can have identical skin colour to that of the printer as their colour gamuts are located in a similar position. Skin colour variation within each ethnic group was investigated and the Caucasians were found to have the greatest variation in skin colour.

9 Skin Colour Reproduction Using 3D Colour Printing

9.1 Introduction

3D colour printing is a relatively new technology and for most applications outside of this field, the actual colour is of little consequence. However, for this project to succeed it has to be possible to reproduce as closely as possible the skin shades of the patient for whom the prosthesis is to be made. The input to the 3D printer is based on RGB colour information but the output will be a function not only of the input conditions but also the base material used, the materials used as infiltrates and of course the process itself. Thus there are a number of variables involved in the process of colour reproduction. Parraman et al (2008) evaluated the colour output of the Z-Corp (Z510) printer using horizontal colour charts and assessing colour output on the vertical and horizontal surface of printed cubes. Furthermore, the samples were finished with wax infiltration, and prior to infiltration the detached powder was removed carefully using a soft brush and colour measurement undertaken by using a spectrophotometer. Result showed more than noticeable differences between the output on horizontal surfaces and vertical surfaces of the cubes. This study was considered as a reference for colour reproduction by the Z-Printer (Parraman et al., 2008).

Another study by Stanić et al (2008) evaluated the capability of Z-Printer (Z510) by using plaster powder (zp131) and the correspondent binder (zb60). This study was based on the type of infiltrant used being cyanoacrylate and an epoxy-based resin. The study recorded decreases in the lightness and chroma values according to the infiltrants used (Stanić et al., 2008). Investigation of colour reproduction by 3D colour printing based on testing the basic colours used has correlated the colour reproduction to the position and texture of the printed surface, infiltrant and type of Z-Printer used. Black binder was added to the Z-Corp 650 printer by adding an additional print head to it in order to expand the range of colour reproduction and expanding its colour gamut. In addition to clear, cyan, yellow and magenta heads, the black print head is the 5^{th} head added to the

later model of Z-Printer (Z650). The colour output of Z510 and Z650 were evaluated and compared with each other by Walters et al (2009). Furthermore, the effect of infiltrants cyanoacrylate and paraffin wax were compared. Colour differences ranged between ΔE value 3.1 for cyan and 7.09 for black specimens and the average ΔE value between the two models Z510 and Z650 was 4 for both infiltrants used in this study (Walters et al., 2009).

To date, a computer-based colour imaging reproduction systems have slowly been developed and have started to replace conventional colour reproduction technology gradually due to its potential for improved accurate and consistency.

The international colour consortium ICC profile defines a set of data that specify the colour space of the input and the output of a device according to the standard stated by International Colour Consortium (ICC, 1998). It is a method of correctly mapping a colour profile from an input to an output colour space (Stokes et al., 1996). In order to improve the quality of colour reproduction, the colour capture device or the display device should be profiled; this can be achieved by using a tristimulus spectrophotometer or colorimeter, although some of the manufacturers provide the product with its own profile. however, on occasions the user may require generation of a specific profile for each devise used (Lee and Choi, 2008).

For the 3D printed coloured samples, it is necessary to map and profile the colour attributes of the colour capture device - the spectrometer or the 3D photogrammetry system and the output device - the 3D colour printer.

9.2 Aims

The Aims of this part of the study was

1- To determine the degree of colour change/shift that occurs when printing skin shades using 3D colour printing technology and to determine the extent to which there is a colour shift between the input data and the output data.

2- To present procedures of colour profile development – colour reproduction system for a Z-Corp 'Z510' 3D colour printer and to evaluate the performance of colour profile in terms of colour reproduction for a range of human skin colours.

9.3 Materials and Methods

9.3.1 Part One - Testing the Performance of Z-Printer for Colour Reproduction

9.3.1.1 Group 1 - Printing in starch:

The L*a*b* colour values of a set of 13 silicone rubber (SR) skin shade guides, kindly provided by Mrs. L. Gill[8] (25mm diameter. and 6 mm thick) representing a range of ethnic groups, were measured using a Minolta spectrophotometer (Model: CM-2600d), (Figure 9-1).

This group of "standardized" skin colours were considered the control group. These spectrophotometer values were then converted to RGB data sets using a Java colorimetric converter. The RGB values of the 13 Silicone rubber skin shade guides were input into the Z-Corp 3D colour printer in order to print a similar set of skin shade guides (25 mm diam. and 6 mm thick) with starch powder. Prior to infiltration the loose powder was removed carefully by using a soft brush. The 13 discs were immersed in a translucent maxillofacial SP (Sil-25) for 25 minutes at 3 bar pressure to ensure full penetration of the SP into the coloured starch discs. After 24 hours the L*a*b* values of the discs were measured using the Minolta spectrophotometer. The difference in the input and output values of the L*a*b* data and delta E (ΔE) values related to the various ethnic groups was determined.

Furthermore, the spectral reflectance graph for each pair of discs (the original SR and the printed starch discs) was plotted using a PC controlled spectrophotometer system operating with UV WinLab software using 2° observation with spectral wavelength 380 nm to 700 nm (Figure 9-2) - PerkinElmer – Lambda 2S, UV/V spectrometer. After zero calibration and white calibration, the samples were fitted into position as shown in Figures 9-3 and 9-4 in order to plot the spectral reflectance curve

[8] Acknowledgment to Mrs. Liz Gill – Maxillofacial technologist – BSc (HONS) C&G – Advanced Max-Fac. General - Senior Lecturer at Manchester University.

for each pair of samples - the SR and the printed starch, and to determine the amount and the areas of colour shift on the reflectance graph.

Figure 9-1: Minolta spectrophotometer (Model: CM-2600d).

Figure 9-2: PerkinElmer "Lambda 25" spectrophotometer.

Colour differences ‘ΔE’ was calculated by the following equation:

$$\Delta E = \sqrt[2]{(L^*2 - L^*1)^2 + (a^*2 - a^*1)^2 + (b^*2 - b^*1)^2}$$

L*2, a*2 and b*2 stand for L*,a*, and b*Values of the printed starch discs - the output, while L*1, a*1 and b*1 stand for the L*, a*, and b* Values of the silicone rubber discs - the input.

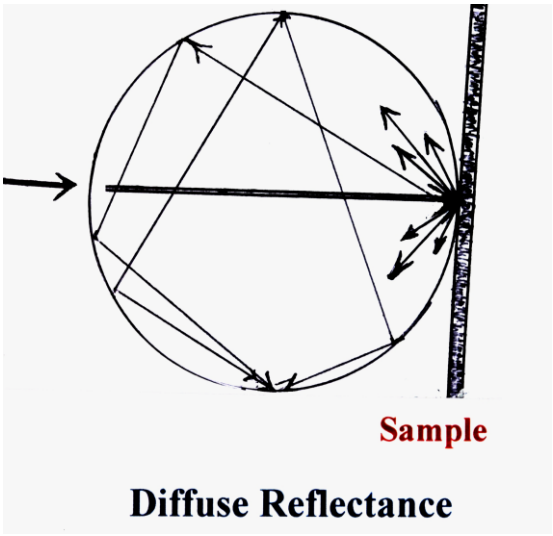

Figure 9-3: Diagram illustrating the position of the sample and the reflectance light.

Figure 9-4: The sample compartment and the sample.

9.3.1.2 Group 2 - Printing in plaster:

As with group one, measuring the L*a*b* colour values of the 13 silicone rubber skin shade guides was undertaken and converting them to RGB values was completed using a Java colorimetric converter. Again the RGB values were input into a 3D colour printer and discs of the same dimensions as the originals were printed in plaster and then infiltrated with cyanoacrylate. After 24 hours the L*a*b* values of the coloured discs were measured. The difference in the input and output values of the L*a*b* data and

ΔE values were determined and the spectral curve for each pair of discs (the original SR and the printed – cyanoacrylate infiltrated plaster discs) was plotted too.

9.3.1.3 Group 3 - Plain starch discs infiltrated with coloured SP:

In a third set of experiments plain non-coloured discs of the printed starch were infiltrated with coloured silicones (Sil-25), representing a Caucasian and an African skin shade. After 24 hours the L*a*b* values and ΔE values for the infiltrated discs were measured and compared with that of the pure coloured silicone rubber discs.

9.3.2 Part two - Colour Correction[9]

9.3.2.1 Printer colour profiling for Z-Corp Z510 3D printer:

The important step in reproducing colour accurately by the Z-Corp printer was to develop a specific colour profile for the printer (Parraman et al., 2008); this included printing a training colour chart consisting of a set of colour patches using the Z-Corp printer with starch powder. The colour chart was then infiltrated with clear SP; prior to infiltration the chart was brushed to clean unattached powder from the surface. The colour chart was left on a horizontal surface after infiltration for 24 hours for the complete set of the SP, and then the input RGB values and output LAB value for each colour patch in the chart was measured using a spectrophotometer. Finally, a mathematical model was developed to predict the relationship between the printer's RGB values and their corresponding LAB values.

In this study, both GretagMacbeth Colour Checker DC charts (240 colours) and a skin colour chart (14 skin colours plus a peak white) were adopted (Figure 9-5 and Figure 9-6). The relationships of CIE LAB and Z-Corp printer RGB was developed by using a third order polynomial regression[10] with a least square fitting based on 254 training colours.

$$\mathbf{M} = (\mathbf{R}^{\mathbf{T}}\mathbf{R})^{-1}\mathbf{R}^{\mathbf{T}}\mathbf{X}$$

$$R' = \begin{bmatrix} L & a & b & L^2 & a^2 & b^2 & L\cdot a & L\cdot b & a\cdot b & L^3 & a^3 & b^3 & L^2\cdot a & L\cdot a^2 & L^2\cdot b & L\cdot b^2 & a^2\cdot b & a\cdot b^2 & L\cdot a\cdot b & 1 \end{bmatrix}_{254}$$

$$X = \begin{bmatrix} R & G & B \end{bmatrix}_{254}$$

Where

[9] Acknowledgment - This work was performed in collaboration with Dr. Kaida Xiao – PhD in colour imaging – Research Fellow – University of Sheffield.

[10] Details in Appendix D - (Polynomial Regression with Least-Squares Fitting).

R represents the LAB values, X represents printer RGB values and M represents a matrix to have a linear relationship between R and X.

After transformation, the M matrix was obtained and was used to represents the colour profile for Z-Corp Z510 printer. Then, printer RGBs were calculated using the linear transformation from any LAB values directly.

$$X = R \cdot M$$

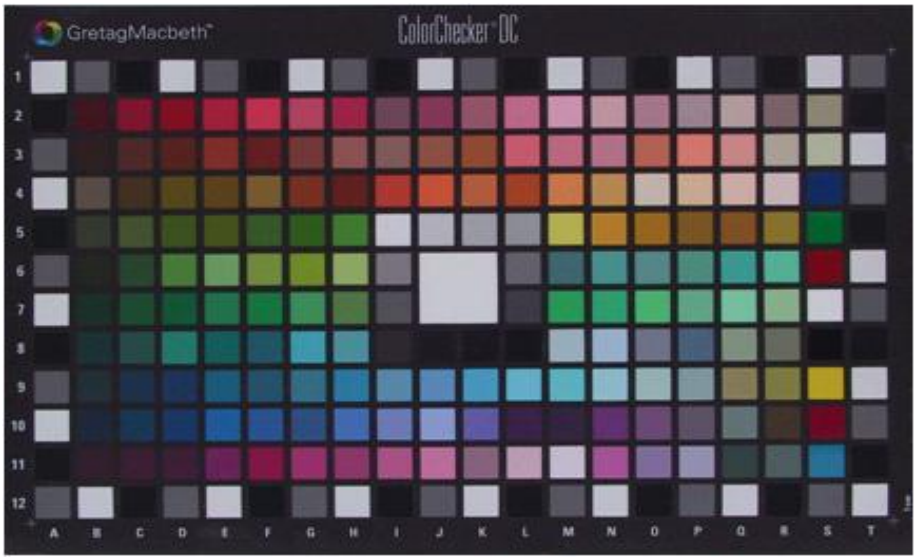

Figure 9-5: GretagMacbeth colour checker DC chart.

Figure 9-6: Skin colour chart.

9.3.2.2 Evaluation of skin colour reproduction:

The printer's performance for skin colour reproduction was evaluated by calculating the colour difference between the original colour samples and the reproduced colour samples. A colour chart including 14 testing skin colours, representing a wide range of skin colours, was employed (Figure 9-6). Note that the 13 coloured silicone discs that had been used previously for evaluation of skin colour reproduction by Z-Corp printer were included. CIELAB colour difference formula was used to measure the colour difference. The method applied for colour reproduction is summarised as follows;

1) Colour transformation:

LAB colour values were measured and sent to the printer to be set into the printer's profile as input values for the samples, then their respective printer RGBs were generated.

2) Colour printing:

Those printer RGBs were sent to the Z-Corp printer and the colour samples were printed on a horizontal chart that included the 13 skin shades, to which a fourth African shade and the white colour were added. The printed chart, infiltrated with clear SP 'Sil-25', was left to dry for 24 hours.

3) Performance evaluation:

Performance of colour reproduction was evaluated by comparing colour difference between the original skin colours and the reproduced skin colours. The respective LAB value of each reproduced skin colour sample was measured using a spectrophotometer. The respective colour differences (ΔE) between the original LAB and the reproduced LAB for each tested pair were then calculated. The grand mean of skin colour difference and the Average (ΔE) values of all tested skin colours were calculated to represent the overall performance of the printer colour profile.

9.4 Results

9.4.1 Part One - Testing the Performance of the Printer for Colour Reproduction

9.4.1.1 Group 1 - Printing in starch:

The L*a*b* values and their colour differences (ΔE) for the 13 SR and the printed starch skin shades are presented in Table 9-1. As the table shows, the ΔE value varies from small in some skin shades to considerable in other skin shades. The table shows a minimum change of 3.4 in Caucasian 1 to a maximum of 12.2 in Caribbean 1, while the other values varied irregularly between these two values. Some skin shades show a minimum amount of colour shift, while others show a high degree of colour shift regardless of the ethnic groups. The average ΔE value was 7.5.

Also the table demonstrates that all a* values of the printed starch colours were higher than the input SR colours, and that indicates a general shift toward the red end of the spectrum in the printing process. On the other hand the L* values shows a general reduction in lighter skin shades - Caucasians, Asians and Pakistanis, whereas the darker skin shade tend to shift to a lighter L* value. This indicates that in general the printer is printing darker shades lighter and lighter shades darker, (please note that these will not be the original colour as printing will have changes them). Visual perception of the colour shift and differences in colour between the original SR discs and the printed starch discs are shown by photographic demonstration for both colours (Figures 9-7, 9-8 and 9-9).

These differences in colour are also confirmed by the spectral reflectance graphs for each pair of discs, the original SR and the printed starch (Figures 9-10 to 9-15). The red line on the graph represents the spectral curve for the printed starch discs, while the blue line represents the spectral curve for the original SR discs. There are some differences in colour reflection for each pair of skin shade discs between the original SR and the printed starch discs. These differences vary between minimal in some skin shades such as Asian, Pakistan, and some of the Caucasian shades, to considerable in African and Caribbean. Generally speaking all the printed colours tended to shift to the red end of the spectrum when compared to the original shade guide. The darker skin tone (Caribbean 2) tended to shift towards a lighter shade. However, the lighter skin

tone (Caucasian 3) tended to shift towards a darker shade. Both show the highest ΔE values, 10.8 and 12.0 respectively. In Caucasian1 and Asian1 the spectral curve of the printed discs runs very close to the original curve. Both show the lowest ΔE values, 3.4 and 4.0 respectively (Table 9-1).

Table 9-1: L*a*b* values for the original rubber and the printed starch shade guides and there colour difference using directly converted RGB values.

	Original Rubber			Printed in Starch			
Ethnic Origin	**L**	**A**	**B**	**L**	**A**	**B**	**ΔE**
Caucasian 1	58.8	9.4	18.4	58.0	10.4	21.5	3.4
Caucasian 2	68.5	10.2	14.7	61.6	14.0	19.1	9.0
Caucasian 3	71.7	3.8	15.2	60.9	7.1	19.4	12.0
Caucasian 4	60.3	8.6	18.6	59.1	9.9	23.1	4.8
Asian 1	61.7	5.7	18.0	58.1	6.3	16.6	4.0
Asian 2	61.2	5.3	17.2	55.7	6.8	18.3	5.7
African 2	32.7	5.0	9.2	42.0	8.4	7.7	10.0
African 3	45.0	11.0	16.2	50.1	9.4	21.0	9.4
African 4	43.3	9.9	12.2	48.1	11.1	14.8	5.0
Caribbean 1	40.8	8.0	17.3	52.9	8.9	18.5	12.2
Caribbean 2	45.7	9.0	19.9	51.6	16.7	24.8	10.8
Pakistan 1	59.4	8.7	16.6	55.4	7.8	19.6	5.1
Pakistan 2	60.1	7.7	17.4	55.3	7.2	20.4	5.7
					Average ΔE		**7.5**

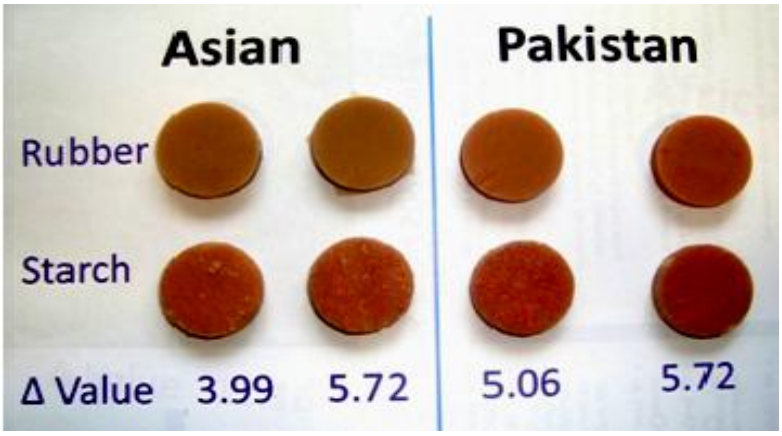

Figure 9-7: Coloured discs for the Asian and Pakistan ethnic group (original rubber and printed starch).

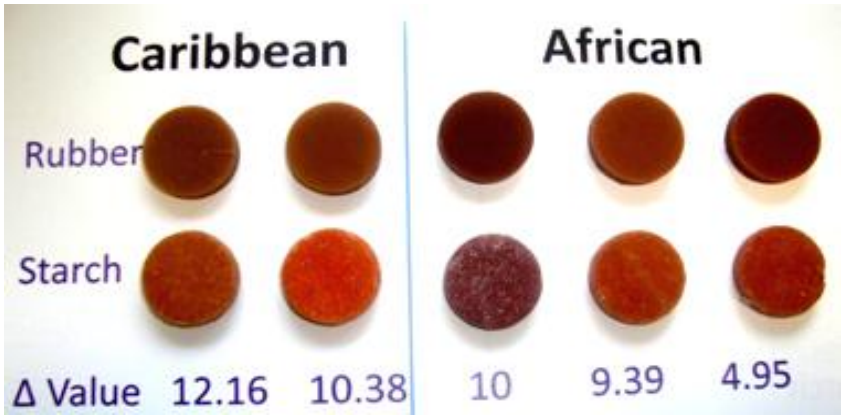

Figure 9-8: Coloured discs for the Caribbean and African ethnic group (original rubber and printed starch).

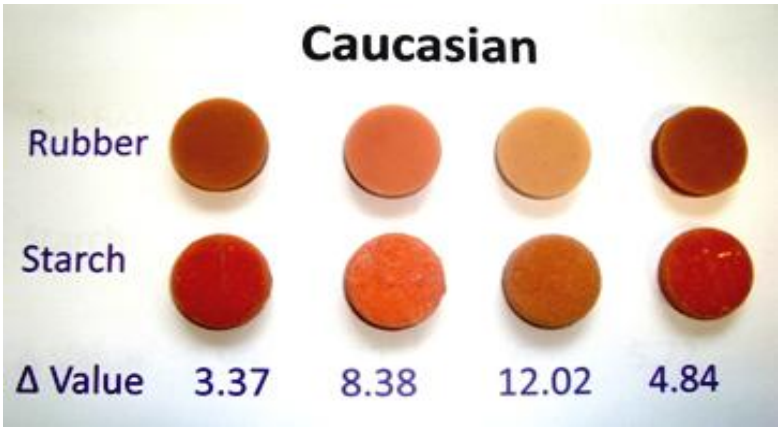

Figure 9-9: Coloured discs for the Caucasian ethnic group (original rubber and printed starch).

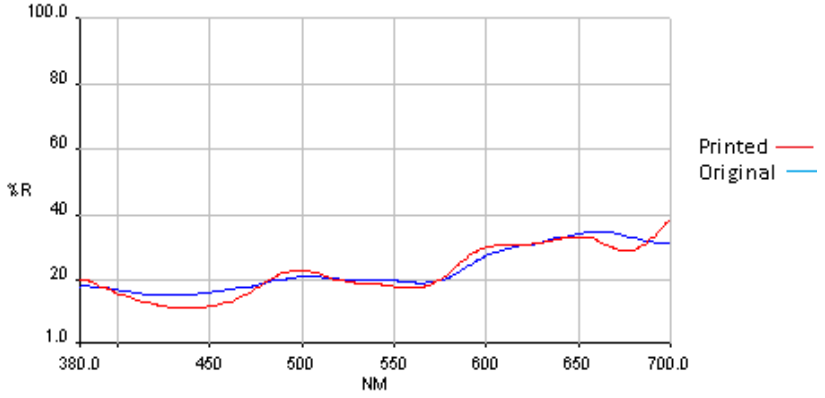

Figure 9-10: Spectral reflectance curve Pakistan 2.

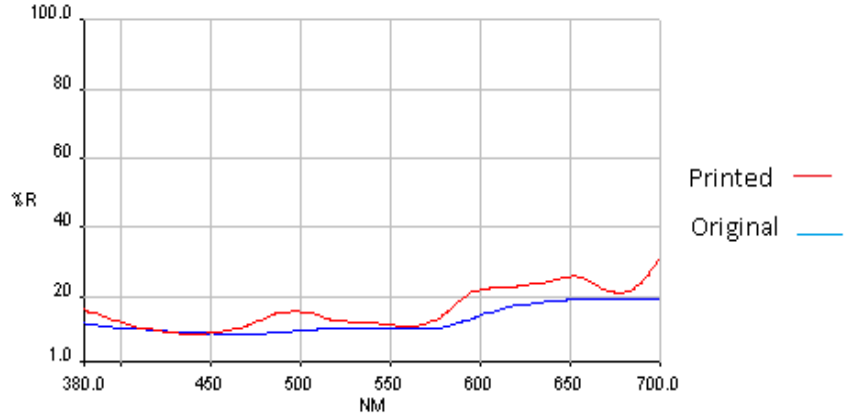

Figure 9-11: Spectral reflectance curve African 4.

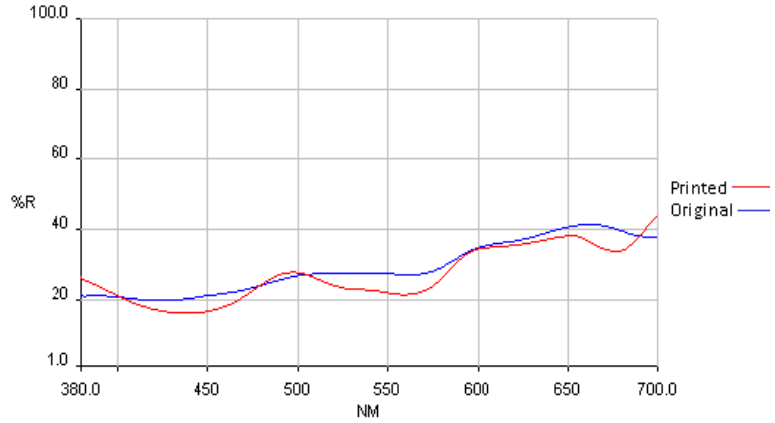

Figure 9-12: Spectral reflectance curve Asian 1.

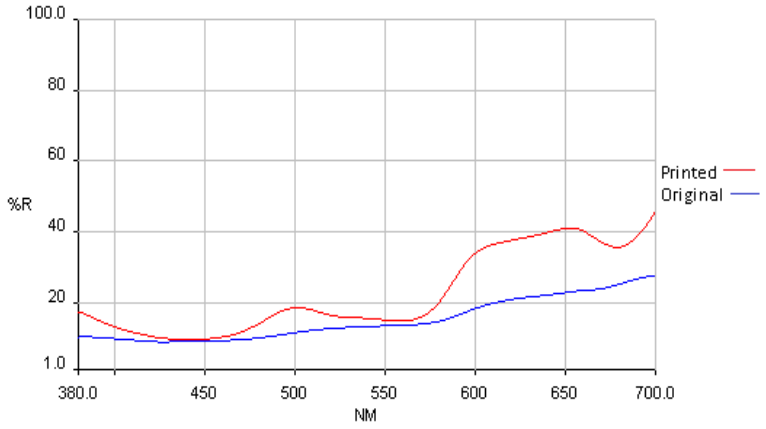

Figure 9-13: Spectral reflectance curve Caribbean 2.

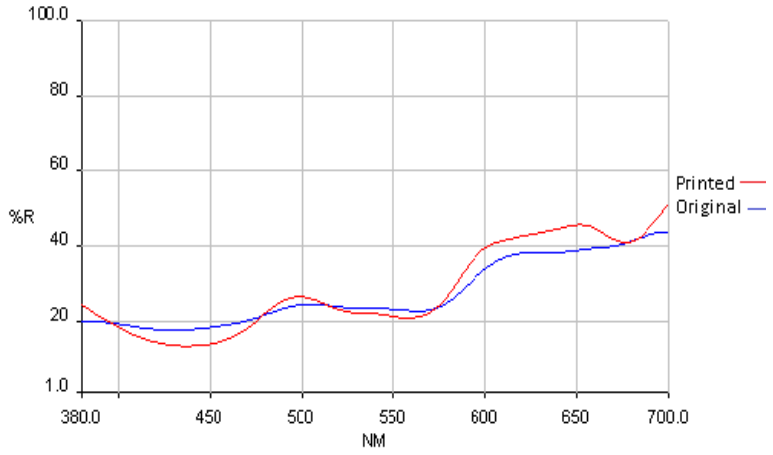

Figure 9-14: Spectral curve Caucasian 1.

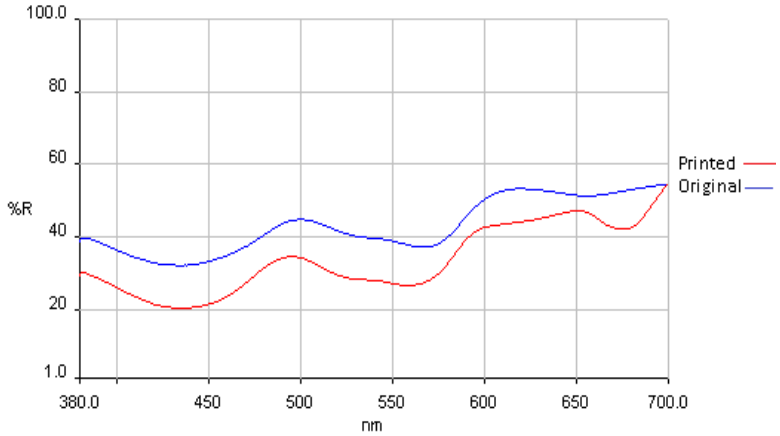

Figure 9-15: Spectral reflectance curve Caucasian 3.

9.4.1.2 Group 2 - Printing in plaster:

Table 9-2 presents the amount of colour shift recorded for group 2 samples, the table demonstrates the L*a*b* values for the 13 SR skin shades, the plaster printed and cyanoacrylate infiltrated shades and their colour differences (ΔE).

A considerable shift in colour was observed for all the shades with the ΔE values varying from a low of 4.5 to a high of 14.6. The greatest ΔE values were obtained for the lighter skin shades (e.g. Caucasian and Asian) as compared with the darker skin shades (e.g. Afro-Caribbean and African). For most shades the biggest changes were observed in the L* values, although for the African and Caribbean shades the shift was mainly due a change in the b* value. The average ΔE Value was 8.5 (Table 9-2).

Visual perception of the colour change is somewhat different from that expected from the ΔE values. Figures 9-16, 9-17, 9-18 show the original SR skin shades compared with the cyanoacrylate infiltrated printed discs using a plaster base (please note there are difficulties reproducing these accurately due to the colour distortion of the printer). The visual impression is that the plaster printed and cyanoacrylate infiltrated discs were darker when compared to those printed in starch and this is confirmed in Table 9-2. This shows a general reduction in L*, a* and b* values. While in starch printed discs the colour was lifted to a lighter shade (L* increased) but also shifted toward the red end of the (–a) to (+a) spectrum/zone, which is demonstrated in an increase in the (a*) value, (Table 9-1).

Table 9-2: L*a*b* values for the original rubber and the plaster printed and cyanoacrylate infiltrated shade guides and their colour difference using directly converted RGB values.

	Silicone Rubber			Printed in plaster			
Ethnic Origin	**L**	**a**	**B**	**L**	**A**	**B**	**ΔE**
Caucasian 1	58.8	9.4	18.4	53.9	6.1	14.4	7.1
Caucasian 2	68.5	10.2	14.7	58.4	7.5	14.2	10.7
Caucasian 3	71.7	3.8	15.2	57.3	2.5	14.7	14.6
Caucasian 4	60.3	8.6	18.6	52.5	6.4	17.5	8.2
Asian 1	61.7	5.7	18.0	53.3	5.8	17.0	8.3
Asian 2	61.2	5.3	17.2	52.7	4.5	16.3	8.5
African 1	32.7	5.0	9.2	39.1	5.3	2.6	9.2
African 2	45.0	11.0	16.2	43.6	9.7	11.3	5.2
African 3	43.3	9.9	12.2	42.4	8.4	8.0	4.5
Caribbean 1	40.8	8.0	17.3	45.7	9.0	19.9	9.4
Caribbean 2	45.7	9.0	19.9	46.4	13.4	15.0	7.0
Pakistan 1	59.4	8.7	16.6	52.8	5.8	14.5	7.5
Pakistan 2	60.1	7.7	17.4	52.0	5.7	16.6	8.4
					Average ΔE		**8.4**

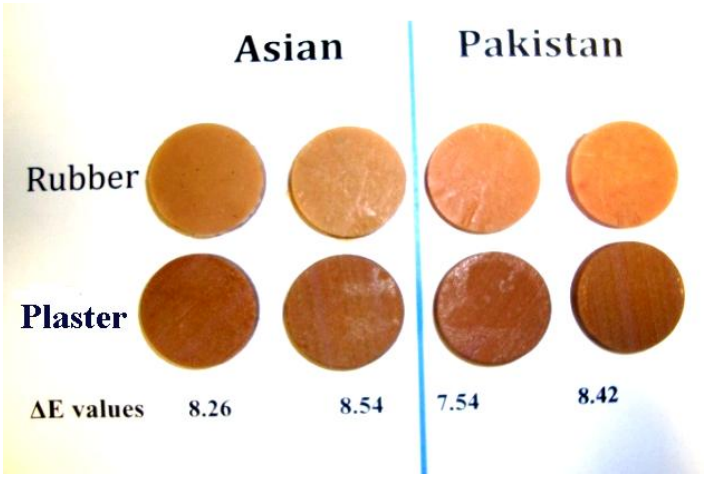

Figure 9-16: Coloured discs for the Asian and Pakistan ethnic group (original rubber and printed plaster).

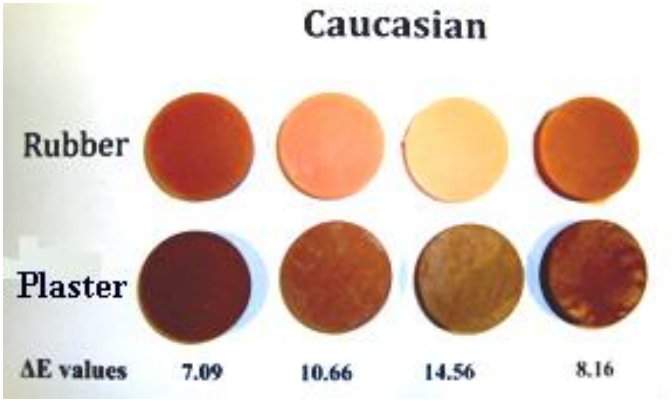

Figure 9-17: Coloured discs for Caucasian ethnic group (original rubber and printed plaster).

Figure 9-18: Coloured discs for the Caribbean and African ethnic group (original rubber and printed plaster).

Figures 9-19 to 9-24 present the spectral reflectance graphs for each pair of the original SR (red lines) and the printed plaster discs (blue lines) for some ethnic shades. The spectral curves show that the printed plaster discs for all ethnic shades shifts toward darker colours. They also demonstrate significant differences through the lighter skin shades than darker shades. The Caucasian and Asian Shades (light skin tone) show a significantly larger shift than the Caribbean and African darker skin tones.

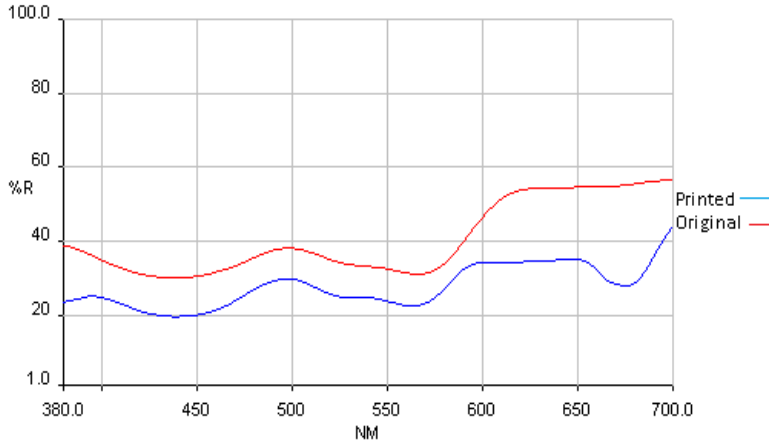

Figure 9-19: Spectral reflectance curve Caucasian 2.

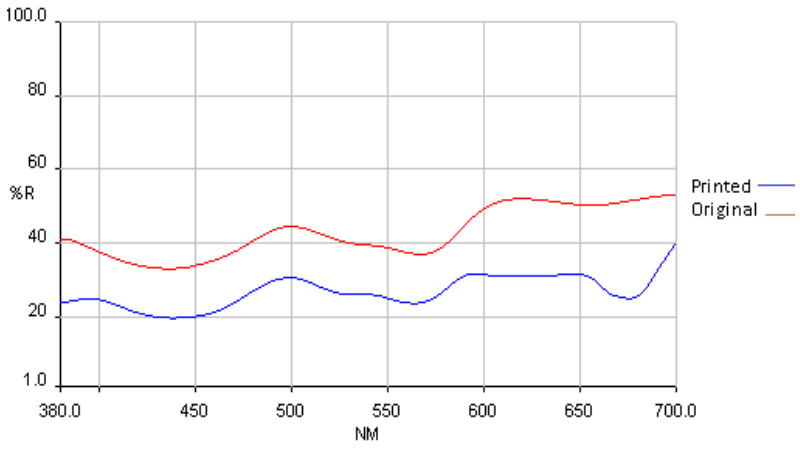

Figure 9-20: Spectral reflectance curve Caucasian 3.

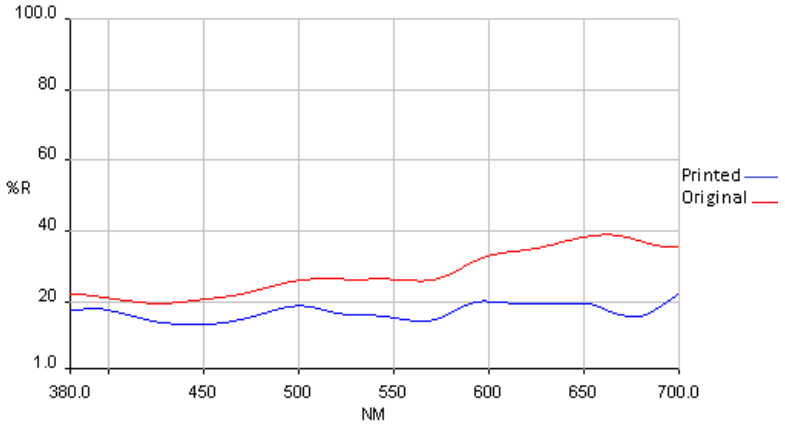

Figure 9-21: Spectral reflectance curve Asian 1.

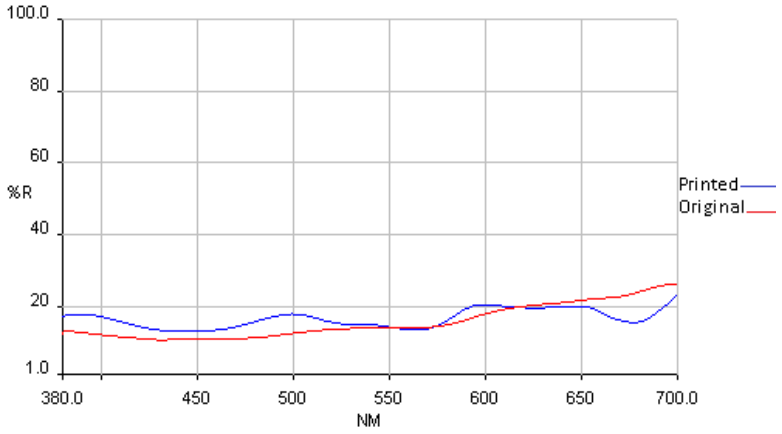

Figure 9-22: Spectral reflectance curve Caribbean 1.

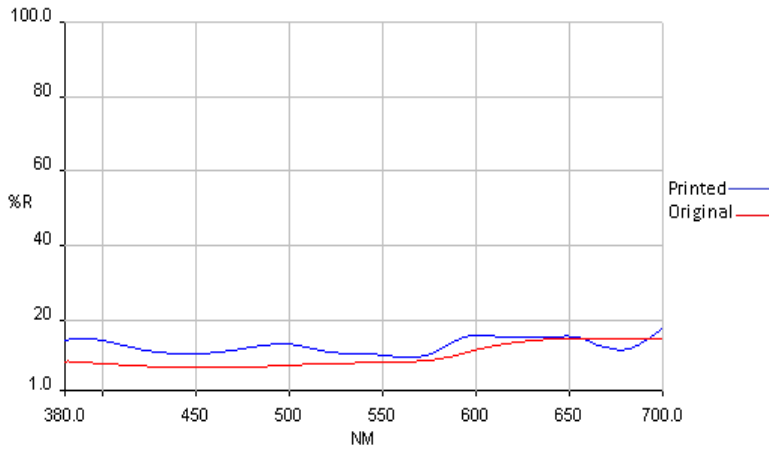

Figure 9-23: Spectral reflectance curve African 1.

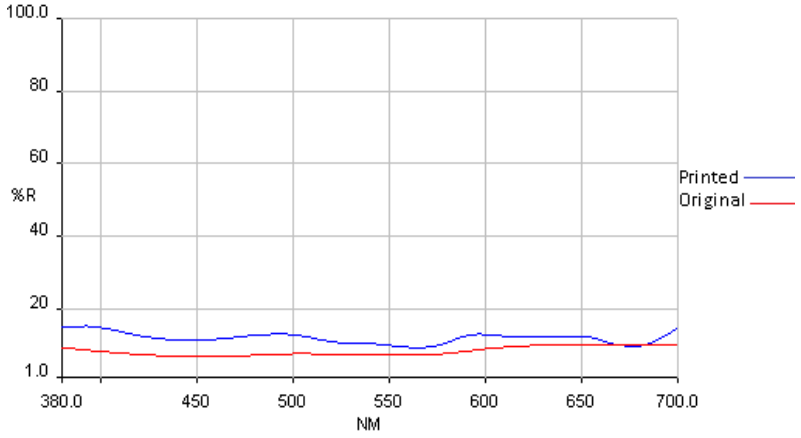

Figure 9-24: Spectral reflectance curve African 3.

9.4.1.3 Group 3 - Plain Starch Discs Infiltrated with Coloured SP:

Table 9-3 illustrates the L*a*b* values and ΔE values for the plain starch discs infiltrated with coloured silicone polymers.

Table 9-3: Effect of infiltration with coloured silicone polymers.

Samples	Silicone Rubber			Printed in Starch			
	L	a	B	L	a	B	ΔE
Caucasian	74.6	14.8	16.3	74.9	12.9	15.0	2.3
African	58.1	10.3	13.2	49.7	11.1	13.8	8.4

Although there is a colour shift, this is quite small in the case of the Caucasian sample. For the African sample the major difference was due to a change in the L* value (lightness) but not in a* and b* values (Colour).

9.4.2 Part Two – Colour Correction

Table 9-4 presents the results of colour correction after profiling the printer colour system. Using a standard printer profile, skin shades produced from SPIS and cyanoacrylate infiltrated plaster were compared to colours produced from SPIS using the 3D Z-Corp printer colour profile. Results showed a demonstrable improvement in

colour production: the average ΔE values were reduced from 8.4 and 7.5 for cyanoacrylate infiltrated plaster and printed SPIS respectively before using the Z-Corp printer profile and then to 4.3 for the printed samples - SPIS after applying the Z-Corp printer colour profile. Figure 9.25 confirms that the proposed method, specially produced for the Z-Corp 510 printer, significantly enhances the performance of colour reproduction when compared to the standard printer colour profile used for this printer. This can also be detected visually in Figures 9-26 and 9-27. The pictures for both original skin colours (a) and reproduced skin colours (b) using the standard printer profile are shown in Figure 9-26. It can be seen that the reproduced colours do not match the originals but are much darker with a significant hue shift, whereas in Figure 9-27, colours were reproduced successfully after applying the Z-Corp printer colour profile.

Table 9-4: Average ΔE Values for printed starch+Z510 profile, printed starch+ standard printer profile and cyanoacrylate infiltrated plaster+standard printer profile[11].

CRS Average ΔE	ΔE Skin Colour – Ethnic groups												
	Cu 1	Cu 2	Cu 3	Cu 4	As 1	As 2	Af 1	Af 2	Af 3	Cr 1	Cr 2	Pk 1	Pk 2
SP+Z510 P ΔE=4.3	3.4	9.7	1.8	4.3	3.8	4.3	0.6	3.9	5.6	4.2	6.1	3.2	5.2
SP+ home P ΔE=7.5	3.4	9.0	12.0	4.8	4.0	5.7	10.0	9.4	5.0	12.2	10.8	5.1	5.7
CY+ home P ΔE=8.4	7.1	10.7	14.6	8.2	8.3	8.5	9.2	5.2	4.5	9.4	7.0	7.5	8.4

[11] - Cu = Caucasian, As = Asian, Af = African, Cr = Caribbean, Pk = Pakistani.

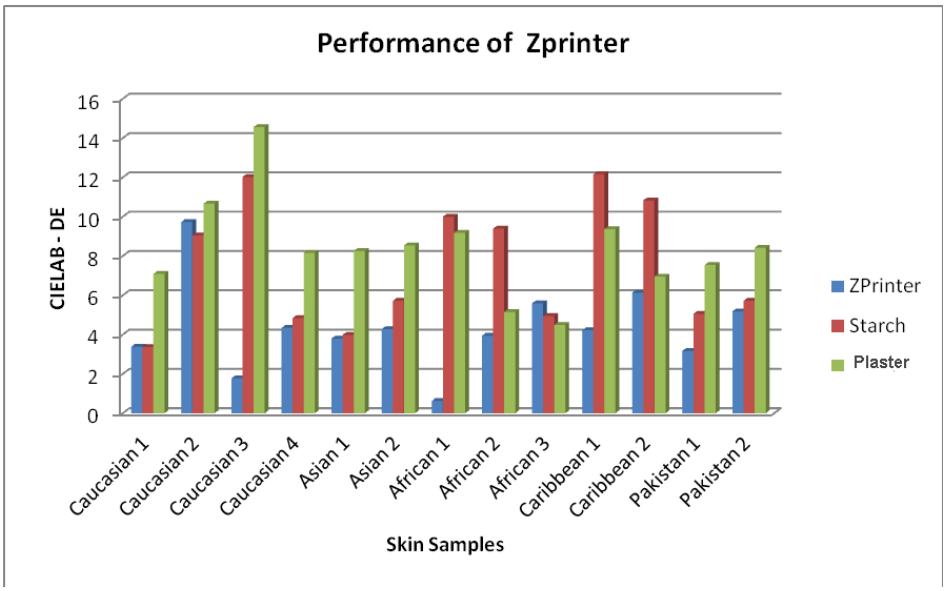

Figure 9-25: Performance of colour reproduction for Printed starch+Z510 profile, printed starch+standard printer profile and cyanoacrylate infiltrated plaster+ standard printer profile.

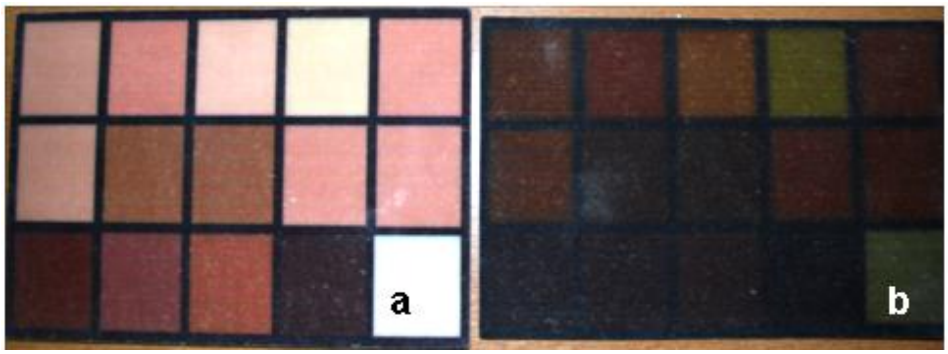

Figure 9-26: Colour reproduction using direct RGB transforms – (a) the original input – (b) the printed output.

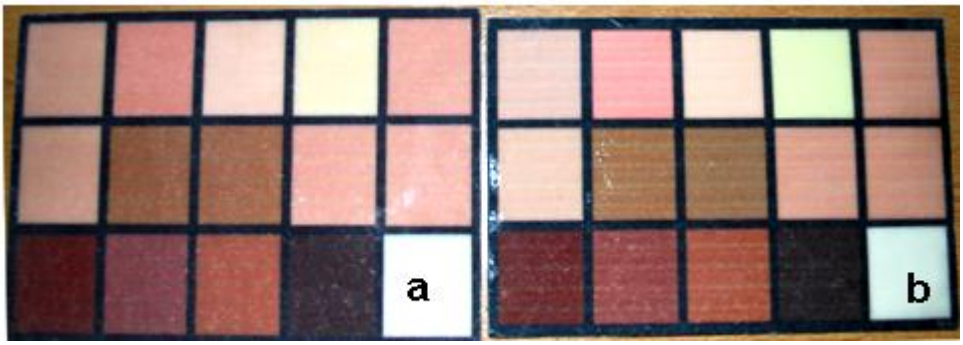

Figure 9-27: Colour reproduction using Z-Corp printer profile – (a) the original input – (b) the printed output.

9.4.3 Performance with Time Spent

In order to investigate the continuity/reproducibility performance of the printer colour reproduction model with time spent, the testing chart was printed 8 times in total (Figure 9-28). They were printed at different intervals within a 28 day period. After printing the average colour difference between the reference colour chart and each test chart was calculated. These values are presented in Table 9-5 and Figure 9-29. It can be seen that the best repeatability/performance was achieved at reproduce 4 with an average colour difference of 2.9 ΔE. In contrast the worst performance was obtained at reproduce 7 with an average colour difference of 5.7 ΔE. It was proposed that the overall model performance within the 20 days was consistent and within the acceptable limits.

Figure 9-28: Colour correction by multiple reproduction of the skin colour chart.

Table 9-5: Performance of the colour reproduction system within 20 days.

Reproduction								
reproduce	**1**	**2**	**3**	**4**	**5**	**6**	**7**	**8**
ΔE	4.3	4.6	3.2	2.9	3.1	4.5	5.7	4.1

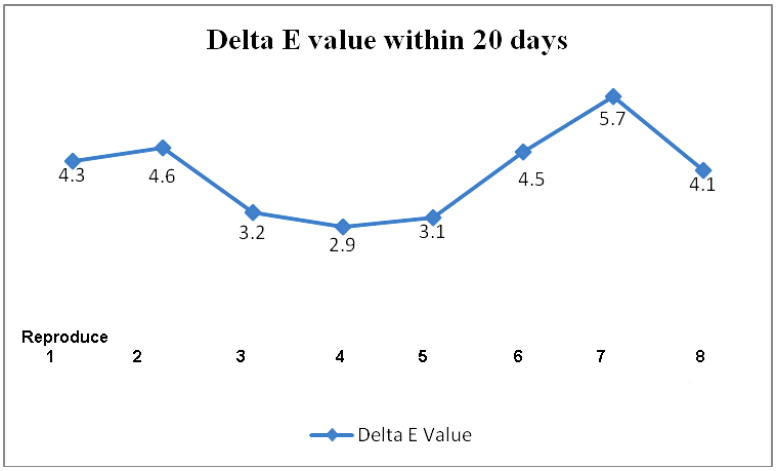

Figure 9-29: Performance of the colour reproduction system within 20 days.

9.5 Discussion

The production of flexible skin shaded prostheses using 3D colour printing can be achieved either by colour printing a 3D model and infiltrating with a clear SP or by printing with a clear binder and infiltration with a coloured SP, or possibly a combination of the two. The first approach would appear to be the most straightforward in that all the features of the patient's skin (base shade, variations, spots, moles and flecks etc.) can be incorporated at the printing stage. However, the drawback with this approach is that it is no simple task to match the output from the printing process with the patient's original skin shade. The data in Table 9-1 clearly identifies the scale of the problem, which appears to be more pronounced with some skin shades than others. It is generally assumes that a ΔE greater than 3 is readily detected by the naked eye. Thus all the printed skin shades differed significantly from their associated original skin shade. Although these values represent the total degree of colour deviation of the printed skin tone and not each particular component of the L*a*b* colour model for each individual colour or skin shade, it is very useful to show the amount of colour shift between the original SR samples and the printed starch discs.

In group one (printed in starch) the difference between the two discs in each pair (the original SR and the starch printed and SP infiltrated) was not significant visually. However ΔE values greater than 3 were recorded in all printed discs and the spectral

curve reflectance of the printed discs shift in various manners. Some show a small shift while others show higher shift. The lighter skin shades tend to shift toward a darker shade while the darker skin shades shift toward lighter shade. There is no clear explanation for this odd behaviour in colour shift, but this phenomenon could be due to the printing process as both, the printer and colour capturing device (Spectrophotometer) have a different colour profile, or due to deviation in the values of the colour space during conversion from L*a*b* to RGB and then from RGB to L*a*b* after printing. Furthermore, it could be related to the translucency factors of the SP used. In general this is a very complex area and requires further investigation.

In group two (printed in plaster), for Caucasian, Asian and Pakistan skin shades the biggest change was in the L* value with only small changes demonstrated in a* and b*. Another prominent feature was that the lighter the skin shades the more the colour mismatched. In contrast the Caribbean and African skin shade match reasonably well in terms of L* but deviate mainly with the b* part of the shade values. Thus it would appear that the colour shift arising during processing varies according to the L*a*b* values of the input data and one cannot assume there is a repeatable shift in each of the individual L*, a* and b* values. The issue becomes yet more complicated when taking into account that the input for the 3D colour printer is in terms of RGB values.

In group three, the use of a coloured silicone polymer infiltrate would appear to work quite well, but again lacked consistency. The Caucasian skin shade produced only a minor shift in the L*a*b* values, whereas for the African skin shade the biggest change was in L*. The change in L* value for the African skin shade contrasts with the colour printing, where the L* value had remained virtually unchanged. Nevertheless, these results are quite encouraging and open up the possibility of using a two stages approach, whereby skin highlights can be printed, followed by infiltration with a suitable base shade. The disadvantage with this approach is that it will require a certain degree of skilled input to get this right, rather than relying on the printer to produce the required appearance of the prosthesis.

The data obtained from the spectral reflectance curves provide a general speculation for the amount of light reflected for each shade and differences in the light reflected for each pair. It can be observed that the higher differences in L* values present a greater variation in the orientation of reflected light on the spectral reflectance

graph, especially in the red portion of the visible wavelengths. Generally the lighter colours such as Caucasian and Asian demonstrated reduced L* values and increased ΔE values and consequently the spectral reflectance graph showed a greater variation in the reflected light for each pair and these variations can be seen on the reflectance graph as a reduction in the amount of reflected light after printing. However, the darker colours, such as the African or the Caribbean shade, showed an increase in L* values followed by an increase in ΔE values and in the amount of light reflected. Furthermore, pairs of discs that revealed slight differences in the L* values before and after printing showed smaller ΔE values and their reflectance curves ran very close to each other along the visible light spectrum.

Human skin colour was produced by printing starch samples infiltrated with clear SP 'Sil-25' and plaster samples infiltrated with cyanoacrylate using a standard printer profile. This method of colour reproduction was not compatible with the RGB colour model adopted by the Z-Printer and resulted in a big difference between the input and the output L*a*b* values and an increased ΔE value for each pair.

In general, a colour reproduction model for digital imaging is conducted for different devices - from digital scanners to colour printer or even monitors/display. Colours in each device are controlled by their own RGB system and therefore true colour communication cannot be achieved without colour management processing between the different devices. Device colour profiling is considered to be a first step of colour management in connecting the device's own colour system (RGB values) to the human eye system (CIE XYZ or CIE LAB values) under a specific viewing condition.
System error for the Z-Corp Z510 3D printing system was evaluated. The effect of system error on colour reproduction was investigated and used as a threshold for assessment of the whole colour reproduction system for facial soft tissues prostheses. A number of algorithms for building specific device profiles were also compared and the one with the best performance for each device was identified. According to the results obtained from these investigations it can be suggested not only did the processes put in place improve colour accuracy/reproducibility but also the colour production system applied in this study for skin colour was adequate for the purpose of reproducing the skin shades for facial prostheses using the Z-Corp 3D colour printer.

9.6 Conclusion

1- The skin shade guide printed using the 3D colour printer and direct RGB transformation was unable to reproduce the skin shades of the original silicone rubber shade guide.

2- Colour shift varied from small in some skin shades to considerable in others, with variation from one ethnic group to another.

3- The quality of colour reproduction was improved by developing a colour reproduction system according to the Z-Corp printer colour profile.

10 Effect of Weathering and Exposure to UV light on the Colour Stability of Silicone Polymer Infiltrated Starch Models[12]

[12] Part of this work on colour stability of SP prostheses has been presented as a poster in BDOSR 2011, Sheffield 12th – 15th September – Appendix A -The Abstract.

10.1 Introduction

Colour instability is considered one of the most significant problems for patients provided with maxillofacial prostheses. Fading of pigments and/dye changes the visual properties of the facial prostheses due to photo-oxidative reaction between the pigments and the UV radiation in the presence of oxygen and moisture. The reaction breaks down the pigments within the prostheses and then alters the reflective properties of the prostheses – these results in a gradual colour fade during its service life. Deterioration of the prostheses due to change in colour is problematic as this is a key aspect in the overall performance of any prosthesis (Chen et al., 1981, Lemon et al., 1995).

A number of studies have investigated the colour stability of maxillofacial SP under different weathering conditions; these have shown colour changes of the SP after artificial and natural weathering and that colour instability was a function of the exposure time and the colorants used. Furthermore, the inherent properties of the original uncoloured SP also contribute to the colour deterioration of the soft tissue prostheses (Hatamleh and Watts, 2010b, Haug et al., 1999b, Haug et al., 1999a, Mancuso et al., 2009c, dos Santos et al., 2010).

10.2 Aim

The aim of this part of the project was to test the effect of natural and accelerated weathering on the colour stability of SPIS specimens compared to the SP.

10.3 Materials and Methods

10.3.1 Part one – Exposure to Accelerated Weathering Conditions

10.3.1.1 Group 1 – Accelerated weathering for 6 weeks:

Testing the effect of 6 weeks exposure to accelerated weathering on the optical Properties of the SPIS samples was performed as detailed bellow.

Group 1 - Series 1: Pure coloured silicone polymer:

Three sets of 25 mm diameter and 6 mm thick, coloured discs prepared from Sil-25 maxillofacial SP representing 5 different ethnic groups were produced using a stainless steel custom made mould. The average L*a*b* colour values for the discs were then measured using the Minolta spectrometer (Model: CM-2600d). These represented the control samples.

Group 1 – Series 2: Coloured discs infiltrated with clear SP:

L*a*b* colour value for each sample was then converted to RGB. These RGB values were utilized by the Z-Corp printer after designing similar discs with identical measurements using SolidWorks 2008 CAD software (25 mm diameter and 6 mm thickness). Colour information for the 5 different ethnic groups was then added to the models during the printing process and 3 sets of coloured discs were printed for use as test samples.

The printed coloured discs were then infiltrated with clear SP as per our protocol - 3 bar pressure in a pressure vessel for 25 minutes. The discs were then left to dry in ambient air at room temperature for 24 hours.

L*a*b* Values for these discs were measured using the Minolta spectrometer.

Both SP (control) discs and SPIS (test) discs were inserted inside the Q-Sun Xenon test chamber (Xe-1-BC1/SC - ASTM G155) in order to expose them to cycles of UV radiation, humidity and temperature for 6 weeks.

At the end of the experiment, the discs were cleaned and L*a*b* colour values taken and ΔE values for each pair of discs were then calculated. A comparison between the control and test groups was then undertaken to determine the degree of colour shift and in order to understand the colour change behaviour of both printed coloured discs and SP discs under accelerated weathering conditions.

10.3.1.2 Group 2 - Accelerated weathering for 2 weeks:

Group 2 - Series 1: Pure coloured Silicone Polymer:

Three sets of 4 pure SP discs (control) were produced to represent 4 different skin shades (2 Caucasians and 2 Africans) and exposed to accelerated weathering inside the Q-Sun chamber for 2 weeks.

Group 2 – Series 2: Coloured discs infiltrated with clear SP:

Three sets of coloured discs were printed and infiltrated with clear SP after converting the L*a*b* colour values of the SP discs in series 1 to RGB. These RGB values were then utilized by the Z-Corp printer. Samples were inserted inside the Q-Sun chamber for 2 weeks.

Group 3 – White starch discs infiltrated with coloured SP:

A third group was also made by printing plain white starch discs, which were infiltrated with a coloured SP – representative of African and Caucasian shades. The samples were similarly placed in the weathering machine (Q-Sun) for 2 weeks.

10.3.2 Part two – Exposure to Natural "Outdoor" Weathering Conditions

Two sets of coloured discs were produced from Sil-25 maxillofacial SP in order to represent 5 different ethnic groups. L*a*b* colour values were measured using Minolta spectrometer and then converted to RGB colour values in order to print the correspondent coloured discs from starch. Their L*a*b* were measured after infiltration with Sil-25 SP and used as a test group. The SP discs (Control) and the printed discs (test) samples were placed in a basket and left exposed to the natural weathering conditions by placing them on a window ledge outside the office for 4 months - May, Jun, July and August 2012 (Figure 10-1).

The specimens were checked regularly during the exposure time. After the scheduled timeframe (4 months) the samples were cleaned and their L*a*b* values were measured, the average L*a*b* and ΔE values were estimated.

Figure 10-1: SP discs and the printed discs exposed to outdoor weathering.

10.3.3 Part Three - Exposure to Ambient Room Environments

Two coloured noses where printed in starch and infiltrated with clear SP "Sil-25", after 24 hours their L*a*b* colour values were measured and the specimens then left on a window ledge in order to be exposed to sun light at daytime and ambient room temperature and humidity for 18 months. After the test period, L*a*b* values were measured and colour differences "ΔE" values for the two noses were obtained.

10.4 Results

10.4.1 Part one - Exposure to Accelerated Weathering Conditions

10.4.1.1 Group 1 – Exposure to 6 weeks accelerated weathering conditions:

The average ΔE value for the SP (control) discs after 6 weeks exposure was 12.5. This compared to a ΔE value of 28.7 for the SPIS (test) discs. The SP and SPIS discs demonstrated a sharp reduction in both a* and b* component of the L*a*b* value for

each individual colour. The detailed information for the L*a*b* values and ΔE values are presented in Table 10.1 for SP and Table 10.2 for SPIS samples.

Table 10-1: L*a*b* colour values for SP (control) discs before and after 6 weeks weathering time.

Lab-SP discs before weathering				Lab-SP discs after weathering			
Shade	**L***	**a***	**b***	**L***	**a***	**b***	**ΔE**
Caucasian	70.1	10.4	15.9	72.2	3.9	11.6	8.1
Asian	72.4	7.2	20.8	63.9	4.7	10	14.3
Pakistan	62.4	8.6	16.2	61.4	7.4	18.1	2.4
Caribbean	59.6	19.8	31.4	74.4	2.2	11.8	30.2
African	39.2	5.0	6.5	40.1	4.4	3.2	3.2
					Average & SD		**12.5±1**

Table 10-2: L*a*b* colour values for coloured SPIS discs before and after 6 weeks weathering time.

Lab-SPIS discs before weathering				Lab-SPIS discs after weathering			
Shade	**L***	**a***	**b***	**L***	**a***	**b***	**ΔE**
Caucasian	76.0	10.6	19.2	81.3	-0.5	11.3	14.7
Asian	70.7	8.9	21.6	84.3	-1.7	7.8	22.1
Pakistan	68.1	9.2	14.5	77.4	1.7	26.7	17.1
Caribbean	61.8	24.7	30.6	78.9	0.1	11.6	35.5
African	34.7	7.0	3.6	58.4	-7.1	11.8	28.7
					Average & SD		**28.7±8.6**

However, L* values which represent lightness, demonstrated a modest increase in some SP (control) colours after 6 weeks exposure (Figure 10-2), where as the SPIS samples showed a considerable increase in L* values for all colours (Figure 10-3).

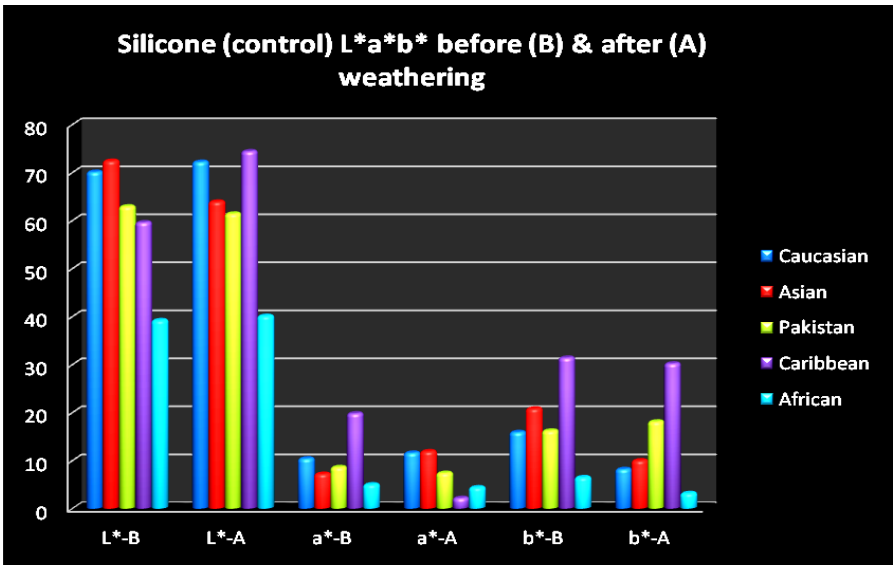

Figure 10-2: L*a*b* values for SR (control) discs before (B) and after (A) 6 weeks weathering time.

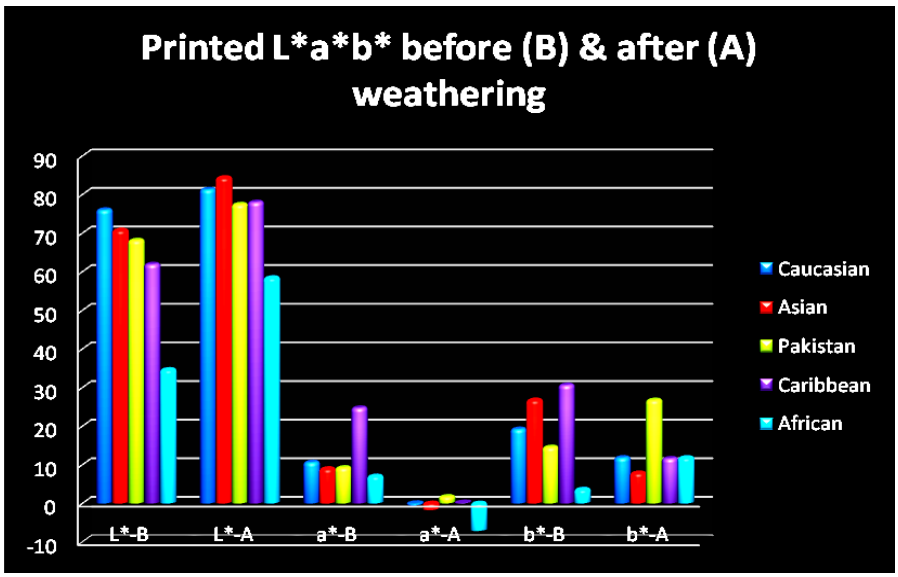

Figure 10-3: L*a*b* values for SPIS (test) samples before (B) and after (A) 6 weeks weathering time.

10.4.1.2 Group 2 – Exposure to 2 weeks accelerated weathering

The data for the SP discs are presented in Table 10-3 and shows an average ΔE of 8.5 with 1.8 SD after 2 weeks exposure to the accelerated weathering conditions. All values of L* increased after weathering, whereas values of a* and b* decreased except a slight increase in b* value was shown for African 2 and Caucasian 1 shades as shown in Table 10-3 and Figure 10-4.

Table 10-3: L*a*b* colour values for SP (control) discs before and after 2 weeks weathering time.

Lab - test discs before weathering				Lab - test discs after weathering			
Clear SP, Coloured discs	**L***	**a***	**b***	**L***	**a***	**b***	**ΔE**
African 1	35.7	7.2	8.4	41.2	4.8	7.9	6.02
African 2	43.5	6.6	11.2	49.6	3.3	16.9	9.0
Caucasian 1	70.6	9.2	15.6	79.2	3.9	16.7	10.2
Caucasian 2	67.7	11.2	18.8	75.7	8.4	15.9	8.8
			Average ΔE & SD			**8.5±1.8**	

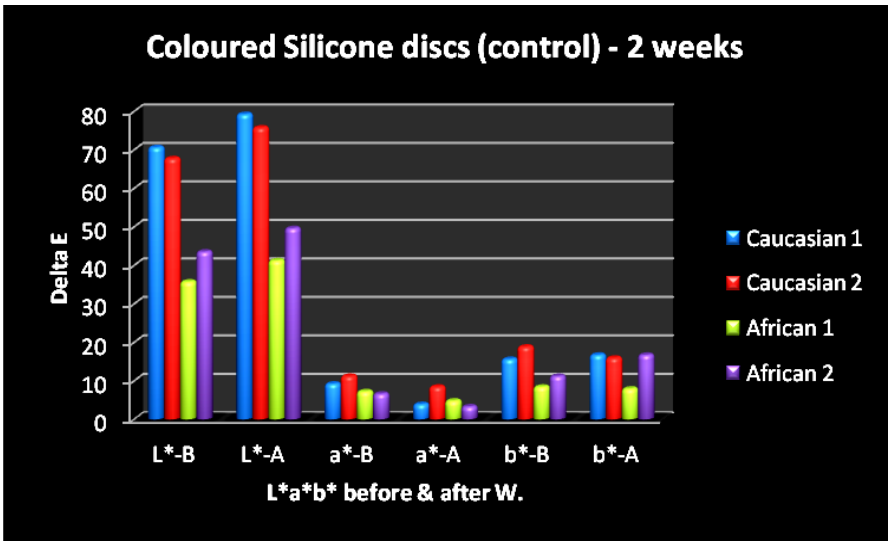

Figure 10-4: L*a*b* values for SP (control) discs before (B) and after (A) 2 weeks weathering time.

The average ΔE values following two-week exposure of the SPIS samples and the plain starch infiltrated with coloured infiltrated SP to accelerated weathering were 12.4 with 9.4 SD and 2.7 at 0.2 SD respectively (Table 10-4). A significant reduction in ΔE value was recorded for the coloured SP infiltrated plain starch discs. The table shows a sharp increase in the L* value (lightness) for African 1 and Caucasian 2 and a considerable reduction in a* value for all colours after weathering (Figure 10-5).

Two weeks exposure to accelerated weathering showed less effect on colour stability of the plain (white) starch samples infiltrated with coloured SP for African and Caucasian shades (Table 10-4). The samples showed a slight increase in L* values, after 2 weeks. The L* value for the African shade slightly increased from 55.7 before weathering to 57.1 after weathering, whilst b* value increased from 8.4 before weathering to 12.6 after weathering. These increases in L* and b* values were followed by a slight reduction in a* value, from 8.5 before weathering to 7.7 after weathering. Similarly the Caucasian shade demonstrated only a very slight increase in L* value, from 71.4 before to 72.7 after weathering (Figure 10-6).

Table 10-4: L*a*b* colour values for the clear SP infiltrated coloured starch and coloured SP infiltrated white starch following 2 weeks weathering time.

Lab - test discs before weathering				**Lab - test discs after weathering**			
Clear SP Coloured discs	**L***	**a***	**b***	**L***	**a***	**b***	**ΔE**
African 1	32.2	10.0	5.2	52.6	-4.4	10.9	25.2
African 2	42.9	5.6	10.9	42.6	4.7	6.2	4.8
Caucasian 1	72.8	7.2	16.8	73.8	4.3	11.7	5.9
Caucasian 2	65.7	7.6	19.0	74.1	-1.0	12.6	13.8
			Average ΔE & SD			**12.4± 9.4**	
Coloured SP Plane discs	**L***	**a***	**b***	**L***	**a***	**b***	**ΔE**
African	55.7	8.5	8.4	57.1	7.7	12.6	2.8
Caucasian	71.4	5.4	12.6	72.6	3.9	11.0	2.5
			Average ΔE & SD			**2.7±0.2**	

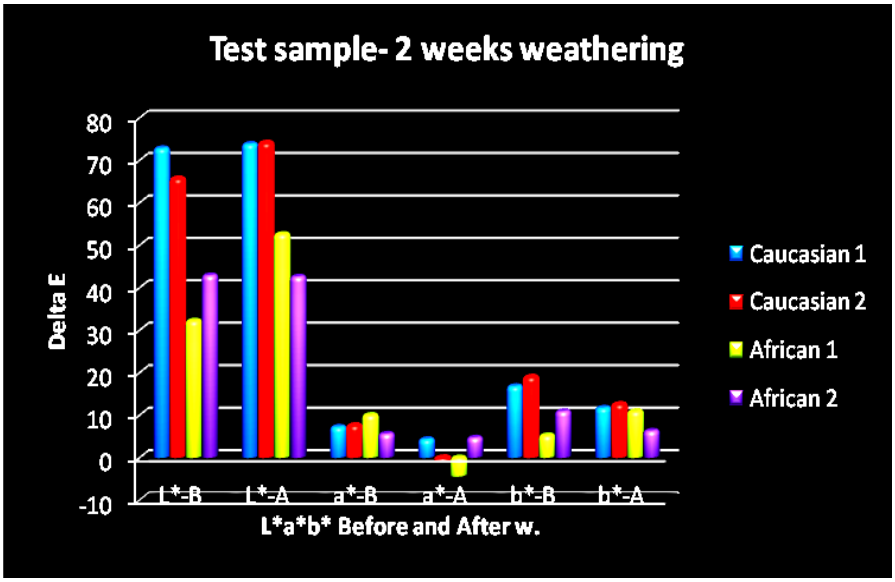

Figure 10-5: L*a*b* values for clear SP infiltrated coloured starch (test) samples before (B) and after (A) 2 weeks weathering time.

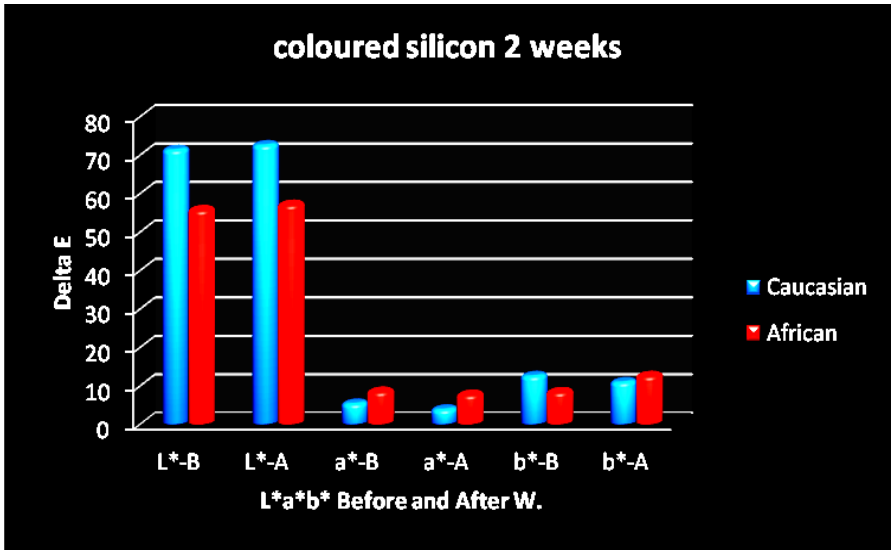

Figure 10-6: L*a*b* colour values for coloured SP infiltrated plain starch (test) samples before (B) and after (A) 2 weeks weathering time.

10.4.2 Part two - Exposure to Natural Weathering Conditions

The detailed information of the L*a*b* value and the average ΔE value for the SP (control) discs and SPIS (test discs) before and after 4 months exposure to outdoor weathering is presented in Tables 10-5 and 10-6. Outdoor weathering had a very little effect on SP samples compared to SPIS samples. Colour differences 'ΔE' values were 3.6 and 9.0 for SP and SPIS samples respectively. L*a*b* values for both groups- the control and the test groups, before and after outdoor weathering are demonstrated in Figures 10-7 and 10-8.

Table 10-5: L*a*b* colour values for SP (control) discs before and after 4 months natural weathering time.

Lab- SR discs before weathering				Lab - SR discs after weathering			
Shade	**L***	**a***	**b***	**L***	**a***	**b***	**ΔE**
Caucasian	68.7	9.9	17.3	69.4	5.0	14.1	5.9
Asian	73.8	4.8	14.2	72.3	3.3	13.7	2.2
Pakistan	63.7	7.1	13.6	62.2	5.6	11.9	2.7
Caribbean	60.2	10.7	31.4	59.2	7.1	28.6	4.7
African	41	5.0	5.7	38.4	4.9	5.8	2.6
	Average & SD						**3.6±1.6**

Table 10-6: L*a*b* colour values for SPIS (test) discs before and after 4 months natural weathering time.

Lab- SPIS discs before weathering				Lab - SPIS discs after weathering			
Shade	**L***	**a***	**b***	**L***	**a***	**b***	**ΔE**
Caucasian	74	11.5	21.6	75.6	0.3	20	11.4
Asian	71.9	5.1	11.5	68.1	5.2	12.3	3.9
Pakistan	63.7	9.9	16.9	64.7	-0.4	19	10.6
Caribbean	60.7	22.8	31.2	60.1	12.7	31	10.1
African	41.8	7.1	6.5	43	-1.5	8.2	8.9
	Average & SD						**9.0±3**

The greater changes for both SP and SPIS samples were in a* value, where as both L* and b* values has shown no changes. The results showed a sharp reduction in a* value of some shades such as Caucasian, Pakistan and African for SPIS samples; this indicates that SPIS samples lose colour faster than SP samples under the effect of natural weathering.

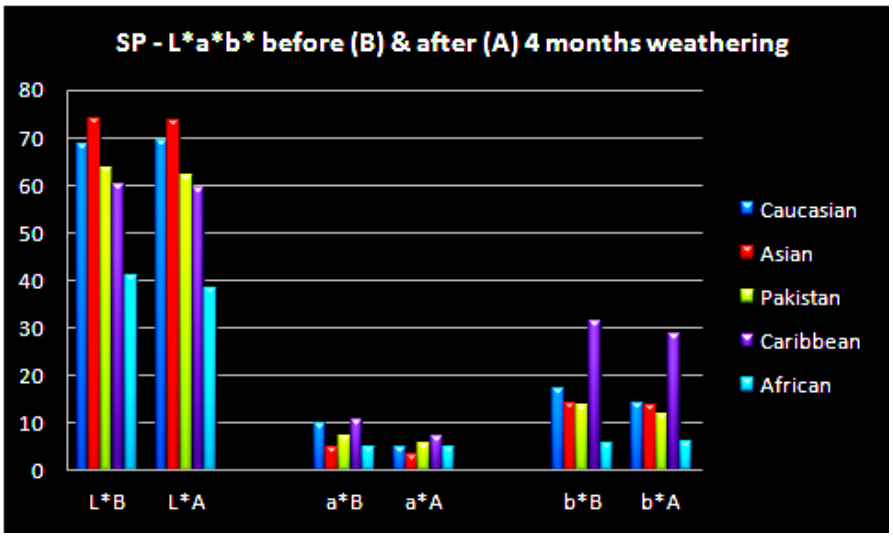

Figure 10-7: L*a*b* colour values for SP (control) discs before and after 4 months natural weathering time.

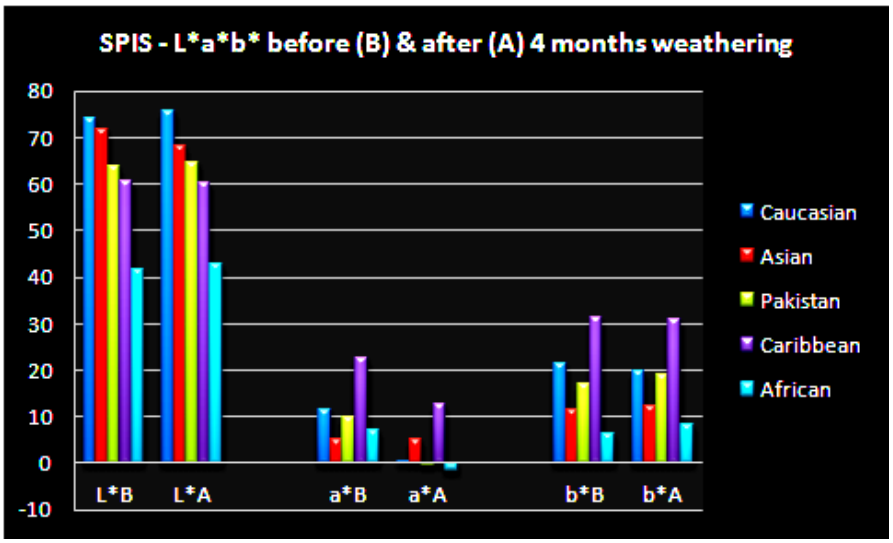

Figure 10-8: L*a*b* colour values for SPIS (test) discs before and after 4 months natural weathering time.

10.4.3 Part three – Exposure to Ambient Room Environments

Figures 10-9 show the differences in colour immediately after printing/infiltration (A) and after 18 months exposure to ambient room environments (B) – light, heat, cold and moisture. Table 10-7 shows the L*a*b* values and ΔE for two printed prostheses at fabrication and after 18 months of normal lifetime. The only detectable change was in the L* value of one of the samples, from 63.3 at fabrication to 70.1 after 18 months lifetime.

Table 10-7: L*a*b* values and ΔE value for nose sample at fabrication and after 18 months lifetime.

L*a*b* Value at fabrication			**L*a*b* Value after 18 months**			
L*	**a***	**b***	**L***	**a***	**b***	**ΔE**
63.3	13.4	11.6	70.1	14.4	14.2	7.3
70.0	14.1	12.3	72.7	14.8	13.8	3.2
				Average ΔE		**5.2**

It is acknowledged that although objective L*a*b* values have been obtained from subjective test/exposure conditions these results appear to reflect what occurs in "real life" more closely than outdoor weathering and accelerated weathering methods. Therefore, it can be suggested that the SPIS formulation can resist colour change and is adequate for the purpose of real life service.

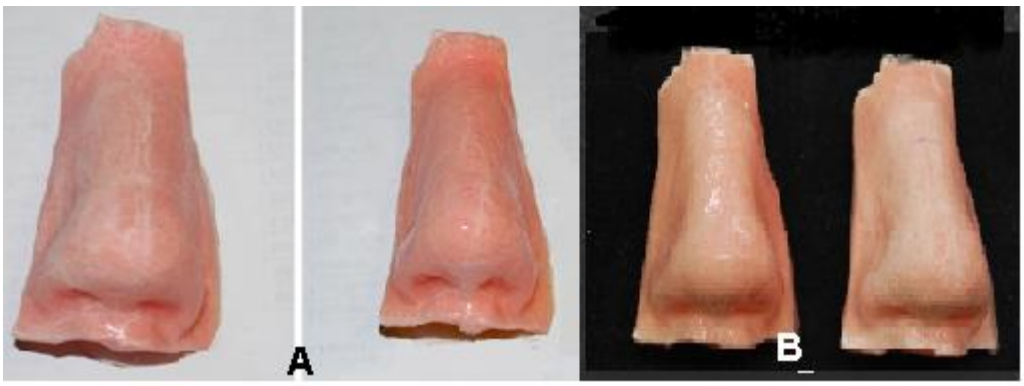

Figure 10-9: The noses at fabrication (A) and after 18 months (B).

10.5 Discussion

Several reports have debated the validity of using artificial weathering to simulate natural weathering conditions as is mentioned in Chapter 6 (Haug et al., 1999b, Haug et al., 1999a). The main criticism is that the two methods do not represent the real life use of facial prostheses.

The outdoor weathering provides a natural aging mechanism but this method has no control over the deterioration factors, whilst the accelerated method is an extreme testing method over a very short time frame but it does have control over the aging factors. Both methods were applied in this study as they are the methods usually used for testing the effects of UV light, humidity and temperature on the optical and mechanical properties of the materials used for soft tissue prostheses.

The data obtained from these studies indicate that all discs – control and test samples – lost some of their colour, and they were bleached under the effect of UV light and other weathering factors. There was a shift toward –a* in 3 samples in the SPIS discs after 6 weeks exposure to accelerated weathering, which indicates a shift from the red to the green part of the colour spectrum. Furthermore, b* values also decreased sharply, which indicates a shift from the yellow to the blue part of the spectrum as shown in Table 10-2 and Figure 10-3. An atypical value can also be noticed in this table: the considerable increase in b* value of the Pakistan shade from 14.5 to 26.7. However, the other samples in the same group showed a remarkable decrease in the b* values. Furthermore, the pure SP (control) samples demonstrated a slight increase in the b* value of Pakistanis, though all other b* values within the same group showed a considerable reduction (table 10-1).

The considerable colour loss in SPIS samples was probably due to the extreme weathering condition used. We understand from the equipment documentation and previous investigations that 6 weeks exposure to accelerated weathering equates to approximately 12 months exposure to outdoor weathering and even more within the lifetime of existing prostheses. Therefore, the testing duration may have been too long/extreme for this purpose, particularly for starch infiltrated silicone samples. As a result of this, further investigations were undertaken to assess a short-term exposure to UV and weathering condition to equate to approximately 4 months of outdoor natural

weathering conditions. Furthermore, a 4 month timeframe of outdoor weathering was applied to assess the effect of outdoor weathering on colour stability of the samples.
Two weeks exposure demonstrated less colour fade than 6 weeks for both SP and SPIS samples. Generally there was a slight increase in L value and a slight reduction in a* and b* values; the average ΔE for the control samples and test samples were 8.5 and 12.4 respectively (Tables 10-3 and 10-4).

The results of Four months exposure to outdoor weathering conditions showed that 2 weeks exposure to accelerated weathering caused more damage to SP and SPIS samples than 4 months exposure to natural weathering. This indicates that 2 weeks exposure to artificial weathering is not corresponding to 4 months natural weathering, it should be equivalent to 6 months or a year and this is dependent on patient's different circumstances.

Colour fading occurs naturally and, in the case of existing prostheses, as a result of photo-oxidative attack of the polymers by UV radiation (Chen et al., 1981, Lemon et al., 1995). However, in this case it is interesting to note that even the control samples consisting of pure silicone were affected – and significantly so.

Visual evaluation of two silicone polymers, Silastic 732 RTV and Silastic MDX 4-4210, by Mancuso et al. (2009) following exposure to accelerated aging showed both silicone polymers behaved similarly in losing their pigments due to the aging mechanism. Furthermore, the time factor was strongly related to pigment loss (Mancuso et al., 2009a). A similar study by Eleni et al. (2009) showed colour loss of maxillofacial silicone polymer on exposure to artificial weathering; results were also dependent on the irradiation time and the basic colours of the sample; African colour was less affected by irradiation; in general, colour change was clinically acceptable (N Eleni et al., 2009). Santos et al. (2010) investigated the effect of three weathering exposures: 252 hours, 504 hours and 1008 hours on MDX4-4210; results showed statistically significant differences between the 3 time periods used for testing the effect of aging mechanisms. Furthermore, exposure to 1008 hours showed a higher influence on colour alteration (dos Santos et al., 2010). Moreover, numerous studies have indicated the deteriorative effect of natural and artificial weathering on the optical properties and colour instability of maxillofacial silicone polymers. (Haug et al., 1999a, Haug et al., 1999b, Eleni et al., 2009a, Mancuso et al., 2009a, Hatamleh and Watts, 2010b, dos Santos et al., 2010) have all reported different degrees of colour change under natural and artificial weathering

conditions. Furthermore, their results were dependent on the duration of exposure, the nature of the weathering condition and type of maxillofacial SPs and the colorant used. Coloured SP - plain discs showed even better resistance after 2 weeks exposure to accelerated weathering conditions. Colour differences before and after weathering showed 2.65 ΔE value, which is considered an acceptable value since it is less than 3. Human eyes detect colour differences when ΔE is more than 3. It is acknowledged that these values may be susceptible to repeatability issues when measuring the values with the spectrometer but these issues should occur consistently across the groups. These investigations revealed that test samples impregnated with coloured SP consistently produce reduced ΔE values and appear more resistant to UV light and other weathering conditions. This demonstrates that they are potentially more durable than pigments or dyes incorporated into the starch discs during printing as part of the print/binder combination. This would be comparable to the pure SP samples and therefore may suggest that colour stability could be improved by applying a coloured silicone to neutral starch models.

In contrast, prolonged exposure (18 months) of the printed prostheses to "natural" conditions - coloured starch infiltrated with clear SP, has shown that the deterioration in colour is comparable to those seen with existing prostheses. As expected, a slight change in colour does occur beyond this time frame.

10.6 Conclusion

1- Accelerated weathering conditions caused a considerable change in the optical properties of both SP and SPIS coloured samples which was dependent on the exposure time.
2- Natural weathering conditions caused a very slight change in the colour of SP samples and a higher change in SPIS coloured samples.
3- "Real life" exposure appears to have little effect on colour stability.

11 Biocompatibility of the Materials Used for Printing Soft Tissue Prostheses[13,14]

[13] Acknowledgment - This work was performed in collaboration with Dr. Nishant Yadev – PhD Tissue engineering.
[14] An overview of the project and part of this work was presented by Professor Yates in 26th annual IAA Conference held in Ghent, Belgium, May 30-June 2, 2012 – Abstract found in appendix E.

11.1 Introduction

The word biocompatibility refers to the ability of an element to operate with an appropriate host response in a certain situation (Williams, 1987). Biocompatibility analysis is performed for materials that are either placed in contact with the skin or implanted inside the body. The body reacts to these elements in different ways according to their location within the body and materials used. The issue of biocompatibility is considered highly critical; implant materials must be tested at an early stage of development for their biocompatibility and their ability to coexist with human tissues (Kammula and Morris, 2001).

Biocompatibility/cytotoxicity testing is performed by cell culture assay in order to investigate the toxic effect of medical devices and implant materials on human cells by applying one or more of the following methods; scanning electron microscopy, enzyme assay, cytokine expression, MTT, LDH and Alamar Blue assay.

The Alamar Blue assay is designed to determine cell line proliferation for different types of living cells. This assay displays the cytotoxic level of an agent among different chemical classes (Fields and Lancaster, 1993). It is a straightforward cell vitality assay, a rapid, reliable and non-radioactive assay which requires a minimum of 80 cells to show positive results (Ahmed et al., 1994). The Alamar Blue assay provides the essential data for predicting the cytotoxic effect of a novel agent by comparing these data with known *in-vitro* data (Fields and Lancaster, 1993).

Recently several models of 3D printers have been developed and commercialised by the Z-corporation; the Z510 is one of these printers that utilize a natural polymer such as cornstarch and water based binder for printing 3D parts. However, the powders and the binders employed by the printer are used for industrial rather than medical applications (Lam et al., 2002). To date, these materials have not been investigated for use in medical applications; therefore, it was necessary to perform the biocompatibility test for the materials used in the manufacture of soft tissue facial prostheses.

11.2 Aim

The aim of this study was to assess the biocompatibility of the binders 'ZB58' and the starch powder 'ZP15e' used by the Z510 colour printer for printing soft tissue facial prostheses.

11.3 Materials and Methods

11.3.1 Part one - Biocompatibility of the Binders

The biocompatibility of the binders was tested on two types of cells stored in liquid nitrogen: the rat osteosarcoma derived cells ROS 17/2.8 (Majeska and Rodan, 1982) and L929 cells, derived from an immortalized mouse fibroblast cell line (Cochrane et al., 2003). Three concentrations (0.1%, 0.5% and 1.0%) of the four binders (clear, yellow, cyan and magenta) were used for the cell vitality assay. The biocompatibility assay included several different procedures, which can be summarised as follows:

11.3.1.1 Growth medium preparation:

500 ml of Complete growth medium was prepared by adding 50 ml of bovine calf serum (BCS), 5 ml of glutamine and 5 ml of P/S (penicillin and streptomycin) to 440 ml of DMEM (Dulbecco's Modified Eagle's Medium) in a sterile bottle, stored at 4°C and to be used within 4 weeks.

11.3.1.2 Cell culture procedure:

1) ROS cells and L929 cells were obtained from stocks stored in liquid nitrogen; recovery of the cells was performed by warming up the vials in a water bath to 37ºC and shaking the vials until 80% had thawed.
2) ROS and L929 cells were cultured in a Complete growth medium, cell suspensions were added to two 'Falcon' 75 ml culture flasks for each cell type and incubated at 37ºC in a humidified atmosphere of 5% CO_2 and 95% O_2 for 72 hours.
3) After the incubation period, the flasks were checked under the light microscope for monolayer cell growth, then the medium was discarded, and the flasks were washed

twice in 5 ml phosphate buffered saline (PBS). 2 ml of Trypsin-Ethylenediaminetetraacetic acid (Trypsin-EDTA) was added to the flasks and the flasks were incubated for 3-4 minutes to allow the cells to split.

4) Two ml of BCS was added to the flasks in order to stop the action of trypsin; the flasks were then gently rinsed several times by drawing the liquid and dropping it back again gently to run against the bottom of the flask in order to detach the remaining cells.
5) The cell suspension was transferred to a 15 ml tube, and centrifuged at 1000 RPM for 5 minutes. Then, the content (supernatant) was discarded leaving the cells densely attached to the bottom of the tube. 10 ml of growth medium was added to the tube and the tube was shaken gently in order to achieve homogeneous cell suspension.

11.3.1.3 Cell counting procedure:

1) A haemocytometer was used for this purpose, 10 micro litres of cell suspension was placed inside and allowed to drain completely beneath the cover slip.
2) The cells were counted systematically in four selected squares using the manual counter. Only live cells were counted; those cells reflected light and appeared shiny, whitish and spherical. Dead or damaged cells, which appeared blue and showed shrinkage of the outer walls, were ignored. The total number of cells in those squares was calculated and divided by the number of squares in order to obtain the average number of cells in each square.
3) The number of cells in 1 millilitre of the original suspension was calculated by applying the following formula

Cells/1ml = $n \times 10^4$

Where n is the average cell count per square

Cell density was calculated using the following formula:

Cell density (µl /ml) = (1.25 / n) x 1000 (µl /ml)

Where 1.25 is the dilution factor

11.3.1.4 Cell vitality assay:

A 12 well plate was used for each binder (clear, yellow, magenta and cyan) and $1.75x10^4$ of each cell (ROS and L929) in medium was added to each well. The plates were incubated at 37ºC for 48 hours at 5% CO_2 and 95% O_2. After the incubation period the medium was discarded and the cells were exposed to three concentrations (1.0%, 0.5% and 0.1%) of each of the four binders (clear, yellow, magenta and cyan) in growth medium, then the plates were incubated at 37ºC for 3 days, 5 days and 7 days. Control groups (cells and medium) also were set for each type of cells.

11.3.1.4.1 Day 3:

Following 3 days exposure to the different concentration of the dyes, unattached cells were removed by washing the monolayer with PBS twice, then one ml of 10 % Alamar Blue (Invitrogen, UK) in medium was added to each well, and the plates were incubated for 2 and 4 hours. After the incubation periods 200 µl for each test and control sample was placed into 96-well plates (Greiner Bio-One, Germany). The fluorescence intensity was measured using a fluorescent plate reader (Infinite® 200 PRO, Tecan, Reading, UK) at an excitation wavelength of 570 nm and an emission wavelength of 600 nm.

11.3.1.4.2 Day 5 and day 7:

As on day 3, at day 5 and day 7, the cells in the 12 well plates were washed with PBS. Then, 1 ml of 10% Alamar Blue in medium was added to each well and the plates were incubated for 2 and 4 hours. After each incubation time, 200 µl samples were placed into a 96-well plate in order to measure the fluorescence intensity.

11.3.2 Part two - Biocompatibility of the Starch Powder

As in part one, biocompatibility of the starch powder was investigated by suspending the ‘ZP15e’ powder in sterile PBS and testing three concentrations (0.025, 0.05 and 0.1 mg/ml) on two cell lines (ROS - osteoblasts and L929 - fibroblasts) (Rae et al., 1989). $120x10^4$ ROS cells in 1 ml DMEM and $5.25x10^4$ L929 cells in 1 ml DMEM per well were cultured. The cells were exposed to the three concentrations in 12 well plates and incubated at 37ºC, for 3, 5 and 7 days hours at 5% CO_2 and 95% O_2. Next the cells were

treated with 10% Alamar Blue (Invitrogen, UK) and incubated for 2 and 4 hours. At the end of this time, 200 µl from each test and control samples was placed into a 96-well plate, and the fluorescence intensity of each well was measured using a fluorescent plate reader (Infinite® 200 PRO, Tecan UK) at an excitation wavelength of 560 nm and emission wavelength of 600 nm. Starch toxicity was measured as a comparison against the uninfected media and cells only 'control'.

Statistical analysis: one way ANOVA was conducted to analyze the toxic effect of the starch powder on the cell lines and to compare the effects of the three concentrations of the starch powder with the control group 'cells only'.

11.3.3 Part three - Biocompatibility of Manufactured Prosthesis

11.3.3.1 Histological examination:

The method used to assess the biocompatibility of manufactured prostheses on intact tissue was an *in vitro* 3-D human skin tissue model - EpiDerm. The tissue samples were obtained from MatTek Corporation (USA). The system consists of cultured normal, human-derived epidermal keratinocytes, which form a "3D", multilayered, highly differentiated model of the human epidermis.

Histological examination was undertaken to evaluate the effect of direct contact between the sample/specimen and the 3D-human skin tissue model. Test specimens in the form of small discs of 2.5 mm diameter and 1 mm thickness were prepared from pure SP (sample A) and colour printed SPIS (sample B). The specimens were kept in contact with the EpiDerm for one hour. Histological examination was undertaken of the test specimens and control specimens (EpiDerm alone) to record the histological changes that occurred in the 3D tissue model as a result of direct contact between the test samples and the EpiDerm compared to the EpiDerm alone (control samples). This investigation allowed visualization of any potential disruption/destruction of the cells within the *in-vitro* skin model.

11.3.3.2 Methylthiazol Tetrazolium (MTT) Assay:

The MTT assay is a convenient, consistent and safe method for determining the number of live cells and their activity following exposure to a stimulus (chemical, thermal, molecular, etc). The MTT assay is a colorimetric assay that relies on the enzymatic

reduction of a yellow tetrazolium salt to a purple formazan derivative in metabolically active cells. The formazan can then be analysed using a colorimetric signal at 570 nm. The outcome is a linear optical density value that is directly proportional to the cell number and activity.

The medium that was removed from the 3D tissue model growth 'EpiDerm' was used for MTT assay and LDH assay after 12 and 24 hours. The MTT was dissolved in phosphate buffered saline PBS at a concentration of 2.5 mg/ml. A supplemented medium was added to it and (200 µl) of the resulting solution was transferred to 96-well plates and absorbance was recorded at 560 nm using the microplate spectrophotometer system.

11.3.3.3 Lactate Dehydrogenase (LDH) Assay:

The lactate dehydrogenase (LDH) assay can be used as an indicator of cell membrane integrity and therefore serves as a general means to assess cytotoxicity resulting from exposure to chemical compounds or other toxic products. LDH is a soluble cytosolic enzyme that is released following loss of cellular membrane integrity from either apoptosis and/or necrosis. The assay measures LDH concentrations using a two-step coupled reaction. In the first step, the LDH released catalyzes the reduction of NAD^+ to NADH and H^+ by oxidation of lactate to pyruvate. In the second step, the newly formed NADH and H^+ are used to catalyze the reduction of a tetrazolium salt (INT) to a highly-coloured formazan derivative which absorbs strongly at 490-520 nm. Again this is an optical density value that is linear and directly proportional to the level of cell death/inactivity. One way analysis of variance ANOVA used to analyse the optical density of the medium after 12 and 24 hours.

11.4 Results

11.4.1 Part one - Biocompatibility of the Binders

After the incubation period the plates showed a change in colour from blue to red in all control and most of the test plates. This conversion is a reflection of cell vitality and continued cell growth in the medium that leads to reduction of non-fluorescent blue dye resazurin to fluorescent red dye resorfurin (Nakayama et al., 1997, Lancaster and Fields,

1996). The detailed information of the Alamar Blue assay is presented in Table 11-1 for ROS cells and Table 11-2 for L929 cells; the tables demonstrate the effect of the 3 concentrations of the four binders on these cells at days 3, 5 and 7.

Table 11-1: Alamar Blue assay for the binders on ROS cell lines.

Concentration	Control and Test Samples –Fraction				
	ROS - Day 3				
	Control	Clear	Cyan	Magenta	Yellow
0.1%	100	88.4	102.8	100.1	93.1
0.5%	100	90.4	99.9	100.2	106.9
1.0%	100	58.0	97.6	101.2	102.1
	ROS - Day 5				
0.1%	100	98.4	100.6	96.2	97.5
0.5%	100	69.6	83.7	86.5	85.5
1.0%	100	69.2	80.9	77.3	81.8
	ROS - Day 7				
0.1%	100	111.2	110.6	118.3	109.8
0.5%	100	9.6	59.9	100.1	59.3
1.0%	100	0	12.7	33.2	36.5

11.4.1.1 Day 3:

At day 3, cell vitality assay showed normal cell growth for both cell lines for the three concentrations of the four binders compared to their control groups (Figures 11-1 and 11-2). Furthermore, photographs were prepared for the different cell lines under light microscopy for the four inks at different concentrations and for the control wells, some of these photographs are demonstrated in Figures 11-3 to 11-8.

Table 11-2: Alamar Blue assay for the binders on L929 cell lines.

Concentration	Control and Test Samples –Fraction				
	L929 - Day 3				
	Control	Clear	Cyan	Magenta	Yellow
0.1%	100	92.9	95.4	92.0	93.6
0.5%	100	94.2	96.1	94.1	94.0
1.0%	100	87.9	99.2	98.4	101.7
	L929 - Day 5				
0.1%	100	98.4	100.6	96.2	97.5
0.5%	100	69.6	83.7	86.5	85.5
1.0%	100	69.2	80.9	77.3	81.8
	L929 - Day 7				
0.1%	100	65.41	81.5	74.0	106.6
0.5%	100	36.3	56.2	75.3	82.3
1.0%	100	0	39.1	104.6	41.1

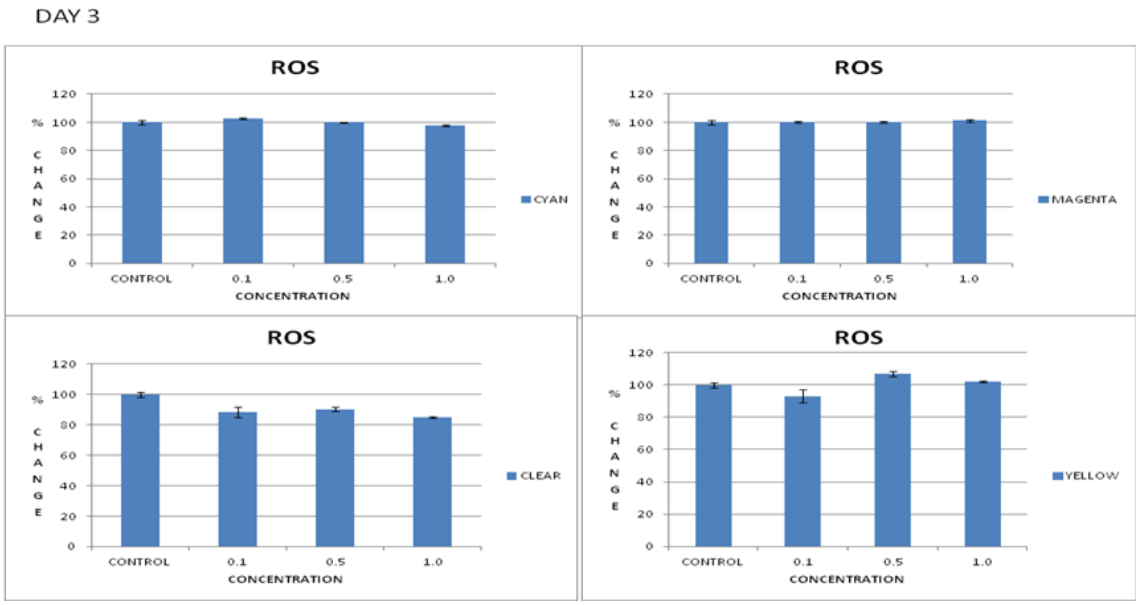

Figure 11-1: Alamar Blue assay of ROS cells for the four binders at day 3.

Figure 11-2: The Alamar Blue assay of L929 for the four inks at day 3.

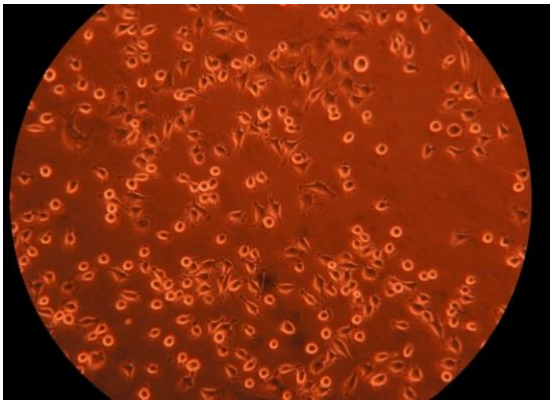

Figure 11-3: Light microscopy of L929 cell line for control well.

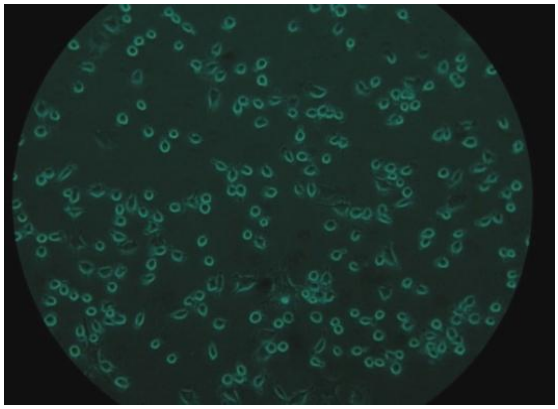

Figure 11-4: Light microscopy of L929 cell line at 1.0% cyan binder.

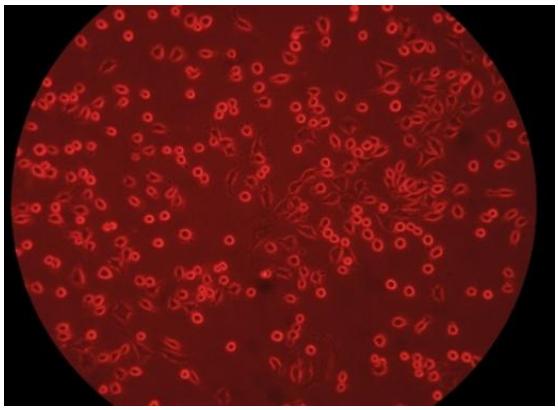

Figure 11-5: Light microscopy of L929 cell line at 0.5% magenta binder

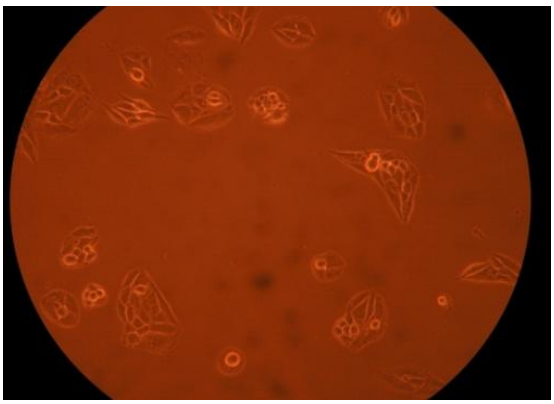

Figure 11-6: Light microscopy of ROS cell line for the control group.

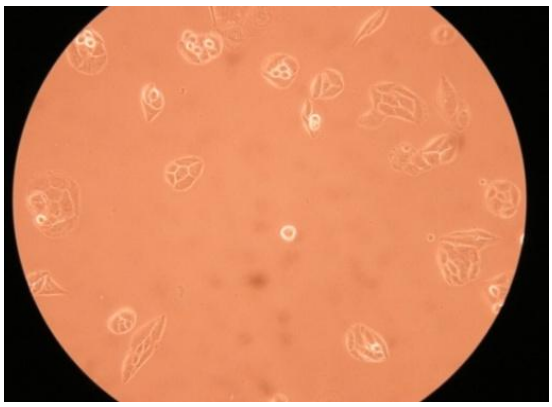

Figure 11-7: Light microscopy of ROS cell lines at 0.1% clear binder.

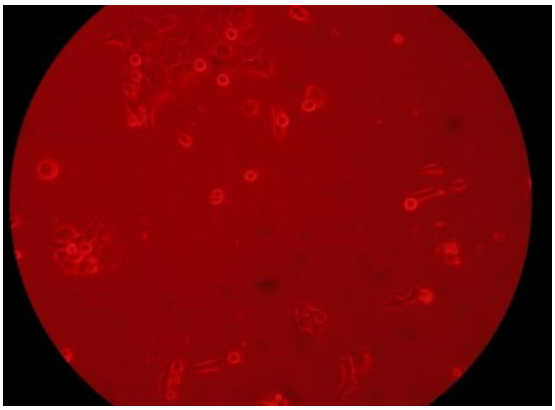

Figure 11-8: Light microscopy of ROS cell lines at 0.1% magenta binder.

11.4.1.2 Day 5:

All cell line growth for the four binders had shown a similar level of growth and cellular activities at all concentrations. There was a slight reduction in cellular activities for both types of cells after 5 days exposure to 0.5% and 1.0% concentrations of the four binders as presented in Figures 11-9 and 11-10.

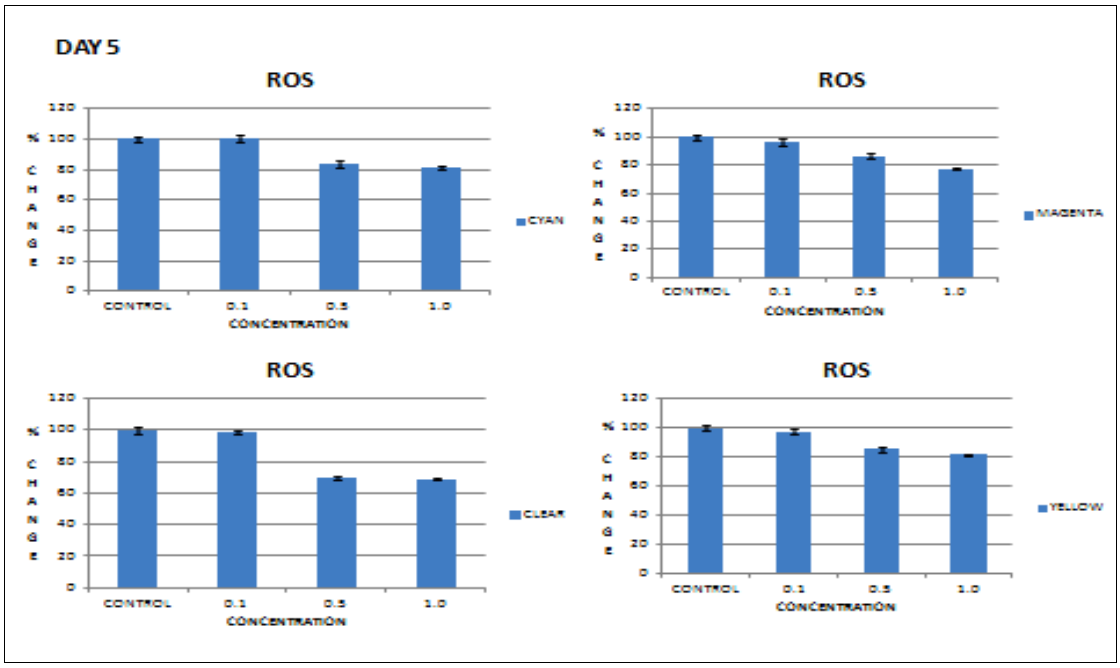

Figure 11-9: Alamar Blue assay of ROS cells for the four binders at day 5.

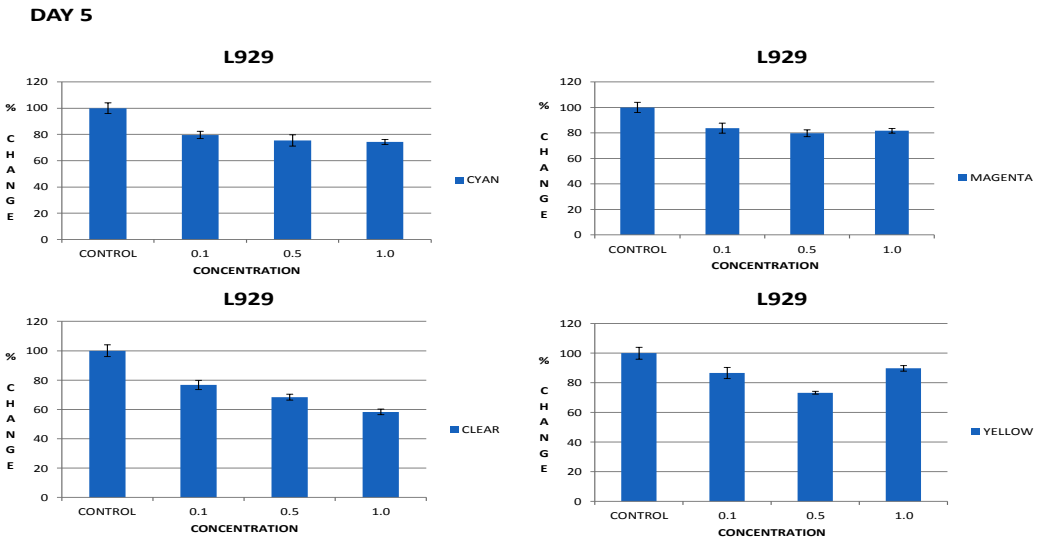

Figure 11-10: Alamar Blue assay of L929 cells for the four binders at day 5.

11.4.1.3 Day 7:

The detailed data for 7 days exposure of the cell lines to different concentrations of the four binders are presented in Figures 11-11 and 11-12. At day 7, the picture was different especially with the higher concentrations of the binders for ROS cell lines. At 0.5% and 1.0% concentrations of the binders results showed a gradual reduction in cell activities.

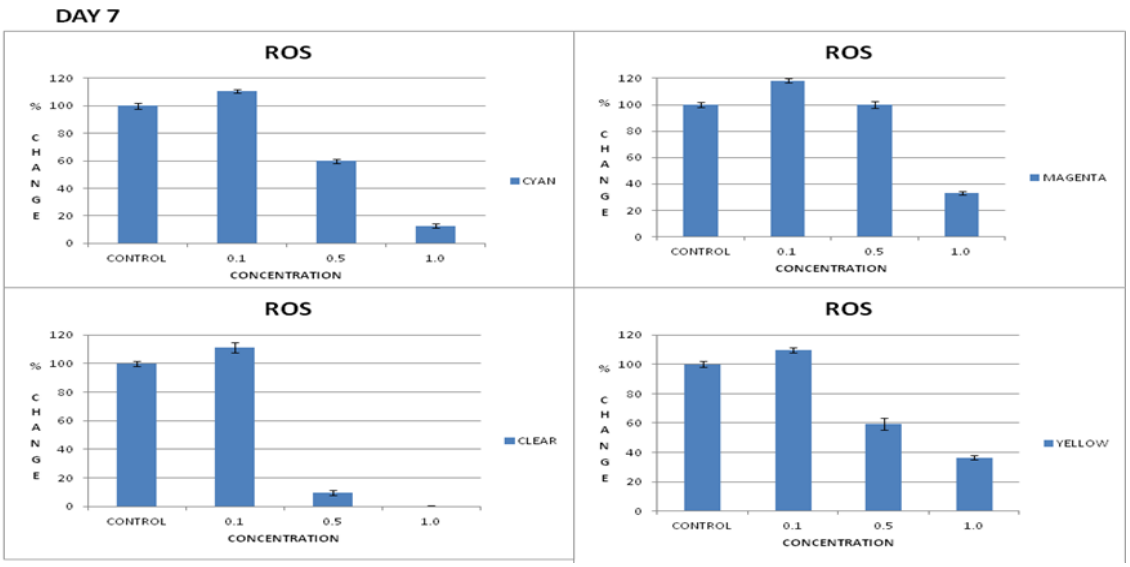

Figure 11-11: Alamar Blue assay of ROS cells for the four binders at day 7.

Exposure of ROS and L929 cell lines to a concentration of 1.0% of the clear binder showed no cellular activity, which indicates that these cells had died. However, the yellow binder and the magenta showed considerable cellular activity, with less toxicity of all concentrations on ROS cell lines and L020 cell lines.

Furthermore, light microscopy revealed no evidence of live cells for the clear binder at 1.0% concentration and only a few cells were detected for the cyan binder at 1.0 % (Figures 11-13 and 11-14).

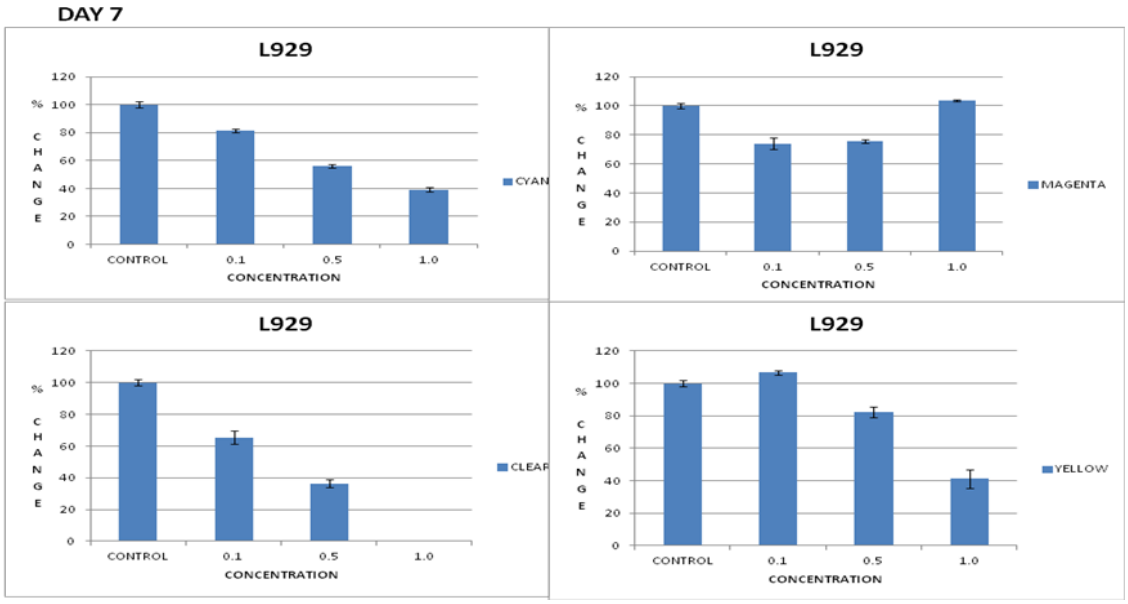

Figure 11-12: Alamar Blue assay of L929 cells for the four binders at day 7.

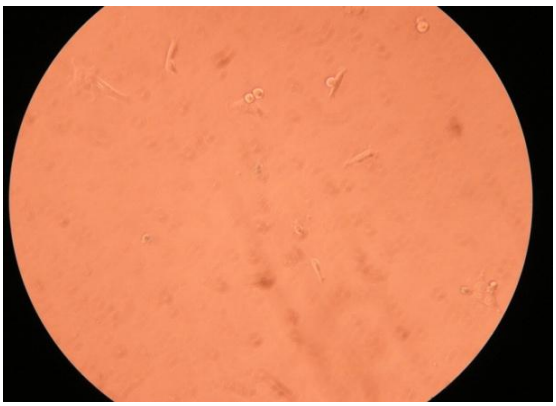

Figure 11-13: Clear binder 1.0% at day 7.

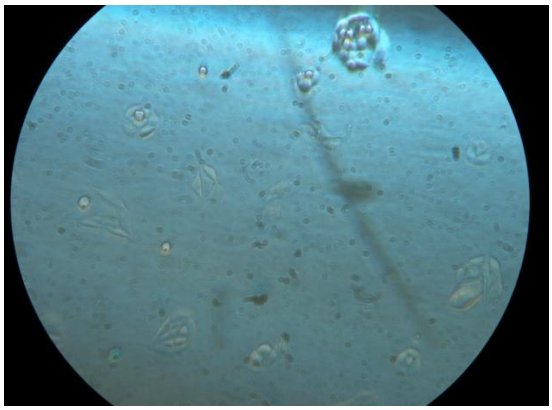

Figure 11-14: Cyan binder 0.5 % few cells were detected at day 7.

11.4.2 Part Two – The Starch

Detailed information on the Alamar Blue assay is presented in Table 11-3 for the cytotoxic effect of three concentrations of starch powder (0.01 mg/ml, 0.005 mg/ml and 0.0025 mg/ml) on two cell line growth (ROS and L929) after 3 days, 5 days and 7 days exposure to these concentrations.

Table 11-3: Alamar Blue assay for 3 concentrations of starch on ROS & L929 cell lines at days 3, 5, & 7.

Days	Samples- ROS - Alamar Blue 4 hours			
	Control	0.01 mg/ml	0.005 mg/ml	0.0025 mg/ml
3	100	84.8	102.2	129.8
5	100	38.8	80.5	105.6
7	100	49.9	78.4	76.3
Days	Samples- L929 - Alamar Blue 4 hours			
3	100	93.8	111.4	119.1
5	100	62.8	81.4	83.7
7	100	61.7	88.6	80.2

11.4.2.1 Day 3:

After three days exposure to the three concentrations of the starch powder statistical analysis revealed no significant effect *(p>0.05)* of the three concentrations of starch powder used in this study on cell line growth of ROS and L929 when compared to their control groups 'cells only' (Figure 11-15 and 11-16).

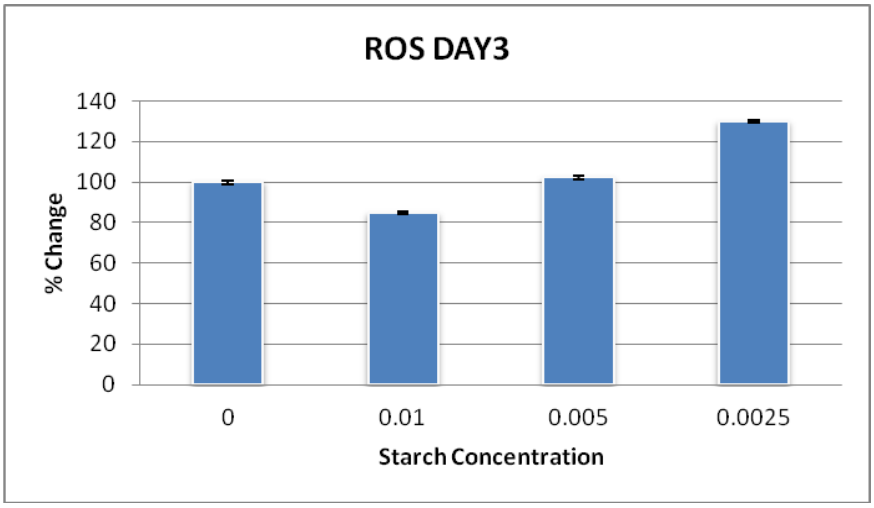

Figure 11-15: Alamar Blue assay for 3 starch concentrations on ROS at day 3.

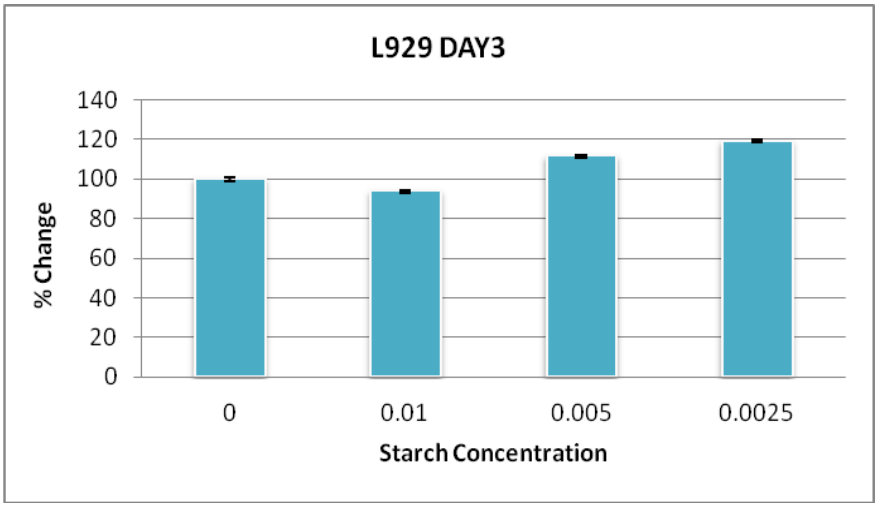

Figure 11-16: Alamar Blue assay for 3 starch concentrations on L929 at day 3.

11.4.2.2 Day 5:

Statistically there was no significant difference *(p>0.05)* in cell growth between the control group and the two concentrations of starch '0.005 mg/ml and 0.0025 mg/ml' for ROS cell lines and L929 cell lines. Statistically there was a significant difference *(p<0.05)* between the control group and 0.01 mg/ml concentration for both cell lines (Figures 11-17 and 11-18).

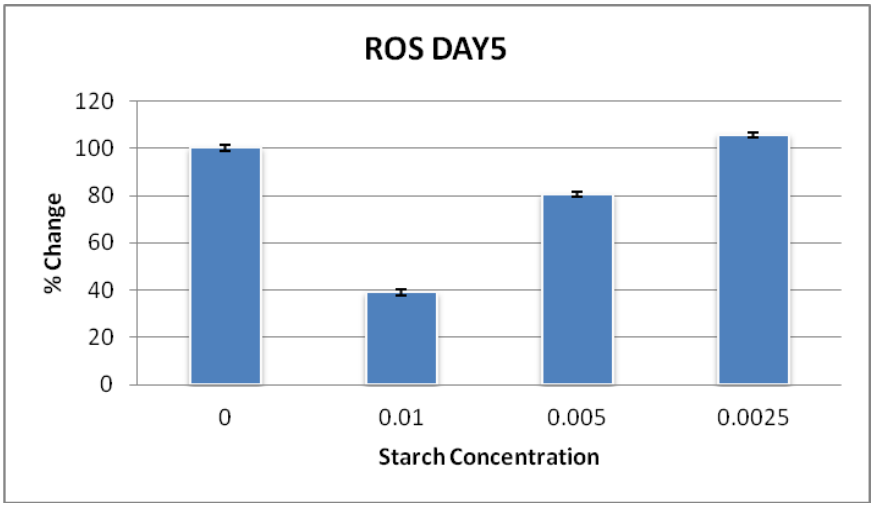

Figure 11-17: Alamar Blue assay for 3 starch concentrations on ROS at day 5.

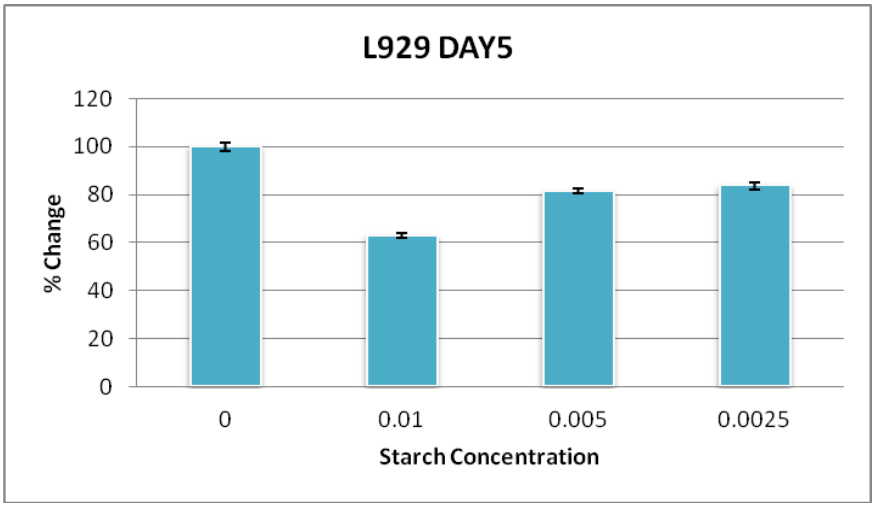

Figure 11-18: Alamar Blue assay for 3 starch concentrations on L929 at day 5.

11.4.2.3 Day 7:

ROS cell lines demonstrated a significant difference *($p<0.05$)* at a concentration of 0.1 mg/ml compared to the control group. There was no significant difference *($p>0.05$)* for 0.005 mg/ml and 0.0025 mg/ml, whereas L929 showed a significant difference *($p<0.05$)* at 0.01 mg/ml and 0.0025 mg/ml when results were compared statistically to the control samples (Figures 11-19 and 11-20).

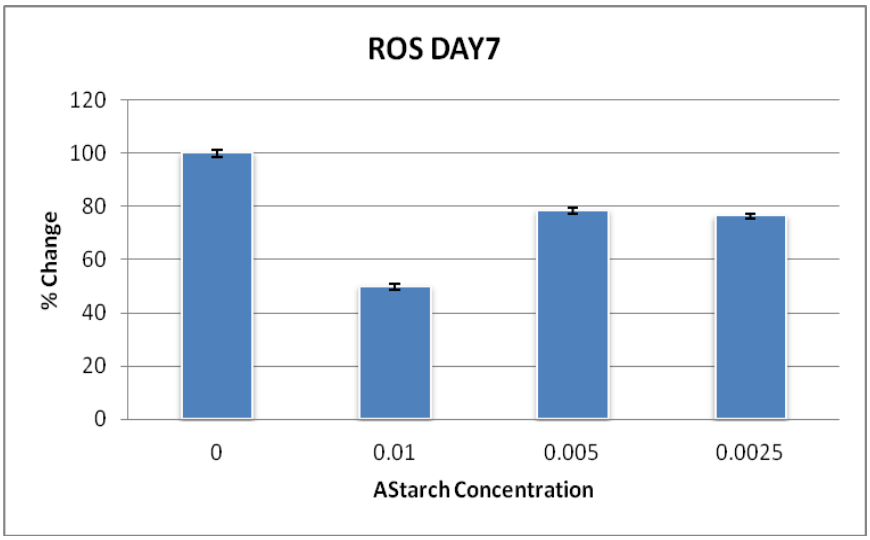

Figure 11-19: Alamar Blue assay for 3 starch concentrations on ROS at day 7.

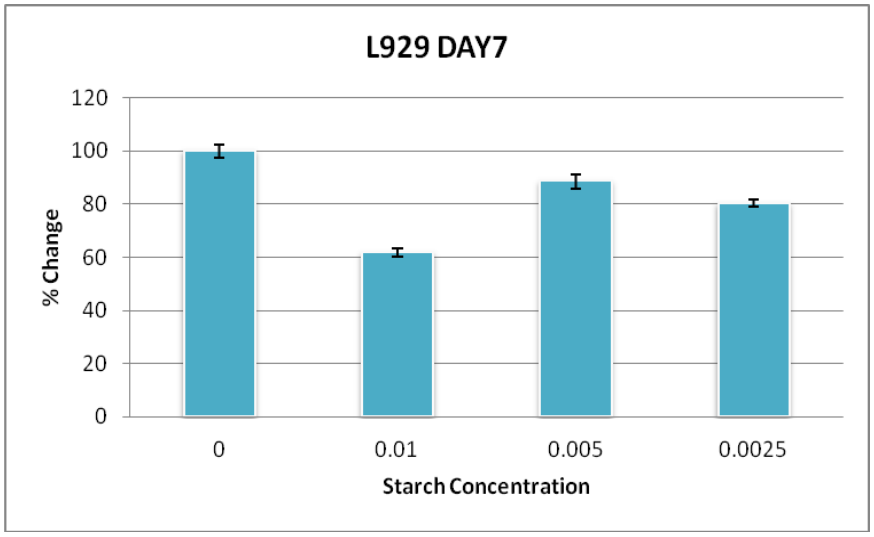

Figure 11-20: Alamar Blue assay for 3 starch concentrations on L929 at day 7.

11.4.3 Part three – Manufactured Prosthesis

11.4.3.1 Histology:

Following histological examination of the specimens, subjective assessment of the tissue samples was made after 12 and 24 hours. Figure 11-21 presents a normal tissue section for the control sample; no disruption of the cellular architecture is apparent in any region of the tissue layer.

Pure SP discs (sample A) presented significant disruption of the cellular architecture, with vacuolation throughout the stratum spinosum and stratum basale leading to loss of tissue characteristics/atypia (Figure 11-22).

Coloured starch discs infiltrated with clear SP (sample B) showed no obvious disruption of tissue architecture anywhere within the tissue layer. There is no evidence of vacuolation or atypia (Figure 11-23).

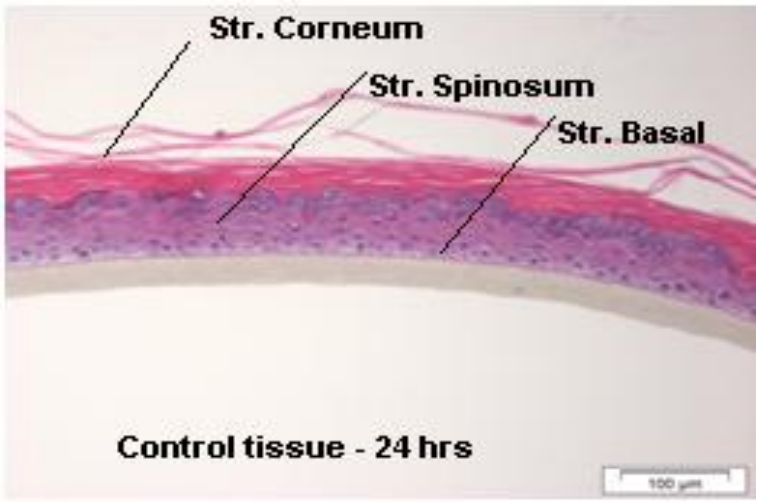

Figure 11-21: Histological section for the control EpiDerm showing normal tissue architecture.

Figure 11-22: Histological section for sample A showing significant disruption of the cellular architecture.

Figure 11-23: Histological section for sample B showing no evidence of tissue disruption.

11.4.3.2 MTT assay:

The results of MTT assay are demonstrated in Table 11-4, statistical analysis using Post-Hoc tests – one way ANOVE statistical analysis show that there was no significant difference *($p>0.05$)* in the optical density observed between the two samples tested after 12 and 24 hours. Furthermore, there appeared to be no significant difference *($p>0.05$)* between the two samples tested and the controls used in this investigation: sample A –

SP, sample B – silicone/starch SPIS and control – no sample. The results are summarised in the histogram below (Figure 11-24).

Table 11-4: MTT assay for test samples SP and the whole compound SP+Starch powder after 12 and 25 hours contact.

Time	MTT – Optical Density – Average + SD		
	Control	Silicone P.	Whole Compound
12 h	1.22±0.05	1.12±0.05	1.14±0.04
24 h	1.21±0.03	1.12±0.04	1.14±0.01

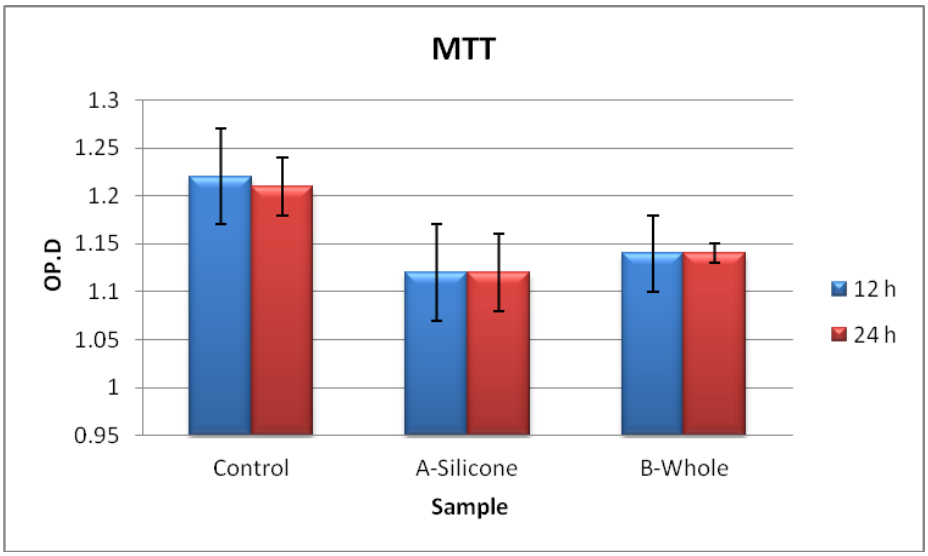

Figure 11-24: Optical density obtained from the MTT assay for the test and control samples.

11.4.3.3 LDH assay:

LDH assay - The results show that there was no significant differences *(p>0.05)* were observed in the optical density after 12 hours and 24 hours contact between the cells and test materials A and B compared to control group. However, there also appeared to be

no significant difference *(p>0.05)* between Sample A – Silicone, Sample B – Silicone/Starch. The results are summarised in the histogram below (Figure 11-25).

Table 11-5: LDH assay for test samples SP and the whole compound SP+Starch powder after 12 and 25 hours contact.

Time	LDH - Sample - Average + SD		
	Control	**Silicone P**	**Whole Compound**
0 h	0.09±0.00	0.09±0.00	0.09±0.00
12 h	0.14±0.03	0.15±0.01	0.13±0.02
24 h	0.16±0.08	0.29±0.00	0.12±0.01

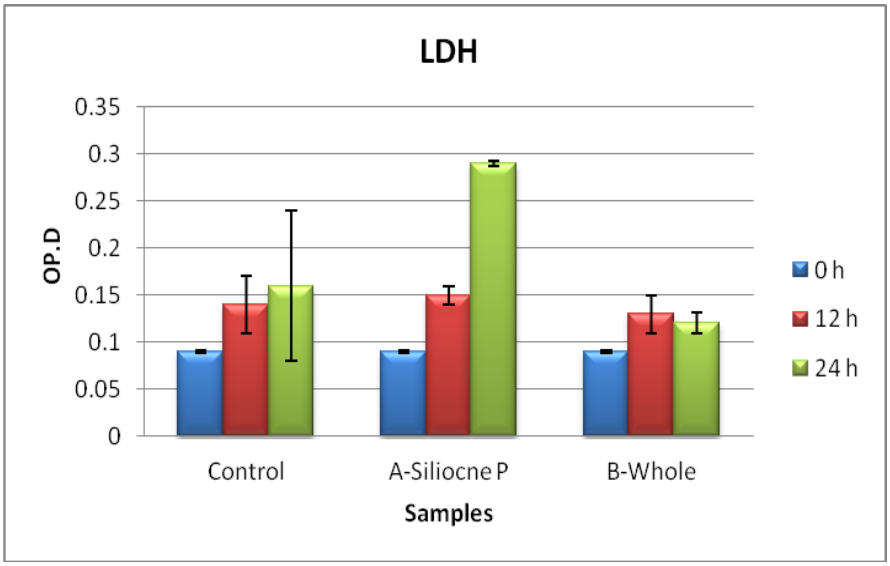

Figure 11-25: histogram demonstrating the optical density obtained from the LDH assay for the test and control samples.

11.5 Discussion:

The Alamar Blue assay was performed to determine the level of toxicity of the binders and the starch powder on two cell lines (ROS and L929). These cells are derived to simulate osseous tissues and fibroblasts respectively and they are commonly used for Alamar Blue assay for evaluation of the cytotoxic effects of implant materials on human cells. L929 mouse fibroblasts have been widely used for biocompatibility assessment of dental materials because of their reproducible growth rate and biological responses (ISO, 1992), (Thonemann et al., 2002, Eldeniz et al., 2007).

Alamar Blue is reduced by living cells through a mechanism whereby as cells start to grow, chemical reduction takes place in the growth medium and then the non-fluorescent dye 'resazurin' is changed to a fluorescent dye 'resorfurin'. Continued cell growth sustains a reduced environment and alters the oxidation reduction 'REDOX' indicator from an oxidized non-fluorescent blue colour to a reduced, fluorescent red colour (Nakayama et al., 1997, Lancaster and Fields, 1996). The fluorescent signal is observed under 530-560 nm excitation wavelength and 590 nm emission wavelength, while the absorbance is monitored at 570 nm and 600 nm and the generated signals usually are comparative to the number of living cells in the specimen (Yu et al., 2003).

Furthermore, an *in-vitro* 3-D human skin tissue model – EpiDerm was undertaken in order to evaluate the biocompatibility of the printed prosthesis in its basic form – the whole compound as it is produced compared to the material currently used – silicone polymer. This work also investigated the biocompatibility/toxicity of traditional SP and a new silicone-starch compound. Industry standard assays are used to assess cell/tissue viability and cell death following exposure to potentially toxic compounds. More specifically, the MTT assay investigates intra-cellular mitochondrial activity, and thus cellular activity. The LDH assay investigates leaked intra-cellular lactate dehydrogenase following cell membrane disruption, and thus cell death. Both cell activity and cell death can be influenced by exposure to potentially toxic compounds.

The result of Alamar Blue assay after 3 and 5 days exposure of the cell lines to three concentrations of four binders did not show toxic effects to any concentration of the four binders on the 2 cell lines used compared to the control cell cultures. However, some growth inhibitions were found at day 7, particularly for the clear binder and cyan. The reduction in cell vitality was dose-dependent and also correlated to the exposure

times: the higher concentrations - 0.5% and 1.0% of cyan and clear binders showed the greatest reduction in vitality on ROS and L929 cell line growth at day 7. There was no evidence of cell activity/growth for 1.0 % clear binder at day 7 for either ROS or L929 cells. However, no toxic effect for 0.1 % of all binders on both cells at the three timeframes was detected.

Furthermore, the Alamar Blue assay showed a similar result for the starch powder. No significant differences were detected between the lower concentrations on any of the test days. The only significant results were reported for 0.01 mg/ml at day 5 and 7 on ROS and L929 cell lines. Also, L929 showed a significant effect on 0.0025 mg/ml at day 7.

The MTT assay demonstrated that after exposure to both Sample A (SP) and Sample B (SPIS) there was no obvious difference in the cellular activity of the remaining cells at either 12 or 24 hours when compared to the control tissue. The LDH assay indicated that there was no difference in the level of cell death between the two samples or when compared to the control sample at 12 hours. However, there appeared to be a demonstrable increase in cell death following exposure to Sample A when compared to both sample B and the control tissue at 24 hours. Histological evaluation would also appear to confirm these results with sample A.

The printing binders are water based (Wohlers, 2009) and the infiltrants are maxillofacial SP, as medical grade silicone elastomers have already been used for decades in the manufacture of soft tissue prostheses; however, some traditional maxillofacial SPs have in some cases caused a degree of inflammation and irritation to the skin varying from mild to moderate (Polyzois et al., 1994, Hensten-Pettersen and Hulterström, 1980).

Furthermore, starch powder has caused some irritation when used in other medical practices, such as lubrication of surgical gloves. Varying degrees of inflammatory reaction were reported in surgical wounds as a result of contamination of those wounds by the powder used on the surgical teams' gloves (Hunt et al., 1994).

Several studies in vitro have investigated the ability of 3D printing technology to produce external and internal designs of scaffolds for tissue engineering and bone regeneration purposes using different types of starch based polymers and biodegradable powders combined with a water based ink (Lam et al., 2002) (Vlasea et al., 2011). However, the main concern of the researchers was binder cytotoxicity, especially in the

event of not all the binder being removed during post processing. Therefore, it can be assumed that any new material, or combination of materials, should be at least as biocompatible.

The above results can be summarised as follows: the investigations of Alamar Blue for the assessment of the binders and the starch powder revealed a slight toxicity at the higher concentrations after prolonged contact between the test material and the cell line growth. However, lower concentrations and shorter contact time between the test materials and the cell lines revealed normal cell activities. The histological findings for the 3D tissue model 'EpiDerm' and MTT and LDH colorimetric assays based on contact with the whole compound for 12 and 24 hours showed no toxic effect of the printed samples on this tissue and this will lead us to a speculation that the prostheses can coexist with the skin without causing any undesirable reaction.

The biocompatibility testing is a risk assessment, and the toxicity testing of these materials was done to determine if these materials are likely cause toxic response to the patient. Exposure of these materials to cells provided us with some information about the level of their toxicity and most materials at some concentrations produce a toxic response, no product is ever 100% safe. The question is it ever likely that the patient would be exposed to those source of levels or concentrations of the ingredients to cause a toxic response? It is unlikely that the patient will actually be exposed to the level of binder or starch as used in these experiments was started causing toxic response. The binder is mostly binding to the starch particles so the chance to release from these particles is very low and even if it leaches out, it has to leach through the silicone. Therefore, the chances of coming out is very small, and it hasn't come out in the amount to cause a toxic reaction. Similarly the starch powder is encapsulated in the silicone it is unlikely to be in contact with the skin unless the materials start disintegration and tearing of the prosthesis takes place and in that case the prosthesis should be replaced anyway. Therefore, we can suggest that the risk of causing any toxicity to the patient is low. However, it is probably to perform some experiments to reveal the amount of binder leaches out from the prostheses or doing a contact experiment with the skin by using skin patch test hold in contact with the skin over 24 hours time or more.

11.6 Conclusion

1- The binders ‘ZB58’ and the starch powder ‘ZP15e’ used by Z510 colour printer for production of soft tissue prostheses are found to be toxic at higher concentrations and prolonged contact with the cell line growth.

2- The silicone-starch material produced during the RP manufacture of soft tissue prostheses appears to be less toxic, and thus more biocompatible with *in-vitro* human skin cells than traditional silicone polymer.

12 General Discussion, General Conclusions and Recommendations for Future Work

12.1 General Discussion

A maxillofacial prosthetic patient usually encounters many challenges after losing part/parts of the face. After surgery, when trying to come to terms with results of the surgery, patients start to fear not being able to cope in the family and in society (Sykes et al., 1972), not being able to find suitable employment to support themselves and not being able to afford the high cost of prosthesis, especially on realising that they might need several/many prostheses during their lifetime.

These problems may force patients into a long-term struggle to adapt to a new way of life and indeed a significant number of patients end up in a state of severe depression. Prosthetic rehabilitation for these patients increases their satisfaction and well-being in relation to family and society by responding to their aesthetic and functional demands (Goiato et al., 2009). However, they encounter a new set of problems such as technical difficulties in getting a prosthesis or difficulties in gaining access to a highly skilled technician who will be able to construct an anatomically and aesthetically accurate prosthesis for them, problems of time, effort and high cost involved in the construction of such a prosthesis.

The limitations of the traditional method of producing this type of prosthesis led a research team at the University of Sheffield, with the help and support of Fripp Design and Research, to investigate the feasibility of producing soft tissue facial prostheses using additive manufacturing through the use of 3D colour printing and medical imaging systems (DICOM). The project aimed to use 3D colour printing to produce low cost facial prostheses, which would match the patient's skin shade and incorporate the desirable mechanical properties.

This has been achieved by layered fabrication of a starch powder joined together with an aqueous binder containing a resin and inks and then infiltrated with a medical grade silicone polymer.

One of the basic concerns was how to achieve an optimal infiltration depth of the silicone polymer inside the printed starch scaffold. Only a small amount of the binder is used to hold the starch particle together and produce a scaffold for the prosthesis. The silicone polymer is considered the main binder for the printed structures;

therefore, in order to achieve optimal performance the scaffold must be infiltrated with maxillofacial silicone polymers. An investigation into elastomer infiltration depth and methods of enhancing their characteristics was performed under pressure; an encouraging result was achieved in that a total infiltration depth of 8 mm of 2 silicone polymers – Sil-25 and Matrix-3428 – inside the starch cubes from each side was achieved under 3 bar pressure after 25 minutes. This depth is sufficient for prostheses that are about 15 mm thick. However, SEM revealed the presence of porosity and lack of integration between the starch particles and the silicone polymers within the infiltrated areas of the printed blocks. As starch powder is a hydrophilic powder and deteriorates easily, it was expected that this would show a negative effect on the mechanical and the optical properties of the composite.

Durability of the printed parts in terms of mechanical and optical properties was tested under different natural and artificial weathering conditions. The mechanical properties of the printed prostheses were also assessed after infiltration with a SP as well as their durability under different natural and accelerated weathering conditions. The mechanical properties and the durability of the SPIS specimens differed from those made of pure SP; this was dictated by an increase in the hardness and a decrease in tensile, tear strength and percentage elongation due to the amount of starch which constitutes 40% of the total weight of the composite.

Until now the ideal properties of the materials used to produce facial prostheses have not been identified and it is not yet clear how far the composite produced in this project is from the ideal. Therefore, the limitations in its mechanical properties will not be of critical importance providing that the patient takes good care of the prosthesis and handles it gently during maintenance and cleaning, particularly in the case of implant retained prostheses that do not rely on adhesive for retention.

Retention of soft tissue prostheses by magnets was also investigated in this project in order to present suitable retention designs for the implant retained prosthesis and to test the feasibility of potential methods for securing the prosthesis to the underlying skin. Four designs provided with different mechanical retention means were tested and the most retentive design is identified as a standard retention pattern for prostheses produced by the 3D printer. It is not necessary to use adhesive for retention of the prosthesis as magnets provide better retention and greater durability.

Furthermore, skin colour data was collected for the face and forearm from a wide range of people from different ethnic groups using a spectrophotometer in order to generate a comprehensive skin colour database, to plot their colour gamut and to analyse factors that might affect the skin colour's appearance. The collected skin data showed that individuals across the three ethnic groups have a similar skin colour gamut to that reproduced by the printer. In other words all the skin colour data collected in this experiment fall within the range of the printer colour gamut, which indicated that the printer would be able to produce skin colour for the volunteers participating in this study. However, further data collection from other ethnic groups is required to plot a full colour gamut for human skin colours.

Colour reproduction by Z510 colour printer was also investigated in this project by printing the L*a*b* colour values of a set of skin colours produced from Sil-25 maxillofacial SP. The corresponding printed coloured starch samples showed different colours after their infiltration with Sil-25 and the printer failed to reproduce the original skin shades accurately using a direct RGB colour transformation. Colour shift varied irregularly from small in some skin shades to considerable in others. However, the quality of colour reproduction was improved by developing a colour reproduction system according to the Z-Corp printer colour profile.

The effects of different natural and accelerated weathering conditions and real life exposure on colour stability of prostheses coloured in different ways were also investigated. The results of colour stability after exposing the samples to accelerated weathering for 2 weeks and 6 weeks and also after 4 months of exposure to natural weathering showed that the colour of the printed samples infiltrated with clear SP is less durable than that of coloured silicone polymers alone. Accelerated weathering conditions caused a considerable change in the optical properties of SPIS coloured samples which was dependent on the exposure time, whereas natural weathering conditions were less detrimental to colour stability of the printed samples. Moreover, white starch samples infiltrated with coloured SP showed only slight colour changes after 2 weeks exposure to artificial weathering. Real life exposure also appeared to have little effect on colour.

Investigation of the problem of durability is inherent in the methodologies used in this study. Natural and artificial weathering tests were performed to determine the durability of the printed prostheses. In terms of using these tests it is quite difficult to

devise a consistent methodology for testing the durability because neither of these methods truly represents the real life use by patients. The proper way of testing the durability of the prostheses is for patients to wear them, but that was not possible because we are at the research experimental stage and the project is still at the developmental stage. The results show that the properties are different from those of silicone polymers and the question is whether they differ to the extent of being unacceptable. This is not the case because there is inherent difficulty in judging what is acceptable. Whilst colour reproduction, biocompatibility, marginal fitting and anatomy were all acceptable, the biggest question about the prostheses relates to their durability. My testing has only partly answered that question; really accurate testing can only be carried out on patients. What my results do show is that the material does not last forever. Although the durability cannot be accurately assessed, the indication is that it is not as good as that of silicone polymer prostheses. While silicone polymer prostheses need to be replaced every 4 months to 12 months, the lifespan of printed prostheses probably will be shorter. However, this issue can be resolved by printing multiple prostheses quickly and at low cost.

The simple way of resolving the problem of durability is by providing the patient with three or four prostheses at a time. The extra cost will be less than that of the anaplastologist making replacements in the traditional way which involves multiple visits and stages, whilst large parts of the process need to be repeated. In contrast, the proposed prostheses require only a visit or two for rescanning and fitting by an anaplastologist. All this could be done in one visit if there were no changes in the area of the defect that required rescanning, while it is difficult to remake the traditional prostheses on the basis of one visit. One of the major advantages of additive manufacture technology is its capacity to print multiple parts at the time of manufacture. Replacement of the prostheses will not create a problem since the method used to design and manufacture the prostheses is based on a CAD/CAM system that has the capability of modifying a previous design. It is very easy to replace the prosthesis at a low cost and in a very short period time. Furthermore, data and designs can be saved and used afterwards for printing additional copies of the prosthesis, especially when the area of the defect has settled after healing and no further tissue changes are expected.
Furthermore the issue of durability is considered a minor problem if the prosthesis is used as an interim prosthesis that will be in use for a short period of time during the

process of healing. At this time the patient need not be subjected to the trauma of having impressions taken as this will be performed by surface scanning of the defective area or by 3D photogrammetry imaging system which has the advantage of being a quick, more accurate, non-contact and non-invasive imaging process. In addition, the tissues undergo continuous change during the healing period which leads to ill-fitting at the margins and the prostheses to be need to be replaced frequently. Therefore, the existing design can easily be modified based on the new imaging data and a replacement prosthesis can be produced within two or three days.

The primary concern was whether the powder and the binder used by the Z-Printer would have any adverse effects on the skin as these materials are utilised for industrial purposes rather than medical applications and their biocompatibility has not previously been investigated. Our early assessments of the biocompatibility of the whole compound – the starch, the binder and the silicone polymer – showed no obvious toxic effects in *vitro* on a 3D EpiDerm tissue model; Histological evolution, MTT and LDH assays revealed similar results following direct contact between the whole compound and the EpiDerm. This investigation was followed by further assessments of the starch powder and the binders on specific - ROS and L929 cell lines. The results showed that the binders 'ZB58' and the starch powder 'ZP15e' used by Z510 colour printer are found to be toxic only at higher concentrations and with prolonged contact with the cell line growth; no evidence of toxicity was reported on ROS and L929 cells at lower concentrations and over a shorter period of contact between the cells and the powder or the binders. It is expected that the amount of binder leached from the prosthesis during service is very small and the starch powder will not come into contact with the skin at a concentration that might cause toxicity since these elements are encapsulated in the silicone polymer. Therefore, it was suggested that the binder and the starch would not induce any toxic effect on the skin. Furthermore, the whole composite was shown to be non-toxic to the human skin tissue in *vitro*.

12.2 General conclusions

Facial prostheses that match the patient's skin shade were successfully manufactured using 3D colour printing with biocompatible materials and desirable mechanical

properties. Based on the mechanical properties and colour measurements the recommendation is that the prostheses will need to be replaced every 6 to 12 months.

If the prosthesis is going to be used as an interim prosthesis for a patient who is healing, durability is not an issue; the speed and cost of manufacturing are big issues as are comfort and acceptability to the patient. In that respect this technology wins easily; the patient is not made to suffer discomfort because the scanning and data capturing process is non-contacting, very simple and very quick. If the prosthesis has to be replaced every few weeks this can be achieved by rescanning the patient and producing the prostheses much more quickly than could be done by the traditional method of manufacture. The major question with regard to definitive prostheses is how they compare with the silicone polymer prostheses. The method that has been applied probably could not produce a prosthesis that looked totally natural. However, it can produce the right fit, the right anatomy, the right colour and appearance. In terms of durability it is probably not going to be as long-lasting as the silicone polymer prostheses.

These prostheses can also be considered as definitive prostheses for those patients in different parts of the world who cannot gain access to highly skilled maxillofacial technicians and what has been produced here is much better than available alternatives. Moreover, these prostheses could last for a long time if they are handled and maintained in a proper way.

12.3 Recommendations for Future Work

1) One of the major issues that have yet to be resolved effectively relates to the durability of the prostheses. Natural and artificial weathering processes revealed deterioration in mechanical and optical properties but it is hard to assess how rapid this deterioration will be when the prostheses are being used by patients. There is some deterioration in colour, but again it is hard to assess how rapidly that will happen on the patient; the only real way of testing colour stability is when the prostheses are being used by patients.

   More needs to be done to determine how long the prostheses will last. The work that has been done so far suggests that they will need to be replaced on a regular basis. It is not clear yet how often they will need to be replaced; that will become

clearer when large numbers of patients have used the prostheses. They could last from a few weeks to 12 months. As the project was at the experimental stage of development it wasn't possible to perform these tests on patients. Therefore, real life exposure tests on patients are required to assess accurately the durability of the prostheses.

2) Further work is required on skin colour measurement; the work performed so far was not sufficiently extensive to represent the whole range of skin colours. Skin colour measurements were performed on a limited group. More data is required from people from different ethnic backgrounds all around the world in order to build a full colour database that can produce a skin colour shade guide to cover all skin shades and all ethnic groups.

3) Further investigations into the translucency factors and surface texture that may affect colour presentation and colour reproduction are required. In this study the thickness of the samples used for colour reproduction was 6 mm, which allowed measurement of the reflected colours and plotting of spectral reluctance curves for the samples. It was not possible to measure the light transferred through these samples. One mm thick samples could be used for this purpose as they would permit the transfer of a certain amount of light.

4) There is a need to investigate replacement of the printing materials with more durable materials. Corn starch powder is highly hydrophilic and considered a weak material that deteriorates easily and despite being encapsulated with a silicone polymer it will contribute significantly to the limited lifespan of the prosthesis. It is recommended that it be replaced with materials that can resist deterioration during service life, such as cellulose powder or silicone powder. Perhaps the binders should be changed or modified according to the type of powder used. Furthermore, it might be an advantageous if different types of infiltrants were investigated, such as polyurethane polymer which is hydrophilic and has a very low viscosity and can be diffused properly within the scaffold particles. This will allow more homogeneous distribution of the infiltrant inside the powder thus improving the quality of infiltration and thereby the quality of the prosthesis.

5) Further investigations are required for assessment of the biocompatibility of materials used by the printer as the binder and the starch powder had shown some toxicity at a higher concentrations and prolonged contact with cells. One option is to perform

some experiments to reveal if all amount of binder leaches out from the prostheses. Another study that could be carried out is to perform contact experiment with the skin by using a skin patch test held in contact with the skin over 24 hours time or more.

12.4 Novelty

The current PhD thesis covers the manufacturing aspect of a novel project employed for rapid manufacturing of soft tissue prosthesis by layer fabrication of these prostheses using Z-Printer (Z510) for layer manufacture with starch powder and an aqueous binder containing a small amount of polymer in order to bind the starch particles together and to provide the printed parts with colour according to colour information of the 3D design. The thesis raises several novelty issues and the novelty lies in providing new ideas, approaches and methodologies applied to investigate several aspects of this project.

Novelty of this thesis lies in the following sections:

1) Section 4 – providing an infiltration protocol that ensures optimal infiltration of the printed parts with a silicone polymer and providing a method of enhancing the penetration depth.

2) Section 5 and 6 - investigation of the mechanical properties of the printed parts after their infiltration with a maxillofacial elastomer and investigation their durability under different natural and accelerated weathering conditions.

3) Section 7 providing the prosthesis with a suitable extension with different mechanical retention means to hold the magnet appropriately opposite to the implant when implant is the method of retention and investigating the capability of the magnet to resist dislodgment during service.

4) Section 8 - methodology used to identify the capability of Z-printer 510 to print the entire range of skin colour measured for groups of people from 3 countries - the UK, China and Iraq by overlapping their skin colour gamut with the printer’s colour gamut thus identifying if these colours fall within the colour printing range of Z510 printer.

5) Section 9 - improving skin colour reproduction of Z510 colour printer by profiling the printers colour system and providing a colour reproduction system able to reduce the error margin that could happen during the printing process.

6) Section 10 – investigating colour stability of the starch printed samples infiltrated with Sil-25 maxillofacial silicone rubber by exposing the samples to outdoor and accelerated weathering conditions and investigating colour differences before and after exposure.

7) Section 11 – investigating the biocompatibility of the prosthesis after infiltration with Sil-25 maxillofacial silicone polymer and each ingredients – the starch and the binder separately as such investigation has not been performed before.

13 References

AGAR, N. & YOUNG, A. R. 2005. Melanogenesis: a photoprotective response to DNA damage? *Mutation Research/Fundamental and Molecular Mechanisms of Mutagenesis,* 571**,** 121-132.

AHMED, S. A., GOGAL, R. M., JR. & WALSH, J. E. 1994. A new rapid and simple non-radioactive assay to monitor and determine the proliferation of lymphocytes: an alternative to [3H]thymidine incorporation assay. *J Immunol Methods,* 170**,** 211-24.

AL MARDINI, M., ERCOLI, C. & GRASER, G. N. 2005. A technique to produce a mirror-image wax pattern of an ear using rapid prototyping technology. *J Prosthet Dent,* 94**,** 195-8.

ANDERL, H., ZUR NEDDEN, D., TWERDY, K., ZANON, E., WICKE, K. & KNAPP, R. 1994. CT-guided stereolithography as a new tool in craniofacial surgery. *British journal of plastic surgery,* 47**,** 60-64.

ANDRES, C. J., HAUG, S. P., BROWN, D. T. & BERNAL, G. 1992. Effects of environmental factors on maxillofacial elastomers: Part II--Report of survey. *J Prosthet Dent,* 68**,** 519-22.

ARVIER, J., BARKER, T., YAU, Y., D'URSO, P., ATKINSON, R. & MCDERMANT, G. 1994. Maxillofacial biomodelling. *British Journal of Oral and Maxillofacial Surgery,* 32**,** 276-283.

ASTM-D412 1981. American Society for Testing and Materials. ASTM Designation: D412 Standard Test Methods for Rubber Properties in Tension. *Annual Book of ASTM Standards. Philadelphia*.

ASTM-D624 1981. ASTM Designation: D624 Standard Test Method for Rubber Property-Tear Resistance. . *Annual Book of ASTM Standards. Philadelphia,* 37.

AZARI, A. & NIKZAD, S. 2009. The evolution of rapid prototyping in dentistry: a review. *Rapid Prototyping Journal,* 15**,** 216-225.

AZIZ, T., WATERS, M. & JAGGER, R. 2003. Analysis of the properties of silicone rubber maxillofacial prosthetic materials. *J Dent,* 31**,** 67-74.

BARNHART, G. W. 1960. A new material and technic in the art of somato-prosthesis. *J Dent Res,* 39**,** 836-44.

BEATTY, M. W., MAHANNA, G. K. & JIA, W. 1999. Ultraviolet radiation-induced color shifts occurring in oil-pigmented maxillofacial elastomers. *J Prosthet Dent,* 82**,** 441-6.

BEDER, O. E. 1974. Fundamentals for Maxillofacial Prosthetics. *Spring field, Illinois: Charles C Thomas Publisher*.

BEUMER, J., CURTIS, T. A. & MARUNIK, M. T. 1996. Maxillofacial rehabilitation; Prosthodontic and surgical reconsiderations *St Louis; Ishiyaku Euro America Inc*.

BEUMER, J. C., T.A .MARUNIK, M.T. 1996. Maxillofacial rehabilitation; Prosthodontic and surgical reconsiderations *St Louis; Ishiyaku Euro America Inc*.

BRÅNEMARK, P. I. & DE OLIVEIRA, M. F. 1997. *Craniofacial prostheses: Anaplastology and osseointegration*, Quintessence Publishing Company.

BROWN, E., HOPPER JR, J., HODGES JR, J., BRADLEY, B., WENNESLAND, R. & YAMAUCHI, H. 1962. Red cell, plasma, and blood volume in healthy women measured by radiochromium cell-labeling and hematocrit. *Journal of Clinical Investigation,* 41**,** 2182.

BROWN, R. P., KOCKOTT, D., TRUBIROHA, P., KETOLA, W. & SHORTHOUSE, J. 1995. A Review of Accelerated Durability Tests. *VAMAS Report No.18*.

BULBULIAN 1954a. prosthetic reconstructions of facial defects by use Latex compounds. *Proc. Maya Clinic***,** 721-727.

BULBULIAN, A. H. 1954b. prosthetic reconstructions of facial defects by use Latex compounds. *Proc. Maya Clinic***,** 721-727.

BULBULIAN, A. H. 1973. Facial Prosthetics *Charlis C. Thomas*.

CANTOR, R., WEBBER, R. L., STROUD, L. & RYGE, G. 1969. Methods for evaluating prosthetic facial materials. *J Prosthet Dent,* 21**,** 324-32.

CARRION, A. 1997. Technology forecast on ink-jet head technology applications in rapid prototyping. *Rapid Prototyping Journal,* 3**,** 99-115.

CHALIAN, V. A. & BARNETT, M. O. 1972. A new technique for constructing a one-piece hollow obturator after partial maxillectomy. *J Prosthet Dent,* 28**,** 448-53.

CHALIAN, V. A. & PHILLIPS, R. W. 1974. Materials in maxillofacial prosthetics. *J Biomed Mater Res,* 8**,** 349-63.

CHANG, C., LEE, M. & WANG, S. 2006. Digital denture manufacturing-An integrated technologies of abrasive computer tomography, CNC machining and rapid prototyping. *The International Journal of Advanced Manufacturing Technology,* 31**,** 41-49.

CHANG, T. L., GARRETT, N., ROUMANAS, E. & BEUMER, J., 3RD 2005. Treatment satisfaction with facial prostheses. *J Prosthet Dent,* 94**,** 275-80.

CHEAH, C. M., CHUA, C. K. & TAN, K. H. 2003a. Integration of laser surface digitizing with CAD/CAM techniques for developing facial prostheses. Part 2: Development of molding techniques for casting prosthetic parts. *Int J Prosthodont,* 16**,** 543-8.

CHEAH, C. M., CHUA, C. K., TAN, K. H. & TEO, C. K. 2003b. Integration of laser surface digitizing with CAD/CAM techniques for developing facial prostheses. Part 1: Design and fabrication of prosthesis replicas. *Int J Prosthodont,* 16**,** 435-41.

CHEN, L., TSUTSUMI, S. & LIZUKA, D. 1997a. A CAD/CAM technique for fabricating facial prostheses; a preliminary report. *Int J Prosthodont,* 10**,** 467-472.

CHEN, L. H., TSUTSUMI, S. & IIZUKA, T. 1997b. A CAD/CAM technique for fabricating facial prostheses: a preliminary report. *Int J Prosthodont,* 10**,** 467-72.

CHEN, M. S., UDAGAMA, A. & DRANE, J. B. 1981. Evaluation of facial prostheses for head and neck cancer patients. *J Prosthet Dent,* 46**,** 538-44.

CHEUNG, L. K., WONG, M. C. M. & WONG, L. L. S. 2001. The application of stereolithography in facial reconstructive surgery. *IEEE***,** 10-15.

CHIU, W. & YU, K. 2008. Direct digital manufacturing of three-dimensional functionally graded material objects. *Computer-Aided Design,* 40**,** 1080-1093.

CHUNG, R. W. C., SIU, A. S. C., CHU, F. & CHOW, T. W. 2003. Magnet-retained auricular prosthesis with an implant-supported composite bar: a clinical report. *The Journal of Prosthetic Dentistry,* 89**,** 446-449.

CIOCCA, L., FANTINI, M., DE CRESCENZIO, F., PERSIANI, F. & SCOTTI, R. 2010. New protocol for construction of eyeglasses-supported provisional nasal prosthesis using CAD/CAM techniques. *J Rehabil Res Dev,* 47**,** 595-604.

COCHRANE, C. A., SHEARWOOD, C., WALKER, M., BOWLER, P. & KNOTTENBELT, D. C. 2003. The application of a fibroblast gel contraction model to assess the cytotoxicity of topical antimicrobial agents. *Wounds,* 15**,** 265-271.

COWARD, T., WATSON, R. & WILKINSON, I. 1999. Fabrication of a wax ear by rapid prototyping modeling using stereolithography. . *Int J prosthodont 1999,* 12**,** 20-7.

COWARD, T. J., SEELAUS, R. & LI, S. Y. 2008. Computerized color formulation for African-Canadian people requiring facial prostheses: a pilot study. *J Prosthodont,* 17**,** 327-35.

CRAIG, R. G., KORAN, A., YU, R. & SPENCER, J. 1978. Color stability of elastomers for maxillofacial appliances. *J Dent Res,* 57**,** 866-71.

D'URSO, P. S., HALL, B. I., ATKINSON, R. L., WEIDMANN, M. J. & REDMOND, M. J. 1999. Biomodel-guided stereotaxy. *Neurosurgery,* 44**,** 1084.

DAVIS, B. K. & EMERT, R. 2010. The Role of Technology in the Maxillofacial Prosthetic Setting. *Printed Biomaterials***,** 111-120.

DIMITROV, D., SCHREVE, K., BEER, N. D. & CHRISTIANE, P. 2008. Three dimensional printing in the South African industrial environment. *South African Journal of Industrial Engineering***,** 208.

DIMITROV, D., SCHREVE, K. & DE BEER, N. 2006a. Advances in three dimensional printing–state of the art and future perspectives. *Rapid Prototyping Journal,* 12**,** 136-147.

DIMITROV, D., WIJCK, W. V., SCHREVE, K. & BEER, N. D. 2006b. Investigating the achievable accuracy of three dimensional printing. *Rapid Prototyping Journal,* 12.

DOOTZ, E. R., KORAN, A., 3RD & CRAIG, R. G. 1994. Physical properties of three maxillofacial materials as a function of accelerated aging. *Journal of Prosthetic Dentistry,* 71**,** 379-83.

DOS SANTOS, D. M., GOIATO, M. C., SINHORETI, M. A. C., FERNANDES, A. Ú. R., RIBEIRO, P. P. & DEKON, S. F. C. 2010. Color stability of polymers for facial prosthesis. *Journal of Craniofacial Surgery,* 21**,** 54.

DURET, F. & PRESTON, J. 1991. CAD/CAM imaging in dentistry. *Current opinion in dentistry,* 1**,** 150.

EBOOK-1 Rapid Prototype Basics Vol. 1. *eBook-1,* 1**,** 1-72.

EGGBEER, D., BIBB, R., EVANS, P. & JI, L. 2012. Evaluation of direct and indirect additive manufacture of maxillofacial prostheses. *Proceedings of the Institution of Mechanical Engineers, Part H: Journal of Engineering in Medicine,* 226**,** 718-728.

ELDENIZ, A., MUSTAFA, K., ØRSTAVIK, D. & DAHL, J. 2007. Cytotoxicity of new resin-, calcium hydroxide-and silicone-based root canal sealers on fibroblasts derived from human gingiva and L929 cell lines. *International endodontic journal,* 40**,** 329-337.

ELENI, P., KATSAVOU, I., KROKIDA, M., POLYZOIS, G. & GETTLEMAN, L. 2009a. Mechanical behavior of facial prosthetic elastomers after outdoor weathering. *Dental Materials,* 25**,** 1493-1502.

ELENI, P., KROKIDA, M. & POLYZOIS, G. 2009b. The effect of artificial accelerated weathering on the mechanical properties of maxillofacial polymers PDMS and CPE. *Biomedical Materials,* 4**,** 035001.

FARAH, J. W., ROBINSON, J. C., KORAN, A., CRAIG, R. G. & HOOD, J. A. 1987. Properties of a modified cross-linked silicone for maxillofacial prostheses. *J Oral Rehabil,* 14**,** 599-605.

FELDMAN, J. F. B. I. M., JG. (ED.) 1990. Plastic Surgery. *Philadelphia: WB Saunders,* 3**,** 2153 - 2236.

FIELDS, R. D. & LANCASTER, M. V. 1993. Dual-attribute continuous monitoring of cell proliferation/cytotoxicity. *Am Biotechnol Lab,* 11**,** 48-50.

FORTNEY, S., NADEL, E., WENGER, C. & BOVE, J. 1981. Effect of blood volume on sweating rate and body fluids in exercising humans. *Journal of Applied Physiology,* 51**,** 1594-1600.

FROST, P. 2006. European hair and eye color: A case of frequency-dependent sexual selection? *Evolution and Human Behavior,* 27**,** 85-103.

FULLERTON, A. & SERUP, J. 1997. Site, gender and age variation in normal skin colour on the back and the forearm: tristimulus colorimeter measurements. *Skin Research and Technology,* 3**,** 49-52.

GARY, J. J., HUGET, E. F. & POWELL, L. D. 2001. Accelerated color change in a maxillofacial elastomer with and without pigmentation. *J Prosthet Dent,* 85**,** 614-20.

GARY, J. J. & SMITH, C. T. 1998. Pigments and their application in maxillofacial elastomers: a literature review. *J Prosthet Dent,* 80**,** 204-8.

GATTO, M., MEMOLI, G., SHAW, A., SADHOO, N., GELAT, P. & HARRIS, R. A. 2011. Three-Dimensional Printing (3DP) of neonatal head phantom for ultrasound: Thermocouple embedding and simulation of bone. *Medical Engineering & Physics*.

GIANLUCA, C., GIOVANNA, S., ANGELO, V. & FRANCO, D. 2010. 3D Optical Body Scanning: Application to Forensic Medicine and to

Maxillofacial Reconstruction. *International Conference on 3D Body Scanning Technologies, Lugano, Switzerland*.

GIANNATSIS, J. & DEDOUSSIS, V. 2009. Additive fabrication technologies applied to medicine and health care: a review. *The International Journal of Advanced Manufacturing Technology,* 40**,** 116-127.

GIBSON, T. 1955. The prostheses of Ambroise Pare. *Br J Plast Surg* 3**,** 3-8.

GLOSSARY 2005. The glossary of prosthodontic terms. *Journal of Prosthetic Dentistry,* 94**,** 10-92.

GOIATO, M. C., FERNANDES, A., SANTOS, D. & BARÃO, V. A. R. 2007. Positioning magnets on a multiple/sectional maxillofacial prosthesis. *J Contemp Dent Pract,* 8**,** 101-107.

GOIATO, M. C., PESQUEIRA, A. A., RAMOS DA SILVA, C., GENNARI FILHO, H. & MICHELINE DOS SANTOS, D. 2009. Patient satisfaction with maxillofacial prosthesis. Literature review. *J Plast Reconstr Aesthet Surg,* 62**,** 175-80.

GOLDBERG, A. J., CRAIG, R. G. & FILISKO, F. E. 1978. Polyurethane elastomers as maxillofacial prosthetic materials. *J Dent Res,* 57**,** 563-9.

GONZALEZ, J. B. 1978. Polyurethane elastomers for facial prostheses. *J Prosthet Dent,* 39**,** 179-87.

HAJEER, M. Y., AYOUB, A. F., MILLETT, D. T., BOCK, M. & SIEBERT, J. P. 2002. Three-dimensional imaging in orthognathic surgery: the clinical application of a new method. *Int J Adult Orthodon Orthognath Surg,* 17**,** 318-30.

HAN, K., CHOI, T. & SON, D. 2006. Skin color of Koreans: statistical evaluation of affecting factors. *Skin Research and Technology,* 12**,** 170-177.

HANSON, M. D., SHIPMAN, B., BLOMFIELD, J. V. & JANUS, C. E. 1983. Commercial cosmetics and their role in the coloring of facial prostheses. *J Prosthet Dent,* 50**,** 818-20.

HATAMLEH, M. M. & WATTS, D. C. 2010a. Bonding of maxillofacial silicone elastomers to an acrylic substrate. *Dental Materials,* 26**,** 387-395.

HATAMLEH, M. M. & WATTS, D. C. 2010b. Effect of extraoral aging conditions on color stability of maxillofacial silicone elastomer. *Journal of Prosthodontics,* 19**,** 536-543.

HATAMLEH, M. M. & WATTS, D. C. 2010c. Mechanical properties and bonding of maxillofacial silicone elastomers. *Dent Mater,* 26**,** 185-91.

HAUG, S. P., ANDRES, C. J. & MOORE, B. K. 1999a. Color stability and colorant effect on maxillofacial elastomers. Part III: weathering effect on color. *J Prosthet Dent,* 81**,** 431-8.

HAUG, S. P., MOORE, B. K. & ANDRES, C. J. 1999b. Color stability and colorant effect on maxillofacial elastomers. Part II: weathering effect on physical properties. *J Prosthet Dent,* 81**,** 423-30.

HECKMANN, S. M., WICHMANN, M. G., WINTER, W., MEYER, M. & WEBER, H. P. 2001. Overdenture attachment selection and the loading of

implant and denture-bearing area. Part 1: In vivo verification of stereolithographic model. *Clinical oral implants research,* 12**,** 617-623.

HEIKE, C. L., UPSON, K., STUHAUG, E. & WEINBERG, S. M. 2010. 3D digital stereophotogrammetry: a practical guide to facial image acquisition. *Head Face Med,* 6**,** 18.

HENSTEN-PETTERSEN, A. & HULTERSTRÖM, A. 1980. Assessment of in vitro cytotoxicity of four RTV-silicone elastomers used for maxillofacial prostheses. *Acta Odontologica,* 38**,** 163-167.

HOGAN, B. J. 2009. Why Herbert Voelcker. *Manufacturing engineering, Internet Article*.

HONIBALL, J. R. 2010. The Application of 3D Printing in reconstructive surgery. *MSc Theses, University of Stellenbosch*

HOOPER, S., WESTCOTT, T., EVANS, P., BOCCA, A. & JAGGER, D. 2005. Implant-Supported Facial Prostheses Provided by a Maxillofacial Unit in a UK Regional Hospital: Longevity and Patient Opinions. *Journal of Prosthodontics,* 14**,** 32-38.

HULL, C. W. 1986. Apparatus for production of three-dimensional objects by stereolithography. Google Patents.

HULTERSTROM, A. K. & RUYTER, I. E. 1999. Changes in appearance of silicone elastomers for maxillofacial prostheses as a result of aging. *Int J Prosthodont,* 12**,** 498-504.

HUNT, T. K., SLAVIN, J. P. & GOODSON, W. H. 1994. Starch powder contamination of surgical wounds. *Archives of Surgery,* 129**,** 825.

HUNTER, R. S. 1948. Proceedings of the Winter Meeting of the Optical Society of America. *JOSA, Jornal of Optical Sociaty of America,* 38 (7)**,** 661.

ICC 1998. ICC Profile Format Specification, Version ICC.1:1998-09. *International Color Consortium*.

IRELAND, A. J., MCNAMARA, C., CLOVER, M. J., HOUSE, K., WENGER, N., BARBOUR, M. E., ALEMZADEH, K., ZHANG, L. & SANDY, J. R. 2008. 3D surface imaging in dentistry - what we are looking at. *Br Dent J,* 205**,** 387-92.

ISMAIL, J. Y. & ZAKI, H. S. 1990. Osseointegration in maxillofacial prosthetics. *Dent Clin North Am,* 34**,** 327-41.

ISO 1992. biologicalevaluation of medical devices—part 5: tests for cytotoxicity: in vitro methods. Geneva, Switzerland: ISO. . *International Organization for Standardization. ISO 10993-5*.

ITO, S. & WAKAMATSU, K. 2003. Quantitative analysis of eumelanin and pheomelanin in humans, mice, and other animals: a comparative review. *Pigment Cell Res,* 16**,** 523-31.

JABLONSKI, N. G. & CHAPLIN, G. 2010. Colloquium paper: human skin pigmentation as an adaptation to UV radiation. *Proc Natl Acad Sci U S A,* 107 Suppl 2**,** 8962-8.

JANI, R. M. & SCHAAF, N. G. 1978. An evaluation of facial prostheses. *J Prosthet Dent,* 39**,** 546-50.

JAYASEKARA, R., HARDING, I., BOWATER, I., CHRISTIE, G. & LONERGAN, G. T. 2004. Preparation, surface modification and characterisation of solution cast starch PVA blended films. *Polymer testing,* 23**,** 17-27.

JEBREIL, K. 1980. Acceptability of orbital prostheses. *The Journal of Prosthetic Dentistry,* 43**,** 82-85.

JIN SUN, JUNTONG XI, CHEN, X. & XIONG, Y. 2011. A CAD/CAM system for fabrication of facial prostheses. *Rapid Prototyping Journal,* 17**,** 235-261.

KAI, C., LS., M., LS., C., LS., T. & SC, A. 2000. Facial prosthetic model fabrication using rapidprototyping tools. *J integrated manufacturing systems* 11**,** 42-53.

KAMMULA, R. G. & MORRIS, J. M. 2001. Considerations for the Biocompatibility Evaluation of Medical Devices. *Medical Plastics and Biomaterials*.

KAU, C. H., RICHMOND, S., INCRAPERA, A., ENGLISH, J. & XIA, J. J. 2007. Three-dimensional surface acquisition systems for the study of facial morphology and their application to maxillofacial surgery. *The International Journal of Medical Robotics and Computer Assisted Surgery,* 3**,** 97-110.

KELLY, J. R. 2007. Developing meaningful systematic review of CAD/CAM reconstructions and fiber-reinforced composites*. *Clinical oral implants research,* 18**,** 205-217.

KHAN, Z., GETTLEMAN, L. & JACOBSON, C. S. 1992. Conference report: materials research in maxillofacial prosthetics. *J Dent Res,* 71**,** 1541-2.

KHINDRIA, S. K., BANSAL, S. & KANSAL, M. 2009. Maxillofacial prosthetic material. *The Journal of Indian Prosthodontic Sociaty,* 9.

KIAT-AMNUAY, S., GETTLEMAN, L., KHAN, Z. & GOLDSMITH, L. J. 2000. Effect of adhesive retention on maxillofacial prostheses. Part I: skin dressings and solvent removers. *J Prosthet Dent,* 84**,** 335-40.

KIAT-AMNUAY, S., LEMON, J. C. & POWERS, J. M. 2002. Effect of opacifiers on color stability of pigmented maxillofacial silicone A-2186 subjected to artificial aging. *J Prosthodont,* 11**,** 109-16.

KLEIN, H., SCHNEIDER, W., ALZEN, G., VOY, E. & GÜNTHER, R. 1992. Pediatric craniofacial surgery: comparison of milling and stereolithography for 3D model manufacturing. *Pediatric radiology,* 22**,** 458-460.

KRUTH, J. P., FROYEN, L., VAN VAERENBERGH, J., MERCELIS, P., ROMBOUTS, M. & LAUWERS, B. 2004. Selective laser melting of iron-based powder. *Journal of materials processing technology,* 149**,** 616-622.

KRUTH, J. P., MERCELIS, P., VAN VAERENBERGH, J., FROYEN, L. & ROMBOUTS, M. 2005. Binding mechanisms in selective laser sintering and selective laser melting. *Rapid Prototyping Journal,* 11**,** 26-36.

LAI, J. H., WANG, L. L., KO, C. C., DELONG, R. L. & HODGES, J. S. 2002. New organosilicon maxillofacial prosthetic materials. *Dental Materials,* 18**,** 281-6.

LAM, C. X. F., MO, X., TEOH, S. H. & HUTMACHER, D. 2002. Scaffold development using 3D printing with a starch-based polymer. *Materials Science and Engineering: C,* 20**,** 49-56.

LANCASTER, M. V. & FIELDS, R. D. 1996. Antibiotic and Cytotoxic Drug Susceptibility Assays using Resazurin and Poising Agents. *U.S. Patent No. 5,501,959.*

LEE, S. H. & CHOI, J. S. 2008. Design and implementation of color correction system for images captured by digital camera. *Consumer Electronics, IEEE Transactions on,* 54**,** 268-276.

LEIFER, J. 2003. A close-range photogrammetry laboratory activity for mechanical engineering undergraduates. *Frontiers in Education, 2003. FIE 2003. 33rd Annual,* 2**,** 7-12.

LEMON, J. C., CHAMBERS, M. S., JACOBSEN, M. L. & POWERS, J. M. 1995. Color stability of facial prostheses. *J Prosthet Dent,* 74**,** 613-8.

LEONARDI, A., BUONACCORSI, S., PELLACCHIA, V., MORICCA, L. M., INDRIZZI, E. & FINI, G. 2008. Maxillofacial prosthetic rehabilitation using extraoral implants. *J Craniofac Surg,* 19**,** 398-405.

LEVY, G. N., SCHINDEL, R. & KRUTH, J. P. 2003. Rapid manufacturing and rapid tooling with layer manufacturing (LM) technologies, state of the art and future perspectives. *CIRP Annals-Manufacturing Technology,* 52**,** 589-609.

LEWIS, D. H. & CASTLEBERRY, D. J. 1980. An assessment of recent advances in external maxillofacial materials. *J Prosthet Dent,* 43**,** 426-32.

LI, X. N., ZHAO, Y. M., LI, S. B., LIU, X. C., WU, G. F., ZHEN, L. L. & WU, N. 2007. Comparison of mechanical properties of cosmesil M511 and A-2186 maxillofacial silicone elastomers. *Journal of US-China Medical Science,* 4**,** 34-37.

LIU, Q., LEU, M. C. & SCHMITT, S. M. 2006. Rapid prototyping in dentistry: technology and application. *The International Journal of Advanced Manufacturing Technology,* 29**,** 317-335.

LONTZ, J. F. 1990. State-of-the-art materials used for maxillofacial prosthetic reconstruction. *Dent Clin North Am,* 34**,** 307-25.

LOWENTAL, U. & SELA, M. 1982. Evaluating cosmetic results in maxillofacial prosthetics. *Journal of Prosthetic Dentistry,* 48**,** 567-70.

MAJESKA, R. J. & RODAN, G. A. 1982. Alkaline phosphatase inhibition by parathyroid hormone and isoproterenol in a clonal rat osteosarcoma cell line. Possible mediation by cyclic AMP. *Calcified tissue international,* 34**,** 59-66.

MAJID, Z., SETAN, H. & CHONG, A. 2008. Integration of stereoohotogrammetry and triangulation-based laser scanning system for precise mapping of craniofacial morphology. *The International Archives*

of the Photogrammetry, Remote Sensing and Spatial Information Sciences, XXXVII.

MALLER, U. S., KARTHIK, K. & MALLER, S. V. 2010. Maxillofacial Prosthetic Materials-Past and Present Trends. *JIADS,* 1**,** 25.

MANCUSO, D. N., GOIATO, M. C., DEKON, S. & GENNARI-FILHO, H. 2009a. Visual evaluation of color stability after accelerated aging of pigmented and nonpigmented silicones to be used in facial prostheses. *Indian Journal of Dental Research,* 20**,** 77.

MANCUSO, D. N., GOIATO, M. C., DEKON, S. F. & GENNARI-FILHO, H. 2009b. Visual evaluation of color stability after accelerated aging of pigmented and nonpigmented silicones to be used in facial prostheses. *Indian J Dent Res,* 20**,** 77-80.

MANCUSO, D. N., GOIATO, M. C. & SANTOS, D. M. 2009c. Color stability after accelerated aging of two silicones, pigmented or not, for use in facial prostheses. *Braz Oral Res,* 23**,** 144-8.

MANKOVICH, N. J., CHEESEMAN, A. M. & STOKER, N. G. 1990. The display of three-dimensional anatomy with stereolithographic models. *Journal of Digital Imaging,* 3**,** 200-203.

MARION, L. R., ROTHENBERGER, S. L. & MINSLEY, G. E. 1997. Judson C. Hickey Scientific Writing Award Winner. A method of fabrication of a facial prosthesis that improves retention and durability: a clinical report. *J Prosthet Dent,* 77**,** 457-60.

MARKT, J. C. & LEMON, J. C. 2001. Extraoral maxillofacial prosthetic rehabilitation at the M. D. Anderson Cancer Center: a survey of patient attitudes and opinions. *J Prosthet Dent,* 85**,** 608-13.

MAXWELL, R. S., COHENOUR, R., SUNG, W., SOLYOM, D. & PATEL, M. 2003. The effects of γ-radiation on the thermal, mechanical, and segmental dynamics of a silica filled, room temperature vulcanized polysiloxane rubber. *Polymer degradation and stability,* 80**,** 443-450.

MCKINSTRY, R. E. 1983. Fundamentals of Facial Prosthetics. *North Carolina: Abi Professional Pubns*.

MCKINSTRY, R. E. 1995. Fundamentals of facial prosthetics. *Clearwater (FL): ABI Professional Publications***,** 161-7 , 169-79.

MCMAINS, S. 2005. Layered manufacturing technologies. *Communications of the ACM,* 48**,** 50-56.

MING, L. W. & GIBSON, I. 2009. Specification of VRML in color rapid prototyping. *International Journal of CAD/CAM,* 1.

MINNS, R., BIBB, R., BANKS, R. & SUTTON, R. 2003. The use of a reconstructed three-dimensional solid model from CT to aid the surgical management of a total knee arthroplasty: a case study. *Medical Engineering & Physics,* 25**,** 523-526.

MIYAZAKI, T., HOTTA, Y., KUNII, J., KURIYAMA, S. & TAMAKI, Y. 2009. A review of dental CAD/CAM: current status and future perspectives from 20 years of experience. *Dent Mater J,* 28**,** 44-56.

MOORE, D. J. 1994. overview of materials for extra – oral prosthesis. *First international congress on maxillofacial prosthetics. California, H Plus Inc.*,**,** 108-115.

MORTON M 1987. Rubber Technology. *Van Nostrand, New York***,** 375-409.

N ELENI, P., KATSAVOU, I., K KROKIDA, M. & L POLYZOIS, G. 2009. Color stability of facial silicone prosthetic elastomers after artificial weathering. *Dental Research Journal,* 5.

NAKAYAMA, G. R., CATON, M. C., NOVA, M. P. & PARANDOOSH, Z. 1997. Assessment of the Alamar Blue assay for cellular growth and viability in vitro. *Journal of immunological methods,* 204**,** 205.

NUSINOV, N. & GAY, W. 1980. A method for obtaining the reverse image of an ear *J Prosthet Dent,* 44**,** 68-71.

OVER, L. M., ANDRES, C. J., MOORE, B. K., GOODACRE, C. J. & MUNOZ, C. A. 1998. Using a colorimeter to develop an intrinsic silicone shade guide for facial prostheses. *J Prosthodont,* 7**,** 237-49.

PARAVINA, R. D., MAJKIC, G., DEL MAR PEREZ, M. & KIAT-AMNUAY, S. 2009. Color difference thresholds of maxillofacial skin replications. *Journal of Prosthodontics,* 18**,** 618-625.

PAREL, S. M., BRANEMARK, P. I., OHRNELL, L. O. & SVENSSON, B. 2001. Remote implant anchorage for the rehabilitation of maxillary defects. *Journal of Prosthetic Dentistry,* 86**,** 377-381.

PAREL, S. M., BRANEMARK, P. I., TJELLSTROM, A. & GION, G. 1986. Osseointegration in maxillofacial prosthetics. Part II: Extraoral applications. *J Prosthet Dent,* 55**,** 600-6.

PARRAMAN, C., WALTERS, P., REID, B. & HUSON, D. 2008. Specifying colour and maintaining colour accuracy for 3D printing. *Proceedings of Electronic Imaging, Society for Imaging Science and Technology/Society of Photographic Instrumentation Engineers, San Jose, CA, USA, 26-31 January 2008*.

PATTON, T. 1973. Pigment handbook. volume 1: properties and economics. 1**,** 1-20,333-49,389-92.

PETZOLD, R., ZEILHOFER, H. F. & KALENDER, W. 1999. Rapid prototyping technology in medicine—basics and applications. *Computerized Medical Imaging and Graphics,* 23**,** 277-284.

PHAN, X. & LING, P. H. 2007. Clinical limitations of Invisalign. *Journal-Canadian Dental Association,* 73**,** 263.

PHILIP, M., ATTWOOD, J., HULME, A., WILLIAMS, G. & SHIPTON, P. 2004. Evaluation of weathering in mixed polyethyline and polypropylene products. *WRAP***,** 6.

POLYZOIS, G. L. 1999. Color stability of facial silicone prosthetic polymers after outdoor weathering. *J Prosthet Dent,* 82**,** 447-50.

POLYZOIS, G. L., ELENI, P. N. & KROKIDA, M. K. 2011. Effect of Time Passage on Some Physical Properties of Silicone Maxillofacial Elastomers. *Journal of Craniofacial Surgery,* 22**,** 1617.

POLYZOIS, G. L., HENSTEN-PETTERSEN, A. & KULLMAN, A. 1994. Effects of RTC-silicone maxillofacial prosthetic elastomers on cell cultures. *The Journal of Prosthetic Dentistry,* 71**,** 505-510.

POLYZOIS, G. L., TARANTILI, P. A., FRANGOU, M. J. & ANDREOPOULOS, A. G. 2000. Physical properties of a silicone prosthetic elastomer stored in simulated skin secretions. *J Prosthet Dent,* 83**,** 572-7.

POTAMIANOS, P., AMIS, A., FORESTER, A., MCGURK, M. & BIRCHER, M. 1998. Rapid prototyping for orthopaedic surgery. *Proceedings of the Institution of Mechanical Engineers, Part H: Journal of Engineering in Medicine,* 212**,** 383-393.

QUAIL, F., STICKLAND, M. & SCANLON, T. Year. Rapid manufacturing technique used in the development of a regenerative pump impeller. *In,* 2009.

QUV&Q-SUN 2012. QUV & Q-Sun Acomarison of two effective approaches to accelerated weathering and light stability testing. *technical Bulletin LU-8009*.

RAE, T., MCCORMICK-THOMSON, L., MURRAY, D. & RUSHTON, N. 1989. The effect of starch glove powder on joint and other tissues. *Annals of The Royal College of Surgeons of England,* 71**,** 361.

RAHIMI, A. 2004. Inorganic and organometallic polymers: a review. *Iranian Polymer Journal,* 13**,** 149-164.

RAYMOND, P. 1977. Some observations on silicone materials and their application in the maxillofacial field. *Proc Inst Maxillofac Technol***,** 177-95.

REPORT, C. 1966. Maxillofacial prosthetic-Proceedings of an interprofessional conference. Sponsered by The . , September. *American Academy of maxillofacial prosthetics. Washongton, D. C.*

ROBERTS, A. C. 1971a. *Facial prostheses: the restoration of facial defects by prosthetic means,* Kimpton.

ROBERTS, A. C. 1971b. Silicones for facial prostheses. *Dent Pract Dent Rec,* 21**,** 276-84.

ROH, K. Y., KIM, D., HA, S. J., RO, Y. J., KIM, J. W. & LEE, H. J. 2001. Pigmentation in Koreans: study of the differences from Caucasians in age, gender and seasonal variations. *British Journal of Dermatology,* 144**,** 94-99.

RUNTE, C., DRIKSEN, D., DELERE, H., THOMAS, C., RUNTE, B., MEYER, U. & VOART 2002. design and n Bally G, Bollman F. Optical data acqusition for computer assessted design of facial prostheses. *Int J prosthodont,* 15**,** 129-132.

SACHS, E., CORNIE, J., BRANCAZIO, D., BREDT, J., CURODEAU, A., FAN, T., KHANUJA, S., LAUDER, A., LEE, J. & MICHAELS, S. 1993. Three dimensional print- ing: the physics and implications of additive manu- facturing. *Ann. CIRP,* 42**,** 257-260.

SAUNDERS, K. J. 1985. Organic Polymer Chemistry. *Chapman and Hall, New York, USA***,** 360.

SHAH, G. B. & WINTER, R. W. 1996. Effect of bimodality on tear properties of silicone networks. *Macromolecular Chemistry and Physics,* 197**,** 2201-2208.

SHAW, W. W. & AHN, C. Y. 1992. Microvascular free flaps in breast reconstruction. *Clin Plast Surg,* 19**,** 917-26.

SHERMAN, L. M. 2004. 3D Printers Lead Growth of Rapid Prototyping. *Plastic Technology*.

SHERMAN, L. M. 2009. Additive Manufacturing New Capabilities for Rapid Prototypes And Production Parts. *Plastic Technology*.

STANIĆ, M., LOZO, B., MUCK, T., JAMNICKI, S. & KULČAR, R. 2008. Color Measurements of Threedimensional Ink-jet Prints. *Proceedings of NIP 24, 6-11 September 2008, Pittsburgh, Pennsylvania*.

STATHI, K., TARANTILI, P. & POLYZOIS, G. 2010. The effect of accelerated ageing on performance properties of addition type silicone biomaterials. *Journal of Materials Science: Materials in Medicine,* 21**,** 1403-1411.

STEINHILP, W. M. & KIAS, U. 2009. Comparison of 3-D Printing Techniques Usable in Digital Landscape Architecture.

STOKES, M., ANDERSON, M., CHANDRASEKAR, S. & MOTTA, R. 1996. A standard default color space for the internet-srgb. *Microsoft and Hewlett-Packard Joint Report*.

STONE, M. C., COWAN, W. B. & BEATTY, J. C. 1988. Color gamut mapping and the printing of digital color images. *ACM Transactions on Graphics (TOG),* 7**,** 249-292.

SUN, J., XI, J., CHEN, X. & XIONG, Y. 2011. A CAD/CAM system for fabrication of facial prostheses. *Rapid Prototyping Journal,* 17**,** 253–261.

SWEENEY, W. T., FISCHER, T. E., CASTLEBERRY, D. J. & COWPERTHWAITE, G. F. 1972. Evaluation of improved maxillofacial prosthetic materials. *J Prosthet Dent,* 27**,** 297-305.

SYKES, B. E., CURTIS, T. A. & CANTOR, R. 1972. Psychosocial aspects of maxillofacial rehabilitation. II. A long-range evaluation. *Journal of Prosthetic Dentistry,* 28**,** 540-5.

TAKAMATA, T., MOORE, B. & CHALIAN, V. 1989. Evaluation of color changes of silicone maxillofacial materials after exposure to sunlight. *Dental materials journal,* 8**,** 260.

TAYLOR, R. L., LIAUW, C. M. & MARYAN, C. 2003. The effect of resin/crosslinker ratio on the mechanical properties and fungal deterioration of a maxillofacial silicone elastomer. *J Mater Sci Mater Med,* 14**,** 497-502.

TECHNOVENT 2012. Magna-Cap, Magnetic Attachment System. *Dental Product Catalogue*.

THONEMANN, B., SCHMALZ, G., HILLER, K. A. & SCHWEIKL, H. 2002. Responses of L929 mouse fibroblasts, primary and immortalized bovine

dental papilla-derived cell lines to dental resin components. *Dental Materials,* 18**,** 318-323.

THONG, H. Y., JEE, S. H., SUN, C. C. & BOISSY, R. E. 2003. The patterns of melanosome distribution in keratinocytes of human skin as one determining factor of skin colour. *Br J Dermatol,* 149**,** 498-505.

UDAGAMA, A. & DRANE, J. B. 1982. Use of medical-grade methyl triacetoxy silane crosslinked silicone for facial prostheses. *J Prosthet Dent,* 48**,** 86-8.

UPCRAFT, S. & FLETCHER, R. 2003. The rapid prototyping technologies. *Assembly Automation,* 23**,** 318-330.

VALAURI, A. J. 1982. Maxillofacial prosthetics. *Aesthetic Plast Surg,* 6**,** 159-64.

VAN NOORT, R. 2011. The future of dental devices is digital. *dental materials*.

VANNIER, M., PILGRAM, T. & BHATIA, G., R. 1993. Quantitative three-dimensional assessment of face-lift with an opti- cal facial surface scanne. *Ann Plast Surg* 30**,** 204-211.

VERRAN, J. & MARYAN, C. J. 1997a. Retention of Candida albicans on acrylic resin and silicone of different surface topography. *J Prosthet Dent,* 77**,** 535-9.

VERRAN, J. & MARYAN, C. J. 1997b. Retention of Candida albicans on acrylic resin and silicone of different surface topography. *The Journal of Prosthetic Dentistry,* 77**,** 535-539.

VLASEA, M., SHANJANI, Y., BASALAH, A. & TOYSERKANI, E. 2011. Additive Manufacturing of Scaffolds for Tissue Engineering of Bone and Cartilage.

WALTERS, K. A. & ROBERTS, M. S. 2008. Dermatologic, cosmeceutic, and cosmetic development: Therapeutic and novel approaches. *New York: Informa Healthcare*.

WALTERS, P., HUSON, D., PARRAMAN, C. & STANIĆ, M. Year. 3D printing in colour: technical evaluation and creative applications. *In*, 2009.

WANG, R. 1999. Preoperative auricular wax pattern duplication for surgical template fabrication. *J Prosthet Dent,* 81**,** 634-7.

WATERS, M., JAGGER, R., POLYZOIS, G. & WILLIAMS, K. 1997. Dynamic mechanical thermal analysis of maxillofacial elastomers. *J Prosthet Dent,* 78**,** 501-5.

WATERS, M. G., JAGGER, R. G. & POLYZOIS, G. L. 1999. Wettability of silicone rubber maxillofacial prosthetic materials. *J Prosthet Dent,* 81**,** 439-43.

WAZEN, J. J., WRIGHT, R., HATFIELD, R. B. & ASHER, E. S. 1999. Auricular rehabilitation with bone-anchored titanium implants. *Laryngoscope,* 109**,** 523-7.

WHITE, J. R. & TURNBULL, A. 1994. Review: Weathering of polymers: mechanisms of degradation and stabilization, testing strategies and modelling. *J. Mat. Sci.,* 29**,** 584-613.

WIECHMANN, D., RUMMEL, V., THALHEIM, A., SIMON, J. S. & WIECHMANN, L. 2003. Customized brackets and archwires for lingual

orthodontic treatment. *American journal of orthodontics and dentofacial orthopedics,* 124**,** 593-599.

WILLIAMS, D. 1987. Definitions in biomaterials. *Amsterdam: Elsevier website*.

WILLIAMS, R., KOMARAGIRI, S., MELTON, V. & BISHU, R. 1996. Investigation of the effect of various build methods on the performance of rapid prototyping (stereolithography). *Journal of materials processing technology,* 61**,** 173-178.

WINDER, J. 1999. Medical rapid prototyping and 3D CT in the manufacture of custom made cranial titanium plates. *Journal of medical engineering & technology,* 23**,** 26-28.

WINDER, J. & BIBB, R. 2005. medical rapid prototyping technologies: State of art and current limitations for application in oral and maxillofacial surgery. *J maxillofac surg,* 63**,** 1006-1015.

WOHLERS, T. 2009. Rapid Prototyping, Tooling & Manufacturing State of the Industry, Annual Worldwide Progress Report, Wohlers Associates Inc., Colorado, USA. *Wohlers Report 2009*.

WOLF, A., DOW CORNING, S., BOLTE, H. & BOTTGER, T. 1999. IX. ATTEMPTS AT CORRELATING ACCELERATED LABORATORY AND NATURAL OUTDOOR AGEING RESULTS. *Durability of building sealants: state-of-the-art report of RILEM Technical committee 139-DBS, Durability of building sealants,* 21**,** 181.

WOLFAARDT, J., SUGAR, A. & WILKES, G. 2003. Advanced technology and the future of facial prosthetics in head and neck reconstruction. *Int J Oral Maxillofac Surg,* 32**,** 121-3.

WORTHINGTON, P. & BRANEMARK, P. 1992. Advanced osseointegration surgery: applica- tions in the maxillofacial region. *Chicago: Quintessence*.

WRIGHT, D. C. 2001. Failure of Plastics and Rubber Products – Causes, Effects and Case Studies involving Degradation. *Rapra Technology Report,* ISBN: 1-85857**,** 261-8.

XIAO, K., LIAO, N., ZARDAWI, F., LIU, H., VAN NOORT, R., YANG, Z., HUANG, M. & YATES, J. M. 2012. Investigation of Chinese skin colour and appearance for skin colour reproduction. *中国光学快报* 10**,** 83301.

YU, H. G., CHUNG, H., YU, Y. S., SEO, J. M. & HEO, J. W. 2003. A new rapid and non-radioactive assay for monitoring and determining the proliferation of retinal pigment epithelial cells. *Korean J Ophthalmol,* 17**,** 29-34.

YU, R., KORAN, A., 3RD & CRAIG, R. G. 1980. Physical properties of maxillofacial elastomers under conditions of accelerated aging. *J Dent Res,* 59**,** 1041-7.

YU, R., KORAN, A., CRAIG, R. & RAPTIS, C. 1982. Stain Removal from a Pigmented Silicone Maxillofacial Elastomer. *Journal of dental research,* 61**,** 993-996.

YU, R., KORAN, A., RAPTIS, C. & CRAIG, R. 1981. Stain removal from a silicone maxillofacial elastomer. *Journal of Dental Research,* 60**,** 1754-1758.

YU, R., KORAN, A., RAPTIS, C. & CRAIG, R. 1983. Cigarette staining and cleaning of a maxillofacial silicone. *Journal of dental research*, 62**,** 853-855.

14 Appendices

14.1 Appendix A

Abstract

Evaluation of the environmental durability of a silicone elastomer used in facial soft tissue prostheses.

Faraedon Zardawi, Kaida Xiao, Richard Van Noort and Julian Yates. School of Clinical Dentistry, University of Sheffield, UK

Aim: To test the effect of UV light and weathering conditions on the mechanical properties and colour stability of a maxillofacial silicone polymer.

Materials & Methods: Samples for testing the tensile strength, tear strength and hardness were manufactured from Sil-25 using custom made stainless steel moulds designed according to ASTM specifications. Six specimens were used for testing tensile and tear strength using a tensile tester (Lloyd instruments LRX Mod.23), and hardness (Sure A Durometer 4478). Coloured silicone discs, representing 5 ethnic skin tones, were fabricated using a stainless steel mould (dimensions: 25x6 mm) from Sil-25 silicone polymer. L*a*b* were measured by using Minolta spectrophotometer (CM-2600d) before and after exposure to UVL and weathering conditions in a Q-U-V Accelerated weathering tester (ASTM G154) for 1 week and 6 weeks, which is approximately equivalent to 3 years and 18 years normal life exposure respectively according to manufactures instruction. ΔE values for all samples were calculated and results analyzed to determine changes in colour.

Results: The average values of both the tensile and tear strength were significantly reduced after 1 and 6 weeks exposure. In contrast both the % of elongation and hardness increased after 6 weeks of exposure to UV light and weathering condition. Six week exposure resulted in a considerable shift in L*a*b* values (ΔE=12.52). The a* and b* values reduced more than L*, which indicates a loss of red and yellow components in the coloured silicone samples and a deterioration towards a lighter tone. No significant effect was detected after one week exposure to UV light and weathering conditions on the samples.

Conclusion: Six weeks exposure to UVL and weathering condition resulted in a demonstrable deterioration in the mechanical properties and colour stability of Sil-25 silicone polymer. These changes were noticeably less after one-week exposure. Therefore Sil-25 has a limited capability of withstanding exposure to these conditions.

Acceptance letter:

Subject:	Acceptance of your paper: BSODR 13th - 15th September 2011
From:	peter.g.robinson@sheffield.ac.uk (peter.g.robinson@sheffield.ac.uk)
To:	dr_faraedon@yahoo.com;
Date:	Monday, 13 June 2011, 19:26

Dear Dr. Zardawi

I am delighted to inform you that your abstract 152754 entitled 'Evaluation of The Durability of A Maxillofacial Silicone Elastomer' has been accepted for presentation at this year's British Society for Oral and Dental Research meeting. The meeting will take place in Sheffield between 13th and 15th September this year. Details of the programme are being put together now and we plan to tell you of the exact time and style of your presentation in the next few weeks. Where I can I will attempt to honour existing requests for a particular style of presentation or to avoid certain days. Please do not forget to register at the conference and the social events. Space is limited on some of those events and so it would be wise to register early. The closing date for early registration (at a lower fee) is 31st July. Registration is available at

http://bsodr2011.group.shef.ac.uk/cms/

I look forward to seeing you at what will be a very exciting meeting.

Yours Sincerely

Peter G Robinson

Editor

BSODR.

14.2 Appendix B

COL 10(8), 000000(2012) CHINESE OPTICS LETTERS August 10, 2012

Investigation of Chinese skin colour and appearance for skin colour reproduction

Kaida Xiao[1*], Ningfang Liao[2], Faraedon Zardawi[1], Haoxue Liu[3], Richard Van Noort[1], Zhixiong Yang[2], Min Huang[3], and Julian M Yates[1]

[1] School of Clinical Dentistry, University of Sheffield, 19 Claremont Crescent Sheffield, S10 2TA, UK

[2] National Key Lab of Colour Science and Engineering, Beijing Institute of Technology, Beijing 100081, China

[3] Beijing Institute of Graphic Communication, Beijing 102600, China

Corresponding author: kaidaxiao@yahoo.co.uk

Received December 1, 2011; accepted February 24, 2012; posted online, 2012

A Chinese skin colour database is established based on measurements taken from nine bodies are as of 202 Chinese individuals to move towards accurate skin colour reproduction. The colour appearance of each skin point is predicted, and a comprehensive colour gamut for Chinese skin is determined. A consistent colour shift between facial and arm colours is identified, in which facial colour tends to be more reddish, more colourful, and darker than arm colour. Moreover, Chinese females are found to have lighter, paler, and more yellowish skin than Chinese males. Variations in Chinese skin colour are quantified, and body area differences and gender differences are shown to have significant effects on Chinese skin colour.

OCIS codes: 330.1690, 330.1710, 330.1730, 170.1850.

doi: 10.3788/COL201210.000000.

Appendix C

The University Of Sheffield.

School Of Clinical Dentistry.

University Research Ethics Committee (School of Clinical Dentistry)

Research Ethics Lead - Dr Lynne Bingle
Claremont Crescent
Sheffield S10 2TA
Telephone: +44 (0)114 271 7954/51
Fax: +44 (0)114 271 7894
Email: l.bingle@sheffield.ac.uk

21st December 2010

Full title of study: Development of a human skin shade guide
Reference number: 9

On behalf of the committee, I am pleased to confirm a favourable ethical opinion for the above research based on your revised application form, information sheet and supporting documentation. If any further changes are made to these documents the Ethics Committee should be informed and their opinion requested.

With the Committee's best wishes for the success of this project

Yours sincerely
Lynne Bingle Research Ethics Lead

14.3 Appendix D

Polynomial Regression with Least-Squares Fitting

Polynomial regression based on the least-squares fitting method has been widely employed for device characterisation due to its accuracy results and ease of implementation. To characterise a camera, a set of camera RGB signals (represented by vector s[r g b]) needs to be mapped onto the corresponding CIE XYZ tri-stimulus values (represented by vector p[x y z]). Suppose that *N* reference colours are used in the characterisation process. Then all the camera RGB responses ($\mathbf{s_i}$ for $i=1..N$) form a *N* by 3 matrix R, and their corresponding CIE XYZ values ($\mathbf{p_i}$ for $i=1..N$) form a *N* by 3 matrix X. If a linear mapping is required, the following objective function minimizes the sum of squared residuals for such a mapping:

$$E = \sum_{i=1}^{N} (\mathbf{p_i^T} - \mathbf{s_i^T M})^2 \quad \text{(a1)}$$

where **M** is the unknown transfer matrix sought. Taking partial derivatives with respect to the elements of **M**, one arrives at the Euler equations:

$$\mathbf{R^T(X - RM) = 0} \quad \text{(a2)}$$

therefore, a least-squares solution is

$$\mathbf{M = (R^T R)^{-1} R^T X} \quad \text{(a3)}$$

where $\mathbf{R}^T$ denotes the transpose of **R**, and $\mathbf{R}^{-1}$ the inverse. The basic idea underpinning this simple linear transformation is that each column of **X** can be written as a linear combination of the columns of **R**. That is,

$$\mathbf{x} = \alpha\mathbf{r} + \beta\mathbf{g} + \gamma\mathbf{b} \quad \text{(a4)}$$

where α, β and γ are scalars. However, a simple linear transformation often does not produce adequate results and so the procedure above can easily be extended to higher-order polynomial terms so that the model derived can be more accurate. In a second-order polynomial function, each column of **X** can be represented as a linear combination of not just the columns of **R**, but also the columns of **R** squared ($\mathbf{r^2}$, $\mathbf{g^2}$, $\mathbf{b^2}$). Moreover, cross-column and translational terms can also be added into the function. So the $N \times 3$ matrix **R** can be expanded to the $N \times 11$ matrix $\mathbf{R'}$:

$$\mathbf{R}' = \begin{bmatrix} \mathbf{r} & \mathbf{g} & \mathbf{b} & \mathbf{r^2} & \mathbf{g^2} & \mathbf{b^2} & \mathbf{rg} & \mathbf{rb} & \mathbf{gb} & \mathbf{rgb} & \mathbf{1} \end{bmatrix} \quad \text{(a5)}$$

where **1** denotes the $N \times 1$ vector with all N components equal to 1 and accounts for translations. Similarly, a third-order polynomial function consisting 20 terms as listed in Equation (a6) was also investigated,

$$R' = \begin{bmatrix} r & g & b & r^2 & g^2 & b^2 & rg & rb & gb & r^3 & g^3 & b^3 & r^2g & rg^2 & r^2b & rb^2 & g^2b & gb^2 & rgb & 1 \end{bmatrix}^t \quad \text{(a6)}$$

In theory, there is no limit to the order and number of terms of the polynomial; in practice, it is constrained by the accuracy required, the computational cost, and the number of samples available.

14.4 Appendix E

26th Annual IAA Conference

Julian M Yates*, Kaida Xaio, Fareadon Zardawi, David Wildgoose, Richard van Noort and Fripp Design and Research Limited.

CAD/CAM Design and Manufacture of Maxillofacial Soft Tissue Prostheses Using 3D Color Printing
friday, june 1, 15.30-15.45

Julian M Yates BSc BDS PhD,MFDSRCPS, FDSRCPS, FDSRCS
Professor of Oral and Maxillofacial Surgery, School of Dentistry, University of Manchester, UK

abstract:
Purpose: A collaborative research team at the University of Sheffield and Fripp Design and Research Ltd, a Sheffield based industrial design company; have developed a method of manufacturing facial soft tissue prostheses using CAD/CAM and additive manufacturing techniques with the use of 3D color printing. This has been achieved by layered fabrication of a biocompatible powder held together by an aqueous binder containing a resin and colored inks, and then processed with a medical grade silicone polymer. The scope of this project was to utilize modern CAD/CAM and manufacturing technologies to enhance and support the traditional skills of the maxillofacial anaplastologist and provide a method of provision where these skills are not available.
Method: Data capture: Three dimensional patient data (geometry and color) was captured using a 3D camera system (3dMD, UK). Alternative methods of capturing/replacing missing facial tissues using stock CAD images or “mirrored” facial parts were also utilized. Additional color information was also captured using 2D photography, and data utilized within the CAD/CAM process.
Data manipulation: CAD manipulation of the captured data was then undertaken using both standard and project specific computer software to refine the shape of the potential prosthesis, provide an optimal fitting surface (facial contour and feathered edge),

attachment points (for magnets or bars), create surface texture and provide the patient specific color to the prosthesis.

Manufacture: To manufacture the prosthesis 3D color printing was then used to achieve layered fabrication of a biocompatible powder held together by aqueous binders containing resin and colored inks. This was then processed with a medical grade silicone polymer in order to produce the final prosthesis. Final touches were then made using matting dispersion solution if required.

Results: The development of this unique and innovative method utilizing additive 3D color printing has allowed the research team to produce custom made/ patient specific silicone based facial soft tissue prostheses. The prostheses produced are biocompatible, lightweight, flexible, color matched and can utilize attachment points to increase retention. Furthermore, it allows for the utilization of patient and stock prostheses to be stored electronically in an image library for subsequent prosthesis replacement. This results in a significant reduction in both production time and cost.

Conclusion: CAD/CAM and additive manufacturing techniques – 3D color printing, have been used to successfully produce custom made lifelike facial soft tissue prostheses.

Clinical significance: This method of soft tissue prosthesis production may supplement or enhance those methods already employed by anaplastologists. Furthermore, it may also allow for the provision of prostheses in areas where these skills are not available.

Julian M. Yates, MD BSc
BDS PhD MFDSRCPS FDSRCPS

CAD/CAM Design and
3D Color Orienting of
Maxillofacial Soft Tissue
Prostheses

friday, june 1, 15.30-15.45

abstract:

A research team at the University of Sheffield with the help and support Fripp Design and Research, a Sheffield based Industrial Design Company; have developed a novel method of manufacturing soft tissue facial prostheses using additive manufacturing with the use of 3D color printing. This has been achieved by layered fabrication of a starch

powder held together by an aqueous binder containing a resin and inks and then infiltrated with a medical grade silicone polymer. Earlier work has shown that the prosthesis thus produced does not cause any cytotoxic reaction. However, the powders and the binders employed by the printer are used for industrial rather than medical applications. To date, these powders and binders have not been tested for their suitability in medical applications. Therefore the aim of this study was to evaluate the biocompatibility of the binders used in the printing of these soft tissue facial prostheses. Biocompatibility was investigated by testing four binders (clear, magenta, cyan and yellow) at three concentrations (0.1, 0.5 and 1.0%) on two cell lines (ROS -osteoblasts and L929 - fibroblasts).

The binders were exposed to the cells for 3, 5 and 7 days, after which the cells were treated with 10% Alamar Blue (Invitrogen, UK) and incubated for 4 h. After this time, samples from each test were placed into a 96-well plate, and the fluorescence intensity of each well was 26th Annual IAA Conference / 31measured using a fluorescent plate reader (InfiniteR 200 PRO, Tecan, Reading, UK) at an excitation wavelength of 570 nm and emission wavelength of 600 nm. Binder toxicity was measured as a comparison against the uninfected media only cell control. The Alamar Blue assays of the binders are shown in Table 1 and Table 2 for the ROS cell line and the L929 cell line respectively.

For the ROS cell line for all days no significant toxic effects were observed at a binder concentration of 0.1% when compared with the control group. At a 0.5% concentration of the four binders there is evidence of a reduction in cell viability and it appears to be more pronounced at seven days, especially for the clear binder. At 1.0% concentration the clear binder showed a toxic effect at 3, 5 and 7 days, becoming most pronounced at seven days, causing complete cell death.

The results for the L929 cell line were very similar in that an increase in concentration an exposure time resulted in measurable cell death and again the clear binder caused a more significant reduction in cell viability than the other binders. The Alamar Blue assay highlighted the potentially toxic effect for the four colored binders used in the manufacture of soft tissue facial prostheses when used in concentrations greater than 0.1%. This effect was most pronounced for the clear binder at seven days exposure. There was no difference in the results obtained with the two types of cell lines used in this study (ROS and L929).

14.5 Appendix F

Tensile Strength

nQuery Advisor

One-way analysis of variance (equal n's)

Column	1	2	3
Test significance level, α	0.050	0.050	0.050
Number of groups, G	3	3	3
Variance of means, $V=\Sigma(\mu_i-\mu)^2 / G$	4.850	1.860	3.860
Common standard deviation, σ	0.380	0.220	0.410
Effect size, $\Delta^2 = V/\sigma^2$	33.5873	38.4298	22.9625
Power (%)	95	95	95
n per group	2	2	2

STORED STATEMENTS for MGT0-tmpA23B.nqa:

When the sample size in each of the 3 groups is 2, a one-way analysis of variance will have 95% power to detect at the 0.050 level a difference in means characterized by a Variance of means, $V=\Sigma(\mu_i-\mu)^2 / G$ of 4.850, assuming that the common standard deviation is 0.380.

REFERENCES for MGT0-tmpA23B.nqa:

O'Brien, R.G., Muller, K.E. Applied Analysis of Variance in Behavioral Science Marcel Dekker, New York (1993) Chapter 8 pp. 297-344

Tear Strength

nQuery Advisor

One-way analysis of variance (equal n's)

Column	1	2	3
Test significance level, α	0.050	0.050	0.050
Number of groups, G	3	3	3
Variance of means, $V=\Sigma(\mu_i-\mu)^2 / G$	6.550	6.520	7.040
Common standard deviation, σ	1.730	1.810	2.150
Effect size, $\Delta^2 = V/\sigma^2$	2.1885	1.9902	1.5230
Power (%)	95	95	95
n per group	4	4	5

STORED STATEMENTS for MGT0-tmpEFFE.nqa:

When the sample size in each of the 3 groups is 5, a one-way analysis of variance will have 95% power to detect at the 0.050 level a difference in means characterized by a Variance of means, $V=\Sigma(\mu_i-\mu)^2 / G$ of 7.040, assuming that the common standard deviation is 2.150.

REFERENCES for MGT0-tmpEFFE.nqa:

O'Brien, R.G., Muller, K.E. Applied Analysis of Variance in Behavioral Science Marcel Dekker, New York (1993) Chapter 8 pp. 297-344

USER NOTES for MGT0-tmpEFFE.nqa

HATAMLEH, M. M. & WATTS, D. C. 2010. Mechanical properties and bonding of maxillofacial silicone elastomers. Dent Mater, 26, 185-91.

Hardness

nQuery Advisor

One-way analysis of variance (equal n's)

Column	1	2	3
Test significance level, α	0.050	0.050	0.050
Number of groups, G	3	3	3
Variance of means, $V=\Sigma(\mu_i-\mu)^2 / G$	25.420	12.460	36.440
Common standard deviation, σ	0.540	0.790	1.810
Effect size, $\Delta^2 = V/\sigma^2$	87.1742	19.9647	11.1230
Power (%)	95	95	95
n per group	2	2	2

STORED STATEMENTS for MGT0-tmp329A.nqa:

When the sample size in each of the 3 groups is 2, a one-way analysis of variance will have 95% power to detect at the 0.050 level a difference in means characterized by a Variance of means, $V=\Sigma(\mu_i-\mu)^2 / G$ of 36.440, assuming that the common standard deviation is 1.810.

REFERENCES for MGT0-tmp329A.nqa:

O'Brien, R.G., Muller, K.E. Applied Analysis of Variance in Behavioral Science Marcel Dekker, New York (1993) Chapter 8 pp. 297-344

USER NOTES for MGT0-tmp329A.nqa

HATAMLEH, M. M. & WATTS, D. C. 2010. Mechanical properties and bonding of maxillofacial silicone elastomers. Dent Mater, 26, 185-91.

14.6 Appendix G

Table showing the mechanical properties of some maxillofacial elastomers

N	Maxillofacial elastomer	Tensile strength	Tear strength	% Elongation	Hardness	Manufacture
1	**Sil-25**	870 psi	12 N/mm	550	22 Shore A	Abacus-UK
2	**Matrix-M-3428**		20 K/m	600	28 Shore A	Abacus-UK
3	**Cosmesil**	4.24 MPa	4.87 N/mm	577	45 (I.R.H.D)	Dow-Coring
4	**Prestige**	2.55 MPa	4.53 N/mm	725	16 (I.R.H.D)	Prestige-Dental-UK
5	**MED-4920 Nusil**	8.36 MPa	14.5 N/mm	1700	24 (I.R.H.D)	Nusil Technology
6	**Silastic-81Standard**	4.9 MPa	26 KN/m	560	21 Shore A	Dow-Corning
7	**A-103 MG Elastomer**	650 psi	90 ppi	500	27 Shore A	Factor 11 Inc
9	**A-588-1 Realistic**	600 psi	45 ppi	700	12 Shore A	Factor 11 Inc
10	**A-588-2 Realistic**	700 psi	45 ppi	600	22 Shore A	Factor 11 Inc
11	**A-2000**	800 psi	12 ppi	500	25 Shore A	Factor 11 Inc

Data obtained from manufacture product specifications and a controlled study by Aziz et al (2003).

1- AZIZ, T., WATERS, M. & JAGGER, R. 2003. Analysis of the properties of silicone rubber maxillofacial prosthetic materials. *J Dent,* 31**,** 67-74.
2- http://www.factor2.com/
3- http://www.notcutt.co.uk/docs/pss/Silastic%203495.pdf
4- http://www.factor2.com/Silicone_Elastomer_RTV_Facial_Prosthetic_p/a-588-1.htm
5- http://www.factor2.com/Medical_Grade_Elastomer_p/a-103.htm